

N73-28977

VOLUME II

STUDIES IN TILT-ROTOR VTOL AIRCRAFT AEROELASTICITY

by

RAYMOND GEORGE KVATERNIK

Submitted in partial fulfillment of the requirements
for the Degree of Doctor of Philosophy

Thesis Advisor: Professor Robert H. Scanlan

Department of Solid Mechanics, Structures, and Mechanical Design

CASE WESTERN RESERVE UNIVERSITY

June 1973

CHAPTER 6

NATURAL MODE VIBRATION ANALYSIS OF STRUCTURAL SYSTEMS

BY DIRECT AND COMPONENT MODE SYNTHESIS TECHNIQUES

Introduction

Natural vibration modes constitute the basic ingredient in many flutter and dynamic response analyses procedures currently employed for aerospace structures. Flutter analyses based on the use of natural modes enjoy the convenience of having the structural dynamic characteristics completely describable in terms of the natural frequencies and generalized masses, the mode shapes being employed in the formulation of the generalized aerodynamic forces. In transient aeroelastic problems related to response in gust encounters or in maneuvers or dynamic response problems such as landing impact the use of a normal mode methodology provides an effective and systematic approach to the formulation of the governing equations of motion. For aircraft having rotating components such as propellers or rotors a complete knowledge of the vibratory characteristics of the airframe is necessary in order to avoid resonances with the airframe frequencies and to be able to assess the effects of the external excitation forces generated by the oscillatory aerodynamic loading. It is also common practice to make resonance tests of flight vehicle structures and/or their components (or suitable models thereof) on the ground and compare the experimental modes and frequencies with calculated values. This serves to validate the mathematical

model as regards the inertial and elastic properties to be used in subsequent flutter and dynamic response analyses.

In recognition of the fundamental role assumed by natural modes in aeroelastic and dynamic analyses and in structural design verification this chapter is concerned with the development of utilitarian computational procedures for the natural mode vibration analysis of linear structural systems. Following customary engineering practice in dealing with complicated structures, recourse is had to the approximation of replacing the continuous structural system having an infinite number of degrees of freedom by an "equivalent" discrete system having a finite number of degrees of freedom. Herein this discretization is made by replacing the structure with a finite element mathematical model based on the stiffness method of structural analysis. Attention is directed to two methods for natural mode vibration analysis. The first consists of a direct approach based on a finite element representation of the complete structure as an entity, the mass and stiffness matrices for the complete structure being assembled by properly combining the mass and stiffness matrices of the individual "elements" into which the structure has been divided. Such procedures are described in Refs. 6-1 and 6-2 for example. For large, complex structural systems, the determination of these modes by a direct method often leads to a problem size which is unwieldy or which exceeds the storage capacity of available computing machinery. An alternative approach to natural mode vibration analysis in such circumstances is that of component mode synthesis. This method is based on the concept of synthesizing the

natural modes of the complete structure from modes* of conveniently defined substructures, or components, into which the structure has been partitioned. In this way the expedient of reducing the system degrees of freedom, and thus the size of the eigenvalue problem, can be introduced by partial modal synthesis wherein only a relatively few of the modes from each component are chosen as degrees of freedom and employed in the synthesizing procedure. The total number of selected component modes, and hence modal coordinates, is then significantly less than the number of discrete degrees of freedom established by the finite-element modeling process. In addition to the obvious advantage of reducing the size of the overall system eigenvalue problem, the component mode approach can be so formulated as to provide the added flexibility of including several types of component deflection shapes such as calculated or measured natural modes, assumed deflection shapes, or static deflection shapes. The chosen shapes may be based on interface restraint conditions which differ from those that exist in the assembled configuration. To judge from the number of recent additions to the literature the modal synthesis method of natural mode vibration analysis appears presently to be experiencing a "renaissance." This renewed interest is undoubtedly a consequence of the many attendant advantages which the modal synthesis scheme offers over that of the direct method, particularly in dynamic analyses of large complex structural systems. For this

* More generally, any suitable set of linearly independent shape functions and not necessarily the calculated natural modes, as will be pointed out later.

reason a brief historical synopsis of this method seems appropriate here.

The method which is now referred to in various terms as component mode synthesis, modal synthesis, or modal coupling was implicit in the early work of Scanlan (Ref. 6-3), among others. He used normal coupled vibration modes of airplane components as generalized coordinates in a Rayleigh-type analysis of the transient response resulting from landing impact. Later Hunn (Ref. 6-4) presented a similar procedure for calculating the free vibration modes of an aircraft. Both these authors were motivated by the need for reducing the system eigenvalue problem to an order suitable for hand calculation. The mechanics of component mode synthesis were quite extensively developed in an early work of MacNeal (Ref. 6-5). However, because his work was stated primarily in terms of electrical analogies, being addressed to electrical engineers, it generally remained "inaccessible" to structural dynamicists. In 1960 Hurty (Ref. 6-6) described the rudiments of component mode synthesis in terms more familiar to structural dynamicists and illustrated its use by applying it to a simple frame structure, thereby making it "available" to structural dynamicists. A comprehensive account of many of the mathematical aspects of component mode synthesis as applied to dynamic analyses was given by Hurty several years later (Ref. 6-7).^{*} Central to Hurty's scheme was the separation of the calculated component modes into fixed constraint normal modes,

^{*} A condensed version of this JPL report is also available as "Dynamic Analysis of Structural Systems Using Component Modes," AIAA Journal, Vol. 3, April 1965, pp. 678-685.

constraint modes, and rigid-body modes. A "Branch Mode" analysis scheme was given by Gladwell (Ref. 6-8) at about the same time. This method featured the imposition of a sequence of sets of constraints on the system, each set being chosen so that for each constrained configuration only one component or "branch" could vibrate elastically. These branch modes and appropriate rigid-body modes were then employed in a Rayleigh type analysis of the complete system. Goldman (Ref. 6-9)* used rigid-body modes and free-free elastic modes of components for synthesis. Bamford (Ref. 6-10) included so-called "attachment modes" in the selected mode sets to account for concentrated loads at unconstrained points of the complete structure. An application to a launch vehicle was given by McAleese (Ref. 6-11). Bajan and Feng (Ref. 6-12) suggested an iterative procedure, which they termed modal substitution, for improving the system modes and frequencies calculated by partial modal synthesis. These works, for the most part, represent the developments pertaining to modal synthesis available in the open literature at the time the comparable work to be described herein was initiated. More recent additions to this literature, appearing while this work was in progress, are given in Refs. 6-13 to 6-19.

Chronologically, the direct method of natural mode vibration analysis was first developed to serve as a stand-alone procedure for problems having up to about 200 degrees of freedom. With a view primarily toward allowing significantly more degrees of freedom

* A condensed version, under the same title, is given in AIAA Journal, Vol. 7, June 1969, pp. 1152-1154.

in the finite-element discretization without a corresponding increase in computer storage requirements a component mode synthesis method was next developed. The analytical bases of both these methods as developed herein are believed to be rather different in approach and to contain several new and novel features: Both analyses enforce inter-substructure deflection compatibility according to a new algorithm conceived by Walton and Steeves (Ref. 6-20) in which independent system coordinates are established by solving an eigenvalue problem associated with a symmetric matrix formed from the coefficients of the constraint equations. The concept of a gyroscopic finite element is further introduced. Based on this artifice both analyses are extended to include the effects of gyroscopic coupling forces induced by large rotating components such as propellers, propellers, or fans. Several additional features are included in the modal synthesis formulation. A "hybrid" representation can be employed for the substructures whereby some substructures may be described in terms of modal coordinates established on the basis of selected component modes while the remaining substructures are described in terms of discrete coordinates. Substructure modal information, either for free-free or constrained boundary conditions, can be specified in the form of calculated or measured natural modes, static deflection shapes, assumed deflection shapes, or any combination of these. These deflection shapes need not be orthogonal or normalized in any consistent manner.

Both the direct and component mode synthesis analyses presented herein are, in principle, applicable to a structural idealization based on any type of finite element (segments of beams, plates, shells, etc.). The computer programs based on these analyses* are, however, limited to structures which admit of a "stick" model representation. The latter refers to a structural idealization in which the structure is taken to be composed of an assemblage of beams, springs, and rigid bodies. Since many structures of practical interest can be represented in this manner for dynamic analyses the corresponding computer programs have a relatively wide range of engineering applicability.

The Mathematical Model

(a) Nature of the Finite-Element Stiffness Matrix Method of Structural Analysis

The idea of replacing a continuous structure by pieces, generating the stiffness matrix for each piece, and from these assembling the stiffness matrix for the complete structure was originally suggested by Levy (Ref. 6-21). However, Turner, Clough, Martin, and Topp (Ref. 6-22) are generally credited with developing the concept to the point at which it was amenable to automation on digital computers, thereby firmly establishing the procedure which is now referred to as the finite element stiffness

* These are given in Appendix H. Only the case of zero gyroscopic coupling has as yet been programmed, however.

or displacement method of structural analysis. Briefly, the finite element method as applied to the analysis of complex structural systems is based on replacing the structure by an idealization consisting of a large number of small discrete "standard" structural elements (such as beam, plate, or shell segments) which are interconnected at discrete node points, the loading on each element being represented by a set of discrete forces and/or moments acting at the node points on the boundary of the element. Element force-deflection relationships, established on the basis of some simple assumed deformation which relates internal displacements of the element to its nodal displacements, lead to a set of stiffness influence coefficients, or stiffness matrix, which embodies the elastic characteristics of the element. The individual unassembled elements are combined to form a mathematical model of the complete structure by conceptually joining all elements at their node points in a manner which insures that the elements are in equilibrium subject to the external loads and the forces they exert on each other and that no discontinuities of deformation occur at element juncture points. These conditions are generally only approximately satisfied. In the stiffness method continuity of deformation is satisfied a priori while the equilibrium requirements are implicit in the mechanics of the method. The resultant system stiffness matrix then defines the elastic characteristics of the structure in terms of force-deflection relationships for a finite number of coordinates (nodes). These force-deflection relations constitute

a set of algebraic equilibrium equations, having deflections as unknowns, which approximate the differential equations of equilibrium for the elastic continuum. The interested reader will find detailed considerations relating to the finite-element method of structural analysis in several excellent books (see, for example, Refs. 6-23 to 6-25).

(b) The "Stick" Model Structural Representation Employed in the
Computer Programs

The analyses and associated computer programs for natural mode vibration analysis by direct and component mode synthesis techniques are based on a substructures approach in which the structure is first partitioned or divided into several separate smaller components or substructures, such as schematically depicted in Fig. 6-1. Based on the known inertial and elastic properties a finite-element mathematical model of each substructure is then established. If the direct method of vibration analysis is to be employed the inertial and elastic characteristics of the substructures remain in the discrete coordinates established by the finite-element modeling process. If the intent is to employ model synthesis the modes of each substructure are first determined on the basis of the discrete-coordinate mathematical model. A selected few of the modes from each substructure modal set are then used in an assumed-modes type procedure to effect a coordinate transformation to distributed (modal) coordinates. In either case the mathematical model of the complete structure is arrived at by reassembling the

components in a manner consistent with the equations of constraint which insure deflection compatibility at the interfaces of the components.

The "stick" model approach to dynamic analysis as embodied in the computer programs assumes that the structure is composed of an assembly of beams, springs, and rigid bodies. Use of these structural building blocks to represent an aircraft structure for a symmetric vibration analysis is schematically illustrated in Fig. 6-2.* The fuselage/engine combination, the wings, and horizontal tails are replaced by equivalent nonuniform beams lying along the calculated elastic axes of the respective components; the wing and horizontal tail carry-through structures are treated as massless uniform beams (i.e., beam-springs), their mass being included with the mass of the fuselage/engine beam; the vertical tails are taken to be rigid bodies rigidly attached to the fuselage/engine beam.

Since the substructures are treated as distinct and separate components in a substructuring methodology their structural properties are most conveniently defined relative to axes local to each component. The specification of the mass and stiffness matrices corresponding to each of the three types of structural members employed in the stick model representation of a structure herein is the subject of the following subsections.

* The silhouette corresponds to that of an actual aircraft for which the stick model shown was used to represent the structure for symmetric natural mode analysis.

Beam Substructures: The beam elastic properties are defined in terms of the distribution of flexural, torsional, and axial stiffness (EI , GJ , and AE , respectively) along the local elastic axis. The continuous distortion of the beam is approximated by specifying both the deflection and rotation at a number of discrete points or stations along the beam. A beam segment or element is defined to be the length between two such stations. The stiffness of each element is assumed to be constant and given by the average value of the stiffnesses at the two adjacent stations. The distributed mass of the beam is discretized by simply replacing the distributed mass by statically equivalent concentrated masses at the discrete stations along the beam, each mass having both translational and rotational inertia. This lumped mass approach is consistent with the fact that weights data is generally available in a lumped form wherein the inertial properties given are the total weight, center of gravity location, and moments and products of inertia of discrete small regions of a structure. In contrast, use of the celebrated "consistent mass matrix" of Archer (Ref. 6-26) would require a knowledge of the mass distribution.

The mass and stiffness matrices of an unrestrained arbitrarily oriented beam element are each of order 12×12 . If the local coordinate axes are chosen to coincide with the principal axes of the cross section the 12×12 stiffness matrix can be expressed in terms of 4×4 and 2×2 submatrices located on the principal diagonal. Should the center of gravity of the lumped masses lie

on the elastic axis of the beam segment a similar partitioning is possible for the mass matrix. We will assume this to be the case for the present and indicate later how to account for any mass coupling terms. The manner in which the computer programs generate these submatrices for a beam substructure is illustrated below with reference to the two-element beam shown in Fig. 6-3.

(1) Beam Bending - The stiffness matrix for vertical bending is put into the partitioned form:

$$[K]_B = \begin{array}{c} \begin{array}{|c|c|} \hline w & \theta \\ \hline \end{array} \\ \left[\begin{array}{c|c} [A] & [B] \\ \hline [B]^T & [C] \end{array} \right] \begin{array}{|c|} \hline w \\ \hline \theta \\ \hline \end{array} \end{array} \quad (6-1)$$

where

$$[A] = \begin{array}{c} \begin{array}{|c|c|c|} \hline w_1 & w_2 & w_3 \\ \hline \end{array} \\ \left[\begin{array}{ccc} \frac{12EI_1}{L_1^3} & -\frac{12EI_1}{L_1^3} & 0 \\ -\frac{12EI_1}{L_1^3} & \frac{12EI_1}{L_1^3} + \frac{12EI_2}{L_2^3} & -\frac{12EI_2}{L_2^3} \\ 0 & -\frac{12EI_2}{L_2^3} & \frac{12EI_2}{L_2^3} \end{array} \right] \begin{array}{|c|} \hline w_1 \\ \hline w_2 \\ \hline w_3 \\ \hline \end{array} \end{array} \quad (6-2)$$

$$[B] = \begin{array}{c} \begin{array}{|c|c|c|} \hline \theta_1 & \theta_2 & \theta_3 \\ \hline \end{array} \\ \left[\begin{array}{ccc} \frac{6EI_1}{L_1^2} & \frac{6EI_1}{L_1^2} & 0 \\ -\frac{6EI_1}{L_1^2} & -\frac{6EI_1}{L_1^2} + \frac{6EI_2}{L_2^2} & \frac{6EI_2}{L_2^2} \\ 0 & -\frac{6EI_2}{L_2^2} & -\frac{6EI_2}{L_2^2} \end{array} \right] \begin{array}{|c|} \hline w_1 \\ \hline \\ \hline w_2 \\ \hline \\ \hline w_3 \\ \hline \end{array} \end{array} \quad (6-3)$$

$$[C] = \begin{array}{c} \begin{array}{|c|c|c|} \hline \theta_1 & \theta_2 & \theta_3 \\ \hline \end{array} \\ \left[\begin{array}{ccc} \frac{4EI_1}{L_1} & \frac{2EI_1}{L_1} & 0 \\ \frac{2EI_1}{L_1} & \frac{4EI_1}{L_1} + \frac{4EI_2}{L_2} & \frac{2EI_2}{L_2} \\ 0 & \frac{2EI_2}{L_2} & \frac{4EI_2}{L_2} \end{array} \right] \begin{array}{|c|} \hline \theta_1 \\ \hline \\ \hline \theta_2 \\ \hline \\ \hline \theta_3 \\ \hline \end{array} \end{array} \quad (6-4)$$

The bending displacements and slopes have each been grouped together and placed in the order shown in Eq. 6-1 for computational convenience. Extension to additional elements is apparent in the distinctive forms of [A], [B], and [C]. The corresponding inertia matrix is given by

$$[M]_B = \begin{array}{c} \begin{array}{|ccc|ccc|} \hline w_1 & w_2 & w_3 & \theta_1 & \theta_2 & \theta_3 \\ \hline \end{array} \\ \begin{array}{|ccc|ccc|} \hline M_1 & & & & & \\ & M_2 & & & & \\ & & M_3 & & & \\ \hline & & & RI_1 & & \\ & 0 & & & RI_2 & \\ & & & & & RI_3 \\ \hline \end{array} \\ \begin{array}{|c|} \hline w_1 \\ w_2 \\ w_3 \\ \hline \theta_1 \\ \theta_2 \\ \theta_3 \\ \hline \end{array} \end{array} \quad (6-5)$$

Similar matrix expressions describe lateral bending.

(2) Beam Torsion - The torsional stiffness matrix is given by

$$[K]_T = \begin{array}{c} \begin{array}{|ccc|} \hline \phi_1 & \phi_2 & \phi_3 \\ \hline \end{array} \\ \begin{array}{|ccc|} \hline \frac{GJ_1}{L_1} & -\frac{GJ_1}{L_1} & 0 \\ -\frac{GJ_1}{L_1} & \frac{GJ_1}{L_1} + \frac{GJ_2}{L_2} & -\frac{GJ_2}{L_2} \\ 0 & -\frac{GJ_2}{L_2} & \frac{GJ_2}{L_2} \\ \hline \end{array} \\ \begin{array}{|c|} \hline \phi_1 \\ \phi_2 \\ \phi_3 \\ \hline \end{array} \end{array} \quad (6-6)$$

and the inertia matrix by

$$[M]_T = \begin{matrix} & \boxed{\begin{matrix} \phi_1 & \phi_2 & \phi_3 \end{matrix}} \\ \begin{bmatrix} I_1 & & \\ & I_2 & \\ & & I_3 \end{bmatrix} & \boxed{\begin{matrix} \phi_1 \\ \phi_2 \\ \phi_3 \end{matrix}} \end{matrix} \quad (6-7)$$

Extension to more elements is obvious.

(3) Beam Axial - The stiffness matrix describing axial deformation has the form

$$[K]_A = \begin{matrix} & \boxed{\begin{matrix} u_1 & u_2 & u_3 \end{matrix}} \\ \begin{bmatrix} \frac{AE_1}{L_1} & -\frac{AE_1}{L_1} & 0 \\ -\frac{AE_1}{L_1} & \frac{AE_1}{L_1} + \frac{AE_2}{L_2} & -\frac{AE_2}{L_2} \\ 0 & -\frac{AE_2}{L_2} & \frac{AE_2}{L_2} \end{bmatrix} & \boxed{\begin{matrix} u_1 \\ u_2 \\ u_3 \end{matrix}} \end{matrix} \quad (6-8)$$

while the inertia matrix is

$$[M]_A = \begin{matrix} & \boxed{\begin{matrix} u_1 & u_2 & u_3 \end{matrix}} \\ \begin{bmatrix} M_1 & & \\ & M_2 & \\ & & M_3 \end{bmatrix} & \boxed{\begin{matrix} u_1 \\ u_2 \\ u_3 \end{matrix}} \end{matrix} \quad (6-9)$$

Again, the extension to additional elements is obvious.

Spring Substructures: In many instances actual springs may comprise some of the structural components of a structure (or various members may be treated as one-degree-of-freedom springs). These springs are defined by 1×1 stiffness matrices having spring constants as matrix elements and associated 1×1 null inertia matrices. The use of these springs will be illustrated in a qualitative manner later.

It is often convenient to account for the elasticity of short beam members while including their inertia with other members (such as suggested for the wing and tail carry-through structures in Fig. 6-2). A massless, uniform beam segment is employed for this purpose. Since only the elastic properties of this beam segment are considered it has the character of a spring and it seems appropriate to include its description here. For descriptive purposes this massless beam segment will be referred to as a "beam-spring". For the particular coordinate ordering shown in Fig. 6-4 the associated 12×12 stiffness matrix has the form given in Fig. 6-5. The corresponding inertia matrix is taken to be null. The use of the beam-spring is illustrated qualitatively later in this chapter and in the detailed example in Appendix E.

Rigid-Body Substructures: Various components can often be treated as rigid in dynamic analyses. For example: ordnance, external fuel tanks, engine/nacelle combinations, etc. With respect

to a local axis system located at the center of gravity the inertia matrix of a rigid body has the general form

$$\begin{array}{c}
 \boxed{\begin{array}{cccccc} x & y & z & \alpha & \beta & \gamma \end{array}} \\
 [M]_{RB} = \left[\begin{array}{ccc|ccc} M & & & & & \\ & M & & & & 0 \\ & & M & & & \\ \hline & & & I_{xx} & I_{xy} & I_{xz} \\ & 0 & & I_{yx} & I_{yy} & I_{yz} \\ & & & I_{zx} & I_{zy} & I_{zz} \end{array} \right] \boxed{\begin{array}{c} x \\ y \\ z \\ \alpha \\ \beta \\ \gamma \end{array}} \quad (6-10)
 \end{array}$$

The corresponding stiffness matrix is of course null since a rigid body has no strain energy associated with its motion.

It may often be necessary to account for either the translational or rotational rigid-body motion of a beam substructure while neglecting the corresponding elastic motion. This situation is easily accommodated by the availability of this rigid-body element, as will be demonstrated somewhat later. This expedient will also be exercised in the numerical examples given in Appendices E and F.

(c) Formation of the Mass and Stiffness Matrices for the Partitioned Structure

The "building blocks" for constructing the mass and stiffness matrices corresponding to each substructure based on a "stick" model structural representation have been given above. Once the substructure mass and stiffness matrices have been determined the mass and stiffness matrices for the partitioned structure are given

by the composite matrices containing as submatrices the mass and stiffness matrices of the individual substructures on the principal diagonal. These composite matrices are denoted by $[\bar{M}]$ and $[\bar{K}]$, respectively. For the "stick" model shown in Fig. 6-6, for example, both the mass and stiffness matrices for the partitioned structure (ie., $[\bar{M}]$ and $[\bar{K}]$) would have the general form shown in Fig. 6-7.* Each block in Fig. 6-7 corresponds to a matrix. The ordering of blocks within a substructure and the ordering of substructure matrices within $[\bar{M}]$ and $[\bar{K}]$ is, in principle, arbitrary. Since the mass and stiffness matrices for each substructure have been generated independently, no inter-substructure coupling will exist in $[\bar{M}]$ and $[\bar{K}]$. However, intra-substructure coupling (ie., coupling between the blocks within a substructure) will generally exist. For example, if the sectional centers of gravity of the wing or tail surfaces are displaced horizontally from their local elastic axes mass static unbalance terms are introduced which will couple vertical bending displacement with torsion. This will couple the bending and torsion blocks of the wing or tail substructures in $[\bar{M}]$.

Components idealized as rigid bodies can be treated as discrete substructures or, alternately, have their inertia properties combined with the inertia matrix associated with the elastic member to which they are attached. If, for example, the main landing gear assembly of the aircraft shown in silhouette in Fig. 6-6 were treated

*The "stick" model of Fig. 6-6 and the particular freedoms indicated in Fig. 6-7 would be appropriate to a symmetric vibration analysis.

as a rigid mass and its inertial properties combined with the forward fuselage beam, the vertical bending and axial rigid-body blocks of the forward fuselage substructure in $[\bar{M}]$ would be coupled.* Coupling terms would also arise within the vertical bending block, leading to a non-diagonal mass matrix for beam bending. Inter- and intra-substructure coupling terms arise in the stiffness matrix of the partitioned structure, $[\bar{K}]$, when the stiffness characteristics of physical springs are combined with the stiffness matrices of members to which they are attached rather than treated as separate substructures. The preceding remarks are elucidated below in several simple illustrative examples.

Wing Static Unbalance: Consider the sectionalized wing planform shown in Fig. 6-8. The sectional (lumped) masses, bending inertias, and torsional inertias (about the cg) are denoted by m_i , RI_i , and I_i , respectively. The perpendicular distance between the sectional cg locations (assumed to be in the wing chord plane) and the wing elastic axis are denoted by e_i . The kinetic energy of each section, T_i , expressed in terms of displacements and rotations of the elastic axis station, has the form indicated in Fig. 6-8. Substituting each of these expressions into Lagrange's equation and performing the appropriate differentiations leads to

* Figs. 6-6 and 6-7 are appropriate to a symmetric vibration analysis. For an anti-symmetric analysis the lateral bending and torsion blocks of the substructure would be coupled.

the coupled bending-torsion mass matrix shown in Fig. 6-9. By way of illustration assume that Fig. 6-8 is appropriate to the wing of the aircraft depicted in Fig. 6-6. Then $[\bar{M}]$ would have the form shown in Fig. 6-7, the first two blocks of substructure #3 being given by twice the mass matrix of Fig. 6-9. If the sectional cg were also displaced vertically from the wing elastic axis (ie., not in the wing chord plane) additional coupling terms would arise and the vertical bending, torsion, and fore-and-aft bending blocks of substructure #3 would be coupled.

Alternate Treatment of Rigid Bodies: As an alternative to treating each rigid body as an individual substructure the inertial properties of the rigid body (total mass lumped at the cg and moments and products of inertia relative to axes fixed in the body at the cg) can be combined with the inertia matrix of the elastic member to which it is attached. This alternative scheme has the attendant advantage of not explicitly introducing the degrees of freedom associated with the rigid body into the resulting eigenvalue problem.

(1) Rigid Attachment - If the rigid body is, or can be taken as, rigidly attached to an elastic substructure other than a beam-spring the procedure consists in suitably modifying the kinetic energy expression for the substructure to include the effects of the concentrated mass, inertia, and static unbalance about its point of attachment. A formal procedure for effecting such a modification in the general case of an arbitrarily oriented six-degree-of-freedom

rigid body is given in Appendix A. In many instances the necessary additions to the mass matrix of the component to which the rigid body is attached can be obtained directly without recourse to the general results of Appendix A. For example, consider the situation depicted in Fig. 6-10. Suppose one wishes to combine the inertial properties of the center-line fuel tank, taken as a rigid body, with the inertia matrix of the fuselage beam. Assume that each fuselage mass has both vertical bending and longitudinal degrees of freedom. If the principal inertia axes of the fuel tank are parallel to the principal geometric axes of the fuselage beam the kinetic energy of the tank expressed in terms of the motion at the n^{th} mass station has the form given at the bottom of Fig. 6-10. Substituting this expression into Lagrange's equation gives the matrix of additional terms which must be added to the (diagonal) mass matrix for the fuselage beam. The final mass matrix is given in Fig. 6-11.

(2) Flexible Attachment - If the fuel tank of Fig. 6-10 were attached to the fuselage beam through a flexible member which could be treated as a spring substructure (either an actual spring or a beam-spring) the inertia properties of the tank could be combined with the null inertia matrix of the spring substructure using a procedure similar to that described in (1) directly above.

Alternate Treatment of Actual Springs: For convenience actual springs can be divided into those which have one end tied to ground and those which have both ends "free" in the sense that

while both ends attach to some component neither end is tied to ground.

(1) Springs Having One End Tied to Ground - If the spring attachment point on the structure is at a mass station the spring constant(s) can be simply added to the appropriate diagonal term(s) of the stiffness matrix of the component. If the point of attachment is not at a mass station coupling among the blocks within the substructures comprising $[\bar{K}]$ will occur. In the latter case it is sometimes convenient to introduce an auxiliary massless station at the spring attachment point.

(2) Free-Free Springs - The spring constants of springs which have neither end tied to ground can be combined with the stiffness matrices of the substructures to which they are attached by writing the potential energy of the springs in terms of the coordinates at the points of attachment. A simple illustration of the use of this expedient in the realm of launch vehicle dynamics may be given with the aid of Fig. 6-12. In dynamic analyses of launch vehicles the dynamic effects of sloshing propellants are usually included by introducing a dynamically equivalent mechanical analogy, composed of fixed and oscillating masses connected to the tank by springs or pendulums, to account for each important vibration mode of the liquid as a degree of freedom (Ref. 6-27). This equivalent lumped parameter mathematical model can then be combined with appropriate discrete element representations for other components of the vehicle. A spring-mass analogy is shown in Fig. 6-12. One such spring-mass

assembly is provided to represent the dynamic effects of sloshing in vertical bending (translation and rotation) and longitudinal oscillation. For illustrative simplicity, all three sloshing masses are taken to be attached to the same beam station*. The potential energy of the springs, expressed in terms of the deflections of the n^{th} beam station (w_n, θ_n, u_n) and the deflections of the slosh masses (w, θ, u) , is given by V_s in the figure. Substituting this expression into Lagrange's equation leads to the matrix shown in Fig. 6-13. $[\Delta K]$ is the matrix of spring stiffness terms which must be added to the stiffness matrix for the beam.

Establishing the System Equations of Motion

Denoting the composite matrices containing the mass and stiffness matrices of the individual substructures as submatrices on the principal diagonal by $[\bar{M}]$ and $[\bar{K}]$, respectively, the Lagrangian of the partitioned structure can be written as

$$L = \frac{1}{2} \{\dot{z}\}^T [\bar{M}] \{\dot{z}\} - \frac{1}{2} \{z\}^T [\bar{K}] \{z\} \quad (6-11)$$

where $\{z\}$ is a column matrix containing the coordinates of all the substructures. A consequence of any substructuring procedure is the introduction of coordinates which are not generalized coordinates in the Lagrangian sense but are related by equations of constraint which must be imposed to restore geometric compatibility at the

* The non-sloshing portion of the fluid (not shown) is treated as rigid and would simply be combined with the mass matrix of the beam.

interfaces. Since the matrices $[\bar{M}]$ and $[\bar{K}]$ in Eq. 6-11 have been established on the basis of such a substructuring procedure the coordinates forming the vector $\{z\}$ are not independent with respect to the total system. Thus, before Eq. 6-11 can be substituted into Lagrange's equation a set of system-independent coordinates consistent with the equations of constraint must be established. Such coordinates can be arrived at in various ways. Herein, recourse is had to a method recently devised by Walton and Steeves (Ref. 6-20) in which solution of the constraint equations (ie., the establishment of independent coordinates) is, in essence, reduced to computing the eigenvalues and eigenvectors of a symmetric matrix formed from the matrix of coefficients appearing in the constraint equations. For completeness, their work is briefly reviewed below.

(a) The Method of Walton and Steeves for Establishing Independent Coordinates*

The linear algebraic equations of constraint which are a consequence of enforcing deflection compatibility at the junctions of the substructures can be written as

$$[C]\{z\} = \{0\} \quad (6-12)$$

where $[C]$ is a constant matrix depending solely on the geometric configuration of the interfaces. In practice $[C]$ is rectangular

* Their original work (Ref. 6-20) is also available as a NASA Technical Report (Ref. 6-28).

with the number of rows generally much less than the number of columns. Since there are many coordinates (degrees of freedom) which do not appear in the constraint equations the matrix [C] is also characterized by the presence of many null (zero) columns. The vector {z} is identical to that appearing in Eq. 6-11. Usual practice when explicitly dealing with equations of constraint is to partition and solve Eq. 6-12 to define L of the z_i in terms of those remaining, where L is equal to the number of independent constraint equations. The method of Ref. 6-20 enjoys several advantages over the usual method. For complex structures, redundancies often appear in the equations of constraint (in the form of linear dependencies among rows of [C]) which can cause problems (Ref. 6-29). The method of Ref. 6-20 eliminates the need to treat the case of redundant equations of constraint in any special manner. The basis of their method is a new mathematical theorem designated the "zero eigenvalues theorem" which expresses the solution of a set of linear homogeneous algebraic equations in terms of eigenvectors of a symmetric matrix constructed from the coefficients of the equations of constraint. The method proceeds as follows. Using [C] from Eq. 6-12 construct the symmetric matrix [E] defined by

$$[E] = [C]^T[C] \quad (6-13)$$

Solve the eigenvalue problem

$$[E]\{x\} = \lambda\{x\} \quad (6-14)$$

Let the resulting set of eigenvalues be arranged in the diagonal matrix $[\lambda]$ and the corresponding eigenvectors in the modal matrix $[X]$. If $[E]$ has no eigenvalues equal to zero the set of equations given by Eq. 6-12 has only the trivial solution. If zero is an eigenvalue of $[E]$ of multiplicity P the most general solution of Eq. 6-12 is given by

$$\begin{array}{l} \{z\} = [\beta] \{q\} \\ N \times 1 \quad N \times P \quad P \times 1 \end{array} \quad (6-15)$$

where $[\beta]$ is a matrix formed from the columns of $[X]$ which correspond to eigenvalues λ_i having the value zero,* $\{z\}$ is a column matrix containing all the substructure coordinates (see Eq. 6-11), and $\{q\}$ is a column matrix of arbitrary elements. With respect to the structural coupling problem of concern herein Eq. 6-15 may be interpreted as defining a suitable transformation matrix $[\beta]$ to effect a transformation from dependent substructure coordinates to independent system coordinates.

In summary, the problem of determining a suitable transformation matrix $[\beta]$ is seen to reduce to that of determining a set of linearly independent eigenvectors of $[E]$ corresponding to eigenvalues of $[E]$ which are zero. The matrix $[\beta]$ is usually not amenable to direct

* Since $[E]$ is a symmetric matrix the eigenvectors corresponding to a multiple eigenvalue are linearly independent, though not necessarily orthogonal.

physical interpretation and the independent coordinates $\{q\}$ are generalized coordinates in the strict sense of the word. In contrast, the independent coordinates obtained by proceeding in the usual manner indicated above are a subset of the original (physical) dependent coordinates.

The manner of introducing the transformation and arriving at the system equations of motion will be outlined below for both the direct and component mode synthesis methods.

(b) Direct Method

The Lagrangian for the partitioned structure is

$$L = \frac{1}{2} \{\dot{z}\}^T [\bar{M}] \{\dot{z}\} - \frac{1}{2} \{z\}^T [\bar{K}] \{z\} \quad (6-16)$$

The constraint equations enforcing inter-substructure deflection compatibility have the matrix form

$$[C]\{z\} = \{0\} \quad (6-17)$$

Proceeding in the manner indicated above a transformation to independent coordinates is effected by substituting

$$\{z\} = [\beta]\{q\} \quad (6-18)$$

into Eq. 6-16. This leads to

$$L = \frac{1}{2} \{\dot{q}\}^T [\beta]^T [\bar{M}] [\beta] \{\dot{q}\} - \frac{1}{2} \{q\}^T [\beta]^T [\bar{K}] [\beta] \{q\} \quad (6-19)$$

Defining

$$[M] \equiv [\beta]^T [\bar{M}] [\beta] \quad (6-20)$$

$$[K] \equiv [\beta]^T [\bar{K}] [\beta]$$

the Lagrangian for the assembled structure is

$$L = \frac{1}{2} \{\dot{q}\}^T [M] \{\dot{q}\} - \frac{1}{2} \{q\}^T [K] \{q\} \quad (6-21)$$

Substituting Eq. 6-21 into Lagrange's equation for a conservative system

$$\frac{d}{dt} \left(\frac{\partial L}{\partial \dot{q}} \right) - \frac{\partial L}{\partial q} = 0 \quad (6-22)$$

there results

$$[M] \{\ddot{q}\} + [K] \{q\} = \{0\} \quad (6-23)$$

as the free vibration equations of motion for the complete structure. $[M]$ and $[K]$ will be symmetric and, in general, positive semidefinite, that is, the eigenvalues of $[M]$ and $[K]$ are greater than or equal to zero.

(c) Component Mode Synthesis

As pointed out earlier component mode synthesis, employed as

a technique for natural mode vibration analysis of complex structural systems, is based on the concept of synthesizing the modes of the complete structure from the modes of conveniently defined substructures or components into which the structure is divided. The substructure modes are used as degrees of freedom, the discrete coordinates of each component being expressed in terms of its modes and normal (modal) coordinates which represent the contribution of each mode to a particular deformation. The expedient of reducing the degrees of freedom and thus the size of the final system eigenvalue problem is introduced by partial modal synthesis wherein only a relatively few of the modes from each component are employed. Selection of modes is generally based on a frequency cut-off criterion wherein all substructure modes below a given frequency of interest for the system are used in the synthesizing procedure and the others discarded.* The rationale for selection of modes on this basis follows from the fact that the higher calculated component modes (based on the discrete mathematical model) generally bear little resemblance to the corresponding modes of the continuous structure. Synthesis of the selected component modes to obtain the generalized coordinates for the structure is then effected by applying the equations of constraint reflecting the compatibility relations at the junctions of the substructures.

Let the selected modes from each substructure be arranged

* A frequency cut-off criterion is, in effect, employed in the computer program.

by columns in the matrices $[U]^{(i)}$, the superscript denoting the assembly of modes from the i^{th} such substructure. The selected substructure modes $[U]^{(i)}$ herein can consist of calculated natural modes, measured modes, static deflection shapes, assumed deflection shapes, or any combination of these. The restraint conditions employed for the substructure analyses need not correspond to the conditions which exist when all the substructures are assembled, in which case appropriate rigid-body modes (and possibly constraint modes) must be included in the selected set of modes. As indicated earlier these "modes" need not be orthogonal or normalized in any consistent manner. Static deflection shapes, assumed modes and rigid-body modes need no special consideration but are simply treated as elastic modes having zero frequencies. In terms of these selected mode sets the transformation from discrete substructure coordinates z_i to substructure modal coordinates ξ_i can be written as

$$\begin{Bmatrix} \{z\}^{(1)} \\ \{z\}^{(2)} \\ \vdots \\ \{z\}^{(NS)} \end{Bmatrix} = \begin{bmatrix} [U]^{(1)} & & \\ & [U]^{(2)} & \\ & & \ddots \\ & & & [U]^{(NS)} \end{bmatrix} \begin{Bmatrix} \{\xi\}^{(1)} \\ \{\xi\}^{(2)} \\ \vdots \\ \{\xi\}^{(NS)} \end{Bmatrix} \quad (6-24)*$$

* NS = total number of substructures into which structure has been partitioned.

or, in condensed notation,

$$\begin{matrix} \{z\} = & [U] & \{\xi\} \\ N \times 1 & N \times NSM & NSM \times 1 \end{matrix} \quad (6-25)$$

The number of rows in the system modal expansion matrix $[U]$ is equal to the total number of discrete degrees of freedom for all the substructures; the number of columns in $[U]$ is equal to the total number of selected modes (NSM). Substituting Eq. 6-25 into the Lagrangian of the partitioned structure as given by Eq. 6-11 gives

$$L = \frac{1}{2} \{\dot{\xi}\}^T [U]^T [\bar{M}] [U] \{\dot{\xi}\} - \frac{1}{2} \{\xi\}^T [U]^T [\bar{K}] [U] \{\xi\} \quad (6-26)$$

where $[\bar{M}]$ and $[\bar{K}]$ are numerically identical to the corresponding matrices in the direct method. Note that if all the mode sets $[U]^{(i)}$ are made up of free-free orthonormal modes we have

$$[U]^T [\bar{M}] [U] = [I] \quad (6-27a)$$

and

$$[U]^T [\bar{K}] [U] = [\Omega^2] \quad (6-27b)$$

where $[I]$ is the unit matrix and the matrix $[\Omega^2]$ has the squares of the substructure natural frequencies (corresponding to the selected modes) on the main diagonal. The Lagrangian given by Eq. 6-26 will then reduce to a quadratic form having only squared terms. Herein, the modes need not be orthogonal or normalized in any

particular manner so the (generally restrictive) simplifications given in Eqs. 6-27 are not employed.

Since equations of constraint have not yet been applied, the coordinates ξ_i in Eq. 6-26 are not generalized system coordinates in the Lagrangian sense. The equations of constraint reflecting inter-substructure deflection compatibility in physical (discrete) coordinates are identical to those appearing in the direct method, that is,

$$[C]\{z\} = \{0\} \quad (6-28)$$

Substituting the transformation of Eq. 6-25 into Eq. 6-28 the constraint equations in terms of the selected modal coordinates ξ_i have the form

$$[C][U]\{\xi\} = \{0\} \quad (6-29)$$

or

$$[D]\{\xi\} = \{0\} \quad (6-30)$$

where the definition of $[D]$ follows from Eq. 6-29. Proceeding in the spirit of Ref. 6-20 we form the symmetric matrix $[E']$ defined by

$$[E'] \equiv [D]^T [D] \quad (6-31)*$$

* Primes are used to distinguish from similar symbols used in describing the direct method to represent matrix quantities which will be different numerically.

and solve the eigenvalue problem

$$[E']\{x'\} = \lambda'\{x'\} \quad (6-32)$$

From the resulting matrix of eigenvectors $[X']$ select those columns corresponding to eigenvalues having the value zero and form a matrix $[\beta']$. A suitable transformation from substructure modal coordinates to system generalized coordinates (which restores geometric compatibility at the interfaces of the substructures) is then given by

$$\{\xi\} = [\beta']\{q'\} \quad (6-33)$$

Substituting Eq. 6-33 into Eq. 6-26 gives

$$\begin{aligned} L = & \frac{1}{2} \{q'\}^T [\beta']^T [U]^T [\bar{M}] [U] [\beta'] \{q'\} \\ & - \frac{1}{2} \{q'\}^T [\beta']^T [U]^T [\bar{K}] [U] [\beta'] \{q'\} \end{aligned} \quad (6-34)$$

Defining

$$[\beta']^T [U]^T [\bar{M}] [U] [\beta'] = [M'] \quad (6-35)$$

$$[\beta']^T [U]^T [\bar{K}] [U] [\beta'] = [K']$$

Eq. 6-34 becomes

$$L = \frac{1}{2} \{\dot{q}'\}^T [M'] \{\dot{q}'\} - \frac{1}{2} \{q'\}^T [K'] \{q'\} \quad (6-36)$$

where $\{q'\}$ is a column vector of independent coordinates. Substituting Eq. 6-36 into Lagrange's equation (Eq. 6-22) yields

$$[M']\{\ddot{q}'\} + [K']\{q'\} = \{0\} \quad (6-37)$$

as the free vibration equations of motion for the assembled structure. Eq. 6-37 is seen to be of the same form as Eq. 6-23. $[M']$ and $[K']$ will be symmetric and, in general, positive semi-definite.

Some Comments on the Form of the Modal Expansion Matrix: Substructures treated either as rigid bodies or springs have no modal expansion associated with them since their degrees of freedom can not be reduced any further. To maintain the definition of such substructures in discrete coordinates the corresponding modal expansion matrices $[U]^{(i)}$ are taken to be unit matrices:

$$\begin{array}{c} \text{Rigid body} \\ \text{or spring} \\ \{z\} \end{array} = \begin{array}{c} \text{Rigid body} \\ \text{or spring} \\ [I]\{\xi\} \end{array} \quad (6-38)$$

$[I]$ is a unit matrix of order equal to the number of degrees of freedom of the rigid body or spring substructure (up to 6 for a rigid body and 12 for a spring). It is in fact possible to use an "identity expansion" of the form given in Eq. 6-38 for any

substructure. This provides the basis for what might be termed a hybrid method of analysis in which the structure is described in terms of both discrete and modal coordinates. The necessity for such a combined approach would, for example, arise in a case in which structural information pertaining to some component were available only in the form of natural vibration modes.*

The matrices $[U]^{(i)}$ contain the selected modes from each substructure mode set. If no intra-substructure coupling exists each of the expansion matrices $[U]^{(i)}$ will itself be composed of submatrices situated along the principal diagonal in a manner similar to that of Eq. 6-24. In general, some of these submatrices will be coupled. By way of illustration the system modal expansion matrix $[U]$ for the airplane of Fig. 6-6, assuming the only intra-substructure coupling to be between vertical bending and torsion for the wing and horizontal tail, would have the form shown in Fig. 6-14. This figure also indicates the manner in which the "identity expansion" is employed for rigid-body and spring substructures and for rigid-body motions of beams which have no corresponding elastic motion.

As a concluding comment it is to be noted that if full modal coupling is employed the resultant mathematical model based on modal coordinates is completely equivalent to a mathematical model

* In such an instance recourse would have to be made to the orthogonality conditions given in Eqs. 6-27 in order to remain independent of the (unknown) mass and stiffness properties.

based on discrete coordinates in that the resultant calculated modes and frequencies will be identical.

Solution of Equations of Motion

(a) Reduction to Standard Eigenvalue Form

The equations of motion for natural mode vibration analysis by either the direct or component mode synthesis methods can, without any loss of generality, be written in the matrix form

$$[M]\{\ddot{q}\} + [K]\{q\} = \{0\} \quad (6-39)$$

Assuming a solution of the form $q = q_0 e^{i\omega t}$ Eq. 6-39 assumes the form

$$[K]\{q_0\} = \omega^2 [M]\{q_0\} \quad (6-40)$$

by removal of the time factor $e^{i\omega t}$. Before the eigenvalue problem defined by Eq. 6-40 can be solved it must be reduced to the standard eigenvalue form

$$[A]\{x\} = \lambda\{x\} \quad (6-41)$$

If $[M]$ (or $[K]$) is positive definite, Eq. 6-40 can be reduced to this form by simply multiplying through by the inverse of $[M]$ (or $[K]$), in which case λ would be identified with ω^2 (or $1/\omega^2$). The matrix $[A]$ arrived at in this manner would, in general, be

nonsymmetric. Since there are several attendant advantages which may be realized if the problem is formulated in symmetric eigenvalue form (cf. Refs. 6-30 and 6-31) an alternative approach would be to reduce Eq. 6-40 to the form of Eq. 6-41 in a manner which leads to a symmetric matrix $[A]$. It will be seen that if both $[M]$ and $[K]$ are positive semidefinite the process of reducing Eq. 6-40 to standard eigenvalue form leads naturally to a symmetric formulation. Algorithms for solving either the symmetric or nonsymmetric eigenvalue problem are well documented in the literature (see, for instance, Refs. 6-30 to 6-32). The particular procedure employed herein is based on the algorithm embodied in a NASA-Langley computer program designated BJD5* which reduces Eq. 6-40 to a symmetric eigenvalue form and employs the Jacobi method[†] for finding eigenvalues and eigenvectors.

The reduction of Eq. 6-40 to a symmetric eigenvalue form consists, in essence, in converting either the mass or stiffness matrices to diagonal form by a transformation of variables using the eigenvectors of the mass or stiffness matrices as the transformation matrix. Since $[K]$ will be singular in any free-free vibration analysis due to the presence of unrestrained rigid-body degrees of freedom it has generally been assumed that $[M]$ is positive definite. In this instance the procedure for

* Barbara J. Durling #5.

† The Jacobi method is a stand-alone procedure for symmetric matrices which leads to all eigenvalues and eigenvectors simultaneously.

reducing Eq. 6-40 to symmetric eigenvalue form is well known.* In general, however, $[M]$ will also be singular and the usual procedure is not directly applicable. The transformation of Eq. 6-40 to symmetric eigenvalue form in the more general case in which the mass matrix $[M]$ is positive semidefinite has been given by Walton and Durling (1966)[†] in what represents a significant extension of the usual procedure. Their method combines the usual procedure for diagonalizing $[M]$ with a reduction scheme to reduce $[M]$ to a smaller, positive definite diagonal matrix. The analytical basis of their procedure is reviewed below for completeness.

The real symmetric matrix $[M]$ can be reduced to a diagonal matrix $[\lambda]$ through the orthogonality transformation

$$[Q]^T[M][Q] = [\lambda] \quad (6-42)$$

where $[Q]$ is a square matrix the columns of which are the eigenvectors of $[M]$ and the diagonal elements of $[\lambda]$ are the eigenvalues of $[M]$. Thus, substituting the coordinate transformation

* Crandall, S. H.: Engineering Analysis, McGraw-Hill Book Co., New York, 1956, pp. 121-122. The triangular decomposition scheme of Cholesky (Ref. 6-30) leads to an alternate procedure for effecting a transformation to symmetric eigenvalue form.

[†] Unpublished work of William C. Walton, Jr. and Barbara J. Durling of the Structural Mechanics Branch of NASA-Langley. Their procedure is embodied in computer program BJD5 written by Barbara Durling. This program forms part of the computer program "packages" for natural mode vibration analysis as listed in Appendix H.

$$\{q_o\} = [Q]\{\eta\} \quad (6-43)$$

into Eq. 6-40 and premultiplying by $[Q]^T$ leads to

$$[Q]^T[K][Q]\{\eta\} = \omega^2 [Q]^T[M][Q]\{\eta\} \quad (6-44)$$

or,

$$[S]\{\eta\} = \omega^2 [-\mu_-]\{\eta\} \quad (6-45)$$

where the definition of $[S]$ follows from Eq. 6-44. If $[M]$ is positive semidefinite some of the eigenvalues μ_i will be zero. Assume that all of the eigenvalues which are zero are arranged so that they constitute the lower diagonal elements of the matrix $[-\mu_-]$.* Eq. 6-45 can then be written in the partitioned form

$$\begin{bmatrix} [S_{11}] & [S_{12}] \\ [S_{21}] & [S_{22}] \end{bmatrix} \begin{Bmatrix} \{\eta_1\} \\ \{\eta_2\} \end{Bmatrix} = \omega^2 \begin{bmatrix} [-\mu_{1-}] & [0] \\ [0] & [0] \end{bmatrix} \begin{Bmatrix} \{\eta_1\} \\ \{\eta_2\} \end{Bmatrix} \quad (6-46)$$

Since $[S]$ is symmetric (an orthogonality transformation preserves symmetry), both $[S_{11}]$ and $[S_{22}]$ are symmetric and $[S_{21}]$ is the transpose

* Either through an appropriate re-arrangement of rows and columns or "automatically" by employing an eigenvalue routine which arranges the eigenvalues in descending order according to magnitude (such as the Jacobi method).

of $[S_{12}]$. The "inertialess" coordinates $\{\eta_2\}$ can now be mathematically removed from the eigenvalue problem in the manner suggested by Turner, et. al. (Ref. 6-22) for free nodes (ie., nodes which have neither applied loads nor specified deflections) in static analyses.* Expanding Eq. 6-46,

$$[S_{11}]\{\eta_1\} + [S_{12}]\{\eta_2\} = \omega^2 [\mu_1]\{\eta_1\} \quad (6-47a)$$

$$[S_{21}]\{\eta_1\} + [S_{22}]\{\eta_2\} = \{0\} \quad (6-47b)$$

Solving Eq. 6-47b for $\{\eta_2\}$ implies the coordinate transformation

$$\{\eta\} = \begin{bmatrix} [I] \\ - [S_{22}]^{-1} [S_{21}] \end{bmatrix} \{\eta_1\} \quad (6-48)$$

Substituting Eq. 6-48 into Eq. 6-46 gives

$$\left[[S_{11}] - [S_{12}][S_{22}]^{-1}[S_{21}] \right] \{\eta_1\} = \omega^2 [\mu_1]\{\eta_1\} \quad (6-49)$$

or, more simply,

$$[\tilde{S}]\{\eta_1\} = \omega^2 [\mu_1]\{\eta_1\} \quad (6-50)$$

* The removal of inertialess coordinates from Eq. 6-46 may also be interpreted as a special case of the Guyan reduction (Ref. 6-33).

where $[\tilde{S}]$ is the "reduced" stiffness matrix. Note that $[\tilde{S}]$ is symmetric. Since all submatrices of the original generalized stiffness matrix appear in $[\tilde{S}]$ there is no loss of structural information in the condensation procedure. Final reduction to symmetric eigenvalue form is accomplished by applying an orthogonality transformation to $[\mu_1]$ using the coordinate transformation

$$\{\eta_1\} = \begin{bmatrix} \frac{1}{\sqrt{\mu_1}} \end{bmatrix} \{\hat{\eta}_1\} \quad (6-51)$$

Substituting Eq. 6-51 into Eq. 6-50 and premultiplying by

$\begin{bmatrix} \frac{1}{\sqrt{\mu_1}} \end{bmatrix}$ gives

$$\begin{bmatrix} \frac{1}{\sqrt{\mu_1}} \end{bmatrix} [\tilde{S}] \begin{bmatrix} \frac{1}{\sqrt{\mu_1}} \end{bmatrix} \{\hat{\eta}_1\} = \omega^2 [I] \{\hat{\eta}_1\} \quad (6-52)$$

or, finally

$$[\hat{S}] \{\hat{\eta}_1\} = \omega^2 \{\hat{\eta}_1\} \quad (6-53)$$

(b) Interpretation of Eigensolutions

Solution of the eigenvalue problem given in Eq. 6-53 leads to a set of eigenvalues ω_i^2 and associated eigenvectors $\{\hat{\eta}_1\}_i$. Since an orthogonal transformation preserves eigenvalues the ω_i^2 are squares of the desired system natural frequencies. The eigenvectors $\{\hat{\eta}_1\}_i$

are generalized mode shapes and must be transformed back to the original coordinates $\{z\}_i$ for physical interpretation. For the direct method this back-transformation is given by

$$\{z\}_i = [\beta][Q] \begin{bmatrix} [I] \\ - [S_{22}]^{-1} [S_{21}] \end{bmatrix} \begin{bmatrix} \frac{1}{\sqrt{\mu_1}} \end{bmatrix} \{\hat{\eta}_1\}_i \quad (6-54)$$

while for component mode synthesis it is

$$\{z\}_i = [U][\beta'][Q'] \begin{bmatrix} [I] \\ - [S'_{22}]^{-1} [S'_{21}] \end{bmatrix} \begin{bmatrix} \frac{1}{\sqrt{\mu'_1}} \end{bmatrix} \{\hat{\eta}'_1\}_i \quad (6-55)*$$

Since no transformation to a global system of coordinates has been employed the mode shapes $\{z\}_i$ are defined in local substructure coordinates. If desired, a transformation to a global set of coordinates could be subsequently carried out.

The substructuring concept, as employed in either the direct or component mode synthesis methods, is applied to a tilt-rotor aircraft configuration in Appendix E to serve as an illustrative example of the manner of forming the substructure mass and stiffness matrices and setting down equations of constraint.

* The primes have been reintroduced for the purpose of distinguishing between common symbols which represent matrix quantities which are different numerically.

Reducing the Order of the Constraint Eigenvalue Problem in the
Direct Method

Three eigenvalue problems require solution under vibration analysis by the direct method as outlined above. By far the largest of these is that associated with the matrix product $[C]^T[C]$, $[C]$ being the matrix of coefficients of the constraint equations. Oftentimes there are many coordinates (degrees of freedom) which do not appear in the constraint equations, leading to a matrix $[C]$ having many columns which are identically zero. Each such null column in $[C]$ will lead to a similarly positioned null column in the product $[C]^T[C]$ and a corresponding null row. Through an appropriate re-arrangement of rows and columns a significant reduction in the size of the eigenvalue problem which must actually be solved in such instances can be achieved.* The analytical basis on which such a reduction can proceed is given below.

As before, from the constraint equations

$$[C]\{z\} = \{0\} \quad (6-56)$$

form the matrix $[E]$ defined by

$$[E] \equiv [C]^T[C] \quad (6-57)$$

* This possibility was pointed out to the author by William C. Walton, Jr. of the Structural Mechanics Branch at NASA-Langley.

and the associated eigenvalue problem

$$[E]\{x\} = \lambda\{x\} \quad (6-58)$$

Let $[S]$ be a matrix which when premultiplied by $[C]$ will re-arrange the columns of $[C]$ so that all null columns are at the right.*

Introducing the transformation

$$\{x\} = [S]\{y\} \quad (6-59)$$

into Eq. 6-58 and premultiplying by $[S]^{-1}$ gives

$$[S]^{-1}[E][S]\{y\} = \lambda[S]^{-1}[S]\{y\} \quad (6-60)$$

Defining

$$[B] \equiv [S]^{-1}[E][S] \quad (6-61)^\dagger$$

Eq. 6-60 can be written as

$$[B]\{y\} = \lambda\{y\} \quad (6-62)$$

*The construction of a matrix $[S]$ having these properties and which is additionally orthogonal is given by Wilkinson (Ref. 6-30). Sciarra (Ref. 6-2) also describes formation of this matrix.

†Eq. 6-61 defines a similarity transformation.

By virtue of the re-arranging properties of [S], the transformation given by Eq. 6-61 permits Eq. 6-62 to be written in the partitioned form

$$\left[\begin{array}{c|c} [B_{11}] & [0] \\ \hline [0] & [0] \end{array} \right] \begin{Bmatrix} \{y_1\} \\ \{y_2\} \end{Bmatrix} = \lambda \begin{Bmatrix} \{y_1\} \\ \{y_2\} \end{Bmatrix} \quad (6-63)$$

where $[B_{11}]$ is a square matrix of order equal to the number of finite (non-zero) columns in [C]. Expanding, Eq. 6-63 reduces to the two uncoupled eigenvalue problems

$$[B_{11}]\{y_1\} = \lambda\{y_1\} \quad (6-64a)$$

$$[0] = \lambda\{y_2\} \quad (6-64b)$$

Since the eigenvalues and eigenvectors of a null matrix (Eq. 6-64b) are known a priori only the eigenvalue problem given by Eq. 6-64a has to actually be solved. Let all the eigenvectors of $[B_{11}]$ and $[0]$ be assembled by columns into the matrices $[Y_1]$ and $[Y_2]$ respectively. The matrix of eigenvectors associated with Eq. 6-63 can then be written in the partitioned form

$$[Y] = \left[\begin{array}{c|c} [Y_1] & [0] \\ \hline [0] & [Y_2] \end{array} \right] \quad (6-65)$$

The matrix of eigenvectors corresponding to the original problem as specified by Eq. 6-58 then follows from

$$[X] = [S][Y] \quad (6-66)$$

The transformation matrix $[\beta]$ is then formed from columns of $[X]$ corresponding to zero eigenvalues* and used in the manner described earlier to enforce inter-substructure displacement compatibility.

A Note on the Inclusion of Gyroscopic Coupling Effects in Natural Mode Vibration Analyses

The gyroscopic coupling forces associated with large rotating components such as propellers or proprotors on propeller- or proprotor-driven aircraft or high-speed fans of turbofan jet powered aircraft may have a non-negligible effect on the vibratory characteristics of an airframe relative to the case in which the spin is zero. One of the earliest attempts to analyze such effects was given by Scanlan and Truman (Ref. 6-34) who considered a 3 degree-of-freedom mathematical model of an elastically supported propeller/engine combination. In a related experimental investigation under the direction of Scanlan, Brower and Lassen (Ref. 6-35) demonstrated that gyroscopic effects due to rotating propellers may manifest themselves by a change in the natural frequency, a change in the mode shape, or the appearance of new modes. The most

* The columns of $[X]$ corresponding to zero eigenvalues will all be grouped at the right in $[X]$ if the Jacobi method is used to solve Eq. 6-64a.

recent treatment of this problem appears to be the work of Griffin (Ref. 6-36).

For dynamic analyses the primary gyroscopic effects of rotating components can be accounted for by treating each such component as a rigid rotating disc. Based on this idealization the concept of a "gyroscopic finite element" is introduced herein and the analyses for natural mode vibration analysis by direct and component mode synthesis techniques analytically extended* to include the effects of gyroscopic coupling forces. The approach taken is that of modifying the Lagrangian potential for the partitioned structure to account for the gyroscopic effects of any rotating components. The concept of a gyroscopic finite element and the proposed approach are believed to be new and have the convenience of being readily incorporated into either direct or modal formulations for dynamic analyses within the Lagrangian scheme for establishing equations of motion. For notational convenience in the analytical development, general matrix expressions are used to illustrate the analytical approach without specifying the exact details.

(a) Inclusion of Gyroscopic Effects in the Direct Method

Let $[\bar{M}]_{NG}$, $[\bar{K}]_{NG}$, and $\{\delta\}$ be the mass, stiffness, and deflection matrices, respectively, of the partitioned structure minus any gyroscopic components. The analogous matrices for the gyroscopic components, from Appendix G, are denoted by $[\bar{M}]_G$, $[\text{Null}]$, and $\{\gamma\}$.

Defining

* These extensions have not yet been programmed, however.

$$\{\tau\} \equiv \left\{ \begin{array}{c} \{\delta\} \\ \hline \{\gamma\} \end{array} \right\} \quad (6-67)$$

the kinetic energy of the total system, including gyroscopic components, can be written as

$$T = \frac{1}{2} \left\{ \begin{array}{c} \dot{\tau} \\ \dot{\psi} \end{array} \right\}^T \left[\begin{array}{cc|cc} \left[\begin{array}{cc} \bar{M} & \\ & \end{array} \right]_{NG} & \begin{bmatrix} [0] \\ [0] \end{bmatrix} & \begin{bmatrix} [0] \\ [0] \end{bmatrix} & \\ \begin{bmatrix} [0] \\ [0] \end{bmatrix} & \begin{bmatrix} [\bar{M}]_G & [\bar{E}] \\ [\bar{E}]^T & [0] \end{bmatrix} & \begin{bmatrix} [\bar{E}] \\ [0] \end{bmatrix} & \end{array} \right] \left\{ \begin{array}{c} \dot{\tau} \\ \dot{\psi} \end{array} \right\} \quad (6-68)$$

or, in abridged notation

$$T = \frac{1}{2} \left\{ \begin{array}{c} \dot{\tau} \\ \dot{\psi} \end{array} \right\}^T \left[\begin{array}{c|c} [\bar{M}] & [\tilde{E}] \\ \hline [\tilde{E}]^T & [0] \end{array} \right] \left\{ \begin{array}{c} \dot{\tau} \\ \dot{\psi} \end{array} \right\} \quad (6-69)$$

where the definition of $[\bar{M}]$ and $[\tilde{E}]$ follow directly from Eq. 6-68.

Expanding Eq. 6-69 we obtain

$$\begin{aligned}
 T &= \frac{1}{2} \{\dot{t}\}^T [\bar{M}] \{\dot{t}\} + \frac{1}{2} \{\dot{t}\}^T [\tilde{E}] \{\psi\} \\
 &\quad + \frac{1}{2} \{\psi\}^T [\tilde{E}]^T \{\dot{t}\}
 \end{aligned}
 \tag{6-70}$$

Since energy is a scalar each term in Eq. 6-70 is a scalar. Hence

$$\{\dot{t}\}^T [\tilde{E}] \{\psi\} \equiv \{\psi\}^T [\tilde{E}]^T \{\dot{t}\}
 \tag{6-71}$$

and Eq. 6-70 can also be written as

$$T = \frac{1}{2} \{\dot{t}\}^T [\bar{M}] \{\dot{t}\} + \{\psi\}^T [\tilde{E}]^T \{\dot{t}\}
 \tag{6-72}$$

The strain energy for the partitioned structure can be written as

$$V = \frac{1}{2} \{\tau\}^T \begin{bmatrix} [\bar{K}]_{NG} & [0] \\ \hline [0] & [0] \end{bmatrix} \{\tau\}
 \tag{6-73}$$

or, more simply,

$$V = \frac{1}{2} \{\tau\}^T [\bar{K}] \{\tau\}
 \tag{6-74}$$

The Lagrangian for the partitioned system is then

$$\begin{aligned}
L &= T - V \\
&= \frac{1}{2} \{\dot{t}\}^T [\tilde{M}] \{\dot{t}\} + \{\psi\}^T [\tilde{E}]^T \{\dot{t}\} \\
&\quad - \frac{1}{2} \{\tau\}^T [\tilde{K}] \{\tau\}
\end{aligned} \tag{6-75}$$

Constraint equations enforcing inter-substructure displacement compatibility have the form

$$[C]\{\tau\} = \{0\} \tag{6-76}^*$$

from which the required transformation to independent coordinates is

$$\{\tau\} = [\beta]\{q\} \tag{6-77}$$

Let the rows in $[\beta]$ which correspond to $\{\psi\}$ in $\{\tau\}$ be designated $[R]$. Then

$$\{\psi\} = [R]\{q\} \tag{6-78}$$

Substituting Eqs. 6-77 and 6-78 into Eq. 6-75 yields

* Both the real and imaginary parts of the complex deflection vector $\{\tau\}$ will satisfy Eq. 6-76; that is, we have $[C]\{\tau_R + i \tau_I\} = \{0\}$.

$$\begin{aligned}
L = & \frac{1}{2} \{\dot{q}\}^T [\beta]^T [\tilde{M}] [\beta] \{\dot{q}\} \\
& + \{q\}^T [R]^T [\tilde{E}]^T [\beta] \{\dot{q}\} \\
& - \frac{1}{2} \{q\}^T [\beta]^T [\tilde{K}] [\beta] \{q\}
\end{aligned} \tag{6-79}$$

or, in more abbreviated form

$$\begin{aligned}
L = & \frac{1}{2} \{\dot{q}\}^T [M] \{\dot{q}\} + \{q\}^T [G] \{\dot{q}\} \\
& - \frac{1}{2} \{q\}^T [K] \{q\}
\end{aligned} \tag{6-80}$$

where the definition of [M], [G], and [K] follow from Eq. 6-79. In Eq. 6-80 [M] and [K] are symmetric while [G] is non-symmetric. Substituting Eq. 6-80 into Lagrange's equation (Eq. 6-22) leads to

$$[M] \{\ddot{q}\} + \left[[G]^T - [G] \right] \{\dot{q}\} + [K] \{q\} = \{0\} \tag{6-81}$$

Defining

$$[\Gamma] \equiv [G]^T - [G] \tag{6-82}$$

The equations of motion assume the final form

$$[M] \{\ddot{q}\} + [\Gamma] \{\dot{q}\} + [K] \{q\} = \{0\} \tag{6-83}$$

where $[\Gamma]$ is skew-symmetric. Although gyroscopic coupling introduces \dot{q} terms in the equations of motion they do not act like damping since there is no energy loss associated with them. This will be shown later.

(b) Inclusion of Gyroscopic Effects in Component Mode Synthesis

In the spirit of the component mode synthesis scheme as developed earlier in this chapter, the transformation from discrete coordinates to modal coordinates is given by

$$\{\tau\} = [U]\{p\} \quad (6-84)$$

where $[U]$ is composed of selected modes from each substructure arranged in the block diagonal form previously indicated in Eq. 6-24. No modal expansion is employed for gyroscopic substructures since they are taken as rigid and the blocks in $[U]$ corresponding to these components are simply unit matrices of order 6. Let the rows in $[U]$ corresponding to $\{\psi\}$ in $\{\tau\}$ be designated $[R']$. Then

$$\{\psi\} = [R']\{p\} \quad (6-85)^*$$

Substituting Eqs. 6-84 and 6-85 into the Lagrangian as given in Eq. 6-75

* Primes are again employed to distinguish between common symbols which represent matrix quantities which are different numerically.

$$\begin{aligned}
L = & \frac{1}{2} \{\dot{p}\}^T [U]^T [\bar{M}] [U] \{\dot{p}\} + \{p\}^T [R']^T [\tilde{E}]^T [U] \{\dot{p}\} \\
& - \frac{1}{2} \{p\}^T [U]^T [\bar{K}] [U] \{p\}
\end{aligned} \tag{6-86}$$

In terms of the substructure modal coordinates the constraint equations (Eq. 6-28) are

$$[C][U]\{p\} = \{0\} \tag{6-87}$$

from which

$$\{p\} = [\beta']\{q'\} \tag{6-88}$$

Substituting Eq. 6-88 into Eq. 6-86 there results

$$\begin{aligned}
L = & \frac{1}{2} \{\dot{q}'\}^T [\beta']^T [U]^T [\bar{M}] [U] [\beta'] \{\dot{q}'\} + \{q'\}^T [\beta']^T [R']^T [\tilde{E}]^T [U] [\beta'] \{\dot{q}'\} \\
& - \frac{1}{2} \{q'\}^T [\beta']^T [U]^T [\bar{K}] [U] [\beta'] \{q'\}
\end{aligned} \tag{6-89}$$

or, in abridged notation

$$L = \frac{1}{2} \{\dot{q}'\}^T [M'] \{\dot{q}'\} + \{q'\}^T [G'] \{\dot{q}'\} - \frac{1}{2} \{q'\}^T [K'] \{q'\} \tag{6-90}$$

Substituting Eq. 6-90 into Lagrange's equation and using Eq. 6-82 the equations of motion are

$$[M']\{\ddot{q}'\} + [\Gamma']\{\dot{q}'\} + [K']\{q'\} = \{0\} \quad (6-91)$$

(c) Inclusion of Gyroscopic Effects Via a Normal Mode Approach

Gyroscopic effects can also be included by proceeding along the lines of the familiar normal mode approach to solution of dynamic response problems. First solve the eigenvalue problem given by Eq. 6-83 assuming that $[\Gamma] = 0$. This leads to a set of modes and frequencies for the complete structure. Assume that the coupled modes of the system with gyroscopic effects included can be given as a linear combination of some of the modes of the complete system for the case of no gyroscopic effects, that is, take

$$\{\tau\} = [\Phi]\{p'\} \quad (6-92)$$

The procedure from this point on is identical to that in section (b) directly above, with $[\Phi]$ replacing $[U]$, and leads to

$$[M'']\{\ddot{q}''\} + [\Gamma'']\{\dot{q}''\} + [K'']\{q''\} = \{0\} \quad (6-93)$$

Again, the primes have been employed to distinguish between common symbols which represent matrix quantities which are different numerically.

(d) Solution of Equations of Motion

The equations of motion for a gyroscopically coupled elastic system as given in Eqs. 6-83, 6-91, or 6-93 may be written, without loss of generality, as

$$[M]\{\ddot{q}\} + [\Gamma]\{\dot{q}\} + [K]\{q\} = \{0\} \quad (6-94)$$

where the primes have been dropped for convenience. The generalized mass and stiffness matrices $[M]$ and $[K]$ are both symmetric; the matrix of gyroscopic terms, $[\Gamma]$, is skew-symmetric. The equations governing the stability of a proprotor/pylon system, as developed in Chapter 3, had a matrix form similar to that of Eq. 6-94. It will be recalled that the reduction of those equations to standard eigenvalue form was complicated by the fact that the damping matrix was not proportional to either the mass or stiffness matrix (or a linear combination of them). Now the skew-symmetry of $[\Gamma]$ leads to a similar situation; that is, $[\Gamma]$ is not proportional to either $[M]$ or $[K]$ (or a linear combination of them). Non-proportionality of the matrix of coefficients of the rate terms is sufficient to ensure that the eigenvectors will be complex, indicating that both amplitude and phase distinguish the components in each vector. Thus if Eq. 6-94 represents N equations, $2N$ equations are required to determine all components of a mode. It is not unexpected, then, that considerations similar to those employed in Chapter 3 for reducing the proprotor equations of motion to standard eigenvalue form must be resorted to for Eq. 6-94. Again, certain aspects of methods which have been developed for uncoupling the forced equations of motion for systems containing non-proportional damping* are relevant to the problem at hand. The particular

* These methods are reviewed in Chapter 3 and more fully described in the references cited therein.

aspect of those procedures which is of direct interest here is the means for effecting a transformation to $2N$ -space, that is, replacing the N equations of second order (6-94) by $2N$ first order equations.

If $[M]$ is positive definite (that is, if $[M]^{-1}$ exists) the appropriate procedure for reducing Eq. 6-94 to standard eigenvalue form is identical to that described in Chapter 3 for reducing Eq. 3-142 to standard eigenvalue form. Since this case is adequately discussed in Chapter 3 it will not be repeated here. The reader may, however, find a review of this case helpful at this time. If $[M]$ in Eq. 6-94 is positive semidefinite its inverse will not exist and the method outlined in Chapter 3 will not work. A procedure which appears suitable in this case is proposed below.

First reduce the matrix $[M]$ to a diagonal matrix by an orthogonality transformation

$$[Q]^T [M] [Q] = [\mu] \quad (6-95)$$

where $[Q]$ is a modal matrix of $[M]$ and $[\mu]$ is a diagonal matrix of eigenvalues of $[M]$. Thus, substituting

$$\{q\} = [Q]\{\eta\} \quad (6-96)$$

into Eq. 6-94 and premultiplying by $[Q]^T$ gives

$$[Q]^T [M] [Q] \{\ddot{\eta}\} + [Q]^T [\Gamma] [Q] \{\dot{\eta}\} + [Q]^T [K] [Q] \{\eta\} = \{0\} \quad (6-97)$$

or, more simply,

$$[-\mu_-]\{\ddot{\eta}\} + [\tilde{\Gamma}]\{\dot{\eta}\} + [\tilde{K}]\{\eta\} = \{0\} \quad (6-98)$$

As before assume that all of the eigenvalues μ_i which are zero are arranged so that they constitute the lower diagonal elements of $[-\mu_-]$. Eq. 6-98 can then be written in the partitioned form

$$\begin{bmatrix} [-\mu_{1-}] & [0] \\ \hline [0] & [0] \end{bmatrix} \begin{Bmatrix} \{\ddot{\eta}_1\} \\ \{\ddot{\eta}_2\} \end{Bmatrix} + \begin{bmatrix} [\tilde{\Gamma}_{11}] & [\tilde{\Gamma}_{12}] \\ \hline [\tilde{\Gamma}_{21}] & [\tilde{\Gamma}_{22}] \end{bmatrix} \begin{Bmatrix} \{\dot{\eta}_1\} \\ \{\dot{\eta}_2\} \end{Bmatrix} + \begin{bmatrix} [\tilde{K}_{11}] & [\tilde{K}_{12}] \\ \hline [\tilde{K}_{21}] & [\tilde{K}_{22}] \end{bmatrix} \begin{Bmatrix} \{\eta_1\} \\ \{\eta_2\} \end{Bmatrix} = \{0\} \quad (6-99)$$

Expanding Eq. 6-99 assuming $[\tilde{\Gamma}] = 0$

$$[-\mu_{1-}]\{\ddot{\eta}_1\} + [\tilde{K}_{11}]\{\eta_1\} + [\tilde{K}_{12}]\{\eta_2\} = \{0\} \quad (6-100a)$$

$$[\tilde{K}_{21}]\{\eta_1\} + [\tilde{K}_{22}]\{\eta_2\} = \{0\} \quad (6-100b)$$

and solving Eq. 6-100b for $\{\eta_2\}$, the matrix of coordinates at which no inertia forces act, implies the coordinate transformation

$$\begin{Bmatrix} \{\eta_1\} \\ \{\eta_2\} \end{Bmatrix} = \begin{bmatrix} [I] \\ \hline -[\tilde{K}_{22}]^{-1} [\tilde{K}_{21}] \end{bmatrix} \{\eta_1\} \equiv [T]\{\eta_1\} \quad (6-101)$$

Guyan (Ref. 6-33) has suggested use of the transformation given in

Eq. 6-101 to simultaneously reduce mass and stiffness matrices in natural mode analyses. Here, however, the mass matrix is already in a reduced form (cf. Eq. 6-99) and we may, in the spirit of Ref. 6-33, employ Eq. 6-101 to alternatively effect a simultaneous reduction of the generalized gyroscopic and stiffness matrices. Thus, substituting Eq. 6-101 into Eq. 6-99 and premultiplying by $[T]^T$ there results

$$[-\mu_1]\{\ddot{\eta}_1\} + [\hat{\Gamma}]\{\dot{\eta}_1\} + [\hat{K}]\{\eta_1\} = \{0\} \quad (6-102)$$

where the reduced gyroscopic and stiffness matrices are given by

$$[\hat{\Gamma}] = \left[\begin{array}{l} [\tilde{\Gamma}_{11}] - [\tilde{\Gamma}_{12}][\tilde{K}_{22}]^{-1}[\tilde{K}_{21}] - \left[[\tilde{K}_{22}]^{-1}[\tilde{K}_{21}] \right]^T [\tilde{\Gamma}_{21}] \\ - [\tilde{\Gamma}_{22}][\tilde{K}_{22}]^{-1}[\tilde{K}_{21}] \end{array} \right] \quad (6-103a)$$

and

$$[\hat{K}] = \left[[\tilde{K}_{11}] - [\tilde{K}_{12}][\tilde{K}_{22}]^{-1}[\tilde{K}_{21}] \right] \quad (6-103b)$$

Since all submatrices of the original stiffness matrix $[\tilde{K}]$ contribute to $[\hat{K}]$ the accuracy of $[\hat{K}]$ is equivalent to the accuracy of the stiffness matrix before reduction. Although the reduced gyroscopic matrix contains all submatrices of the original matrix, these appear in combination with submatrices from the original stiffness matrix so that, as in the case for simultaneous

reduction of mass and stiffness matrices (Ref. 6-33), the eigenvalue problem is not exactly preserved. Eq. 6-102 is now in a form from which the transformation to $2N$ -space can be effected in the usual manner (cf. Chapter 3). Multiplying Eq. 6-102 through by the inverse of $[\mu_1]$

$$[I]\{\ddot{\eta}_1\} + [\mu_1]^{-1}[\hat{F}]\{\dot{\eta}_1\} + [\mu_1]^{-1}[\hat{K}]\{\eta_1\} = \{0\} \quad (6-104)$$

and introducing the identity

$$\{\dot{\eta}_1\} - \{\dot{\eta}_1\} = \{0\} \quad (6-105)$$

Eqs. 6-104 and 6-105 can be written in the combined form

$$\begin{Bmatrix} \{\dot{\eta}_1\} \\ \{0\} \\ \{\ddot{\eta}_1\} \end{Bmatrix} = \begin{bmatrix} [0] & [I] \\ \hline -[\mu_1]^{-1}[\hat{K}] & -[\mu_1]^{-1}[\hat{F}] \end{bmatrix} \begin{Bmatrix} \{\eta_1\} \\ \{0\} \\ \{\dot{\eta}_1\} \end{Bmatrix} \quad (6-106)$$

Defining

$$\{W\} = \begin{Bmatrix} \{\eta_1\} \\ \{\dot{\eta}_1\} \end{Bmatrix} \quad (6-107)$$

Eq. 6-106 can be written in the compact form

$$\{\dot{W}\} = [H]\{W\} \quad (6-108)$$

where the definition of $[H]$ follows directly from Eq. 6-106. $[H]$ is non-symmetric and will, in general, be singular. Assuming a solution of the form

$$\{W\} = \{W_0\} e^{\lambda t} \quad (6-109)$$

Eq. 6-108 reduces to the standard eigenvalue form

$$[H]\{W_0\} = \lambda\{W_0\} \quad (6-110)$$

Eq. 6-110 defines the complex eigenvalue problem for determining the natural modes and frequencies of a gyroscopically coupled elastic system.

A procedure for handling the case of a singular mass matrix based on transforming to $3N$ -space and so on to nN -space (n an integer) until the leading matrix is positive definite is given in Ref. 6-37. What seems to be basically a similar procedure is given in Ref. 6-38. Neither of these methods, however, appears to be suited to routine machine computation, thereby lacking the computational convenience of the Guyan-type reduction proposed above.

(e) Interpretation of Eigensolutions

Solution of Eq. 6-110 leads to $2N$ complex eigenvalues λ_p and eigenvectors $\{W_0\}^{(p)}$. Since $[H]$ is real these occur in N complex conjugate pairs. Discarding the negative frequency roots and their associated eigenvectors the p^{th} eigenvalue has the form

$$\lambda_p = \alpha_p + i\omega_p \quad (6-111)$$

Now the set of equations adjoint to Eq. 6-94 are given by

$$[M]^T \{\ddot{y}\} - [\Gamma]^T \{\dot{y}\} + [K]^T \{y\} = \{0\} \quad (6-112)$$

[M] and [K] are symmetric; since [\Gamma] is skew-symmetric, $[\Gamma]^T = -[\Gamma]$. Thus Eq. 6-112 is identical to Eq. 6-94. For a conservative system the adjoint set is identical in form to the original set (Ref. 6-39). Hence the α_p in Eq. 6-111, which are associated with dissipative forces, are zero and the eigenvalues λ_p are pure imaginary.*

The complex vector associated with the eigenvalue λ_p can be written in the form

$$\{W_o^{(p)}\} = \left\{ \begin{array}{c} \{w^{(p)}\} \\ \text{-----} \\ \lambda_p \{w^{(p)}\} \end{array} \right\} \quad (6-113)$$

The upper N elements $\{w^{(p)}\}$ in each vector of 2N elements define the generalized mode shape.[†] Since these elements are complex, phase differences will exist between the harmonic motions at different points of the system in a given mode of motion. The

* Griffin (Ref. 6-36) shows that the skew-symmetry of [\Gamma] is a necessary and sufficient condition for the net work done by the gyroscopic torques to be zero, thus precluding any energy dissipation.

[†] The lower N elements define the generalized velocity.

relative amplitude and phasing existing in a given mode could be ascertained by converting the complex elements of the mode to polar form and then normalizing on one of them.

The generalized displacement vectors $\{w^{(p)}\}_i$ must be transformed back to the original coordinates for physical interpretation. The back-transformation is given by

$$\{\tau\}_i = [\beta][Q] \begin{bmatrix} [I] \\ -[\tilde{K}_{22}]^{-1} [\tilde{K}_{21}] \end{bmatrix} \{w\}_i \quad (6-114)$$

for the direct method,

$$\{\tau\}_i = [U][\beta'][Q'] \begin{bmatrix} [I] \\ -[\tilde{K}'_{22}]^{-1} [\tilde{K}'_{21}] \end{bmatrix} \{w^{\dagger}\}_i \quad (6-115)$$

for component mode synthesis, and

$$\{\tau\}_i = [\Phi][\beta''][Q''] \begin{bmatrix} [I] \\ -[\tilde{K}''_{22}]^{-1} [\tilde{K}''_{21}] \end{bmatrix} \{w''\}_i \quad (6-116)$$

in the normal mode method. The primes have been reintroduced for the purpose of distinguishing between common symbols which represent matrix quantities which are different numerically. The final mode shapes $\{\tau\}_i$ are defined in local substructure coordinates. If

desired a transformation to a global set of coordinates could be subsequently carried out.

A Remark on Solution of the Free Equations of Motion

In the final equations of free vibration given above for the case of zero and non-zero gyroscopic coupling (Eqs. 6-39 and 6-94, respectively) both $[M]$ and $[K]$ were symmetric. This symmetry has been a consequence of working in orthogonal coordinates. The use of non-orthogonal (ie., oblique) coordinates would lead to $[M]$ and $[K]$ which are not symmetric. The procedures described above for reducing the equations of motion to standard eigenvalue form are, however, still valid since $[M]$ can be reduced to diagonal form in this instance by a similarity transformation:

$$[Q]^{-1} [M] [Q] = [\mu] \quad (6-117)$$

The necessary changes in the steps indicated above are arrived at by merely replacing $[Q]^T$ by $[Q]^{-1}$.

CITED REFERENCES

- 6-1. Archer, J. S.: "A Stiffness Matrix Method of Natural Mode Analysis", Proceedings of the National Specialist Meeting on Dynamics and Aeroelasticity, Fort Worth, Texas, November 1958, pp. 88-97.
- 6-2. Sciarra, J. J.: "Dynamic Unified Structural Analysis Method Using Stiffness Matrices", Presented at the AIAA/ASME 7th Structures and Materials Conference, April 1966.
- 6-3. Scanlan, R. H.: "An Analytical Study of the Landing Shock Effect on an Elastic Airplane", Journal of the Aeronautical Sciences, Vol. 15, May 1948, pp. 300-304.
- 6-4. Hunn, B. A.: "A Method of Calculating Space Free Resonance Modes of an Aircraft", Journal of the Royal Aeronautical Society, Vol. 57, June 1953, pp. 420-422.
- 6-5. MacNeal, R. H.: "Vibrations of Composite Systems", AFOSR TN-55-120, October 1954.
- 6-6. Hurty, W. C.: "Vibrations of Structural Systems by Component Mode Synthesis:", Journal of the Engineering Mechanics Division, Proc. ASCE, EM4, August 1960, pp. 51-69.
- 6-7. Hurty, W. C.: "Dynamic Analysis of Structural Systems by Component Mode Synthesis", Report No. 32-530, January 1964, Jet Propulsion Laboratory, Pasadena, California.
- 6-8. Gladwell, G. M. L.: "Branch Mode Analysis of Vibrating Systems," Journal of Sound and Vibration, 1, 1964, pp. 41-59.
- 6-9. Goldman, R. L.: "Vibration Analysis by Dynamic Partitioning", RM-305, May 1966, Martin Co., Baltimore, Maryland.
- 6-10. Bamford, R. M.: "A Modal Combination Program for Dynamic Analysis of Structures", Technical Memorandum No. 33-290, August 1966, Jet Propulsion Laboratory, Pasadena, California.
- 6-11. McAleese, J. D.: "Method for Determining Normal Modes and Frequencies of a Launch Vehicle Utilizing its Component Normal Modes", NASA TN D-4550, May 1968.
- 6-12. Bajan, R. L. and C. C. Feng: "Free Vibration Analysis by the Modal Substitution Method", Presented at the American Astronautical Society Symposium on Space Projections from the Rocky Mountain Region, Denver, Colorado, July 1968.

- 6-13. Bajan, R. L., C. C. Feng, and I. J. Jaszlics: "Vibration Analysis of Complex Structural Systems by Modal Substitution", Shock and Vibration Bulletin No. 39, Part 3, January 1969, pp. 99-105.
- 6-14. Hou, S. N.: "Review of Modal Synthesis Techniques and a New Approach", TM-69-2031-5, September 1969, Bellcomm, Inc., Washington, D. C.
- 6-15. Bajan, R. L.: "The Free Vibration Analysis of Discrete Systems by Modal Substitution", Ph.D. dissertation, University of Colorado, 1969.
- 6-16. Benfield, W. A. and R. F. Hruda: "Vibration Analysis of Structures by Component Mode Synthesis", Presented at the AIAA/ASME 11th Structures, Structural Dynamics and Materials Conference, Denver, Colorado, April 1970.
- 6-17. Hart, G. C., W. C. Hurty, and J. D. Collins: "A Survey of Modal Synthesis Methods", Presented at the SAE National Aeronautic and Space Engineering and Manufacturing Meeting, Los Angeles, Calif., September 1971.
- 6-18. Hurty, W. C., J. D. Collins, and G. C. Hart: "Dynamic Analysis of Large Structures by Modal Synthesis Techniques", Computers and Structures, Vol. 1, 1971, pp. 535-563.
- 6-19. MacNeal, R. H.: "A Hybrid Method of Component Mode Synthesis", Computers and Structures, Vol. 1, 1971, pp. 581-601.
- 6-20. Walton, W. C. Jr. and E. C. Steeves: "A Practical Computational Method for Reducing a Dynamical System with Constraints to an Equivalent System with Independent Coordinates", Presented at the Air Force Second Conference on Matrix Methods in Structural Mechanics, Wright-Patterson Air Force Base, Ohio, October 1968.
- 6-21. Levy, S.: "Structural Analysis and Influence Coefficients for Delta Wings", Journal of the Aeronautical Sciences, Vol. 20, July 1953, pp. 449-454.
- 6-22. Turner, M. J., R. W. Clough, H. C. Martin, and L. J. Topp: "Stiffness and Deflection Analysis of Complex Structures", Journal of the Aeronautical Sciences, Vol. 23, September 1956, pp. 805-823, 854.
- 6-23. Martin, H. C.: Introduction to Matrix Methods of Structural Analysis, McGraw-Hill Book Co., New York, 1966.
- 6-24. Rubinstein, M. F.: Matrix Computer Analysis of Structures, Prentice-Hall, Inc., Englewood Cliffs, N. J., 1966.

- 6-25. Przemieniecki, J. S.: Theory of Matrix Structural Analysis, McGraw-Hill Book Co., New York, 1968.
- 6-26. Archer, J. S.: "Consistent Mass Matrix for Distributed Mass Systems", Journal of the Structural Division, Proc. ASCE, ST4, August 1963, pp. 161-178.
- 6-27. Bauer, H. F.: "Fluid Oscillations in the Containers of a Space Vehicle and their Influence Upon Stability", NASA TR R-187, February 1964.
- 6-28. Walton, W. C. Jr. and E. C. Steeves: "A New Matrix Theorem and its Application for Establishing Independent Coordinates for Complex Dynamic Systems with Constraints", NASA TR R-326, October 1969.
- 6-29. Greene, B. E., R. E. Jones, R. W. McLay, and D. R. Strome: "Generalized Variational Principles in the Finite-Element Method", AIAA Journal, Volume 7, July 1969, pp. 1254-1260.
- 6-30. Wilkinson, J. H.: The Algebraic Eigenvalue Problem, Oxford University Press, 1965.
- 6-31. Ralston, A.: A First Course in Numerical Analysis, McGraw-Hill Book Co., New York, 1965.
- 6-32. Wilkinson, J. H., and C. Reinsch: Handbook for Automatic Computation, Volume II - Linear Algebra, Springer-Verlag, 1971.
- 6-33. Guyan, R. J.: "Reduction of Stiffness and Mass Matrices," AIAA Journal, Vol. 3, February 1965, p. 380.
- 6-34. Scanlan, R. H., and J. C. Truman: "The Gyroscopic Effect of a Rigid Rotating Propeller on Engine and Wing Vibration Modes", Journal of the Aeronautical Sciences, October 1950, pp. 653-659, 666.
- 6-35. Brower, W. B., and R. H. Lassen: "The Effects of Gyroscopic Coupling of Propulsion Units on the Vibration Modes of a Dynamically Similar Model of the Lockheed Constitution Airplane", Masters Thesis, Rensselaer Polytechnic Institute, Troy, New York, June 1950.
- 6-36. Griffin, J. A., Jr.: "A General Approach to the Vibration and Flutter Analysis of a Gyroscopically Coupled Elastic System," Report No. 2-53450/2R50079, July 1962, Chance Vought Corporation.

- 6-37. Caughey, T. K. and M. E. J. O'Kelly: "General Theory of Vibration of Damped Linear Dynamic Systems", Caltech Dynamics Laboratory Report, June 1963.
- 6-38. Frazer, R. A., W. J. Duncan, and A. R. Collar: Elementary Matrices, Cambridge University Press, 1960, pp. 162-163.
- 6-39. Halfman, R. L.: Dynamics, Vol. 2, Addison-Wesley Publ. Co., Reading, Mass., 1962.

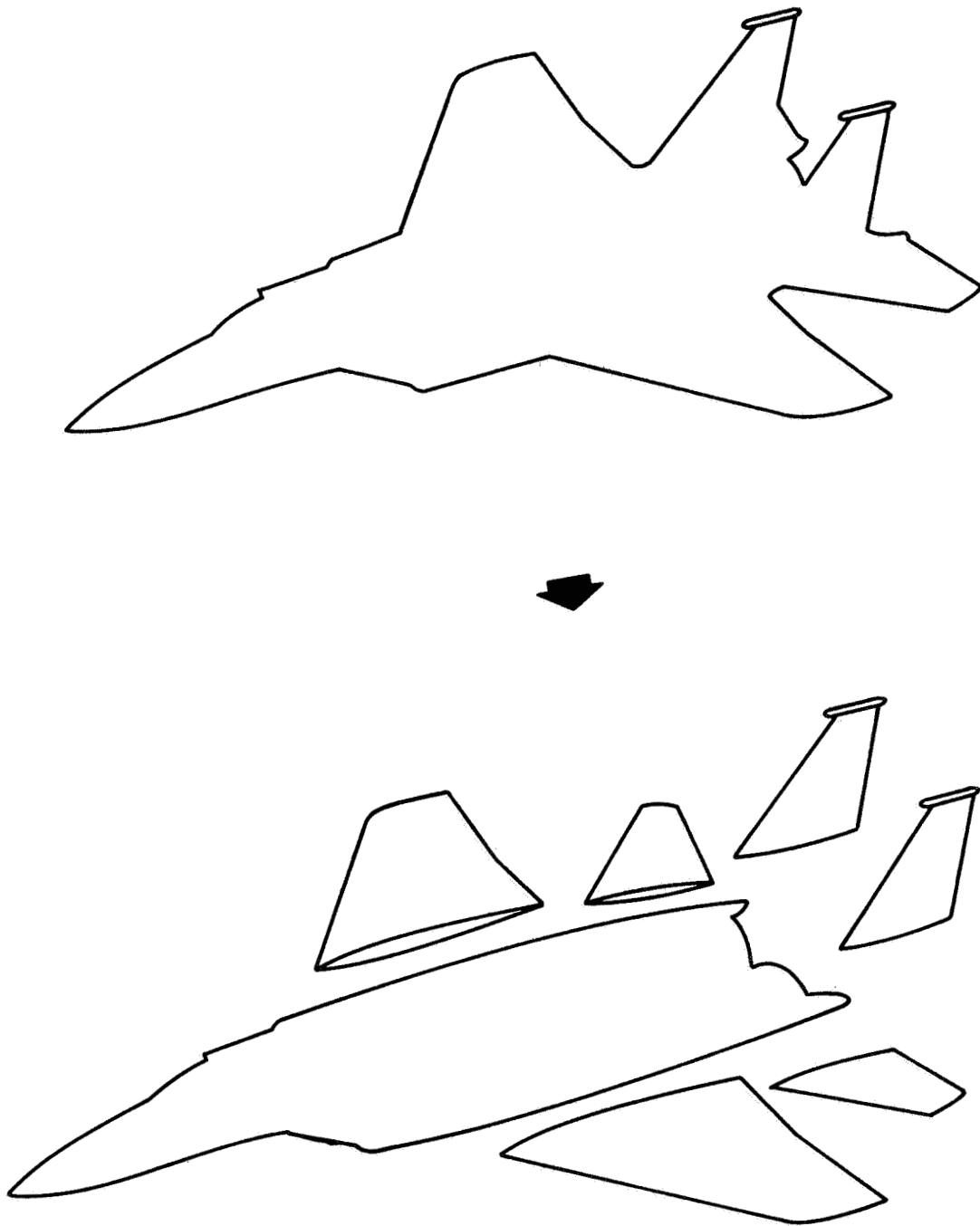


Figure 6-1. Partitioning an aircraft structure into several smaller substructures.

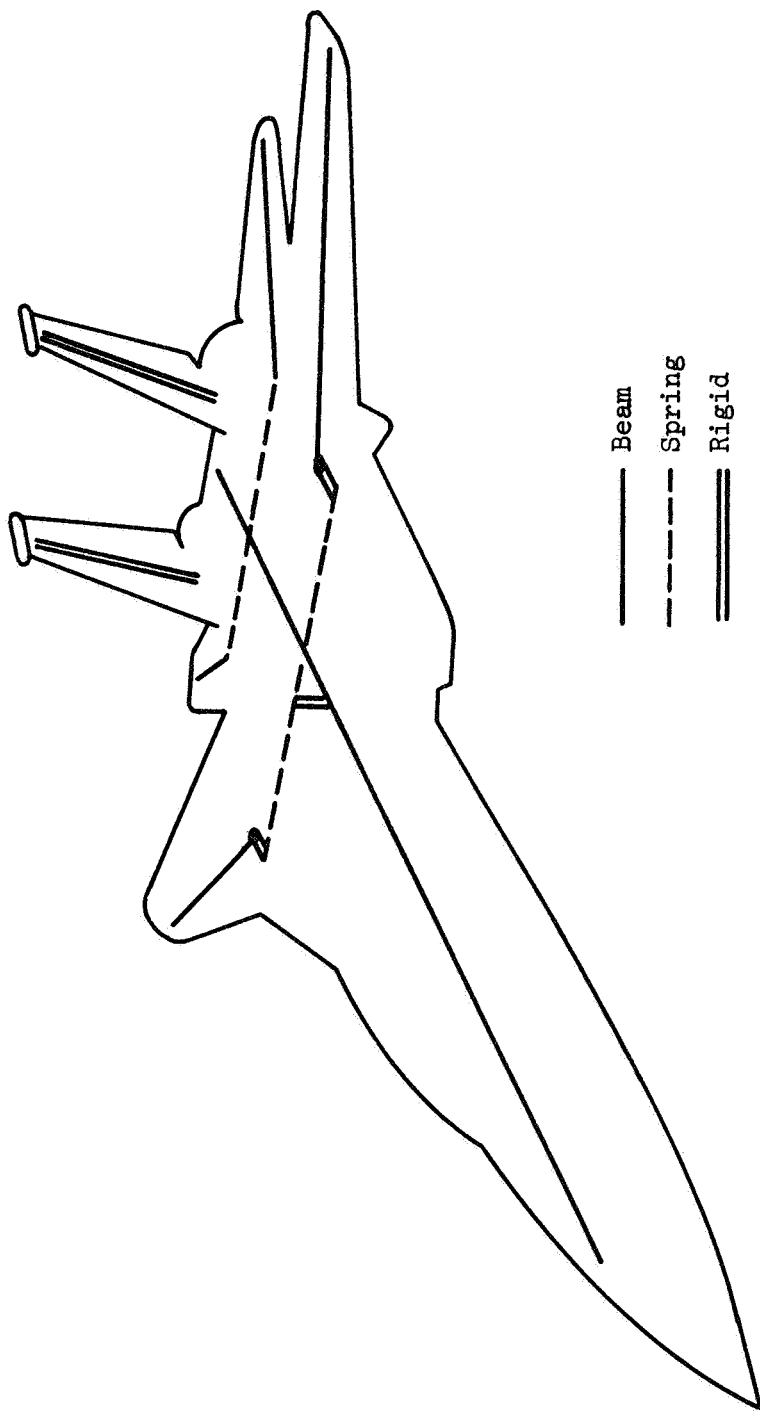


Figure 6-2. "Stick" model of a variable-sweep-wing aircraft for symmetric mode analysis.

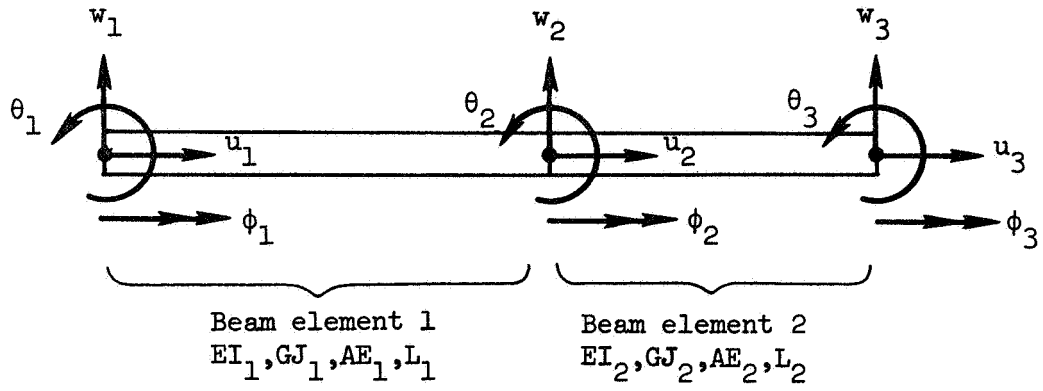


Figure 6-3. A two-element beam substructure.

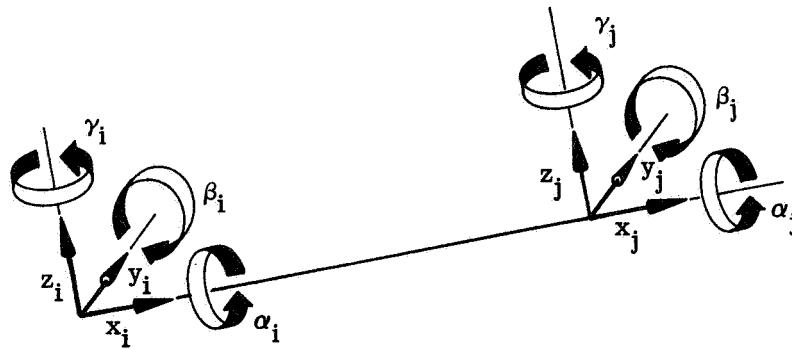


Figure 6-4. Sign convention for end deflections of massless uniform beam segment (beam-spring).

$[K]_{B-S} =$

x_i	y_i	z_i	α_i	β_i	γ_i	x_j	y_j	z_j	α_j	β_j	γ_j
$\frac{AE}{L}$	0	0	0	0	0	$-\frac{AE}{L}$	0	0	0	0	0
$\frac{12EI}{L^3}$	$\frac{12EI}{L^3}$	0	0	0	$\frac{6EI}{L^2}$	0	$-\frac{12EI}{L^3}$	0	0	0	$\frac{6EI}{L^2}$
	$\frac{12EI}{L^3}$	$\frac{12EI}{L^3}$	0	$-\frac{6EI}{L^2}$	0	0	0	$-\frac{12EI}{L^3}$	0	$-\frac{6EI}{L^2}$	0
			$\frac{6EI}{L}$	0	0	0	0	0	$-\frac{6EI}{L}$	0	0
				$\frac{4EI}{L}$	0	0	0	$\frac{6EI}{L^2}$	0	$\frac{2EI}{L}$	0
					$\frac{4EI}{L}$	0	$-\frac{6EI}{L^2}$	0	0	0	$\frac{2EI}{L}$
						$\frac{AE}{L}$	0	0	0	0	0
							$\frac{12EI}{L^3}$	0	0	0	$-\frac{6EI}{L^2}$
								$\frac{12EI}{L^3}$	0	0	0
									$\frac{6EI}{L}$	0	0
										$\frac{4EI}{L}$	0
											$\frac{4EI}{L}$

Symmetric

Figure 6-5. Stiffness matrix of massless uniform beam segment (beam-spring).

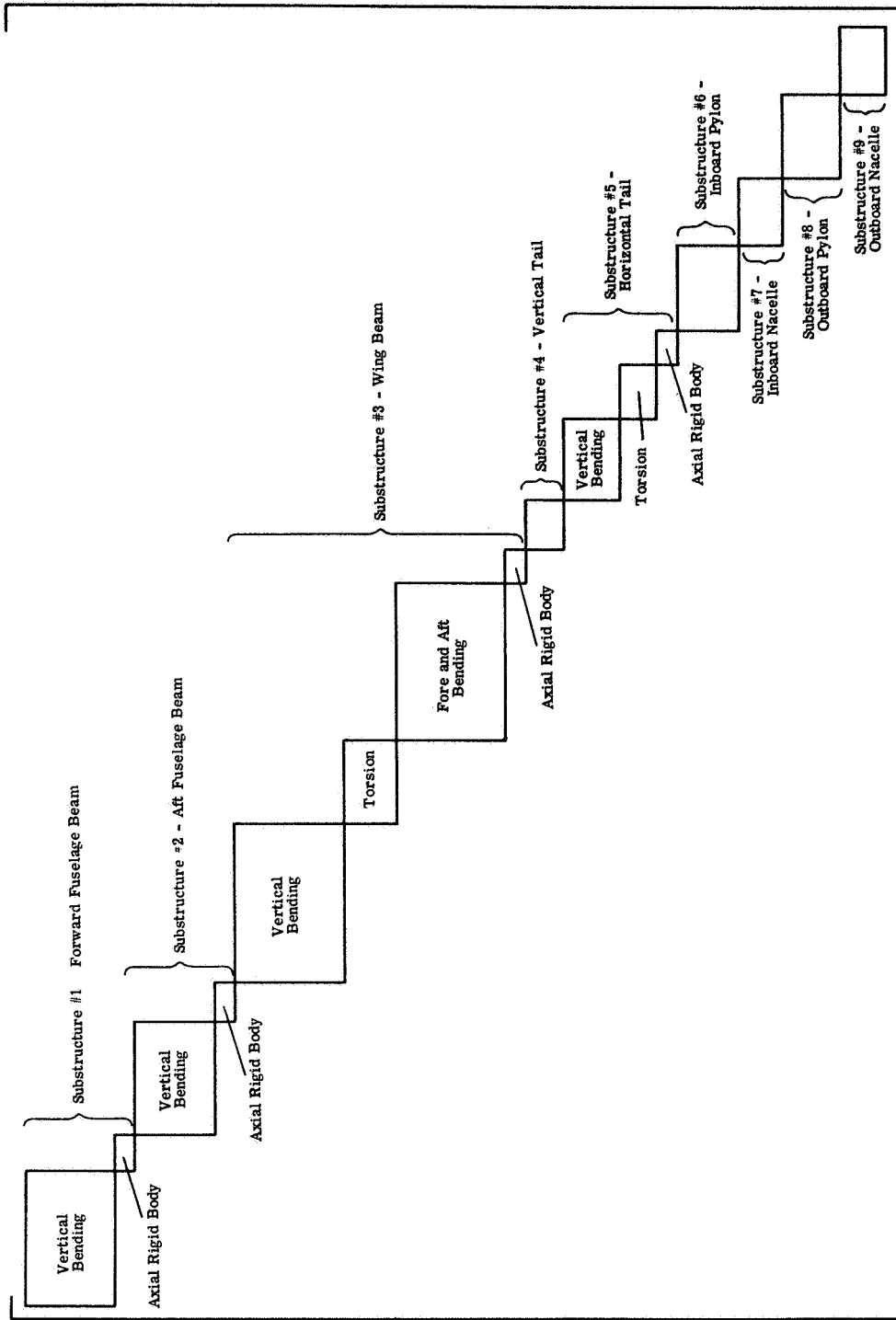
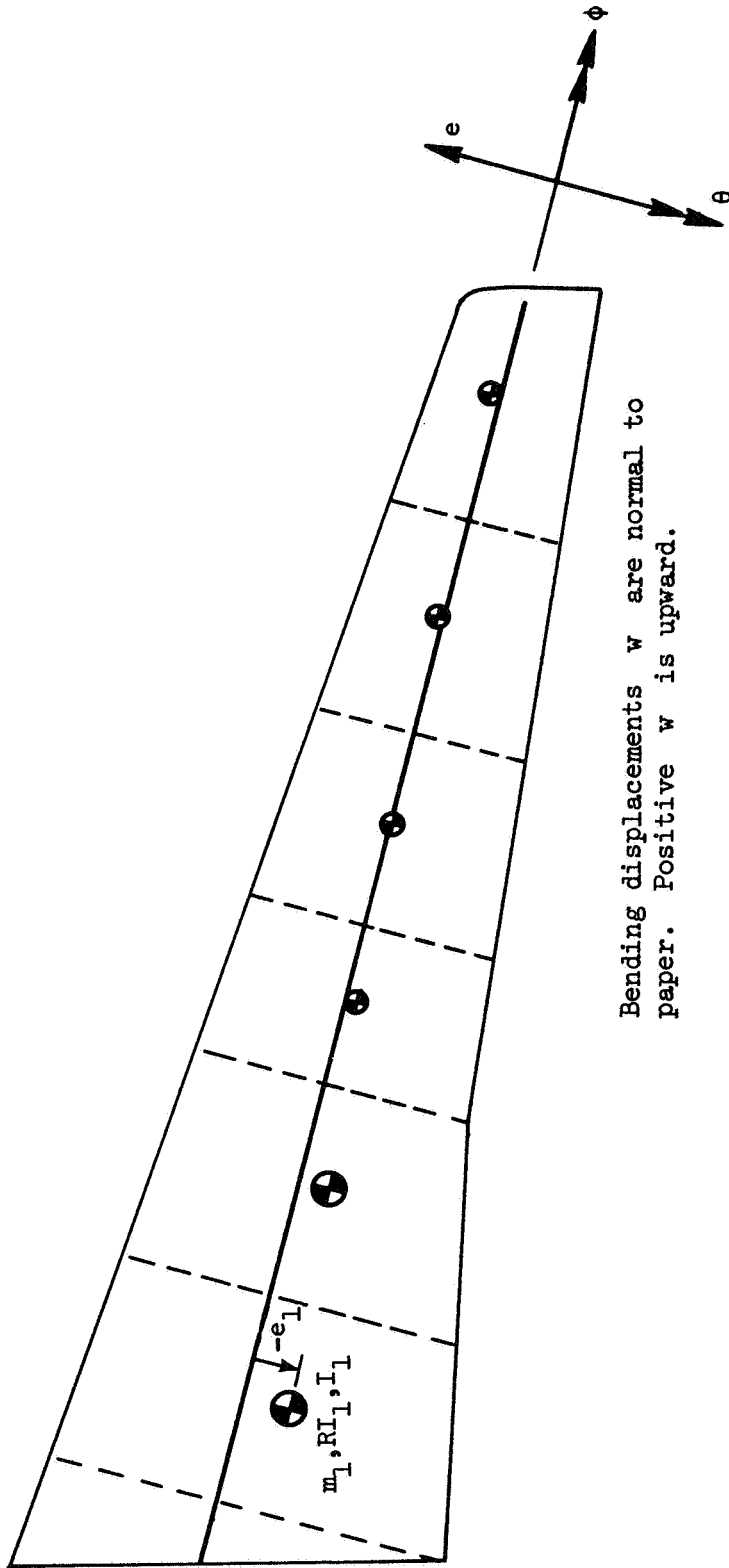


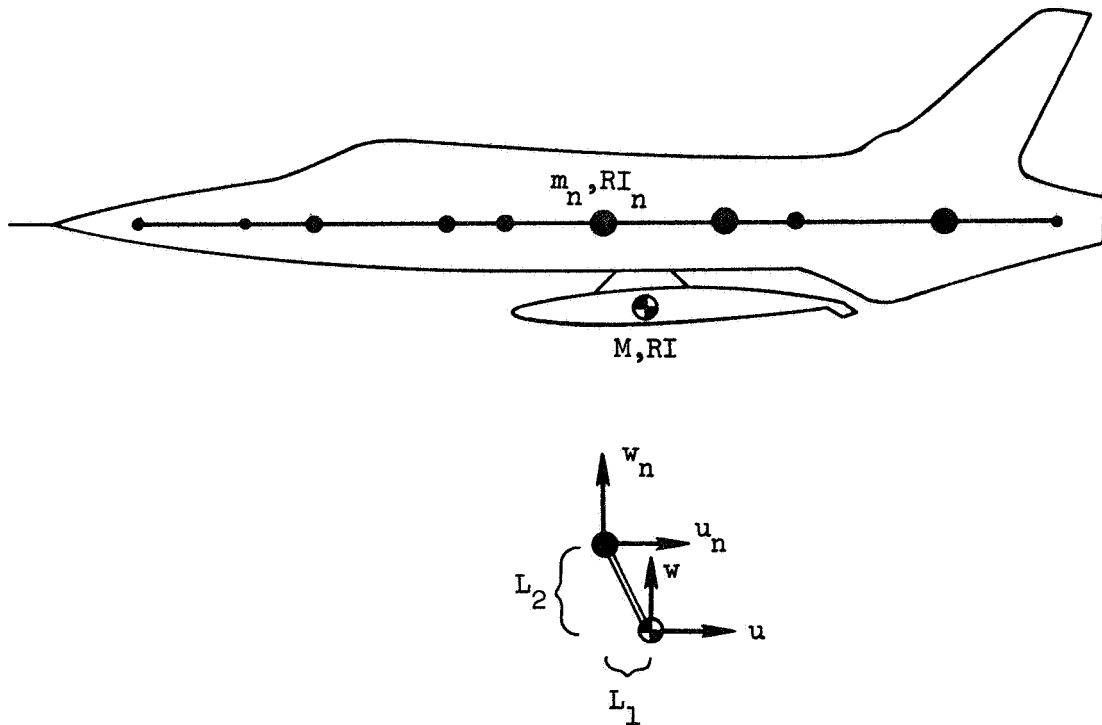
Figure 6-7. Block composition of matrices $[M]$ and $[K]$ for the stick model of Fig. 6-6.



Bending displacements w are normal to paper. Positive w is upward.

$$T_i = \frac{1}{2} m_i \left[\dot{w}_i^2 + 2 e_i \dot{w}_i \dot{\phi}_i + (e_i \dot{\phi}_i)^2 \right] + \frac{1}{2} I_i \dot{\phi}_i^2 + \frac{1}{2} R I_i \dot{\theta}_i^2 \quad i = 1, 2, \dots, 6$$

Figure 6-8. Treatment of mass coupling terms arising from wing static unbalance.



$$\dot{u} = \dot{u}_n + L_2 \dot{\theta}_n$$

$$\dot{w} = \dot{w}_n + L_1 \dot{\theta}_n$$

$$\dot{\theta} = \dot{\theta}_n$$

$$T = \frac{1}{2} M(\dot{u}^2 + \dot{w}^2) + \frac{1}{2} RI \dot{\theta}^2$$

$$T = \frac{1}{2} M(\dot{u}_n^2 + \dot{w}_n^2) + M(L_1 \dot{\theta}_n \dot{w}_n + L_2 \dot{\theta}_n \dot{u}_n) + \frac{1}{2}(RI + ML_1^2 + ML_2^2) \dot{\theta}_n^2$$

Figure 6-10. Manner of assimilating the rigid body inertial properties of a center-line fuel tank into the inertial matrix of the fuselage beam.

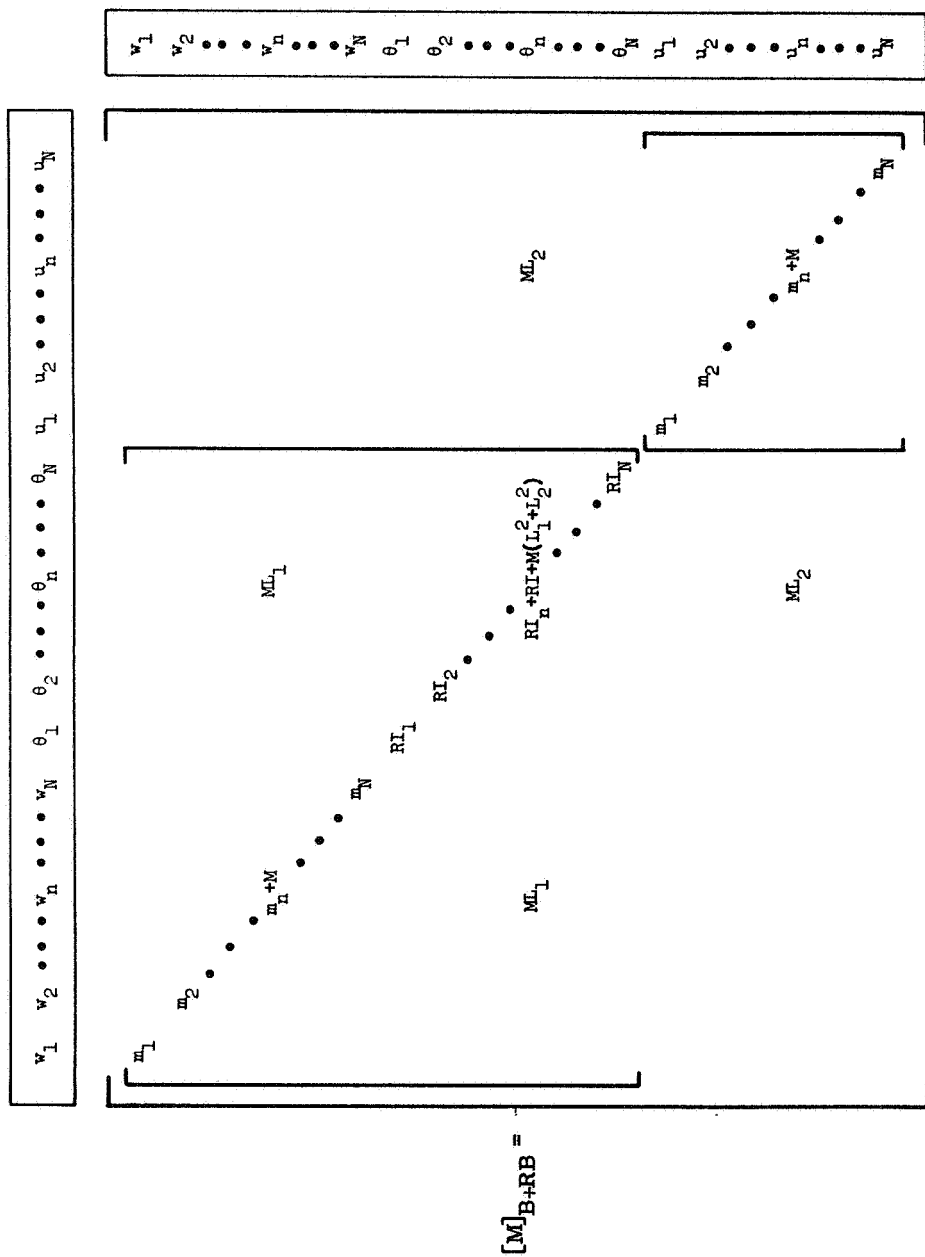
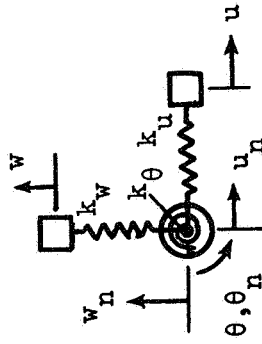
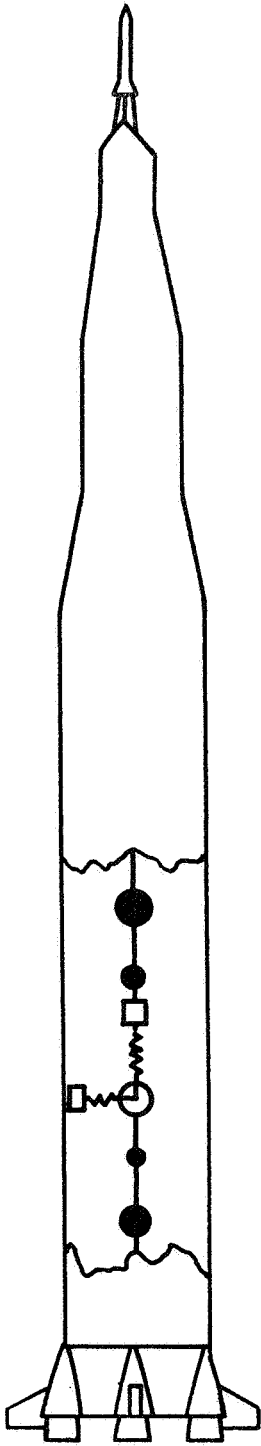


Figure 6-11. Inertia matrix of the fuselage beam/fuel tank combination of Fig. 6-10.



$$V_s = \frac{1}{2} k_w (w - w_n)^2 + \frac{1}{2} k_\theta (\theta - \theta_n)^2 + \frac{1}{2} k_u (u - u_n)^2$$

Figure 6-12. Use of the spring-mass analogy to simulate the dynamics of sloshing propellant in a natural mode analysis.

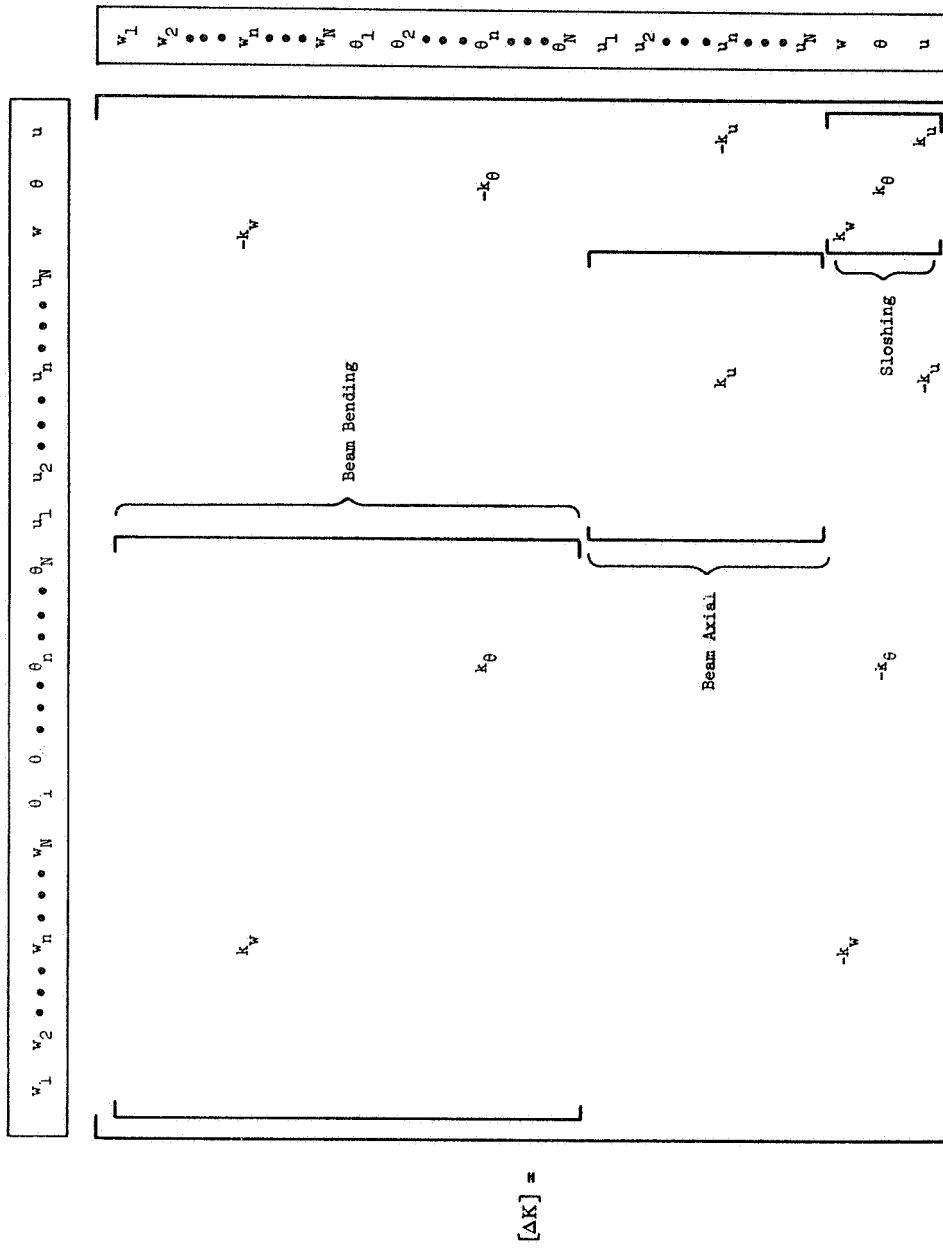


Figure 6-13. Matrix of spring terms introduced by the spring-mass analogy of Fig. 6-12.

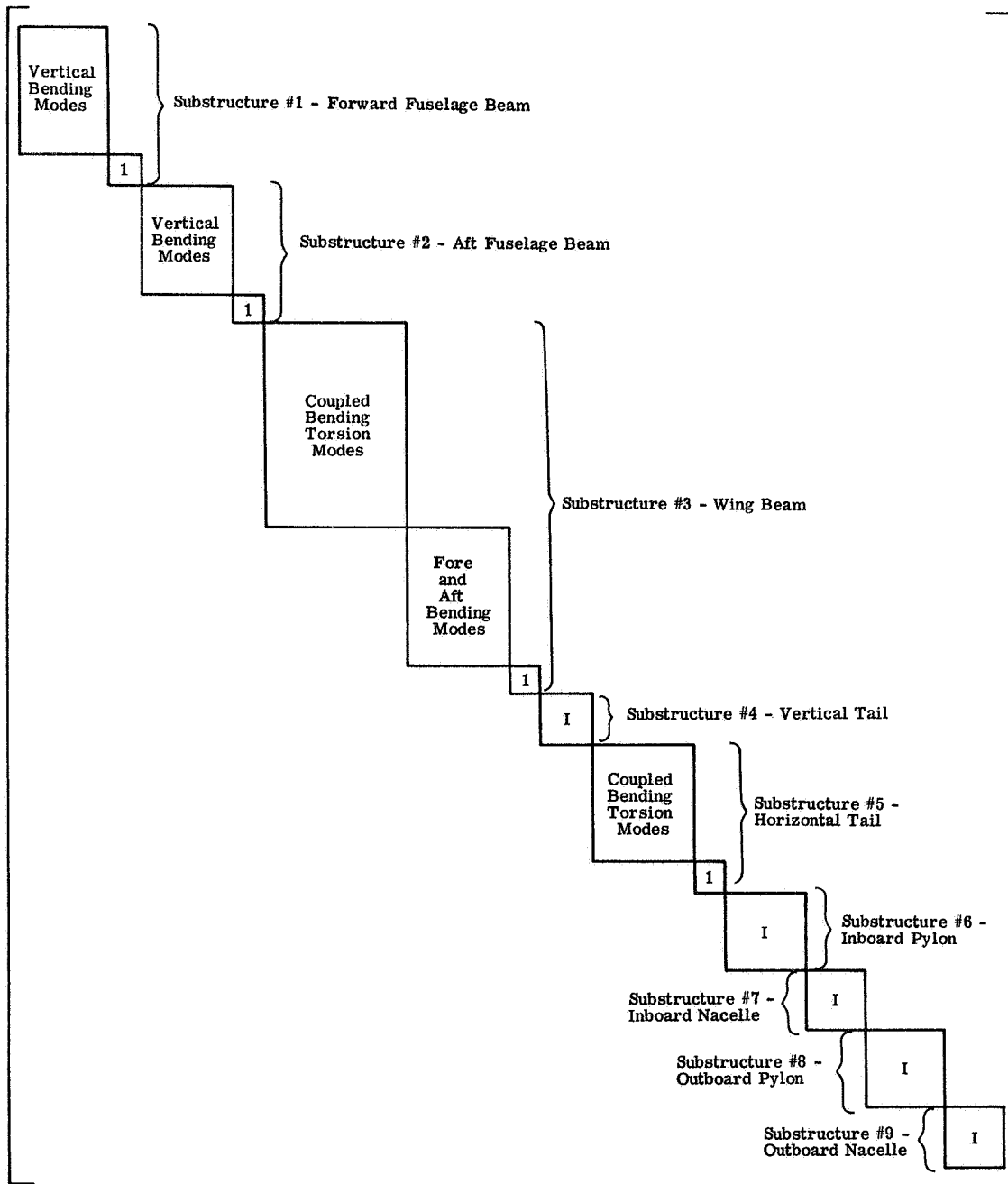


Figure 6-14. Composition of the system modal expansion matrix [U] corresponding to the stick model of Fig. 6-6.

CHAPTER 7

CONCLUDING REMARKS

This dissertation has presented the results of some generalized aeroelastic and dynamic studies which complement and extend various aspects of technology applicable to tilt-rotor VTOL aircraft.

Selected analytical and experimental studies and related discussions have provided insight into several aeroelastic and dynamic aspects associated with tilt-rotor aircraft operating in the high-speed airplane mode of flight with the proprotors fully converted forward. Particular attention has been given to proprotor/pylon whirl instability, a precession-type instability akin to propeller/nacelle whirl flutter, which first came into prominence in 1962 during tests of the Bell XV-3 convertiplane in the NASA-Ames full-scale wind tunnel. Several salient features of propeller- and proprotor-related dynamics were examined and the origin of the forces and moments generated during precessional motion indicated. These considerations have provided additional insight into the mechanism of whirl flutter for both propellers and proprotors. The blade flapping and pitch-change freedoms of a proprotor were shown to introduce new ingredients into the dynamic behavior of a proprotor relative to that of a propeller, thereby leading to a fundamentally different situation as regards the manner in which the precession-generated aerodynamic forces and moments act on the pylon and induce whirl flutter. Whereas aerodynamic cross-stiffness moments are the driving terms for propeller/nacelle whirl flutter, the primary

destabilizing factors on proprotor/pylon motion are the inplane shear forces associated with the airload moments required to precess the rotor in space in response to shaft motions. In addition to a true whirl instability involving both pitching and yawing motions, a proprotor/pylon system can, in contrast to a propeller/nacelle system, exhibit a dynamic instability in either the pitch or yaw direction depending on the pylon support conditions. The flapping and pitch-change freedoms of a proprotor lead to aerodynamic forces and moments the magnitude and phase of which are dependent on the frequency of the precessional motion. The implication of the proprotor forces and moments which are induced during whirling motions were also examined with regard to their capacity for instigating a whirl instability. These considerations have shown, it is believed for the first time, precisely why a proprotor can physically exhibit whirl flutter in either the backward or forward directions in contrast to a propeller which is found to always whirl in the backward direction. The work herein has shown that the ambidextrous behavior of a proprotor as regards the direction in which it can whirl flutter is a direct consequence of the frequency dependency of the aerodynamic forces and moments.

Equations describing the perturbation motions of an idealized proprotor/pylon/wing system encastré at the wing root with the proprotor fully converted forward were derived. The particular mathematical model employed assumed a three-or-more-bladed rotor in an axial flow condition having rigid blades whose flapping motion could be represented by longitudinal and lateral flapping of the

tip-path-plane. The proprotor was taken to be gimbal-mounted to a pylon having three translational and three rotational degrees of freedom and constrained by linear springs and dampers to represent the pylon support conditions. A quasi-steady aerodynamic theory applied stripwise to the blade and integrated along its span was used for the blade loading. The option of employing Theodorsen unsteady aerodynamics to approximate the effects of the shed wake was also provided. Wing and pylon aerodynamics were not included. In addition to providing the analytical basis from which to assess the aeroelastic stability of the system the equations of motion were shown to furnish the basis for deriving the equations for calculating the frequency response characteristics of the proprotor force and moment derivatives and the tip-path-plane flapping derivatives.

Using parameters relevant to the Bell Model 266 tilt-rotor design evolved during the U.S. Army Composite Aircraft Program, the proprotor analyses developed herein were employed in some analytical trend studies to delineate the effects of various system design parameters on proprotor/pylon stability, flapping response, and proprotor force and moment derivatives, the response characteristics being examined in light of their effects on proprotor/pylon aeroelastic stability and aircraft rigid-body stability and response.

Results of experimental studies pertaining mainly to joint NASA/Bell Helicopter Company investigations of a 0.1333-scale, semi-span, dynamic, aeroelastic model of the Model 266 tilt-rotor in the Langley transonic dynamics tunnel were presented. During these investigations an apparently new type of flapping

instability associated with the stopped or slowly turning rotor was identified. The instability was characterized by an essentially rigid-body flapping motion of the blades such that the tip-path-plane of the blades exhibited a wobbling precessional motion in the forward whirl direction (for negative δ_3). Because of the novel character of this instability the effect of various system parameters on the instability was established both experimentally and analytically. Based on these studies it was concluded that rotor precone was the primary factor contributing to the flapping instability at low rpm. To provide additional data for correlation selected results pertaining to a 1/5 scale model of the Bell Model 300 tilt-rotor design as well as some results from tests of a 25-foot flightworthy Model 300 proprotor in the Ames full-scale wind tunnel have also been included.

The analytical predictions were found to be in good agreement with measured dynamic characteristics thereby providing validation of the proprotor/pylon stability and response analyses developed in this dissertation.

Although the proprotor analyses have been developed for a proprotor of the semi-rigid (ie., gimbaled) type characteristic of Bell designs and are thus strictly applicable only to rotors of that type the analyses were found to have a somewhat broader range of applicability. Specifically, the stability analysis herein has also been applied to whirl flutter data obtained during a joint NASA/Grumman test program in the transonic dynamics tunnel employing a research configuration of a semispan model of the Grumman "Helicat" tilt-rotor. This tilt-rotor design is characterized by a proprotor

having blades with offset flapping hinges. For analysis purposes the restoring centrifugal moment from the offset flapping hinge was simulated by introducing an equivalent hub spring. Analyses based on this equivalent gimbaled rotor were in good agreement with the measured stability characteristics over a wide range of variable system parameters. These results are being prepared for publication as a NASA Technical Note.

In recognition of the fundamental role assumed by natural vibration modes in aeroelastic and dynamic response analyses and in structural design verification, this dissertation has also directed attention to the development and computer implementation of utilitarian computational procedures for natural mode vibration analysis of structural systems, particularly aircraft structures. Two methodologies for natural mode analysis have been described; both employ the substructuring technique and are based on the stiffness matrix method of structural analysis. The first consists of a direct approach based on solving the matrix eigenvalue problem resulting from a finite element representation of the complete structure as an entity. The second method is that of component mode synthesis which is based on the concept of synthesizing the vibration modes of the complete structure from modes of conveniently defined substructures, or components, into which the structure has been divided. The latter method provides for a significant reduction in the size of the resulting eigenvalue problem through the expedient of partial modal synthesis wherein only a relatively few of the modes from each component are chosen as degrees of freedom

and employed in the synthesizing procedure. Although both of the analyses as developed in this dissertation are applicable to a structural idealization based on any type of finite element, the computer implementation of these analyses was limited to structures which admit of a stick model representation for dynamic analysis. Since many structures can be represented in this manner, particularly in the preliminary stages of design, the computer programs so established have a relatively wide range of engineering applicability. A stick model of the Model 266 tilt-rotor was employed in a detailed numerical example to illustrate the substructuring approach and the mechanics of setting down the equations of constraint which enforce deflection compatibility at the junctions of the substructures. Both methods of analysis were applied to two simple structural systems in some comparative studies. Validation of both analyses as embodied in the computer programs was demonstrated by showing correlation with experimentally measured modes and frequencies obtained from a model of one of the configurations. To provide for additional validation, mention was also made of related work by the author and others in which the computer programs embodying both methods of analysis have been applied to more complex structural systems.

On the assumption that the primary gyroscopic effects of large rotating components such as propellers or proprotors can be accounted for by idealizing each such component as a rigid rotating disc, the dissertation has introduced the concept of a gyroscopic finite element which has the convenience of being readily incorporated into

either a direct or modal formulation for dynamic analysis. By means of this artifice both analyses for determining natural modes and frequencies of vibration were extended to include the case of a gyroscopically coupled elastic system. The final equations of motion lead to a generalized eigenvalue problem in which both the mass and stiffness matrices can be singular, thereby precluding the usual procedure for reducing the equations to the standard eigenvalue form required for solution. A method which appears suited to routine machine computation has been proposed for effecting such a reduction in the general case in which both the mass and stiffness matrices are singular. These extensions have, however, not yet been programmed and thus lack numerical verification.

The analytical portion of the research reported in this dissertation is continuing. Attention is being directed toward extending the present flutter analysis for an isolated propotor/pylon system encastré' at the wing root to include aircraft rigid-body dynamics and aerodynamics, blade inplane flexibility, and wing aerodynamics. Work is also continuing on refining and extending the computer programs for natural mode analysis, particularly as regards the inclusion of gyroscopic coupling effects.

BIBLIOGRAPHY

- Loewy, R. G.: "Review of Rotary-Wing V/STOL Dynamic and Aeroelastic Problems," AIAA/AHS VTOL Research, Design, and Operations Meeting, February 1969 (AIAA Paper 69-202).
- Richardson, D. A.: "The Application of Hingeless Rotors to Tilting Prop/Rotor Aircraft", Presented at the 26th Annual National Forum of the American Helicopter Society, June 1970.
- Sambell, K. W.: "Application of the Low Disc Loading Proprotor to a Series of Aircraft for the Short-Hall Market", AIAA Paper 71-781, July 1971.
- Many authors: "Design Studies and Model Tests of the Stowed Tilt Rotor Concept", AFFDL-TR-71-62 (Boeing-Vertol) , July 1971.
- Gillmore, K. B.: "Survey of Tilt Rotor Technology Development," Presented at AGARD Flight Mechanics Panel Meeting on Advanced Rotorcraft at NASA Langley Research Center, September 1971.
- Fraga, D. E., and J. Liiva: "Design Studies and Model Tests of the Stowed Tilt-Rotor Aircraft", AIAA Paper 72-804, August 1972.
- Edenborough, H. K., T. M. Gaffey, and J. A. Weiberg: "Analyses and Tests Confirm Design of Proprotor Aircraft", AIAA Paper 72-803, August 1972.
- Marr, R. L., and G. T. Neal: "Assessment of Model Testing of a Tilt-Proprotor VTOL Aircraft", Presented at the American Helicopter Society Mideast Region Symposium on Status of Testing and Modeling Techniques for V/STOL Aircraft, Essington, Pennsylvania, October 1972.
- Emslie, B. and J. L. Kepert: "Whirl Flutter of an Engine-Propeller System", Report ARL/SM 304, August 1965.
- Rodden, W. P. and J. E. Fischler: "The Loads Acting on an Oscillating Jet Engine", Douglas Aircraft Company, Report No. WPR (DAC) TN-66-5, March 1966.
- Smith, G. E.: "Whirl of an Aircraft Power Plant Installation and its Interaction with the Flutter Motion of a Flexible Wing", Reports and Memorandum No. 3636, August 1966.
- Hammond, C. E.: "Compressibility Effects in Helicopter Rotor Blade Flutter", Ph. D. dissertation, Georgia Institute of Technology, December 1969 (GITAER 69-4).

- Langelo, V. A.: "A Simplified Technique for the Development of Aeroelastic Analyses of V/STOL Aircraft", AIAA 8th Aerospace Sciences Meeting, January 1970 (AIAA Paper 70-22).
- Hall, W. E. Jr.: "Application of Floquet Theory to the Analysis of Rotary-Wing VTOL Stability", Stanford University, SUDAAR No. 400, February 1970.
- Peters, D. A., and K. H. Hohenemser: "Application of the Floquet Transition Matrix to Problems of Lifting Rotor Stability", Presented at the 26th Annual National Forum of the American Helicopter Society, June 1970.
- Hobbs, G. K.: "Methods of Treating Damping in Structures", AIAA Paper No. 71-349, April 1971.
- Hasselmann, T. K.: "Method for Constructing a Full Modal Damping Matrix from Experimental Measurements", AIAA Journal, Vol. 10, April 1972, pp. 526-527.
- Hohenemser, K. H. and S. K. Yin: "Some Applications of the Method of Multiblade Coordinates", Journal of the American Helicopter Society, Vol. 17, July 1972.
- Many authors: "V/STOL Dynamics and Aeroelastic Rotor-Airframe Technology", AFFDL-TR-72-40 (Boeing-Vertol) , September 1972.
- Curtiss, H. C., Jr.: "The Use of Complex Coordinates in the Study of Rotor Dynamics", Presented at the AIAA 2nd Atmospheric Flight Mechanics Conference, Palo Alto, California, September, 1972 (AIAA Paper 72-954).
- Loewy, R. G.: "A Review of Aerodynamic and Dynamic V/STOL Model Testing", Presented at the American Helicopter Society Mideast Region Symposium on Status of Testing and Modeling Techniques for V/STOL Aircraft, Essington, Pennsylvania, October 26-28, 1972.
- Albrecht, C. O.: "Factors in the Design and Fabrication of Powered Dynamically Similar V/STOL Wind Tunnel Models", Presented at the American Helicopter Society Mideast Region Symposium on Status of Testing and Modeling Techniques for V/STOL Aircraft, Essington, Pennsylvania, October 1972.
- Lytwyn, R. T., W. Miao, and W. Woitsch: "Airborne and Ground Resonance of Hingeless Rotors", Presented at the 26th Annual National Forum of the American Helicopter Society, June 1970.
- Liu, Y. N.: "Whirl Flutter Analysis of a Propeller-Nacelle-Pylon

System on Large Surface Effect Vehicles", Report 3673,
Naval Ship Research and Development Center, November 1971.

- Scheiman, J.: "Analytical Investigation of the Tilt Rotor Whirl Instability", Ph. D. dissertation, Virginia Polytechnic Institute and State University, January 1972.
- Friedman, P., and P. Tong: "Nonlinear Flap Lag Stability of Hingeless Helicopter Blades", Israel Journal of Technology, Vol. 10, 1972, pp. 133-143.
- Ormiston, R. A., and D. H. Hodges: "Linear Flap-Lag Dynamics of Hingeless Helicopter Rotor Blades in Hover", Journal of the American Helicopter Society, Vol. 17, April 1972.
- Johnston, R. A.: "Parametric Studies of Instabilities Associated with Large, Flexible Rotor Propellers", Presented at the 28th Annual National Forum of the American Helicopter Society, May 1972.
- Burkam, J. E., and W. L. Miao: "Exploration of Aeroelastic Stability Boundaries with a Soft-Inplane Hingeless-Rotor Model", Presented at the 28th Annual National Forum of the American Helicopter Society, May 1972.
- De Larm, L. N.: "Whirl Flutter and Divergence Aspects of Tilt-Wing and Tilt-Rotor Aircraft," Presented at the Air Force V/STOL Technology and Planning Conference, Las Vegas, Nevada, September 1969.
- Baird, E. F., E. M. Bauer, and J. S. Kohn: "Model Tests and Analysis of Prop-Rotor Dynamics for Tilt-Rotor Aircraft," Presented at the American Helicopter Society Mideast Region Symposium on Status of Testing and Modeling Techniques for V/STOL Aircraft, Essington, Pennsylvania, October 1972.
- Pearce, B. F.: Topics on Flexible Airplane Dynamics, Part I - Residual Stiffness Effects in Truncated Modal Analysis ASD-TDR-63-334 (Part I), July 1963.
- Leckie, F. A. and G. M. Lindberg: "The Effect of Lumped Parameters on Beam Frequencies", Aeronautical Quarterly, Vol. 14, August 1963, pp. 224-240.
- Rubinstein, M. F. and W. C. Hurty: "Dynamic Analysis of a Rocket Model by the Component Modes Method", SAE National Aeronautic and Space Engineering and Manufacturing Meeting, October 1964.
- Irons, B.: "Structural Eigenvalue Problems: Elimination of Unwanted Variables," AIAA Journal, Vol. 3, May 1965, pp. 961-962.

- Young, R. and H. McCallum: "The Determination of Frequencies and Modes of Undamped Structures Using Finite-Element Stiffness and Consistent-Mass Matrices", ASRL TR 121-8, Massachusetts Institute of Technology, June 1965.
- McCalley, R. B. Jr.: "Mass Matrix for a Prismatic Beam Segment", Notes for a Short course on Normal Modes, Shock, and Vibrations, Pennsylvania State University, July 1966.
- Zienkeiwicz, O. C.: The Finite Element Method in Structural and Continuum Mechanics, McGraw-Hill Book Co., London, 1967.
- Hurtz, W. C.: "A Criterion for Selecting Realistic Natural Modes of a Structure", Jet Propulsion Laboratory, Technical Memorandum 33-364, November 1967.
- Craig, R. R. and M. C. C. Bampton: "Coupling of Substructures for Dynamic Analyses", AIAA Journal, Vol. 6, July 1968, pp. 1313-1319.
- Mains, R. M.: "Comparisons of Consistent Mass Matrix Schemes," Shock and Vibration Bulletin 39, Part 3, January 1969, pp. 129-142.
- Jensen, F. R. and H. N. Christiansen: "An Application of Component Mode Synthesis to Rocket Motor Vibration Analysis," Shock and Vibration Bulletin No. 40, Part 6, Dynamic and Dynamic Stress Analysis, December 1970, pp. 115-121.
- Mains, R. M.: "Results of Comparative Studies on Reduction of Size Problem", Shock and Vibration Bulletin No. 42, Part 5, January 1972, pp. 135-141.
- Hasselmann, T. K. and G. C. Hart: "Modal Analysis of Random Structural Systems", Journal of the Engineering Mechanics Division, Proc. ASCE, EM3, June 1972, pp. 561-579.
- Gupta, K. K.: "Solution of Eigenvalue Problems by Sturm Sequence Method", Int. J. for Numerical Methods in Engineering, Vol. 4, 1972, pp. 379-404.
- Appa, K., G. C. C. Smith, and J. T. Hughes: "Rational Reduction of Large-Scale Eigenvalue Problems", AIAA Journal, Vol. 10, July 1972, pp. 964-965.
- Johnson, S. E. and W. C. Hurty: "Convergence in Modal Synthesis", Journal of the Engineering Mechanics Division, Proc. ASCE, EM5, October 1972, pp. 1105-1114.

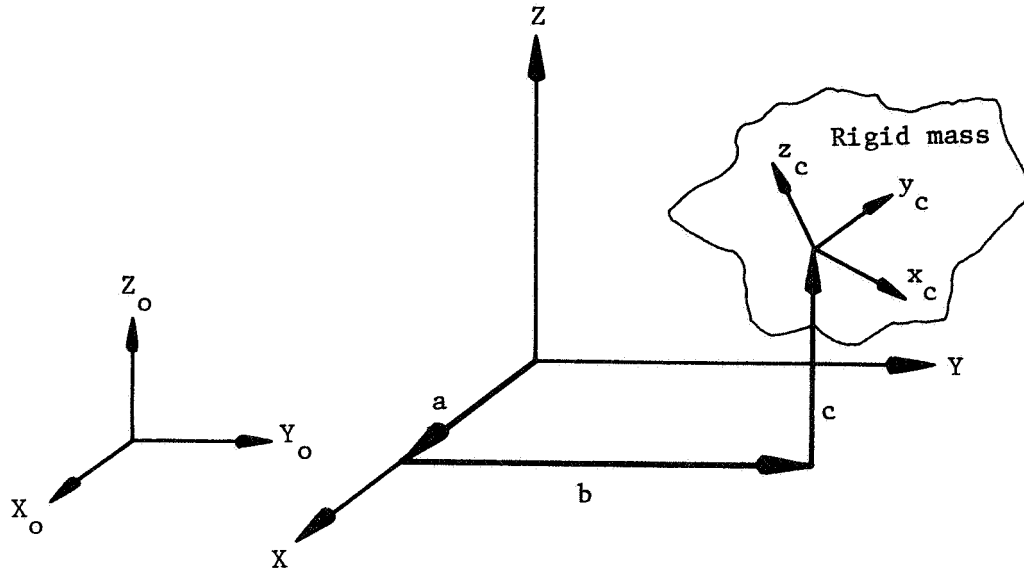
- Schwendler, R. G., and R. H. MacNeal: "Optimum Structural Representation in Aeroelastic Analyses", ASD-TR-61-680, March 1962.
- Duncan, W. J., and A. R. Collar: "Matrices Applied to the Motions of Damped Systems", Philosophical Magazine and Journal of Science, Vol. 19, February 1935, pp. 197-219.
- Fried, I.: "Condensation of Finite Element Eigenproblems", AIAA Journal, November 1972, pp. 1592-1530.
- MacNeal, R. H., ed.: "The NASTRAN Theoretical Manual", NASA SP-222(01), June 1972.
- Dowell, E. H.: "Free Vibrations of an Arbitrary Structure in Terms of Component Modes", Journal of Applied Mechanics, Vol. 39, September 1972, pp. 727-732.
- Hunt, G. K.: "Similarity Requirements for Aeroelastic Models of Helicopter Rotors", RAE TR 72005, January 1972.
- Hart, G. C., and J. D. Collins: "Study of Modeling of Substructure Damping Matrices", Paper No. 720813, Presented at the SAE National Aerospace Engineering and Manufacturing Meeting, October 1972.
- Lee, T. H.: "A Dynamic Analysis for Elastic Structures Interacting With Rotating Machinery", Journal of Aircraft, Vol. 10, January 1973, pp. 45-51.

APPENDIX A

RIGID BODY MASS MATRIX REFERRED TO AN ARBITRARY SYSTEM OF AXES

Various aircraft appendages, such as engine/nacelle combinations, ordnance, external fuel tanks, etc., can often be treated as rigid lumped masses during dynamic analyses of the complete vehicle. Since the inertial properties of such appendages are generally available in the form of lumped values for the mass and moments and products of inertia relative to some axes fixed to the center of mass of the item, it is desirable to retain inertial information in this form. However, quite often in applications, it is necessary to be able to express these inertial properties relative to another axis system which is displaced from and arbitrarily oriented to the axes in which the inertial properties are defined. This requires a transformation of coordinates which can be effected in the manner outlined below.

The situation being addressed is depicted in the sketch shown below. A rigid body is translating and rotating with respect to the axis system X_0, Y_0, Z_0 which is fixed in space. The inertial properties of the rigid body are defined with respect to the axes x_c, y_c, z_c fixed in the body at its center of mass. Relative to



these body axes the kinetic energy of the mass can be written as

$$T_c = \frac{1}{2} \begin{Bmatrix} \dot{x} \\ \dot{y} \\ \dot{z} \\ \dot{\alpha} \\ \dot{\beta} \\ \dot{\gamma} \end{Bmatrix}_c^T \begin{bmatrix} M & & & & & \\ & M & & & & \\ & & M & & & \\ \hline & & & I_{xx} & I_{xy} & I_{xz} \\ & & & I_{yx} & I_{yy} & I_{yz} \\ & & & I_{zx} & I_{zy} & I_{zz} \end{bmatrix} \begin{Bmatrix} \dot{x} \\ \dot{y} \\ \dot{z} \\ \dot{\alpha} \\ \dot{\beta} \\ \dot{\gamma} \end{Bmatrix}_c \quad (A-1)$$

or, in condensed form,

$$2T_c = \{\dot{X}\}_c^T [M]_c \{\dot{X}\}_c \quad (A-2)$$

Since the kinetic energy is independent of the coordinate system used in its calculation, we can also write

$$2T_o = \{\dot{X}\}_o^T [M]_o \{\dot{X}\}_o \quad (A-3)$$

The coordinate transformation from body axes to fixed axes can be formally written in the form

$$\{\dot{X}\}_c = [\theta]\{\dot{X}\}_o \quad (A-4)$$

Substituting Eq. A-4 into Eq. A-2 and equating the resultant expression to that in Eq. A-3

$$2T_c = \{\dot{X}\}_o^T [\theta]^T [M]_c [\theta]\{\dot{X}\}_o = 2T_o = \{\dot{X}\}_o^T [M]_o \{\dot{X}\}_o \quad (A-5)$$

the mass matrix in fixed axes is seen to be given by

$$[M]_o = [\theta]^T [M]_c [\theta] \quad (A-6)$$

It now remains to establish the specific form of the transformation matrix $[\theta]$.

Since the magnitude of the rigid body angular velocity vector is an invariant we can write

$$\dot{\alpha}_o \bar{i}_o + \dot{\beta}_o \bar{j}_o + \dot{\gamma}_o \bar{k}_o = \dot{\alpha}_c \bar{i}_c + \dot{\beta}_c \bar{j}_c + \dot{\gamma}_c \bar{k}_c \quad (A-7)$$

where $\dot{\alpha}_o$, $\dot{\beta}_o$, $\dot{\gamma}_o$ and $\dot{\alpha}_c$, $\dot{\beta}_c$, $\dot{\gamma}_c$ are the angular velocity components with respect to fixed and body axes, respectively, and \bar{i}_o , \bar{j}_o , \bar{k}_o and \bar{i}_c , \bar{j}_c , \bar{k}_c are corresponding unit vector triads. The

angular velocity components in body axes can be expressed in terms of the fixed system components by forming the dot products of \bar{i}_c , \bar{j}_c , and \bar{k}_c respectively with Eq. A-7. This gives

$$\begin{aligned}\dot{\alpha}_c &= \dot{\alpha}_o \bar{i}_c \cdot \bar{i}_o + \dot{\beta}_o \bar{i}_c \cdot \bar{j}_o + \dot{\gamma}_o \bar{i}_c \cdot \bar{k}_o \\ \dot{\beta}_c &= \dot{\alpha}_o \bar{j}_c \cdot \bar{i}_o + \dot{\beta}_o \bar{j}_c \cdot \bar{j}_o + \dot{\gamma}_o \bar{j}_c \cdot \bar{k}_o \\ \dot{\gamma}_c &= \dot{\alpha}_o \bar{k}_c \cdot \bar{i}_o + \dot{\beta}_o \bar{k}_c \cdot \bar{j}_o + \dot{\gamma}_o \bar{k}_c \cdot \bar{k}_o\end{aligned}\tag{A-8}$$

The dot products involving the unit vectors in Eqs. A-8 can be physically interpreted as the projection of the body axes unit vectors onto the fixed axes unit vectors. Defining these "direction cosines" by l_{ij} , Eqs. A-8 can be written as

$$\begin{aligned}\dot{\alpha}_c &= l_{11} \dot{\alpha}_o + l_{12} \dot{\beta}_o + l_{13} \dot{\gamma}_o \\ \dot{\beta}_c &= l_{21} \dot{\alpha}_o + l_{22} \dot{\beta}_o + l_{23} \dot{\gamma}_o \\ \dot{\gamma}_c &= l_{31} \dot{\alpha}_o + l_{32} \dot{\beta}_o + l_{33} \dot{\gamma}_o\end{aligned}\tag{A-9}$$

Equating expressions for the translational velocity vector in fixed and body axes

$$\dot{x}_o \bar{i}_o + \dot{y}_o \bar{j}_o + \dot{z}_o \bar{k}_o = \dot{x}_c \bar{i}_c + \dot{y}_c \bar{j}_c + \dot{z}_c \bar{k}_c\tag{A-10}$$

and proceeding as above leads to

$$\begin{aligned}
 \dot{x}_c &= l_{11}\dot{X}_o + l_{12}\dot{Y}_o + l_{13}\dot{Z}_o \\
 \dot{y}_c &= l_{21}\dot{X}_o + l_{22}\dot{Y}_o + l_{23}\dot{Z}_o \\
 \dot{z}_c &= l_{31}\dot{X}_o + l_{32}\dot{Y}_o + l_{33}\dot{Z}_o
 \end{aligned}
 \tag{A-11}$$

Eqs. A-11 define the translational velocity components in the body axes due to translational velocities in the fixed system. Now fixed system angular velocities will also contribute to the translational velocity in the body axes. The combined effects are obtained by making the substitutions

$$\begin{aligned}
 \dot{X}_o &\longrightarrow \dot{X}_o + c\dot{\beta}_o - b\dot{\gamma}_o \\
 \dot{Y}_o &\longrightarrow \dot{Y}_o + a\dot{\gamma}_o - c\dot{\alpha}_o \\
 \dot{Z}_o &\longrightarrow \dot{Z}_o + b\dot{\alpha}_o - a\dot{\beta}_o
 \end{aligned}
 \tag{A-12}$$

in Eqs. A-11. These results in conjunction with those previously given in Eqs. A-9 can then be put in the combined matrix form

$$\begin{Bmatrix} \dot{x} \\ \dot{y} \\ \dot{z} \\ \dot{\alpha} \\ \dot{\beta} \\ \dot{\gamma}_c \end{Bmatrix} = \begin{bmatrix} l_{11} & l_{12} & l_{13} & | & bl_{13} - cl_{12} & cl_{11} - al_{13} & al_{12} - bl_{11} \\ l_{21} & l_{22} & l_{23} & | & bl_{23} - cl_{22} & cl_{21} - al_{23} & al_{22} - bl_{21} \\ l_{31} & l_{32} & l_{33} & | & bl_{33} - cl_{32} & cl_{31} - al_{33} & al_{32} - bl_{31} \\ \hline & & & & l_{11} & l_{12} & l_{13} \\ & & & & l_{21} & l_{22} & l_{23} \\ & & & & l_{31} & l_{32} & l_{33} \\ \text{Null} & & & & & & \end{bmatrix} \begin{Bmatrix} \dot{x} \\ \dot{y} \\ \dot{z} \\ \dot{\alpha} \\ \dot{\beta} \\ \dot{\gamma}_o \end{Bmatrix}
 \tag{A-13}$$

which defines the transformation relating velocities in the fixed axis system to velocities in the body axis system. The square matrix in Eq. A-13 is the required transformation matrix $[0]$ to be used in Eq. A-6.

APPENDIX B

BLADE FLAPPING NATURAL FREQUENCY

Gimbaled Proprotor

An expression for the blade flapping natural frequency can be derived from the equations of motion developed in Chapter 3 by considering the degenerate case obtained through retaining only the two tip-path-plane degrees of freedom. If precone and gimbal damping are neglected the resulting equations for the case of a symmetric hub restraint reduce to

$$I_R \ddot{a}_1 + 2I_R \Omega \dot{b}_1 + K_H a_1 = M \quad (\text{B-1a})$$

$$I_R \ddot{b}_1 - 2I_R \Omega \dot{a}_1 + K_H b_1 = N \quad (\text{B-1b})$$

where the longitudinal and lateral tip-path-plane flapping moments (from Eqs. 3-129 and 3-130) are given by

$$M = \frac{1}{2} \gamma \Omega^2 I_R \left[-B_3 a_1 \tan \delta_3 - \frac{A_5}{\Omega} \dot{a}_1 - A_5 b_1 \right] \quad (\text{B-2a})$$

$$N = -\frac{1}{2} \gamma \Omega^2 I_R \left[B_3 b_1 \tan \delta_3 + \frac{A_5}{\Omega} \dot{b}_1 - A_5 a_1 \right] \quad (\text{B-2b})$$

Multiplying Eq. B-1a by $\sin \psi$ and Eq. B-1b by $\cos \psi$, subtracting the second equation from the first, and making use of the relations

$$\begin{aligned}
\beta &= a_1 \sin \psi - b_1 \cos \psi \\
\dot{\beta} &= \dot{a}_1 \sin \psi - \dot{b}_1 \cos \psi + \dot{a}_1 \Omega \cos \psi + \dot{b}_1 \Omega \sin \psi \\
\ddot{\beta} &= \ddot{a}_1 \sin \psi - \ddot{b}_1 \cos \psi + 2\dot{a}_1 \Omega \cos \psi + 2\dot{b}_1 \Omega \sin \psi \\
&\quad - a_1 \Omega^2 \sin \psi + b_1 \Omega^2 \cos \psi
\end{aligned} \tag{B-3}$$

defining the transformation between blade flapping motion and tip-path-plane flapping motion, the resulting equation can be put into the form

$$\ddot{\beta} + \frac{1}{2} \gamma \Omega A_5 \dot{\beta} + \left[\Omega^2 + \frac{K_H}{I_R} + \frac{1}{2} \gamma \Omega^2 B_3 \tan \delta_3 \right] \beta = 0 \tag{B-4}$$

Comparing Eq. B-4 to the equation of motion for a viscously damped one degree of freedom system

$$\ddot{x} + 2\zeta \omega_n \dot{x} + \omega_n^2 x = 0 \tag{B-5}$$

the undamped flapping natural frequency is seen to be given by

$$\bar{\omega}_\beta \equiv \frac{\omega_\beta}{\Omega} = \left[1 + \frac{K_H}{I_R \Omega^2} + \frac{1}{2} \gamma B_3 \tan \delta_3 \right]^{\frac{1}{2}} \tag{B-6}$$

and the aerodynamic flap damping by

$$\zeta_\beta = \frac{\gamma A_5}{4 \bar{\omega}_\beta} \tag{B-7}$$

The damped natural frequency is of course given by

$$\bar{\omega}_{\beta_d} = \bar{\omega}_\beta \sqrt{1 - \zeta_\beta^2} \tag{B-8}$$

If a representative section aerodynamic theory is used to specify the blade loading Eqs. B-6 and B-7 are replaced by

$$\bar{\omega}_\beta = \left[1 + \frac{K_H}{I_R \Omega^2} + \frac{\gamma \tan \delta_3}{8 \cos \bar{\phi}} \right]^{\frac{1}{2}} \quad (\text{B-9})$$

$$\zeta_\beta = \frac{\gamma \cos \bar{\phi}}{16 \bar{\omega}_\beta} \quad (\text{B-10})$$

where the bar over ϕ denotes that the inflow angle is to be evaluated at the representative blade spanwise station.

The effect of δ_3 on the blade flapping frequency is seen to be that of an aerodynamic spring which increases or decreases the frequency depending on whether δ_3 is positive or negative.

Offset Flapping Hinge Proprotor

It is of interest to present the analogous expressions for the case of a propotor having blades with offset flapping hinges. Proceeding as above using the equations of motion developed by Richardson and Naylor* for a propeller having hinged blades the analogous expressions can be shown to be

$$\bar{\omega}_\beta = \left[1 + \frac{eS_{R_\epsilon}}{I_{R_\epsilon}} + \frac{K_{H_\epsilon}}{I_{R_\epsilon} \Omega^2} + \frac{\gamma_\epsilon (B_{3_\epsilon} - \epsilon B_{2_\epsilon}) \tan \delta_3}{2} \right]^{\frac{1}{2}} \quad (\text{B-11})$$

* Richardson, J. R., and H. F. W. Naylor: "Whirl Flutter of Propellers with Hinged Blades," Engineering Research Associates, Report No. 24, March 1962.

$$\zeta_{\beta} = \frac{\gamma_{\epsilon}}{4\bar{\omega}_{\beta}} (A_{5\epsilon} - 2\epsilon A_{4\epsilon} + \epsilon^2 A_{3\epsilon}) \quad (\text{B-12})$$

where

$$\gamma_{\epsilon} = \frac{\rho a_o c R^4}{I_{B\epsilon}} \quad (\text{B-13})$$

and the subscript ϵ ($\epsilon \equiv e/R$, e the hinge offset) is used to denote quantities defined with respect to the flapping hinge location. Also, in the aerodynamic integrals the lower limit of integration for no root cutout is $\eta_1 = \epsilon$ rather than $\eta_1 = 0$. Comparing Eqs. B-6 and B-7 to Eqs. B-11 and B-12 it is seen that several additional terms appear for the proprotor having non-centrally hinged blades.

An Equivalent Hub Spring Approximation for a Stiff-Inplane Prop-rotor with Offset Flapping Hinges

A gimbaled proprotor is essentially a zero offset flapping hinge rotor. On the supposition that the principal stability and response characteristics can be approximated by using an equivalent hub spring to represent the restoring centrifugal moment from an offset flapping hinge, analyses developed for the gimbaled proprotor are applicable to a stiff-inplane offset flapping hinge rotor, at least for preliminary design calculations. The equivalent hub spring K_H is established by requiring that

$$\frac{K_H}{I_R \Omega^2} = \frac{e S_{R\epsilon}}{I_{R\epsilon}} + \frac{K_{H\epsilon}}{I_{R\epsilon} \Omega^2} \quad (\text{B-14})$$

so that the in-vacuum blade flapping natural frequency is preserved.* For a given offset flapping hinge proprotor configuration and a selected rotational speed the right hand side of Eq. B-14 and the denominator of the left hand side are known, permitting solution for the equivalent K_H .

A more complete equivalence could be established by retaining all terms in the expressions for $\bar{\omega}_\beta$, both dynamic and aerodynamic, equating Eq. B-6 to Eq. B-11, and solving for K_H . In this case a new equivalent K_H would have to be determined for each (Ω, V) combination rather than for just each Ω as in Eq. B-14 above.

Fixed System Flapping Frequencies

Blade flapping is related to tip-path-plane flapping by Eq. B-3. The relation between the blade flapping frequency and the two tip-path-plane flapping frequencies[†] is given by

$$\omega_{1d}, \omega_{2d} = |\Omega \pm \omega_{\beta_d}| \quad (B-15)$$

The proprotor stability program PRSTAB6 (Appendix G) prints out values for $\bar{\omega}_\beta$ and ζ_β for each airspeed at which the stability determinant is solved. At low airspeeds ω_β is sufficiently close to ω_{β_d} that Eq. B-15 can be used to identify the tip-path-

*This is similar in many respects to an equivalence suggested by M. I. Young for hingeless rotors: "A Simplified Theory of Hingeless Rotors with Application to Tandem Helicopters," Proceedings of the 18th Annual National Forum of the American Helicopter Society, May 1962, pp. 38-45.

[†]These are derived and discussed in Chapter 4.

plane flapping modes at low velocity and hence with increasing air-speed. This obviates the need to inspect the mode shapes for the purpose of identifying these modes.

APPENDIX C

PROPROTOR OSCILLATORY FORCE AND MOMENT DERIVATIVES

As a consequence of the flapping degree of freedom, propotor generated forces and moments, such as those shown in Fig. 2-12, are highly frequency dependent; that is, they are functions of the linear and angular motions of the control axis* in space. The knowledge of these forces and moments as a function of the frequency of motion constitutes a necessary ingredient in an aircraft dynamic stability analysis (airframe plus propotors).

The equations of motion developed in Chapter 3, in addition to providing the basis for an aeroelastic stability analysis, may be used to obtain the expressions required for calculating these oscillatory forces and moments. Briefly, the procedure consists in specifying a sinusoidal motion of the form $e^{i\omega t}$ of given frequency and amplitude in one of the degrees of freedom, assuming that the response in the remaining degrees of freedom is at the same frequency but of unknown amplitude, solving the equations of motion for these unknown amplitudes, and then substituting the known results into the appropriate force and moment expressions (as listed in Chapter 3). Herein, only the longitudinal and lateral propotor forces and moments arising from pylon oscillatory motions in pitch will be treated in detail for illustrative purposes.

*The shaft axis for the case in which the swashplate is rigidly attached normal to the shaft.

Neglecting gimbal damping consider the tip-path-plane equations for the case of the pylon having only the pitch degree of freedom. From Chapter 3 these assume the form

$$I_R \ddot{a}_1 + (I_R + S_R \beta h_1) \ddot{\phi}_y + 2\Omega I_R \dot{b}_1 + K_{a_1} a_1 = M \quad (C-1a)$$

$$I_R \ddot{b}_1 - 2\Omega I_R \dot{a}_1 - 2\Omega I_R \dot{\phi}_y + K_{b_1} b_1 = N \quad (C-1b)$$

where M and N are given by

$$\begin{aligned} M = & \frac{1}{2} \gamma \Omega^2 I_R \left[-B_3 (a_1 \tan \delta_3 + K_1 \phi_y \sin \epsilon) - \frac{A_5}{\Omega} (\dot{\phi}_y + \dot{a}_1) \right. \\ & \left. - A_5 b_1 \right] + \frac{1}{2} \gamma \Omega^2 I_R \lambda \beta_o \left[B_2 (b_1 \tan \delta_3 - K_1 \phi_y \cos \epsilon) \right. \\ & \left. + A_2 \lambda^2 \phi_y + \frac{A_4}{\Omega} \dot{b}_1 - A_4 a_1 - \frac{A_2 \lambda}{\Omega R} h_1 \dot{\phi}_y \right] \quad (C-2a) \end{aligned}$$

$$\begin{aligned} N = & -\frac{1}{2} \gamma \Omega^2 I_R \left[B_3 (b_1 \tan \delta_3 - K_1 \phi_y \cos \epsilon) + A_3 \lambda^2 \phi_y \right. \\ & \left. + \frac{A_5}{\Omega} \dot{b}_1 - A_5 a_1 - \frac{A_3 \lambda}{\Omega R} h_1 \dot{\phi}_y \right] \\ & + \frac{1}{2} \gamma \Omega^2 I_R \lambda \beta_o \left[-B_2 (a_1 \tan \delta_3 + K_1 \phi_y \sin \epsilon) \right. \\ & \left. - \frac{A_4}{\Omega} (\dot{\phi}_y + \dot{a}_1) - A_4 b_1 \right] \quad (C-2b) \end{aligned}$$

Taking the oscillatory pylon motion to be

$$\phi_y = \phi_{y_o} e^{i\omega t} \quad (C-3)$$

the steady-state response of the tip-path-plane to this forced oscillation of the pylon can be written as

$$a_1 = \bar{a}_1 e^{i\omega t} \quad (C-4a)$$

$$b_1 = \bar{b}_1 e^{i\omega t} \quad (C-4b)$$

where \bar{a}_1 and \bar{b}_1 are the unknown complex amplitudes to be determined. Substituting Eqs. C-3 and C-4 into Eqs. C-1 the resulting equations can be put into the form

$$\begin{aligned} & \left[-I_R \omega^2 + K_{a_1} + F_1 B_3 \tan \delta_3 + F_2 A_4 + i\omega \frac{F_1}{\Omega} A_5 \right] \bar{a}_1 \\ & + \left[\left\{ 2I_R \Omega - \frac{F_2}{\Omega} A_4 \right\} i\omega + F_1 A_5 - F_2 B_2 \tan \delta_3 \right] \bar{b}_1 \\ & = \left[\left\{ I_R + S_R \beta_o h_1 \right\} \omega^2 - i\omega \frac{F_1}{\Omega} A_5 - F_1 B_3 K_1 \sin \epsilon \right. \\ & \quad \left. + F_2 \lambda^2 A_2 - F_2 B_2 K_1 \cos \epsilon - i\omega F_2 \frac{\lambda}{\Omega R} A_2 h_1 \right] \phi_{y_o} \end{aligned} \quad (C-5a)$$

$$\begin{aligned} & \left[-F_1 A_5 + F_2 B_2 \tan \delta_3 + i\omega \left\{ F_2 \frac{A_4}{\Omega} - 2I_R \Omega \right\} \right] \bar{a}_1 \\ & + \left[-\omega^2 I_R + K_{b_1} + F_1 B_3 \tan \delta_3 + F_2 A_4 + i\omega F_1 \frac{A_5}{\Omega} \right] \bar{b}_1 \\ & = \left[i\omega 2I_R \Omega - F_1 \lambda^2 A_3 + F_1 \frac{\lambda}{\Omega R} A_3 h_1 i\omega + F_1 K_1 B_3 \cos \epsilon \right. \\ & \quad \left. - i\omega F_2 \frac{A_4}{\Omega} - F_2 B_2 K_1 \sin \epsilon \right] \phi_{y_o} \end{aligned} \quad (C-5b)$$

where F_1 and F_2 are constants defined by

$$\begin{aligned} F_1 & \equiv \frac{1}{2} \gamma \Omega^2 I_R \\ F_2 & \equiv \lambda \beta_o F_1 \end{aligned} \quad (C-6)$$

Eqs. C-5 constitute two non-homogeneous complex algebraic equations in the two unknowns \bar{a}_1 and \bar{b}_1 . Writing these equations in the form

$$\begin{bmatrix} a_{11} & a_{12} \\ a_{21} & a_{22} \end{bmatrix} \begin{Bmatrix} \bar{a}_1 \\ \bar{b}_1 \end{Bmatrix} = \begin{Bmatrix} c_1 \\ c_2 \end{Bmatrix} \phi_{y_0} \quad (\text{C-7})$$

the solutions for \bar{a}_1 and \bar{b}_1 , by Cramer's rule, are given by

$$\bar{a}_1 = \frac{c_1 a_{22} - c_2 a_{12}}{a_{11} a_{22} - a_{21} a_{12}} \phi_{y_0} \quad (\text{C-8a})$$

$$\bar{b}_1 = \frac{a_{11} c_2 - a_{21} c_1}{a_{11} a_{22} - a_{21} a_{12}} \phi_{y_0} \quad (\text{C-8b})$$

where the definitions of $a_{11}, a_{12}, \dots, c_2$ follow directly from Eqs. C-5. The forces and moments acting on the harmonically oscillating proprotor then follow by substituting the solutions for \bar{a}_1 and \bar{b}_1 into

$$\begin{aligned} H = & -\frac{1}{2} \gamma \Omega^2 I_R \frac{\lambda}{R} \left[B_1 \bar{b}_1 \tan \delta_3 - K_1 B_1 \phi_{y_0} \cos \varepsilon \right. \\ & \left. + A_1 \lambda^2 \phi_{y_0} + i\omega \frac{A_3}{\Omega} \bar{b}_1 - A_3 \bar{a}_1 - i\omega \frac{\lambda A_1}{\Omega R} h_1 \phi_{y_0} \right] \quad (\text{C-9}) \end{aligned}$$

$$\begin{aligned} Y = & -\frac{1}{2} \gamma \Omega^2 I_R \frac{\lambda}{R} \left[B_1 \bar{a}_1 \tan \delta_3 + K_1 B_1 \phi_{y_0} \sin \varepsilon \right. \\ & \left. + i\omega \frac{A_3}{\Omega} (\phi_{y_0} + \bar{a}_1) + A_3 \bar{b}_1 \right] \quad (\text{C-10}) \end{aligned}$$

$$\begin{aligned}
M = & -\frac{1}{2} \gamma \Omega^2 I_R \left[B_3 \bar{a}_1 \tan \delta_3 + B_3 K_1 \phi_{y_0} \sin \epsilon + i\omega \frac{A_5}{\Omega} (\phi_{y_0} + \bar{a}_1) \right. \\
& + A_5 \bar{b}_1 \left. \right] + \frac{1}{2} \gamma \Omega^2 I_R \lambda \beta_0 \left[B_2 \bar{b}_1 \tan \delta_3 - B_2 K_1 \phi_{y_0} \cos \epsilon \right. \\
& + A_2 \lambda^2 \phi_{y_0} + i\omega \frac{A_4}{\Omega} \bar{b}_1 - A_4 \bar{a}_1 - i\omega \frac{A_2 \lambda}{\Omega R} h_1 \phi_{y_0} \left. \right] \quad (C-11)
\end{aligned}$$

$$\begin{aligned}
N = & -\frac{1}{2} \gamma \Omega^2 I_R \left[B_3 \bar{b}_1 \tan \delta_3 - B_3 K_1 \phi_{y_0} \cos \epsilon + A_3 \lambda^2 \phi_{y_0} \right. \\
& + i\omega \frac{A_5}{\Omega} \bar{b}_1 - A_5 \bar{a}_1 - i\omega \frac{A_3 \lambda}{\Omega R} h_1 \phi_{y_0} \left. \right] \\
& - \frac{1}{2} \gamma \Omega^2 I_R \lambda \beta_0 \left[B_2 \bar{a}_1 \tan \delta_3 + B_2 K_1 \phi_{y_0} \sin \epsilon \right. \\
& + i\omega \frac{A_4}{\Omega} (\phi_{y_0} + \bar{a}_1) + A_4 \bar{b}_1 \left. \right] \quad (C-12)
\end{aligned}$$

The forces and moments defined by Eqs. C-9 to C-12 are algebraically complex quantities. As discussed in Chapter 4 this indicates that the total force or moment has components which are inphase (or 180° out of phase) with both pitch angle and the pitching angular rate. The maximum value of the component inphase (or 180° out of phase) with the pitch angle is given by the real part of the complex quantity; the maximum value of the component inphase (or 180° out of phase) with the angular pitch rate is given by the imaginary part. If the real part is divided by ϕ_{y_0} and the imaginary part by $\omega \phi_{y_0}$ the resulting quantities can be viewed as force and moment derivatives due to pitch and pitch rate

respectively. In the limiting case of zero pitch frequency the real portions correspond to a situation in which the pitch angle is constant and the imaginary parts to a constant pitch rate.

Computer program HFORCE1 (Appendix G) is based on the equations developed above and evaluates both the complex forces and moments and the component derivatives arising from sinusoidal pitching oscillations of the pylon. A sample output listing is shown in Table C-1. The input corresponding to the case shown is included with the program listing in Appendix G.

The effects of blade flapwise flexibility, included as a virtual hinge dynamic representation in the manner suggested by Young, on the static or zero frequency normal force and pitching moment (H and M in the present notation) were recently treated by Magee and Pruyn.*

* Magee, J. P., and R. R. Pruyn: "Prediction of the Stability Derivatives of Large Flexible Prop/Rotors by a Simplified Analysis," Presented at the 26th Annual National Forum of the American Helicopter Society, June 1970.

TABLE C-1

PROPRTOR OSCILLATORY FORCE AND MOMENT DERIVATIVES - SAMPLE OUTPUT LISTING

RDTR RPM	VELQ CITY		ADVANCE RATIO	PYLON PITCH AMPLITUDE	
	FT/SEC	KNOTS		CEGRFES	RADIANS
2.38000000E+02	5.51216216E+02	3.50000000E+02	3.87132740E+00	6.09000000E+00	1.04715755E-01

PYLON PITCH FREQUENCY			RDTR INPLANE H-FORCE		H-FORCE DERIVATIVES	
CYCLES/REV	CPS	RAD/SEC	REAL	IMAGINARY	H-ALPHA	H-ALPHA DDT
0.	0.	0.	-2.61314011E+03	0.	-2.49536499E+04	IIIII
2.00000000E-02	7.93333334E-02	4.98466035E-01	-2.62654537E+03	-1.08403013E+03	-2.50816608E+04	-2.07671627E+04
4.00000000E-02	1.58666667E-01	9.96932069E-01	-2.67105846E+03	-2.19420863E+03	-2.55067244E+04	-2.10176296E+04
6.00000000E-02	2.38000000E-01	1.49539810E+00	-2.76001549E+03	-3.35598298E+03	-2.63562654E+04	-2.14305988E+04
8.00000000E-02	3.17333333E-01	1.99386414E+00	-2.91707562E+03	-4.59282195E+03	-2.75602035E+04	-2.19965995E+04
1.00000000E-01	3.96666667E-01	2.49233017E+00	-3.17813490E+03	-5.92367957E+03	-3.03489641E+04	-2.26964203E+04
1.20000000E-01	4.76000000E-01	2.99079621E+00	-3.59327762E+03	-7.35831250E+03	-3.43127374E+04	-2.34943151E+04
1.40000000E-01	5.55333334E-01	3.48926224E+00	-4.02743613E+03	-8.89589797E+03	-4.03690144E+04	-2.43287330E+04
1.60000000E-01	6.34666667E-01	3.98772828E+00	-4.51571334E+03	-1.04823937E+04	-4.92469968E+04	-2.51018824E+04
1.80000000E-01	7.14000000E-01	4.48619431E+00	-5.04593765E+03	-1.20607433E+04	-6.16825029E+04	-2.56724536E+04
2.00000000E-01	7.93333334E-01	4.98466035E+00	-5.61887911E+03	-1.34988911E+04	-7.81971951E+04	-2.59603206E+04
2.40000000E-01	9.52000000E-01	5.98159242E+00	-6.33915924E+03	-1.52660524E+04	-1.12555656E+05	-2.43714669E+04
2.80000000E-01	1.11066667E+00	6.97852448E+00	-7.18019842E+03	-1.74646952E+04	-1.42075291E+05	-2.00428511E+04
3.00000000E-01	1.19000000E+00	7.47699052E+00	-8.02468803E+03	-1.93559925E+04	-1.73343665E+05	-1.71853744E+04
4.00000000E-01	1.58666667E+00	9.96932069E+00	-9.46869744E+03	-2.25565646E+04	-2.35743240E+05	-5.03422688E+03
6.00000000E-01	2.38000000E+00	1.49539810E+01	-1.49539810E+01	2.27293055E+03	-2.13598277E+05	1.45144547E+03
8.00000000E-01	3.17333333E+00	1.99386414E+01	-2.07460924E+04	4.90059503E+03	-1.98110589E+05	2.34706242E+03
1.00000000E+00	3.96666667E+00	2.49233017E+01	-2.80255562E+04	6.90834640E+03	-1.91678793E+05	2.66691450E+03
1.20000000E+00	4.76000000E+00	2.99079621E+01	-3.69193800E+04	9.33441548E+03	-1.89251588E+05	2.98038033E+03
1.40000000E+00	5.55333334E+00	3.48926224E+01	-4.73647908E+04	1.19364790E+04	-1.84920130E+05	3.64212537E+03
1.50000000E+00	5.95000000E+00	3.73849526E+01	-5.02356447E+04	1.46601445E+04	-1.74137580E+05	2.55526611E+03
1.50000000E+00	6.34666667E+00	3.98772828E+01	-5.43697307E+04	1.72215457E+04	-1.37220820E+05	5.08186260E+03
1.60000000E+00	6.74333334E+00	4.23696129E+01	-5.91250341E+04	2.02783521E+04	-1.06236251E+05	5.32283269E+03
1.70000000E+00	7.14000000E+00	4.48619431E+01	-6.451914304E+03	2.25198440E+04	-4.00253227E+04	5.07554010E+03
1.74000000E+00	7.53666667E+00	4.73542733E+01	-7.04926206E+02	1.93375752E+04	2.08157752E+03	4.25812666E+03
1.80000000E+00	7.93333334E+00	4.98466035E+01	-7.75270063E+03	1.19451386E+04	2.41311130E+04	2.54263778E+03
1.84000000E+00	8.32000000E+00	5.23000000E+01	-8.58588752E+01	1.27875165E+03	7.84716260E+03	1.62403229E+03
1.90000000E+00	8.71000000E+00	5.46666667E+00	-9.46393084E+03	1.36393084E+03	4.38363358E+03	8.40584666E+03
2.00000000E+00	9.10000000E+00	5.69666667E+00	-1.04267754E+03	2.89905492E+03	-6.23261142E+04	5.55382588E+02
2.40000000E+00	1.19000000E+01	7.47699052E+01	-1.12503341E+04	5.39101370E+03	-1.22068881E+05	6.60646850E+02
3.00000000E+00	1.58000000E+01	9.96932069E+01	-1.45840203E+04	8.87697599E+03	-1.39267133E+05	1.13372989E+03
1.00000000E+01	3.96666667E+01	2.49233017E+02	-1.57674319E+04	3.64260164E+04	-1.50567884E+05	1.39565310E+03

PYLON PITCH FREQUENCY			RDTR INPLANE Y-FORCE		Y-FORCE DERIVATIVES	
CYCLES/REV	CPS	RAD/SEC	REAL	IMAGINARY	Y-ALPHA	Y-ALPHA DDT
0.	0.	0.	2.34616370E+03	0.	2.24042130E+04	IIIII
2.00000000E-02	7.93333334E-02	4.98466035E-01	2.44309534E+03	4.51966929E+02	2.42093010E+04	8.65849617E+03
4.00000000E-02	1.58666667E-01	9.96932069E-01	2.68322820E+03	8.81769557E+02	2.56229419E+04	8.44619135E+03
6.00000000E-02	2.38000000E-01	1.49539810E+00	3.10978169E+03	1.26424400E+03	2.96962277E+04	8.07319526E+03
8.00000000E-02	3.17333333E-01	1.99386414E+00	3.71497796E+03	1.56810157E+03	3.54794264E+04	7.51017419E+03
1.00000000E-01	3.96666667E-01	2.49233017E+00	4.50238705E+03	1.75271215E+03	4.29946293E+04	6.71546986E+03
1.20000000E-01	4.76000000E-01	2.99079621E+00	5.46683774E+03	1.76523451E+03	5.22235366E+04	5.63620746E+03
1.40000000E-01	5.55333334E-01	3.48926224E+00	6.59634524E+03	1.53932889E+03	6.29040511E+04	4.21278398E+03
1.60000000E-01	6.34666667E-01	3.98772828E+00	7.84068933E+03	9.97963386E+02	7.48730111E+04	2.38979381E+03
1.80000000E-01	7.14000000E-01	4.48619431E+00	9.11821846E+03	6.42191809E+01	8.70725533E+04	1.36696710E+02
2.00000000E-01	7.93333334E-01	4.98466035E+00	1.02967495E+04	1.31605643E+03	9.83926714E+04	2.32121755E+03
2.40000000E-01	9.52000000E-01	5.98159242E+00	1.16473366E+04	-5.31808832E+03	1.11223870E+05	-8.49001540E+03
2.80000000E-01	1.11066667E+00	6.97852448E+00	1.07211203E+04	-9.92804451E+03	1.02379157E+05	-1.35853706E+04
3.00000000E-01	1.19000000E+00	7.47699052E+00	9.40951028E+03	-1.18903276E+04	8.98542044E+04	-1.51858244E+04
4.00000000E-01	1.58666667E+00	9.96932069E+00	8.6610777E+02	-1.51998086E+04	8.07880782E+03	-1.45594153E+04
6.00000000E-01	2.38000000E+00	1.49539810E+01	-6.71474900E+03	-1.13142376E+04	-6.41211297E+04	-7.22503324E+03
8.00000000E-01	3.17333333E+00	1.99386414E+01	-9.95204922E+03	-8.6821432E+03	-8.54897730E+04	-4.15817411E+03
1.00000000E+00	3.96666667E+00	2.49233017E+01	-1.03870167E+04	-7.31460223E+03	-9.91887032E+04	-2.80257034E+03
1.20000000E+00	4.76000000E+00	2.99079621E+01	-1.12518120E+04	-6.58971735E+03	-1.14041257E+05	-2.09444851E+03
1.40000000E+00	5.55333334E+00	3.48926224E+01	-1.24520158E+04	-5.73083178E+03	-1.47251668E+05	-1.56839494E+03
1.50000000E+00	5.95000000E+00	3.73849526E+01	-1.48058251E+04	-4.44786265E+03	-1.75762683E+05	-1.13612447E+03
1.60000000E+00	6.34666667E+00	3.98772828E+01	-1.729984264E+04	-4.45821609E+02	-2.15799076E+05	-1.06759600E+02
1.64000000E+00	6.74333334E+00	4.23696129E+01	-2.40118433E+04	2.84900268E+03	-2.29296213E+05	6.65602304E+02
1.70000000E+00	7.14000000E+00	4.48619431E+01	-3.05244178E+04	9.85363307E+03	-2.24641643E+05	2.20819556E+03
1.74000000E+00	7.53666667E+00	4.73542733E+01	-3.81924496E+04	1.43078471E+04	-1.92823640E+05	3.15058245E+03
1.80000000E+00	7.93333334E+00	4.98466035E+01	-4.6419631E+01	1.66805237E+04	-1.20080264E+05	3.50603636E+03
1.84000000E+00	8.32000000E+00	5.23000000E+01	-5.5808752E+01	-8.32624037E+03	-1.54724661E+04	3.22166366E+03
1.90000000E+00	8.71000000E+00	5.46666667E+00	-6.3668637E+03	1.22870526E+04	-4.42770934E+04	2.47176391E+03
2.00000000E+00	9.10000000E+00	5.69666667E+00	-7.27338774E+03	7.81224963E+03	-2.64839021E+04	1.49662130E+03
2.40000000E+00	1.19000000E+01	7.47699052E+01	-3.74356128E+03	1.83571208E+03	-3.57483769E+04	2.93061745E+02
3.00000000E+00	1.58000000E+01	9.96932069E+01	-4.94054265E+03	3.13014386E+02	-4.71787070E+04	3.99768757E+01
1.00000000E+01	3.96666667E+01	2.49233017E+02	-6.21560097E+03	-1.55695470E+02	-5.93546171E+04	-5.96543041E+00

TABLE C-1 (Continued)

PYLON PITCH FREQUENCY			ROTOR PITCHING MOMENT		PITCHING MOMENT DERIVATIVES	
CYCLES/REV	CPS	RAD/SEC	REAL	IMAGINARY	P-ALPHA	M-ALPHA DCT
0.	0.	0.	1.83563336E+03	0.	1.75290C74E+04	IIIIII
2.00000000E-02	7.93333334E-02	4.98466035E-01	2.35331765E+03	3.81149782E+03	2.24725282E+04	7.30182612E+04
4.00000000E-02	1.58666667E-01	9.96932069E-01	3.91922864E+03	7.51225300E+03	7.74258766E+04	7.19574926E+04
6.00000000E-02	2.38000000E-01	1.49539810E+00	6.56977792E+03	1.09728060E+04	6.27367579E+04	7.00700225E+04
8.00000000E-02	3.17333333E-01	1.99386414E+00	1.03575022E+04	1.40249999E+04	9.89686059E+04	6.717C5161E+04
1.00000000E-01	3.96666667E-01	2.49233017E+00	1.53354568E+04	1.84403368E+04	1.46442826E+05	6.29907121E+04
1.20000000E-01	4.76000000E-01	2.99079621E+00	2.15284742E+04	1.79085608E+04	2.05581785E+05	5.71801442E+04
1.40000000E-01	5.55333334E-01	3.48926224E+00	2.88850203E+04	1.80231256E+04	2.75831624E+05	4.93250894E+04
1.60000000E-01	6.34666667E-01	3.98772828E+00	3.72053794E+04	1.62803927E+04	3.55285202E+05	3.90053897E+04
1.80000000E-01	7.14000000E-01	4.48619431E+00	4.60524322E+04	1.21735321E+04	4.35768333E+05	2.59125353E+04
2.00000000E-01	7.93333334E-01	4.98466035E+00	5.46576365E+04	5.24161182E+03	5.22120840E+05	1.00411648E+04
2.40000000E-01	9.52000000E-01	5.98159242E+00	6.68897954E+04	-1.70866119E+04	6.38750494E+05	-2.72778741E+04
2.80000000E-01	1.11056667E+00	6.97852448E+00	8.58849062E+04	-6.91755726E+04	6.28677049E+05	-6.13175006E+04
3.00000000E-01	1.19000000E+00	7.47699052E+00	9.9848493E+04	-5.79244809E+04	5.71667201E+05	-7.39787013E+04
4.00000000E-01	1.58666667E+00	9.96932069E+00	1.20222932E+05	-8.43867716E+04	1.14804444E+06	-8.08314162E+04
6.00000000E-01	2.38000000E+00	1.49539810E+01	1.58262821E+05	-6.60125888E+04	-3.42121007E+05	-4.21542455E+04
8.00000000E-01	3.17333333E+00	1.99386414E+01	-5.10331927E+04	-5.06276120E+04	-4.87331093E+05	-2.42472931E+04
1.00000000E+00	3.96666667E+00	2.49233017E+01	-6.06993452E+04	-4.17999861E+04	-5.79349571E+05	-1.60155332E+04
1.20000000E+00	4.76000000E+00	2.99079621E+01	-1.96020307E+04	-3.59046467E+04	-4.87186774E+05	-1.14639774E+04
1.40000000E+00	5.55333334E+00	3.48926224E+01	-9.18115895E+04	-2.80805779E+04	-8.76736098E+05	-7.68499995E+03
1.50000000E+00	5.95000000E+00	3.73849526E+01	-1.09842377E+05	-1.77359186E+04	-1.04114549E+06	-4.52469327E+03
1.60000000E+00	6.34666667E+00	3.98772828E+01	-1.31095821E+05	1.01308777E+04	-1.25177738E+06	-7.42601172E+03
1.64000000E+00	6.50533334E+00	4.08742148E+01	-1.36820433E+05	3.12621475E+04	-1.30653889E+06	7.30366368E+03
1.70000000E+00	6.74333334E+00	4.23696129E+01	-1.42786516E+05	7.31173322E+04	-1.22102242E+06	1.64792439E+04
1.74000000E+00	6.90200000E+00	4.33665450E+01	-1.40393118E+05	9.70809416E+04	-9.92465713E+05	2.13771861E+04
1.80000000E+00	7.14000000E+00	4.48619431E+01	-5.59948800E+04	1.04725624E+05	-5.34711716E+05	2.22918575E+04
1.84000000E+00	7.29866667E+00	4.58588752E+01	-3.14896609E+04	9.37153615E+04	-3.00704111E+05	1.95145602E+04
1.90000000E+00	7.53666667E+00	4.73542733E+01	-1.21231834E+04	7.12683388E+04	-1.15767874E+05	1.45717231E+04
2.00000000E+00	7.93333334E+00	4.98466035E+01	-4.96130283E+03	6.2654643E+04	-4.73765272E+04	8.1715167E+03
2.40000000E+00	9.52000000E+00	5.98159242E+01	-1.65257841E+04	7.54828666E+03	-1.57809614E+05	1.20554413E+03
3.00000000E+00	1.19000000E+01	7.47699052E+01	-2.55079766E+04	-4.4614213E+02	-2.43583234E+05	-5.64011027E+01
1.00000000E+01	3.96666667E+01	2.49233017E+02	-3.45284673E+04	-1.47675504E+03	-3.29722575E+05	-5.65914756E+01

PYLON PITCH FREQUENCY			ROTOR YAWING MOMENT		YAWING MOMENT DERIVATIVES	
CYCLES/REV	CPS	RAD/SEC	REAL	IMAGINARY	N-ALPHA	N-ALPHA DCT
0.	0.	0.	2.57745792E+03	0.	2.461291C1E+04	IIIIII
2.00000000E-02	7.93333334E-02	4.98466035E-01	2.57101487E+03	-6.19664153E+03	2.49513835E+04	-1.18711334E+05
4.00000000E-02	1.58666667E-01	9.96932069E-01	2.52707580E+03	-1.25705223E+04	2.42121796E+04	-1.20409052E+05
6.00000000E-02	2.38000000E-01	1.49539810E+00	2.36875842E+03	-1.92972851E+04	2.26199767E+04	-1.23228389E+05
8.00000000E-02	3.17333333E-01	1.99386414E+00	1.95791337E+03	-2.65440165E+04	1.86956994E+04	-1.77137943E+05
1.00000000E-01	3.96666667E-01	2.49233017E+00	1.06106717E+03	-3.44657285E+04	1.03234310E+04	-1.2058391E+05
1.20000000E-01	4.76000000E-01	2.99079621E+00	-5.66815948E+02	-4.31646948E+04	-5.41269360E+03	-1.37820314E+05
1.40000000E-01	5.55333334E-01	3.48926224E+00	-3.39334424E+03	-5.26590968E+04	-3.24040506E+04	-1.44104714E+05
1.60000000E-01	6.34666667E-01	3.98772828E+00	-7.89912994E+03	-6.27936171E+04	-7.54311345E+04	-1.50370043E+05
1.80000000E-01	7.14000000E-01	4.48619431E+00	-1.46222962E+04	-7.31892395E+04	-1.39632643E+05	-1.55790344E+05
2.00000000E-01	7.93333334E-01	4.98466035E+00	-2.40085283E+04	-8.31306313E+04	-2.29264557E+05	-1.59256398E+05
2.40000000E-01	9.52000000E-01	5.98159242E+00	-5.08197659E+04	-9.74093912E+04	-4.89283468E+05	-1.55508952E+05
2.80000000E-01	1.11056667E+00	6.97852448E+00	-8.28823630E+04	-9.78204924E+04	-7.91468266E+05	-1.33855931E+05
3.00000000E-01	1.19000000E+00	7.47699052E+00	-7.4496629E+04	-9.24054554E+04	-9.30575733E+05	-1.18014346E+05
4.00000000E-01	1.58666667E+00	9.96932069E+00	-1.31608612E+05	-4.60675303E+04	-1.25676947E+06	-4.41266284E+04
6.00000000E-01	2.38000000E+00	1.49539810E+01	-1.23764962E+05	2.32252806E+03	-1.18186833E+06	1.48311739E+03
8.00000000E-01	3.17333333E+00	1.99386414E+01	-1.15117206E+05	2.00987818E+04	-1.09928834E+06	9.62599330E+03
1.00000000E+00	3.96666667E+00	2.49233017E+01	-1.10907834E+05	3.31018269E+04	-1.05909180E+06	1.26828767E+04
1.20000000E+00	4.76000000E+00	2.99079621E+01	-1.08346660E+05	4.81042969E+04	-1.03463439E+06	1.53591942E+04
1.40000000E+00	5.55333334E+00	3.48926224E+01	-1.03027174E+05	7.16151773E+04	-9.83837081E+05	1.96541363E+04
1.50000000E+00	5.95000000E+00	3.73849526E+01	-9.36894391E+04	9.09866817E+04	-8.94682079E+05	2.324C8696E+04
1.60000000E+00	6.34666667E+00	3.98772828E+01	-6.67567561E+04	1.15014235E+05	-6.37480063E+05	2.75421233E+04
1.64000000E+00	6.50533334E+00	4.08742148E+01	-4.59617963E+04	1.21537198E+05	-4.38902824E+05	2.83943009E+04
1.70000000E+00	6.74333334E+00	4.23696129E+01	-4.58365341E+03	1.13765438E+05	-4.37706659E+04	2.56405437E+04
1.74000000E+00	6.90200000E+00	4.33665450E+01	1.90788865E+04	9.06208482E+04	1.87189946E+05	1.99546760E+04
1.80000000E+00	7.14000000E+00	4.48619431E+01	2.62954278E+04	4.38688392E+04	2.51102839E+05	9.33790485E+03
1.84000000E+00	7.29866667E+00	4.58588752E+01	1.50143060E+04	2.01531036E+04	1.4337661E+05	4.19652604E+03
1.90000000E+00	7.53666667E+00	4.73542733E+01	-7.81880911E+03	1.97051331E+03	-7.46641271E+04	3.97366800E+02
2.00000000E+00	7.93333334E+00	4.98466035E+01	-3.70269690E+04	-3.21983460E+03	-3.53518159E+05	-6.16835521E+02
2.40000000E+00	9.52000000E+00	5.98159242E+01	-7.40316232E+04	1.61955866E+04	-7.06549327E+05	2.5855392E+03
3.00000000E+00	1.19000000E+01	7.47699052E+01	-8.39298849E+04	3.68185288E+04	-8.01471363E+05	4.70230703E+03
1.00000000E+01	3.96666667E+01	2.49233017E+02	-9.00777150E+04	1.75357651E+05	-8.60178816E+05	6.71878164E+03

APPENDIX D

PROPROTOR OSCILLATORY FLAPPING DERIVATIVES

Tip-Path-Plane Flapping Derivatives

The longitudinal and lateral tip-path-plane flapping associated with a sinusoidal pitching oscillation of the pylon follow directly from Eqs. C-8a and C-8b of Appendix C. These flapping components, like the proprotor forces and moments, are algebraically complex quantities indicating that the total longitudinal and lateral flapping have components which are inphase (or 180° out of phase) with both pitch angle and pitch rate. The maximum value of \bar{a}_1 or \bar{b}_1 flapping inphase (or 180° out of phase) with the pitch angle is given by the real parts of the complex quantities; the maximum value of \bar{a}_1 or \bar{b}_1 flapping inphase (or 180° out of phase) with the pitch rate is given by the imaginary parts of the complex quantities. Dividing the real parts of \bar{a}_1 and \bar{b}_1 by ϕ_{y_0} and the imaginary parts by $\omega\phi_{y_0}$ the resulting quantities constitute the tip-path-plane flapping derivatives due to pitch angle and pitch rate, respectively.

Blade Flapping Derivatives

The relation between blade flapping and tip-path-plane flapping can be written in terms of complex flapping amplitudes as

$$\bar{\beta} = \bar{a}_1 \sin \psi - \bar{b}_1 \cos \psi \quad (D-1)$$

Writing

$$\begin{aligned}\bar{\beta} &= \beta_1 + i\beta_2 \\ \bar{a}_1 &= f_1 + if_2 \\ \bar{b}_1 &= g_1 + ig_2\end{aligned}\tag{D-2}$$

Eq. D-1 becomes

$$\bar{\beta} = \beta_1 + i\beta_2 = f_1 \sin \psi - g_1 \cos \psi + i(f_2 \sin \psi - g_2 \cos \psi)\tag{D-3}$$

The azimuthal position for which the total blade flapping $\bar{\beta}$ is a maximum is defined by establishing the ψ for which $\bar{\beta}$ is an extremum; that is, the ψ which satisfy

$$\frac{d\bar{\beta}}{d\psi} = f_1 \cos \psi + g_1 \sin \psi + i(f_2 \cos \psi + g_2 \sin \psi) = 0\tag{D-4}$$

Since Eq. D-4 is complex there are really two extremum situations: β_1 is an extremum for the ψ which satisfy

$$\text{Real } \frac{d\bar{\beta}}{d\psi} = \frac{d\beta_1}{d\psi} = 0\tag{D-5}$$

and β_2 is an extremum for the ψ which satisfy

$$\text{Imag } \frac{d\bar{\beta}}{d\psi} = \frac{d\beta_2}{d\psi} = 0\tag{D-6}$$

Whether the extremum are a maximum or a minimum is determined by substituting the ψ which are zeros of Eqs. D-5 and D-6 into

$$\text{Real } \frac{d^2\bar{\beta}}{d\psi^2} = \frac{d^2\beta_1}{d\psi^2} = -f_1 \sin \psi + g_1 \cos \psi \quad (\text{D-7})$$

$$\text{Imag } \frac{d^2\bar{\beta}}{d\psi^2} = \frac{d^2\beta_2}{d\psi^2} = -f_2 \sin \psi + g_2 \cos \psi$$

Then

$$\frac{d^2\beta_1}{d\psi^2}, \frac{d^2\beta_2}{d\psi^2} > 0 \longrightarrow \text{minimum} \quad (\text{D-8})$$

$$\frac{d^2\beta_1}{d\psi^2}, \frac{d^2\beta_2}{d\psi^2} < 0 \longrightarrow \text{maximum}$$

In this way the azimuthal position where blade flapping is algebraically a maximum and a minimum due to pitch angle and pitch rate and the associated values are determined. It is to be noted that the maximum blade flapping due to angle of attack does not occur at the same azimuth as the maximum flapping due to pitch rate.

Dividing the real parts of Eqs. D-2 by ϕ_{y_0} and the imaginary parts by $\omega\phi_{y_0}$ and defining

$$\begin{aligned} f_1/\phi_{y_0} &= f_{1\alpha} & g_1/\phi_{y_0} &= g_{1\alpha} \\ f_2/\omega\phi_{y_0} &= f_{2q} & g_2/\omega\phi_{y_0} &= g_{2q} \\ \beta_1/\phi_{y_0} &= \beta_{1\alpha} & \beta_2/\omega\phi_{y_0} &= \beta_{2q} \end{aligned} \quad (\text{D-9})$$

the maximum values for $\beta_{1\alpha}$ and β_{2q} are given by

$$\beta_{1\alpha} = \sqrt{f_{1\alpha}^2 + g_{1\alpha}^2} \quad (\text{D-10a})$$

$$\beta_{2q} = \sqrt{f_{2q}^2 + g_{2q}^2} \quad (D-10b)$$

If $\beta_{1\alpha}$ and β_{2q} are calculated by means of the operation

$$\beta_{1\alpha} + i\beta_{2q} = \left[(f_{1\alpha} + if_{2q})^2 + (g_{1\alpha} + ig_{2q})^2 \right]^{\frac{1}{2}} \quad (D-11)$$

the $\beta_{1\alpha}$ of Eq. D-10a agrees with that from Eq. D-11. However, the value of β_{2q} from Eq. D-11 corresponds to the ψ position at which $\beta_{1\alpha}$ is a maximum and is therefore not the maximum value of β_{2q} .

Computer program ROTDER4 (Appendix G) calculates both the tip-path-plane derivatives given by Eqs. D-9 and the blade flapping derivatives of Eqs. D-10 as a function of both pylon pitching and yawing frequency. A sample output listing is given in Table D-1. The corresponding input is included with the program listing in Appendix G.

Blade Steady-State Flapping

The steady-state tip-path-plane and blade flapping derivatives are obtained by setting the pylon pitch frequency to zero. Consider the blade flapping derivative due to constant shaft angle of attack. This is given by

$$\beta_{1\alpha} \Big|_{\omega=0} \equiv \beta_{\alpha} = \sqrt{f_{1\alpha}^2 + g_{1\alpha}^2} \quad (D-12)$$

Assuming a symmetric hub restraint and taking the swashplate/pylon coupling and proprotor precone to be zero,

$$f_{1\alpha} = \frac{F_1^2 \lambda^2 A_3 A_5}{K_H^2 + 2F_1 B_3 K_H \tan \delta_3 + F_1^2 [(B_3 \tan \delta_3)^2 + A_5^2]} \quad (D-13a)$$

$$\varepsilon_{1\alpha} = \frac{-F_1 \lambda^2 A_3 [K_H + F_1 B_3 \tan \delta_3]}{K_H^2 + 2F_1 B_3 K_H \tan \delta_3 + F_1^2 [(B_3 \tan \delta_3)^2 + A_5^2]} \quad (D-13b)$$

Hence,

$$\beta_\alpha = \frac{F_1 \lambda^2 A_3 \left[F_1^2 A_5^2 + (K_H + F_1 B_3 \tan \delta_3)^2 \right]^{\frac{1}{2}}}{K_H^2 + 2F_1 B_3 K_H \tan \delta_3 + F_1^2 [(B_3 \tan \delta_3)^2 + A_5^2]} \quad (D-14)$$

Now, from Eq. B-6 of Appendix B,

$$\bar{\omega}_\beta^2 - 1 = \frac{K_H}{I_R \Omega^2} + \frac{1}{2} \gamma \beta_3 \tan \delta_3 \quad (D-15)$$

from which

$$\begin{aligned} \left[I_R \Omega^2 (\bar{\omega}_\beta^2 - 1) \right]^2 &= [K_H + F_1 B_3 \tan \delta_3]^2 \\ &= K_H^2 + 2F_1 B_3 K_H \tan \delta_3 + F_1^2 B_3^2 \tan^2 \delta_3 \end{aligned} \quad (D-16)$$

where F_1 has the same definition as in Appendix C. Using Eq.

D-16

$$\beta_\alpha = \frac{F_1 \lambda^2 A_3}{\left[F_1^2 A_5^2 + \left\{ I_R \Omega^2 (\bar{\omega}_\beta^2 - 1) \right\}^2 \right]^{\frac{1}{2}}} \quad (D-17)$$

or, finally, $\partial\beta/\partial\alpha$ as a function of blade flapping natural frequency is given by

$$\frac{\partial\beta}{\partial\alpha} = \frac{\lambda^2 A_3}{\left[A_5^2 + \frac{4}{\gamma^2} (\bar{\omega}_\beta^2 - 1) \right]^{\frac{1}{2}}} \quad (\text{D-18})$$

The expression analogous to that in Eq. D-18 for the case in which a representative section aerodynamic theory is employed for the blade loading is given by

$$\frac{\partial\beta}{\partial\alpha} = \frac{\tan^2 \bar{\phi}}{\left[1 + \left\{ \frac{8(\bar{\omega}_\beta^2 - 1)}{\gamma \cos \bar{\phi}} \right\}^2 \right]^{\frac{1}{2}}} \quad (\text{D-19})$$

Hub restraint and/or pitch-flap coupling are seen to decrease flapping by detuning the blade flapping natural frequency from one-per-rev so that it is not in resonance with the one-per-rev airload moments arising from shaft angle of attack. For zero hub restraint it is to be noted that since $(\bar{\omega}_\beta^2 - 1)$ enters as a square in the expressions for $\partial\beta/\partial\alpha$, either positive or negative pitch-flap coupling (negative or positive δ_3) are equally effective in reducing flapping.

TABLE D-1

PROPROPOTR OSCILLATORY FLAPPING DERIVATIVES SAMPLE OUTPUT LISTING

ROTOR RPM	VELOCITY		ADVANCE RATIO		LCKK NUMBER	INFLCW ANGLE PHI
	FT/SEC	KNOTS	KEAS	J		
2.3800000E+32	5.91216216E+02	3.5000000E+02	3.5000000E+02	3.87132740E+00	4.54547485E+00	5.86741761E+01

**** BLADE FLAPPING FREQUENCY(CYCLES/REV) = .756 **** BLADE DAMPING(PERCENT CRITICAL) = 20.197

***** PROPROPOTR DYNAMIC FLAPPING DERIVATIVES DUE TO PYLON PITCH *****

PYLON PITCH FREQUENCY			CCOMPONENT FLAPPING DERIVATIVES				TOTAL FLAPPING DERIVATIVE	
CYCLES/REV	CPS	RAD/SEC	AI/PHIY	AI/PHIY DOT	BI/PHIY	BI/PHIY DOT	BETA/PHIY	BETA/PHIY DOT
1.0000E-04	3.9667E-04	2.4923E-03	8.7645E-01	2.8802E-02	1.2306E+00	-3.5830E-01	1.5108E+00	3.5945E-01
5.0000E-02	1.9833E-01	1.2462E+00	9.4564E-01	2.0206E-02	1.1964E+00	-3.6398E-01	1.5250E+00	3.6454E-01
1.0000E-01	3.9667E-01	2.4923E+00	1.1519E+00	8.5775E-03	1.0669E+00	-3.7908E-01	1.5701E+00	3.7917E-01
2.0000E-01	7.9333E-01	4.9847E+00	1.7547E+00	1.5508E-01	1.4492E+01	-3.8668E-01	1.7607E+00	4.1662E-01
4.0000E-01	1.5867E+00	9.9693E+00	-1.9369E-01	2.4329E-01	-1.7695E+00	-3.6366E-02	1.7801E+00	2.4599E-01
6.0000E-01	2.3800E+00	1.4954E+01	-1.1366E+00	1.1113E-01	-1.1737E+00	2.6890E-02	1.6339E+00	1.1434E-01
8.0000E-01	3.1733E+00	1.9939E+01	-1.3686E+00	-6.4023E-02	-8.9848E-01	2.6958E-02	1.6175E+00	6.5467E-02
1.0000E+00	3.9667E+00	2.4923E+01	-1.5227E+00	-4.4687E-02	-8.1258E-01	2.9477E-02	1.7259E+00	5.1415E-02
1.2000E+00	4.7600E+00	2.9908E+01	-1.7372E+00	-3.5769E-02	-8.2340E-01	2.7123E-02	1.9226E+00	4.4889E-02
1.4000E+00	5.5533E+00	3.4893E+01	-2.1823E+00	-3.1012E-02	-8.7491E-01	3.5288E-02	2.3519E+00	4.6979E-02
1.6000E+00	6.3467E+00	3.9877E+01	-3.3537E+00	-2.6265E-02	-1.9968E-02	-4.6299E-01	3.3855E+00	6.1909E-02
1.8000E+00	7.1400E+00	4.4862E+01	-2.6265E+00	4.7210E-02	2.2671E+00	3.6882E-02	3.4696E+00	5.9785E-02
2.0000E+00	7.9333E+00	4.9847E+01	-9.1040E-01	2.5654E-02	1.4093E+00	-1.5911E-03	1.6771E+00	2.5704E-02
2.2000E+00	8.7267E+00	5.4831E+01	-7.6643E-01	1.2302E-02	7.8804E-01	-4.2046E-03	1.0993E+00	1.3001E-02
2.4000E+00	9.5200E+00	5.9816E+01	-7.8839E-01	6.8798E-03	9.1187E-01	-3.5739E-03	9.1999E-01	7.7527E-03
2.6000E+00	1.0313E+01	6.4801E+01	-8.2251E-01	4.2646E-03	3.6573E-01	-2.8338E-03	9.0016E-01	5.1203E-03
2.8000E+00	1.1107E+01	6.9785E+01	-8.5155E-01	2.8322E-03	7.7777E-01	-2.2594E-03	8.9571E-01	3.6230E-03
3.0000E+00	1.1900E+01	7.4770E+01	-8.7455E-01	1.9759E-03	2.1998E-01	-1.8330E-03	9.0179E-01	2.6952E-03
3.2000E+00	1.2693E+01	7.9755E+01	-9.6114E-01	1.8833E-04	5.5513E-02	-4.6418E-04	9.6274E-01	5.0093E-04
3.4000E+01	3.9667E+01	2.4923E+02	-9.9089E-01	1.0561E-05	1.2201E-02	-9.8503E-05	9.9096E-01	9.9067E-05

***** PROPROPOTR DYNAMIC FLAPPING DERIVATIVES DUE TO PYLON YAW *****

PYLON YAW FREQUENCY			COMPONENT FLAPPING DERIVATIVES				TOTAL FLAPPING DERIVATIVE	
CYCLES/REV	CPS	RAD/SEC	AI/PHIZ	AI/PHIZ DOT	BI/PHIZ	BI/PHIZ DOT	BETA/PHIZ	BETA/PHIZ DOT
1.0000E-04	3.9667E-04	2.4923E-03	-1.2306E+00	3.5830E-01	8.7645E-01	2.8802E-02	1.5108E+00	3.5945E-01
5.0000E-02	1.9833E-01	1.2462E+00	-1.1964E+00	3.6398E-01	9.4564E-01	2.0206E-02	1.5250E+00	3.6454E-01
1.0000E-01	3.9667E-01	2.4923E+00	-1.0669E+00	3.7908E-01	1.1519E+00	-8.5775E-03	1.5701E+00	3.7917E-01
2.0000E-01	7.9333E-01	4.9847E+00	-1.4492E-01	3.8668E-01	1.7547E+00	-1.5508E-01	1.7607E+00	4.1662E-01
4.0000E-01	1.5867E+00	9.9693E+00	1.7695E+00	3.6366E-02	-1.9369E-01	-2.4329E-01	1.7801E+00	2.4599E-01
6.0000E-01	2.3800E+00	1.4954E+01	1.1737E+00	2.6890E-02	-1.1366E+00	-1.1113E-01	1.6339E+00	1.1434E-01
8.0000E-01	3.1733E+00	1.9939E+01	8.9848E-01	2.6958E-02	-1.3686E+00	-6.4023E-02	1.6175E+00	6.5467E-02
1.0000E+00	3.9667E+00	2.4923E+01	8.1258E-01	-2.5427E-02	-1.5227E+00	-4.4687E-02	1.7259E+00	5.1415E-02
1.2000E+00	4.7600E+00	2.9908E+01	8.2340E-01	-2.7123E-02	-1.7372E+00	-3.5769E-02	1.9226E+00	4.4889E-02
1.4000E+00	5.5533E+00	3.4893E+01	8.7691E-01	-3.5288E-02	-2.1823E+00	-3.1012E-02	2.3519E+00	4.6979E-02
1.6000E+00	6.3467E+00	3.9877E+01	4.6299E-01	-5.9815E-02	-3.3537E+00	-1.5968E-02	3.3855E+00	6.1909E-02
1.8000E+00	7.1400E+00	4.4862E+01	-2.2671E+00	-3.6882E-02	-2.6265E+00	4.7210E-02	3.4696E+00	5.9785E-02
2.0000E+00	7.9333E+00	4.9847E+01	-1.4093E+00	1.5911E-03	-9.1040E-01	2.5654E-02	1.6771E+00	2.5704E-02
2.2000E+00	8.7267E+00	5.4831E+01	-7.8804E-01	4.2046E-03	-7.6643E-01	1.2302E-02	1.0993E+00	1.3001E-02
2.4000E+00	9.5200E+00	5.9816E+01	-5.1187E-01	3.5739E-03	-7.8839E-01	6.8798E-03	9.1999E-01	7.7527E-03
2.6000E+00	1.0313E+01	6.4801E+01	-3.6573E-01	2.8338E-03	-8.2251E-01	4.2646E-03	9.0016E-01	5.1203E-03
2.8000E+00	1.1107E+01	6.9785E+01	-2.7777E-01	2.2594E-03	-8.5155E-01	2.8322E-03	8.9571E-01	3.6230E-03
3.0000E+00	1.1900E+01	7.4770E+01	-2.1998E-01	1.8330E-03	-8.7455E-01	1.9759E-03	9.0179E-01	2.6952E-03
3.2000E+00	1.2693E+01	7.9755E+01	-5.5513E-02	4.6418E-04	-9.6114E-01	1.8833E-04	9.6274E-01	5.0093E-04
3.4000E+01	3.9667E+01	2.4923E+02	-1.2201E-02	9.8503E-05	-9.9089E-01	1.0561E-05	9.9096E-01	9.9067E-05

APPENDIX E

APPLICATION OF THE SUBSTRUCTURING CONCEPT TO AN AIRCRAFT NATURAL MODE ANALYSIS

Direct and component mode synthesis procedures for natural mode vibration analysis have been described in Chapter 6. Both methods are based on the substructuring concept wherein the continuous structure is divided into smaller components, or substructures, a mathematical model (either discrete or modal) of each substructure established, and the mathematical model of the complete structure arrived at by reassembling the components in a manner consistent with the equations of constraint which enforce deflection compatibility at the interfaces of the components. Formation of the substructure mass and stiffness matrices and the establishment of the equations of constraint are aspects of the overall problem which are common to both methods of analysis. To illustrate the manner of establishing the substructure mass and stiffness matrices and the mechanics of setting down the equations of constraint the substructuring procedure is applied herein to an aircraft structure which admits of a stick model representation for natural mode analysis. The aircraft configuration selected to form the basis of this exercise is the Bell Model 266 tilt-rotor VTOL design evolved during the Army Composite Aircraft Program.

Stick Model Representation of the Model 266 Tilt-Rotor

An artist's conception of the Bell Model 266 tilt-rotor design

has been given in Fig. 1-6 of Chapter 1. This aircraft is depicted in silhouette form in Fig. E-1 along with the stick model established using the beam, spring, and rigid-body components described in Chapter 6. The fuselage, wing, and empennage structures are replaced by nonuniform beams lying along the elastic axes of the respective components. Since the fuselage elastic axis has two changes in slope, three beams are used to represent the fuselage structure. The wing carry-through structure is idealized as a beam-spring, its (rigid-body) inertial properties being combined with the inertia matrix of the second fuselage beam. The pylon structure, consisting of the transmission/engine assembly, is treated as a rigid body inertially. Elastically, the pylon structure from the conversion axis to the front of the transmission case is assumed to be rigid while the portion between the front of the transmission case and the propotor hub is treated as a beam-spring. The propotor blades are assumed to be rigid. Since the blades are rigidly attached to the hub in a gimbaled propotor design (such as the Model 266) the propotors can then be treated as rigid discs in the analysis. The hub is taken to be rigidly attached to the mast.* The geometric offsets between the fuselage elastic axis and the wing carry-through and vertical tail elastic axes, between the outboard end of the wing elastic axis and the conversion axis, and the conversion axis itself are also assumed to be rigid in the analysis.

*For illustrative purposes, the manner in which one could treat a propotor/hub-assembly which is spring-connected to the mast will also be described.

These particular rigidities are enforced mathematically via equations of constraint, as will subsequently be shown.

Since the substructures are treated as distinct and separate components their structural properties and deflection characteristics are defined relative to axes local to each component. These local right-handed axis systems are also employed to establish the deflection compatibility equations at the junctions of the substructures. With reference to Fig. E-2 the set of local junction coordinate axes used in setting down the equations of constraint is identifiable by subscripts. Each of the directions so indicated is taken to be positive. Vectors representing positive rotations $\alpha_r, \beta_r, \gamma_r$ (not shown) about x_r, y_r, z_r , respectively, are taken in the same direction as vectors representing positive x_r, y_r, z_r . A short-hand notation for a column vector of these junction or connection coordinates is given by $\{X\}_r$ herein, where

$$\{X\}_r \equiv \begin{Bmatrix} x_r \\ y_r \\ z_r \\ \alpha_r \\ \beta_r \\ \gamma_r \end{Bmatrix} \equiv \begin{Bmatrix} x \\ y \\ z \\ \alpha \\ \beta \\ \gamma \end{Bmatrix}_r \quad (E-1)$$

$r = 1, 2, \dots, 15$

Several auxiliary right-handed coordinate systems (which are not associated with degrees of freedom) are employed to facilitate setting down the equations of constraint. These are also shown in Fig. E-2 and are distinguished by Roman numeral superscripts. A short-hand notation for a column vector of these auxiliary connection coordinates is given by $\{X\}^s$ herein, where

$$\{X\}^s \equiv \begin{Bmatrix} x^s \\ y^s \\ z^s \\ \alpha^s \\ \beta^s \\ \gamma^s \end{Bmatrix} \equiv \begin{Bmatrix} x \\ y \\ z \\ \alpha \\ \beta \\ \gamma \end{Bmatrix}^s \quad (E-2)$$

$s = i, ii, \dots, vi$

Employing the available structural data* lumped-mass/stiffness discretizations were established for the fuselage, wing, and empennage beams. These are summarized in Tables E-1 to E-3. Inertial properties of components treated as rigid bodies inertially are given in Table E-4 while the elastic properties of beam-spring components are listed in Table E-5. A summary of the pertinent geometric quantities is contained in Table E-6. Utilizing aircraft symmetry about a vertical plane through the center of the fuselage

*Exploratory Definition Final Report, Model 266 Composite Aircraft Program, Volume 7 - Dynamics, Report 266-099-207, Bell Helicopter Company, July 1967.

attention is directed to separate symmetric and anti-symmetric formulations. A consequence of this analytical separation into symmetric and anti-symmetric problems is the identification of several displacements and rotations which can be set to zero a priori in both formulations. Also, either on the basis of physical considerations or simply for expediency, the displacements and/or rotations in some coordinate directions can be discarded. For this reason it is convenient to distinguish the coordinates constituting the vectors $\{X\}_r$ from the actual (nodal) degrees of freedom. The nodal degrees of freedom are denoted by q_j herein. The column vector containing all these freedoms, $\{q\}$, may be directly identified with the vector $\{z\}$ in Chapter 6.

Symmetric Formulation

The degrees of freedom employed in the symmetric analysis are identified in Table E-7. The airframe is partitioned into 10 substructures having a total of 144 degrees of freedom.

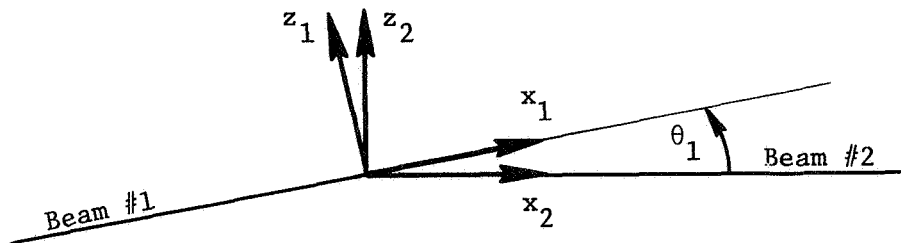
(a) Constraint Equations

The substructures are physically connected to form the total structure by requiring deflection compatibility at the interfaces of the substructures. For compatibility the deflection vectors of adjacent substructures at their point of mutual attachment must be equal when expressed in a common coordinate system. The common coordinates considered here are one or the other of the local coordinate systems of the contiguous substructures. Assuming the displacements and rotations to be small, the deflection vectors of

adjacent substructures at their point of mutual attachment are related by a diagonally partitioned rotational transformation matrix $[R]$. Since rotational deflections can be treated as a vector if the rotations are small the rotational deflections of adjacent substructures at their mutual point of attachment are related by the same coordinate rotation matrix as the displacements. The two submatrices comprising $[R]$ are thus identical and are denoted herein by $[T]$. For the general three-dimensional problem with six coordinates associated with each station, $[R]$ is of order 6×6 and $[T]$ is of order 3×3 .

To aid in setting down the equations of constraint a series of auxiliary sketches showing the substructure junctions and associated coordinate systems will be employed in conjunction with Fig. E-2. For illustrative purposes somewhat more detail is indicated in the example herein than would normally be required in practice.

Fuselage:



At the junction of fuselage beam #1 and #2 the relation expressing the equality of the deflections at the left end of beam #2 and the

deflections at the right end of beam #1 relative to coordinates local to beam #2 has the form

$$\begin{Bmatrix} x \\ y \\ z \\ \alpha \\ \beta \\ \gamma \end{Bmatrix}_2 = \begin{bmatrix} [T_1] & [0] \\ [0] & [T_1] \end{bmatrix} \begin{Bmatrix} x \\ y \\ z \\ \alpha \\ \beta \\ \gamma \end{Bmatrix}_1 \equiv [R_1]\{X\}_1 \quad (\text{E-3})$$

where the connection coordinate vectors $\{X\}_1$ and $\{X\}_2$ are identified with degrees of freedom according to

$$\begin{Bmatrix} x \\ y \\ z \\ \alpha \\ \beta \\ \gamma \end{Bmatrix}_2 = \begin{Bmatrix} q_{24} \\ 0 \\ q_{12} \\ 0 \\ -q_{18} \\ 0 \end{Bmatrix} \quad \begin{Bmatrix} x \\ y \\ z \\ \alpha \\ \beta \\ \gamma \end{Bmatrix}_1 = \begin{Bmatrix} q_{11} \\ 0 \\ q_5 \\ 0 \\ -q_{10} \\ 0 \end{Bmatrix} \quad (\text{E-4})$$

and the appropriate coordinate rotation matrix $[T_1]$ is given by

$$[T_1] \equiv \begin{bmatrix} \cos \theta_1 & 0 & -\sin \theta_1 \\ 0 & 1 & 0 \\ \sin \theta_1 & 0 & \cos \theta_1 \end{bmatrix} \quad (\text{E-5})$$

Since there are no displacements or rotations out of the vertical plane of symmetry in a symmetric formulation $y_1, \alpha_1, \gamma_1, y_2, \alpha_2,$ and γ_2 are zero. The minus signs associated with q_{18} and q_{10} in Eqs. E-4 have been introduced in order to have the usual definition of positive slope. This has been done here merely for convenience. Several sign changes of this type will be introduced during the course of this development for similar reasons. Expanding Eq. E-3 using Eqs. E-4 and E-5, the resultant constraint equations at this junction are given by

$$q_{24} = q_{11} \cos \theta_1 - q_5 \sin \theta_1$$

$$0 = 0$$

$$q_{12} = q_{11} \sin \theta_1 + q_5 \cos \theta_1$$

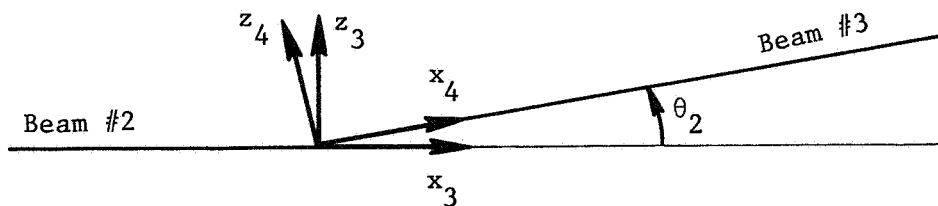
$$0 = 0$$

(E-6)

$$-q_{18} = -q_{10}$$

$$0 = 0$$

At the junction of fuselage beams #2 and #3



we write, in a similar manner,

$$\begin{Bmatrix} x \\ y \\ z \\ \alpha \\ \beta \\ \gamma \end{Bmatrix}_3 = \begin{bmatrix} [T_2] & [0] \\ \hline [0] & [T_2] \end{bmatrix} \begin{Bmatrix} x \\ y \\ z \\ \alpha \\ \beta \\ \gamma \end{Bmatrix}_4 \quad (\text{E-7})$$

where

$$\begin{Bmatrix} x \\ y \\ z \\ \alpha \\ \beta \\ \gamma \end{Bmatrix}_3 = \begin{Bmatrix} a_{24} \\ 0 \\ a_{17} \\ 0 \\ -a_{23} \\ 0 \end{Bmatrix} \quad \begin{Bmatrix} x \\ y \\ z \\ \alpha \\ \beta \\ \gamma \end{Bmatrix}_4 = \begin{Bmatrix} a_{41} \\ 0 \\ a_{25} \\ 0 \\ -a_{33} \\ 0 \end{Bmatrix} \quad (\text{E-8})$$

and

$$[T_2] = \begin{bmatrix} \cos \theta_2 & 0 & -\sin \theta_2 \\ 0 & 1 & 0 \\ \sin \theta_2 & 0 & \cos \theta_2 \end{bmatrix} \quad (\text{E-9})$$

thereby arriving at the constraint equations

$$a_{24} = a_{41} \cos \theta_2 - a_{25} \sin \theta_2$$

$$0 = 0$$

$$a_{17} = a_{41} \sin \theta_2 + a_{25} \cos \theta_2$$

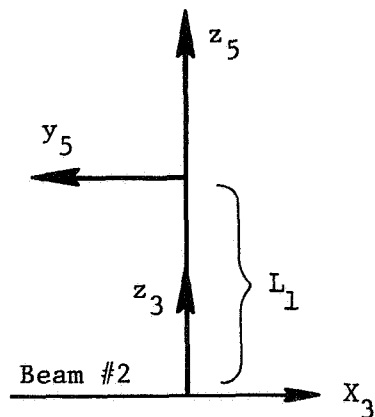
(E-10)

$$0 = 0$$

$$-a_{23} = -a_{33}$$

$$0 = 0$$

Rigid Offset Between Fuselage and Wing Carry-Through Elastic Axes:



The equations relating the deflections at the right end of fuselage beam #2 to the deflections of the inboard end of the wing carry-through beam-spring are given by

$$\begin{Bmatrix} x \\ y \\ z \\ \alpha \\ \beta \\ \gamma \end{Bmatrix}_3 = \begin{bmatrix} 0 & -1 & 0 & | & -L_1 & 0 & 0 \\ 1 & 0 & 0 & | & 0 & -L_1 & 0 \\ 0 & 0 & 1 & | & 0 & 0 & 0 \\ \hline 0 & 0 & 0 & | & 0 & -1 & 0 \\ 0 & 0 & 0 & | & 1 & 0 & 0 \\ 0 & 0 & 0 & | & 0 & 0 & 1 \end{bmatrix} \begin{Bmatrix} x \\ y \\ z \\ \alpha \\ \beta \\ \gamma \end{Bmatrix}_5 \quad (\text{E-11})$$

where $\{X\}_3$ has already been given in Eq. E-8 and

$$\begin{Bmatrix} x \\ y \\ z \\ \alpha \\ \beta \\ \gamma \end{Bmatrix}_5 = \begin{Bmatrix} 0 \\ q_{42} \\ q_{43} \\ q_{44} \\ q_{45} \\ q_{46} \end{Bmatrix} \quad (\text{E-12})$$

Eq. E-11 leads to the constraint equations

$$q_{24} = -q_{42} - L_1 q_{44}$$

$$0 = -L_1 q_{45}$$

$$q_{17} = q_{43}$$

$$0 = -q_{45}$$

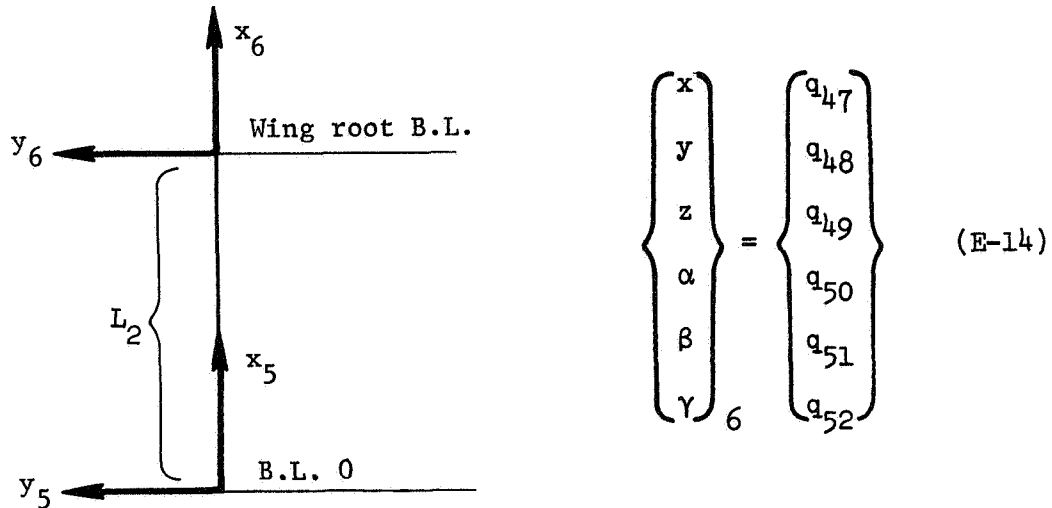
(E-13)*

*Note that this set of constraint equations contains one redundant equation. This redundant equation need not be discarded, however, since use of the method of Walton and Steeves (cf. Chapter 6) for establishing independent system coordinates requires no special consideration in this case.

$$-a_{23} = a_{44}$$

$$0 = a_{46}$$

Wing Carry-Through Structure:



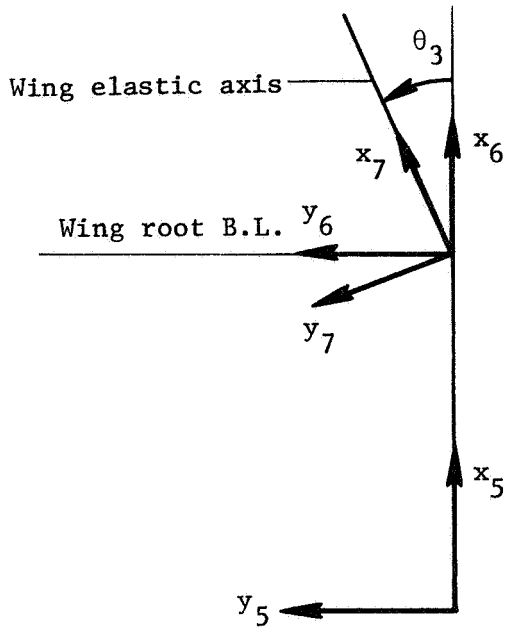
On the basis of considerations related to its structural configuration, twisting of the wing carry-through structure is negligible in a symmetric mode of oscillation. Hence, the beam-spring representation of the wing carry-through structures is taken to be rigid in torsion. This "constraint" is specified by writing

$$a_{50} - a_{44} = 0 \quad (\text{E-15})$$

Axial extensions of this member are also assumed to be negligible. Since $x_5 = 0$ (cf. Eq. E-12) this implies the additional constraint

$$a_{47} = 0 \quad (\text{E-16})$$

Wing:



At the wing elastic axis/wing carry-through elastic axis junction:

$$\begin{Bmatrix} x \\ y \\ z \\ \alpha \\ \beta \\ \gamma \end{Bmatrix}_6 = \begin{bmatrix} & & & & & \\ & [T_3] & & [0] & & \\ & & & & & \\ & & & & & \\ & & & & & \\ & [0] & & [T_3] & & \\ & & & & & \end{bmatrix} \begin{Bmatrix} x \\ y \\ z \\ \alpha \\ \beta \\ \gamma \end{Bmatrix}_7 \quad (E-17)$$

where

$$\begin{Bmatrix} x \\ y \\ z \\ \alpha \\ \beta \\ \gamma \end{Bmatrix}_6 = \begin{Bmatrix} a_{47} \\ a_{48} \\ a_{49} \\ a_{50} \\ a_{51} \\ a_{52} \end{Bmatrix} \quad \begin{Bmatrix} x \\ y \\ z \\ \alpha \\ \beta \\ \gamma \end{Bmatrix}_7 = \begin{Bmatrix} a_{88} \\ a_{67} \\ a_{53} \\ a_{81} \\ -a_{60} \\ a_{74} \end{Bmatrix} \quad (E-18)$$

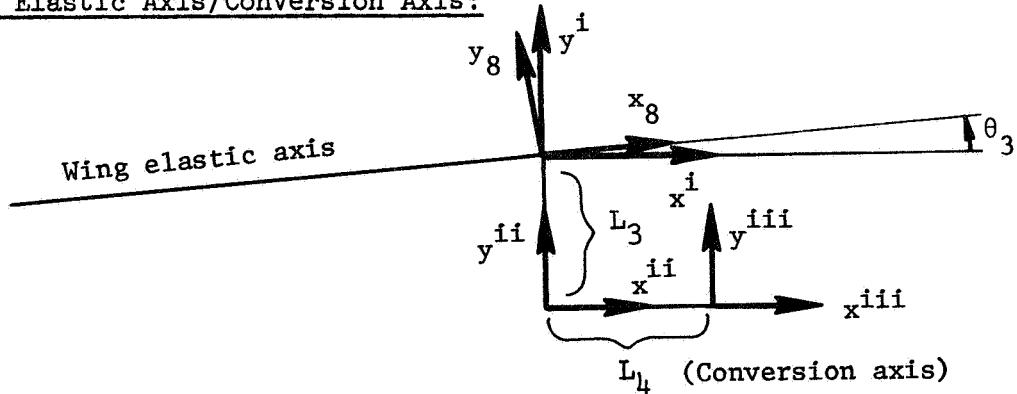
and

$$[T_3] = \begin{bmatrix} \cos \theta_3 & -\sin \theta_3 & 0 \\ \sin \theta_3 & \cos \theta_3 & 0 \\ 0 & 0 & 1 \end{bmatrix} \quad (E-19)$$

The above lead to

$$\begin{aligned} q_{47} &= q_{88} \cos \theta_3 - q_{67} \sin \theta_3 \\ q_{48} &= q_{88} \sin \theta_3 + q_{67} \cos \theta_3 \\ q_{49} &= q_{53} \\ q_{50} &= q_{81} \cos \theta_3 + q_{60} \sin \theta_3 \\ q_{51} &= q_{81} \sin \theta_3 - q_{60} \cos \theta_3 \\ q_{52} &= q_{74} \end{aligned} \quad (E-20)$$

Wing Elastic Axis/Conversion Axis:



An expression relating the coordinates at the last wing elastic axis station, $\{X\}_8$, to the intermediate (auxiliary) coordinates $\{X\}^i$ is given by

$$\begin{Bmatrix} x \\ y \\ z \\ \alpha \\ \beta \\ \gamma \end{Bmatrix}_8 = \begin{bmatrix} [T_4] & [O] \\ [O] & [T_4] \end{bmatrix} \begin{Bmatrix} x \\ y \\ z \\ \alpha \\ \beta \\ \gamma \end{Bmatrix}^i \equiv [\textcircled{1}] \{X\}^i \quad (\text{E-21})$$

As pointed out earlier, the auxiliary coordinates $\{X\}^i$ are not degrees of freedom but have been introduced here merely for convenience in arriving at the equations of constraint. The appropriate values of $\{X\}_8$ and $[T_4]$ to be used in Eq. E-21 are

$$\begin{Bmatrix} x \\ y \\ z \\ \alpha \\ \beta \\ \gamma \end{Bmatrix}_8 = \begin{Bmatrix} a_{88} \\ a_{73} \\ a_{59} \\ a_{87} \\ -a_{66} \\ a_{80} \end{Bmatrix} \quad (\text{E-22})$$

and

$$[T_4] = \begin{bmatrix} \cos \theta_3 & \sin \theta_3 & 0 \\ -\sin \theta_3 & \cos \theta_3 & 0 \\ 0 & 0 & 1 \end{bmatrix} \quad (\text{E-23})$$

From the sketch above the intermediate coordinate vectors $\{X\}^i$ and $\{X\}^{ii}$ are seen to be related as

$$\begin{Bmatrix} x \\ y \\ z \\ \alpha \\ \beta \\ \gamma \end{Bmatrix}^i = \begin{bmatrix} 1 & 0 & 0 & | & 0 & 0 & -L_3 \\ 0 & 1 & 0 & | & 0 & 0 & 0 \\ 0 & 0 & 1 & | & L_3 & 0 & 0 \\ \hline 0 & 0 & 0 & | & 1 & 0 & 0 \\ 0 & 0 & 0 & | & 0 & 1 & 0 \\ 0 & 0 & 0 & | & 0 & 0 & 1 \end{bmatrix} \begin{Bmatrix} x \\ y \\ z \\ \alpha \\ \beta \\ \gamma \end{Bmatrix}^{ii} \equiv [2] \{X\}^{ii} \quad (\text{E-24})$$

If the conversion axis (length L_4 in the sketch) is taken to be flexible and treated as a beam-spring we would have

$$\{X\}^{ii} = \{Q\}_{CA_L} \quad (\text{E-25})$$

where $\{Q\}_{CA_L}$ is a column vector containing the degrees of freedom associated with the inboard end of the conversion axis beam-spring. The appropriate constraint equations would then have the matrix form

$$\{X\}_8 = [1][2]\{Q\}_{CA_L} \quad (\text{E-26})$$

Similarly, at the outboard end of the conversion axis beam-spring we would have

$$\{X\}^{iii} = \{Q\}_{CA_R} \quad (\text{E-27})$$

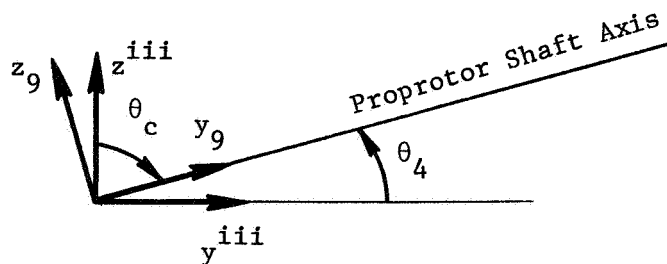
where $\{Q\}_{CA_R}$ is a column vector containing the degrees of freedom

for the outboard end. If the conversion axis is taken as completely rigid $\{X\}^{ii}$ and $\{X\}^{iii}$ are not identified with degrees of freedom so that

$$\begin{Bmatrix} x \\ y \\ z \\ \alpha \\ \beta \\ \gamma \end{Bmatrix}^{ii} = \begin{bmatrix} 1 & 0 & 0 & | & 0 & 0 & 0 \\ 0 & 1 & 0 & | & 0 & 0 & -L_h \\ 0 & 0 & 1 & | & 0 & L_h & 0 \\ \hline 0 & 0 & 0 & | & 1 & 0 & 0 \\ 0 & 0 & 0 & | & 0 & 1 & 0 \\ 0 & 0 & 0 & | & 0 & 0 & 1 \end{bmatrix} \begin{Bmatrix} x \\ y \\ z \\ \alpha \\ \beta \\ \gamma \end{Bmatrix}^{iii} \equiv [3] \{X\}^{iii} \quad (E-28)$$

Herein, the conversion axis is assumed to be completely rigid so that Eq. E-28 is applicable. The portion of the pylon structure between the conversion axis and the front of the transmission case is also assumed to be rigid for the analysis. The flexibility of the pylon mast is accounted for by representing it as a beam-spring. However, the only elastic deformations of the mast which will be admitted analytically are vertical and lateral bending, motion in the remaining two directions being solely of the rigid-body type.

Proprotor Shaft Axis:



Although a portion of the pylon structure forward of the conversion axis is treated as though it were rigid elastically the

coordinate axes fixed to the shaft (axes with subscript 9 in the sketch) will be identified with actual degrees of freedom. This is necessitated by the (arbitrary) decision to define the rigid body inertial properties of the complete pylon relative to coordinate axes at the position of the conversion axis/propertor shaft axis intersection rather than relative to body axes at the center of gravity of the pylon.

$$\{x\}^{iii} = \begin{bmatrix} [T_5] & | & [0] \\ \hline & & \\ [0] & | & [T_5] \end{bmatrix} \{x\}_9 \equiv [4] \{x\}_9 \quad (E-29)$$

where

$$\begin{Bmatrix} x \\ y \\ z \\ \alpha \\ \beta \\ \gamma \end{Bmatrix}_9 = \begin{Bmatrix} q_{89} \\ q_{90} \\ q_{91} \\ q_{92} \\ -q_{93} \\ q_{94} \end{Bmatrix} \quad (E-30)$$

and

$$[T_5] = \begin{bmatrix} 1 & 0 & 0 \\ 0 & \cos \theta_4 & -\sin \theta_4 \\ 0 & \sin \theta_4 & \cos \theta_4 \end{bmatrix} \quad (E-31)$$

On the basis of considerations in the preceding subsection and directly above:

$$\{x\}_8 = [1][2][3][4]\{x\}_9 \quad (E-32)$$

Making the appropriate substitutions into Eq. E-32 and expanding the resulting individual constraint equations become

$$\begin{aligned} a_{88} &= a_{89} \cos \theta_3 + a_{90} \sin \theta_3 \cos \theta_4 - a_{91} \sin \theta_3 \sin \theta_4 \\ &\quad + a_{93} \sin \theta_4 [L_4 \sin \theta_3 + L_3 \cos \theta_3] \\ &\quad - a_{94} \cos \theta_4 [L_4 \sin \theta_3 + L_3 \cos \theta_3] \end{aligned}$$

$$\begin{aligned} a_{73} &= -a_{89} \sin \theta_3 + a_{90} \cos \theta_3 \cos \theta_4 - a_{91} \cos \theta_3 \sin \theta_4 \\ &\quad + a_{93} \sin \theta_4 [L_4 \cos \theta_3 - L_3 \sin \theta_3] \\ &\quad - a_{94} \cos \theta_4 [L_4 \cos \theta_3 - L_3 \sin \theta_3] \end{aligned}$$

(E-33)

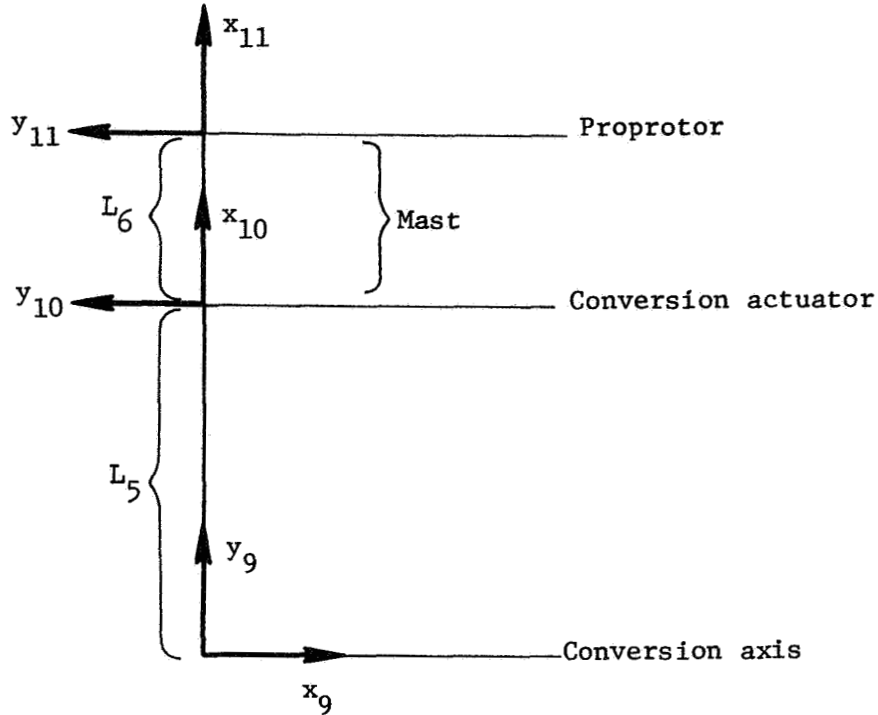
$$a_{87} = a_{92} \cos \theta_3 - a_{93} \sin \theta_3 \cos \theta_4 - a_{94} \sin \theta_3 \sin \theta_4$$

$$a_{59} = a_{90} \sin \theta_4 + a_{91} \cos \theta_4 + L_3 a_{92} - a_{93} L_4 \cos \theta_4 - a_{94} L_4 \sin \theta_4$$

$$-a_{66} = -a_{92} \sin \theta_3 - a_{93} \cos \theta_3 \cos \theta_4 - a_{94} \cos \theta_3 \sin \theta_4$$

$$a_{80} = -a_{93} \sin \theta_4 + a_{94} \cos \theta_4$$

Pylon Mast:



The pylon mast, the portion of the drive shaft between the front of the transmission case (to which the conversion actuator attaches) and the proprotor hub is treated as a beam-spring. Since the length L_5 corresponds to the segment of the pylon which is treated as rigid $\{X\}_9$ and $\{X\}_{10}$ are related as

$$\begin{Bmatrix} x \\ y \\ z \\ \alpha \\ \beta \\ \gamma \end{Bmatrix}_9 = \begin{bmatrix} 0 & -1 & 0 & | & 0 & 0 & L_5 \\ 1 & 0 & 0 & | & 0 & 0 & 0 \\ 0 & 0 & 1 & | & 0 & L_5 & 0 \\ \hline 0 & 0 & 0 & | & 0 & -1 & 0 \\ 0 & 0 & 0 & | & 1 & 0 & 0 \\ 0 & 0 & 0 & | & 0 & 0 & 1 \end{bmatrix} \begin{Bmatrix} x \\ y \\ z \\ \alpha \\ \beta \\ \gamma \end{Bmatrix}_{10} \tag{E-34}$$

where $\{X\}_{10}$, containing the degrees of freedom associated with the aft end of the mast beam-spring, is given by

$$\begin{Bmatrix} x \\ y \\ z \\ \alpha \\ \beta \\ \gamma \end{Bmatrix}_{10} = \begin{Bmatrix} a_{95} \\ a_{96} \\ a_{97} \\ -a_{98} \\ -a_{99} \\ a_{100} \end{Bmatrix} \quad (\text{E-35})$$

Expanding Eq. E-34 and using Eqs. E-30 and E-35 leads to the constraint equations

$$\begin{aligned} a_{89} &= -a_{96} + L_5 a_{100} \\ a_{90} &= a_{95} \\ a_{91} &= a_{97} - L_5 a_{99} \\ a_{92} &= a_{99} \\ -a_{93} &= -a_{98} \\ a_{94} &= a_{100} \end{aligned} \quad (\text{E-36})$$

At the forward end of the mast:

$$\begin{Bmatrix} x \\ y \\ z \\ \alpha \\ \beta \\ \gamma \end{Bmatrix}_{11} = \begin{Bmatrix} a_{101} \\ a_{102} \\ a_{103} \\ -a_{104} \\ -a_{105} \\ a_{106} \end{Bmatrix} \quad (\text{E-37})$$

To analytically suppress the axial and torsional deformations of the mast yet allowing for rigid-body motions in these directions we write

$$q_{101} - q_{95} = 0 \quad (E-38)$$

$$q_{104} - q_{98} = 0$$

These equations stipulate that the relative axial and torsional deformations between the ends of the mast are zero.

Proprotor: The coordinates describing the proprotor disc, $\{X\}_R$, are taken in the same sense as $\{X\}_{11}$. Hence

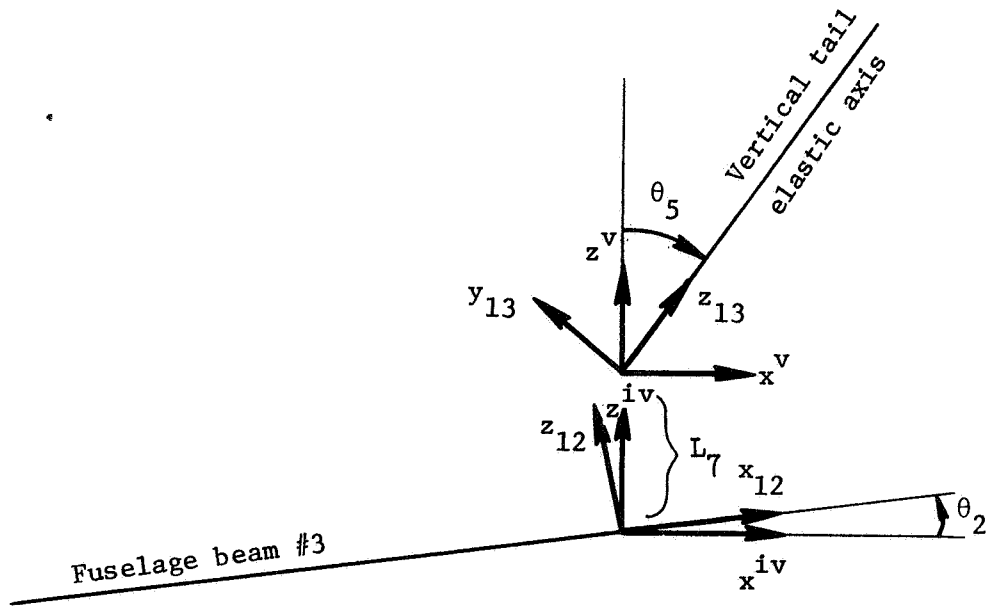
$$\{X\}_R = \begin{Bmatrix} q_{107} \\ q_{108} \\ q_{109} \\ -q_{110} \\ -q_{111} \\ q_{112} \end{Bmatrix} \quad (E-39)$$

Since the proprotor/hub combination is rigidly fastened to the mast*, $\{X\}_{11} = \{X\}_R$ and the constraint equations become

*The case of a spring-connected hub will be described later.

$$\begin{Bmatrix} a_{101} \\ a_{102} \\ a_{103} \\ -a_{104} \\ -a_{105} \\ a_{106} \end{Bmatrix} = \begin{Bmatrix} a_{107} \\ a_{108} \\ a_{109} \\ -a_{110} \\ -a_{111} \\ a_{112} \end{Bmatrix} \quad (E-40)$$

Empennage :



At the aft end of fuselage beam #3 we have

$$\begin{Bmatrix} x \\ y \\ z \\ \alpha \\ \beta \\ \gamma_{12} \end{Bmatrix} = \begin{bmatrix} [T_6] & [0] \\ [0] & [T_6] \end{bmatrix} \begin{Bmatrix} x^{iv} \\ y \\ z \\ \alpha \\ \beta \\ \gamma \end{Bmatrix} \equiv [5] \{x\}^{iv} \quad (E-41)$$

where

$$\begin{Bmatrix} x \\ y \\ z \\ \alpha \\ \beta \\ \gamma_{12} \end{Bmatrix} = \begin{Bmatrix} a_{41} \\ 0 \\ a_{32} \\ 0 \\ -a_{40} \\ 0 \end{Bmatrix} \quad (\text{E-42})$$

and

$$[T_6] = \begin{bmatrix} \cos \theta_2 & 0 & \sin \theta_2 \\ 0 & 1 & 0 \\ -\sin \theta_2 & 0 & \cos \theta_2 \end{bmatrix} \quad (\text{E-43})$$

Since the offset distance L_7 is taken to be rigid the intermediate coordinate vectors $\{X\}^{iv}$ and $\{X\}^v$ are related according to

$$\begin{Bmatrix} x \\ y \\ z \\ \alpha \\ \beta \\ \gamma \end{Bmatrix}^{iv} = \begin{bmatrix} 1 & 0 & 0 & 0 & -L_7 & 0 \\ 0 & 1 & 0 & L_7 & 0 & 0 \\ 0 & 0 & 1 & 0 & 0 & 0 \\ \hline 0 & 0 & 0 & 1 & 0 & 0 \\ 0 & 0 & 0 & 0 & 1 & 0 \\ 0 & 0 & 0 & 0 & 0 & 1 \end{bmatrix} \begin{Bmatrix} x \\ y \\ z \\ \alpha \\ \beta \\ \gamma \end{Bmatrix}^v \equiv [6] \{X\}^v \quad (\text{E-44})$$

At the base of the vertical tail elastic axis, $\{X\}^v$ and $\{X\}_{13}$ are related as

$$\begin{Bmatrix} x \\ y \\ z \\ \alpha \\ \beta \\ \gamma \end{Bmatrix}^v = \begin{bmatrix} [T_7] & [0] \\ \hline [0] & [T_7] \end{bmatrix} \begin{Bmatrix} x \\ y \\ z \\ \alpha \\ \beta \\ \gamma_{13} \end{Bmatrix} \equiv [7] \{X\}_{13} \quad (\text{E-45})$$

where

$$\begin{Bmatrix} x \\ y \\ z \\ \alpha \\ \beta \\ \gamma_{13} \end{Bmatrix} = \begin{Bmatrix} 0 \\ a_{13} \\ a_{123} \\ -a_{118} \\ 0 \\ 0 \end{Bmatrix} \quad (\text{E-46})$$

and

$$[T_7] = \begin{bmatrix} 0 & -\cos\theta_5 & \sin\theta_5 \\ 1 & 0 & 0 \\ 0 & \sin\theta_5 & \cos\theta_5 \end{bmatrix} \quad (\text{E-47})$$

Assembling the series of transformation matrices indicated above:

$$\{X\}_{12} = [5][6][7]\{X\}_{13} \quad (\text{E-48})$$

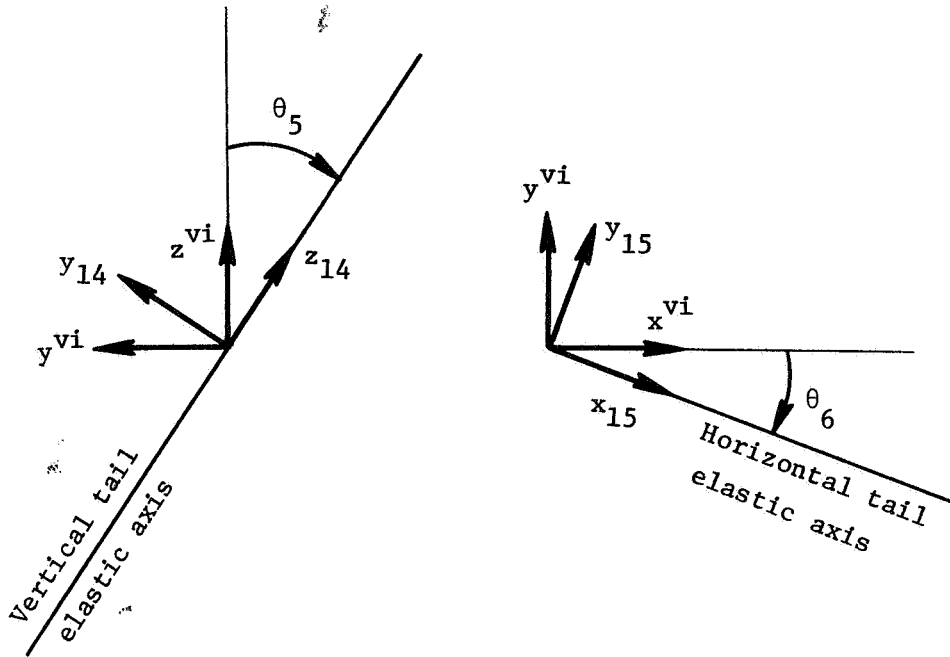
from which we obtain

$$\begin{aligned} a_{41} &= a_{113} [-\cos\theta_2 \cos\theta_5 + \sin\theta_2 \sin\theta_5] \\ &\quad + a_{123} [\cos\theta_2 \sin\theta_5 + \sin\theta_2 \cos\theta_5] \\ &\quad + a_{118} L_4 \cos\theta_2 \\ 0 &= 0 \\ a_{32} &= a_{113} [\sin\theta_2 \cos\theta_5 + \sin\theta_5 \cos\theta_2] \\ &\quad + a_{123} [-\sin\theta_2 \sin\theta_5 + \cos\theta_2 \cos\theta_5] \\ &\quad - a_{118} L_7 \sin\theta_2 \end{aligned} \quad (\text{E-49})$$

$$0 = 0$$

$$-a_{40} = -a_{118}$$

$$0 = 0$$



At the junction of the vertical and horizontal tail elastic axes, $\{X\}_{14}$ and $\{X\}^{vi}$ are related as

$$\begin{Bmatrix} x \\ y \\ z \\ \alpha \\ \beta \\ \gamma \end{Bmatrix}_{14} = \begin{bmatrix} [T_8] & [0] \\ \hline [0] & [T_8] \end{bmatrix} \begin{Bmatrix} x \\ y \\ z \\ \alpha \\ \beta \\ \gamma \end{Bmatrix}^{vi} \equiv [\textcircled{8}] \{x\}^{vi} \quad (E-50)$$

where

$$\begin{Bmatrix} x \\ y \\ z \\ \alpha \\ \beta \\ \gamma \end{Bmatrix}_{14} = \begin{Bmatrix} 0 \\ a_{115} \\ a_{123} \\ -a_{120} \\ 0 \\ 0 \end{Bmatrix} \quad (\text{E-51})$$

and

$$[T_8] = \begin{bmatrix} 1 & 0 & 0 \\ 0 & \cos\theta_5 & \sin\theta_5 \\ 0 & -\sin\theta_5 & \cos\theta_5 \end{bmatrix} \quad (\text{E-52})$$

while $\{X\}^{vi}$ and $\{X\}_{15}$ are related according to

$$\begin{Bmatrix} x \\ y \\ z \\ \alpha \\ \beta \\ \gamma \end{Bmatrix}^{vi} = \begin{bmatrix} [T_9] & [0] \\ \hline [0] & [T_9] \end{bmatrix} \begin{Bmatrix} x \\ y \\ z \\ \alpha \\ \beta \\ \gamma \end{Bmatrix}_{15} \equiv [\textcircled{9}] \{X\}_{15} \quad (\text{E-53})$$

with $\{X\}_{15}$ and $[T_9]$ being given by

$$\begin{Bmatrix} x \\ y \\ z \\ \alpha \\ \beta \\ \gamma \end{Bmatrix}_{15} = \begin{Bmatrix} a_{144} \\ a_{132} \\ a_{124} \\ a_{140} \\ -a_{128} \\ a_{136} \end{Bmatrix} \quad (\text{E-54})$$

and

$$[T_9] = \begin{bmatrix} \cos\theta_6 & \sin\theta_6 & 0 \\ -\sin\theta_6 & \cos\theta_6 & 0 \\ 0 & 0 & 1 \end{bmatrix} \quad (\text{E-55})$$

Eqs. E-50 and E-53 imply the matrix relation

$$\{X\}_{14} \equiv [8][9]\{X\}_{15} \quad (E-56)$$

from which, upon substitution of appropriate quantities, there results

$$\begin{aligned} 0 &= a_{144} \cos \theta_6 + a_{132} \sin \theta_6 \\ a_{115} &= -a_{144} \cos \theta_5 \sin \theta_6 + a_{132} \cos \theta_5 \cos \theta_6 + a_{124} \sin \theta_5 \\ a_{123} &= a_{144} \sin \theta_5 \sin \theta_6 - a_{132} \sin \theta_5 \cos \theta_6 + a_{124} \cos \theta_5 \\ -a_{120} &= a_{140} \cos \theta_6 - a_{128} \sin \theta_6 \\ 0 &= -a_{140} \cos \theta_5 \sin \theta_6 - a_{128} \cos \theta_5 \cos \theta_6 + a_{136} \sin \theta_5 \\ 0 &= a_{140} \sin \theta_5 \sin \theta_6 + a_{128} \sin \theta_5 \cos \theta_6 + a_{136} \cos \theta_5 \end{aligned} \quad (E-57)$$

This completes the derivation of the equations of constraint for the symmetric formulation. For easy reference these equations are summarized in Table E-8. Since there are 49 constraint equations and 144 degrees of freedom, the matrix of coefficients of the constraint equations, [C], will be of order 49 x 144.

(b) Rigid-Mass Components

Wing Carry-Through: The rigid body inertial properties of the wing carry-through structure are combined with the inertia matrix of fuselage beam #2 by treating the center of gravity of the carry-through structure as rigidly attached to the last (right hand) station of that beam, for which (from Eq. E-8)

$$\begin{Bmatrix} x \\ y \\ z \\ \alpha \\ \beta \\ \gamma \end{Bmatrix}_3 = \begin{Bmatrix} q_{24} \\ 0 \\ q_{17} \\ 0 \\ -q_{23} \\ 0 \end{Bmatrix} \quad (\text{E-58})$$

The results of Appendix A will be employed to establish an equivalent inertia matrix relative to the axes $\{X\}_3$ using the inertia properties defined relative to body axes at the center of gravity. Assuming that the principal body axes at the center of gravity of the carry-through structure are parallel to axes x_3 , y_3 , and z_3 the direction cosines l_{ij} (cf. Eq. A-13) are given by

$$l_{ij} = \begin{cases} 1 & i = j \\ 0 & i \neq j \end{cases} \quad (\text{E-59})$$

From Table E-6 we have

$$\begin{Bmatrix} a \\ b \\ c \end{Bmatrix} = \begin{Bmatrix} 0 \\ 0 \\ 46.6 \end{Bmatrix} \quad (\text{E-60})$$

Substituting Eqs. E-59 and E-60 into Eq. A-13, the matrix which effects the desired transformation assumes the form

$$[\theta] = \left[\begin{array}{ccc|ccc} 1 & 0 & 0 & 0 & 46.6 & 0 \\ 0 & 1 & 0 & -46.6 & 0 & 0 \\ 0 & 0 & 1 & 0 & 0 & 0 \\ \hline 0 & 0 & 0 & 1 & 0 & 0 \\ 0 & 0 & 0 & 0 & 1 & 0 \\ 0 & 0 & 0 & 0 & 0 & 1 \end{array} \right] \quad (\text{E-61})$$

For comparative purposes $\{X\}_3$ herein is equivalent to $\{X\}_0$ in Appendix A. Using the data supplied in Table E-4 the inertia matrix of the carry-through structure relative to body axes at the center of gravity is given by the diagonal matrix

$$[M_{cg}]_{CT} = \begin{bmatrix} .88 & & & & & \\ & .88 & & & & \\ & & .88 & & & \\ & & & 0 & & \\ & & & & 725.2 & \\ & & & & & 0 \end{bmatrix} \quad (\text{E-62})^*$$

Substituting Eqs. E-61 and E-62 into Eq. A-6 gives

$$[M]_{CT} = \begin{bmatrix} .88 & 0.0 & 40.6 \\ 0.0 & 0.88 & 0.0 \\ 40.6 & 0.0 & 2595.0 \end{bmatrix} \begin{bmatrix} a_{24} \\ a_{17} \\ -a_{23} \end{bmatrix} \quad (\text{E-63})$$

* $[M_{cg}]_{CT}$ herein is equivalent to $[M]_c$ of Eq. A-6.

Absorbing the minus sign associated with q_{23} into the inertia matrix* and reordering the degrees of freedom finally yields

$$[M]_{CT} = \begin{matrix} & \boxed{\begin{matrix} q_{17} & q_{23} & q_{24} \end{matrix}} \\ \begin{bmatrix} .88 & 0 & 0 \\ 0 & 2595 & -40.6 \\ 0 & -40.6 & .88 \end{bmatrix} & \boxed{\begin{matrix} q_{17} \\ q_{23} \\ q_{24} \end{matrix}} \end{matrix} \quad (E-64)$$

as the matrix of additional terms to be added to the diagonal inertia matrix of fuselage beam #2. The corresponding stiffness matrix is null since there is no strain energy associated with any rigid body motion.

Pylon: As indicated earlier the rigid body inertial properties of the pylon will be defined relative to a coordinate axis system at the junction of the conversion axis and the shaft axis rather than maintaining a center-of-gravity definition. Again, the results of Appendix A will be employed to effect this transformation. From Table E-6 the quantities a, b, and c for use in Eq. A-13 are given by

$$\begin{Bmatrix} a \\ b \\ c \end{Bmatrix} = \begin{Bmatrix} 31.2 \\ 0 \\ -19.0 \end{Bmatrix} \quad (E-65)$$

*By multiplying the third row and column of Eq. E-63 by minus one.

The principal axes at the pylon center of gravity are taken to be parallel to the axes x_g, y_g, z_g so that Eq. E-59 is valid here also. The values given by Eqs. E-59 and E-65 are substituted into Eq. A-13 to obtain the transformation matrix $[\theta]$. Substituting this result into Eq. A-6, using the values in Table E-4 to define the inertia matrix at the center of gravity, and taking into account the difference in orientation of the coordinate directions $\{X\}_g$ relative to those assumed in the derivation contained in Appendix A the desired pylon inertia matrix can be put into the form

$$[M]_{\text{Pylon}} = \begin{matrix} & \begin{matrix} q_{g9} & q_{g0} & q_{g1} & q_{g2} & q_{g3} & q_{g4} \end{matrix} \\ \begin{matrix} 7.25 & 0 & 0 & 0 & 137.8 & -226 \\ 0 & 7.25 & 0 & 137.8 & 0 & 0 \\ 0 & 0 & 7.25 & 226 & 0 & 0 \\ 0 & 137.8 & 226 & 16627 & 0 & 0 \\ 137.8 & 0 & 0 & 0 & 6417 & -4297.8 \\ -226 & 0 & 0 & 0 & -4297.8 & 13180 \end{matrix} & \begin{matrix} q_{g9} \\ q_{g0} \\ q_{g1} \\ q_{g2} \\ q_{g3} \\ q_{g4} \end{matrix} \end{matrix} \quad (\text{E-66})$$

where the minus sign associated with q_{g3} (cf. Eq. E-30) has been absorbed into the inertia matrix. The corresponding stiffness matrix is null.

Proprotor: The proprotor is treated as a rigid circular disc.

Since the coordinate axes at the center of gravity of the proprotor disc are oriented such that they are principal axes the inertia matrix is diagonal and can be constructed directly from the data supplied in Table E-4:

$$[M]_{\text{Rotor}} = \begin{array}{c} \begin{array}{cccccc} q_{107} & q_{108} & q_{109} & q_{110} & q_{111} & q_{112} \end{array} \\ \left[\begin{array}{cccccc} 3.64 & & & & & \\ & 3.64 & & & & \\ & & 3.64 & & & \\ & & & 28476 & & \\ & & & & 14238 & \\ & \text{Null} & & & & 14238 \end{array} \right] \begin{array}{c} q_{107} \\ q_{108} \\ q_{109} \\ q_{110} \\ q_{111} \\ q_{112} \end{array} \end{array} \quad (\text{E-67})^*$$

The companion stiffness matrix is null since the proprotor hub is taken to be rigidly attached to the mast. This matrix would not be null if the hub were spring-connected to the mast, as will be demonstrated below.

(c) Springs

The wing carry-through structure and the pylon mast are both treated elastically as beam-springs, their inertias being incorporated with other components.

Wing Carry-Through: Since x_5 has been set to zero a priori (cf. Eq. E-12) the appropriate beam-spring stiffness matrix is of order 11 x 11 and is given by that in Fig. 6-5 of Chapter 6 with the first row and column struck out. The resultant matrix is shown in Fig. E-3 along with the ordering of the degrees of freedom. Tables E-5 and E-6 contain the necessary data to evaluate the terms of the matrix. Constraint Eqs. E-15 and E-16 in conjunction with

*The minus signs associated with q_{110} and q_{111} (cf. Eq. E-39) have been absorbed into the inertia matrix.

the 11 x 11 stiffness matrix given in Fig. E-3 imply that twisting and both the elastic and rigid-body axial motions of the beam-spring representing the wing carry-through structure are removed as degrees of freedom, in accordance with earlier discussions.

An alternate approach in this situation would be to additionally strike out the rows and columns corresponding to q_{47} , thereby reducing the matrix of Fig. E-3 to one of order 10 x 10, and then deleting constraint equation E-16.

Pylon Mast: The stiffness matrix of the pylon mast beam-spring is given in Fig. E-4. Again, Tables E-5 and E-6 contain the data required to evaluate the individual terms of the matrix.

Some comments are included here to indicate the manner of treating a propotor/hub assembly which is connected to the mast by springs. For illustrative purposes assume that the propotor/hub combination is allowed to flap longitudinally and laterally with respect to the mast, the flapping motion being restrained by linear springs K_{a_1} and K_{b_1} , respectively (cf. Chapter 3). Since longitudinal and lateral angular motions of the propotor disc relative to the mast are permitted the last two constraint equations given in Eq. E-40 must be deleted. Recalling the treatment of springs in the spring-mass analogy employed in Chapter 6 to illustrate the manner of including fuel slosh in a launch vehicle vibration analysis we require an expression for the strain energy stored in the springs. The appropriate expression here is given by

$$V_S = \frac{1}{2} K_{a_1} (q_{105} - q_{111})^2 + \frac{1}{2} K_{b_1} (q_{106} - q_{112})^2 \quad (\text{E-68})$$

Substituting Eq. E-68 into Lagrange's equation then leads to

$$[\Delta K] = \begin{array}{c} \boxed{\begin{array}{cccc} q_{105} & q_{106} & q_{111} & q_{112} \end{array}} \\ \left[\begin{array}{cccc} K_{a_1} & 0 & -K_{a_1} & 0 \\ 0 & K_{b_1} & 0 & -K_{b_1} \\ -K_{a_1} & 0 & K_{a_1} & 0 \\ 0 & -K_{b_1} & 0 & K_{b_1} \end{array} \right] \boxed{\begin{array}{c} q_{105} \\ q_{106} \\ q_{111} \\ q_{112} \end{array}} \end{array} \quad (\text{E-69})$$

as the matrix of spring terms to be added to the partitioned system stiffness matrix, $[\bar{K}]$. Note that the negative terms in Eq. E-69 couple the stiffness matrices for the pylon mast and propotor substructures.

Anti-Symmetric Formulation

The considerations related to the symmetric formulation have illustrated the manner of establishing substructure mass and stiffness matrices and the mechanics of setting down equations of constraint. A corresponding derivation for the anti-symmetric case would, for the most part, be repetitious. For this reason a

summary-type treatment, for the most part listing only final results which are different from the symmetric case, is given here.

The anti-symmetric formulation is based on the same stick model and the same stations employed in the symmetric formulation, leading to a problem having 165 degrees of freedom. These freedoms are identified in Table E-9.

(a) Constraint Equations

For anti-symmetric motions of the airframe the twist of the wing carry-through structure is not negligible and the beam-spring which is taken to represent it must now be permitted freedom in twist. Although axial extensions of the wing carry-through are still negligible the ability to translate axially as a rigid body must be provided for. The final constraint equations, 48 in number, are summarized in Table E-10.

(b) Rigid-Mass Components

Wing Carry-Through: Here the vector $\{X\}_3$ is given by

$$\{X\}_3 = \begin{Bmatrix} 0 \\ q_{21} \\ 0 \\ q_{33} \\ 0 \\ q_{27} \end{Bmatrix} \quad (E-70)$$

so that

$$[M]_{CT} = \begin{array}{|c|} \hline \begin{array}{ccc} q_{21} & q_{27} & q_{33} \end{array} \\ \hline \begin{bmatrix} .88 & 0 & -40.6 \\ 0 & 0 & 0 \\ -40.6 & 0 & 1870.0 \end{bmatrix} \\ \hline \end{array} \begin{array}{|c|} \hline q_{21} \\ q_{27} \\ q_{33} \\ \hline \end{array} \quad (E-71)$$

Pylon:

$$[M]_{Pylon} = \begin{array}{|c|} \hline \begin{array}{cccccc} q_{106} & q_{107} & q_{108} & q_{109} & q_{110} & q_{111} \end{array} \\ \hline \begin{bmatrix} 7.25 & 0 & 0 & 0 & 137.8 & -226 \\ 0 & 7.25 & 0 & 137.8 & 0 & 0 \\ 0 & 0 & 7.25 & 226 & 0 & 0 \\ 0 & 137.8 & 226 & 16627 & 0 & 0 \\ 137.8 & 0 & 0 & 0 & 6417 & -4297.8 \\ -226 & 0 & 0 & 0 & -4297.8 & 13180 \end{bmatrix} \\ \hline \end{array} \begin{array}{|c|} \hline q_{106} \\ q_{107} \\ q_{108} \\ q_{109} \\ q_{110} \\ q_{111} \\ \hline \end{array} \quad (E-72)$$

Proprotor:

$$[M]_{ROTOR} = \begin{array}{|c|} \hline \begin{array}{cccccc} q_{124} & q_{125} & q_{126} & q_{127} & q_{128} & q_{129} \end{array} \\ \hline \begin{bmatrix} 3.64 & & & & & \\ & 3.64 & & & & \\ & & 3.64 & & & \\ & & & 28476 & & \\ & & & & 14238 & \\ & & & & & 14238 \end{bmatrix} \\ \hline \end{array} \begin{array}{|c|} \hline q_{124} \\ q_{125} \\ q_{126} \\ q_{127} \\ q_{128} \\ q_{129} \\ \hline \end{array} \quad (E-73)$$

(c) Springs

Wing Carry-Through: Since axial rigid body motion of the carry-through is included in the anti-symmetric formulation the beam-spring representing it has a stiffness matrix of order 12 x 12 having the form given in Fig. E-4. The degrees of freedom shown there, $(q_{95} - q_{106})$, are replaced by q_{58} through q_{69} respectively. Tables E-5 and E-6 contain the data needed to evaluate the individual terms of the matrix.

Pylon Mast: The pylon mast beam-spring stiffness matrix is also given by Fig. E-4 if we replace q_{95} through q_{106} by q_{118} through q_{123} respectively. Again Tables E-5 and E-6 provide the data required to evaluate the individual terms of the matrix.

*

Numerical Results Using the Direct Method

The direct method of analysis was used to calculate the symmetric and anti-symmetric free-free modes and frequencies for several pylon tilt angles. A summary of these frequencies for the first five elastic modes is given in Table E-11. The modal vectors for the first three symmetric modes for $\theta_c = 90^\circ$ are listed in Table E-12. The first five symmetric modes for $\theta_c = 90^\circ$ are given in Fig. E-5. Corresponding results have been calculated by Bell.* However, since their mathematical model was significantly different from that employed herein a direct

*Ibid.

numerical comparison with their results can not be made.

A sample input for the symmetric case with $\theta_c = 90^\circ$ is included as part of the listing of the computer program package for the direct method of analysis in Appendix H.

Additional Applications of the Direct Method

Two simple applications of the direct method are included in some comparative studies with the method of component mode synthesis in Appendix F. A comparison of the results from the direct analysis with experimentally measured modes and frequencies of a model of one of the configurations is also presented there.

The direct method of analysis as embodied in the computer program package listed in Appendix H has also been employed in two other studies. The first consisted of the determination of the symmetric modes of the aircraft shown in silhouette in Fig. 6-2, using the stick model indicated there, for use in a free-free flutter analysis of the wing and horizontal tail.* The second consisted in generating the modes of a pivoting wing for use in a subsequent flutter analysis.†

*Results of this work given limited distribution.

†Unpublished work.

TABLE E-1
FUSELAGE DISCRETIZATION

Station	Local Coordinate Position (inches)	Mass (lb-sec ² /in)	Torsional Inertia (lb-sec ² -in)	EI vertical (lb-in ²)	EI side (lb-in ²)	GJ (lb-in ²)
Beam #1						
1	0.0	.104	500.	.34x10 ¹⁰	.30x10 ¹⁰	.36x10 ¹⁰
2	35.0	.120	1000.	.80	.75	.84
3	60.0	.300	4000.	1.60	1.50	2.00
4	85.0	1.440	25000.	3.20	2.80	4.00
5	120.0	2.160	15500.	-----	-----	-----
Beam #2						
1	0.0	2.160	15500.	8.00x10 ¹⁰	4.50x10 ¹⁰	7.00x10 ¹⁰
2	40.0	5.280	37200.	13.60	7.60	8.60
3	75.0	2.040	24000.	16.00	9.40	8.80
4	100.0	.240	11000.	16.60	10.00	8.80
5	120.0	.960	23000.	16.80	10.40	8.80
6	140.0	.840	15500.	-----	-----	-----
Beam #3						
1	0.0	.840	15500.	16.80x10 ¹⁰	10.45x10 ¹⁰	8.80x10 ¹⁰
2	35.0	1.878	36500.	16.60	10.40	8.80
3	63.0	2.900	38000.	14.60	8.80	8.80
4	105.0	10.560	41000.	9.00	6.00	8.10
5	150.0	2.556	41000.	4.50	4.00	6.00
6	188.0	.720	9000.	3.00	2.80	4.00
7	235.0	.350	6000.	1.80	1.78	2.60
8	287.0	.600	4000.	-----	-----	-----
Total Mass: Beam #1 = 4.124, Beam #2 = 11.520, Beam #3 = 20.404						

TABLE E-2

WING DISCRETIZATION

Station	Local Coordinate Position (inches)	Mass (lb-sec ² /in)	Static Unbalance* (lb-sec ²)	Torsional Inertia About e.a. (lb-sec ² -in)	EI vertical (lb-in ²)	EI chord (lb-in ²)	GJ (lb-in ²)
1	0.0	.881	-5.18	389.0	15.0x10 ⁹	35.0x10 ⁹	12.3x10 ⁹
2	34.0	.705	-6.48	414.0	12.4	30.0	10.4
3	75.0	.518	-4.92	246.0	9.2	24.0	8.2
4	125.0	.648	-5.57	231.0	6.0	18.0	6.0
5	173.0	.357	-6.48	251.0	4.6	15.0	4.6
6	209.0	1.480	-9.32	526.0	4.15	14.2	4.2
7	222.0	0.0	0.0	0.0	-----	-----	-----
Total Mass = 4.589 lb-sec ² /in							
*Negative static unbalance indicates that section center of gravity is aft of section elastic axis.							

TABLE E-3*

EMPENNAGE DISCRETIZATION

Station	Local Coordinate Position (inches)	Mass (lb-sec ² /in)	Static Unbalance* (lb-sec ²)	Torsional Inertia about e.a. (lb-sec ² -in)	EI side (lb-in ²)	EI chord (lb-in ²)	GJ (lb-in ²)
Vertical Tail							
1	0.0	.0863	1.69	139.4	17.5x10 ⁸	15.2x10 ⁹	13.0x10 ⁸
2	36.4	.1306	1.40	108.5	6.5	8.0	7.9
3	71.5	.1244	1.27	86.8	2.0	3.4	4.0
4	108.0	.1166	1.05	64.0	1.0	1.8	1.8
5	145.0	.0833	.795	43.8	-----	-----	-----
Total Mass = .542 lb-sec ² /in							
Horizontal Tail							
1	0.0	0.0	0.0	0.0	4.5x10 ⁸	3.0x10 ⁹	4.0x10 ⁸
2	35.0	0.0	0.0	0.0	2.0	1.5	2.75
3	65.0	.36	0.0	21.8	1.2	.75	1.0
4	100.0	0.0	0.0	0.0	-----	-----	-----
Total Mass = .36 lb-sec ² /in							
*Positive static unbalance indicates that section center of gravity is forward of section elastic axis.							

TABLE E-4

COMPONENT INERTIAL PROPERTIES TREATED AS RIGID

PROPROPOTOR

Mass	3.64 lb-sec ² /in
Flapping Inertia	
Longitudinal	14238 lb-sec ² -in
Lateral	14238 lb-sec ² -in
Polar Inertia	28476 lb-sec ² -in

PYLON

Mass	7.25 lb-sec ² /in
C. G. Inertia	
Pitch	6950 lb-sec ² -in
Roll	3800 lb-sec ² -in
Yaw	6120 lb-sec ² -in

WING CARRY-THROUGH

Mass	.88 lb-sec ² /in
C. G. Inertia	
Pitch	725.2 lb-sec ² -in
Roll	Not Available
Yaw	Not Available

TABLE E-5

STIFFNESS PROPERTIES OF COMPONENTS TREATED AS SPRINGS

Wing Carry-Through*

EI_{vertical}	=	$15.7 \times 10^9 \text{ lb-in}^2$
EI_{lateral}	=	$36.9 \times 10^9 \text{ lb-in}^2$
GJ	=	$12.8 \times 10^9 \text{ lb-in}^2$

Pylon Mast[†]

EI_{vertical}	=	$2.5 \times 10^9 \text{ lb-in}^2$
EI_{lateral}	=	$2.5 \times 10^9 \text{ lb-in}^2$

* AE is taken to be zero as no axial elastic motion is "allowed"

[†] Both AE and GJ are taken to be zero as only rigid-body axial and torsional motions are admitted.

TABLE E-6

GEOMETRIC QUANTITIES EMPLOYED IN VIBRATION ANALYSIS

ANGLES

θ_1	9.5° (.1658 Radians)
θ_2	5.6° (.09774 Radians)
θ_3	4.5° (.07854 Radians)
θ_4	Variable (90°-conversion angle)
θ_5	25° (.4363 Radians)
θ_6	15° (.2618 Radians)

LENGTHS

L_1	46.1 inches
L_2	42.0 inches
L_3	17.0 inches
L_4	17.0 inches
L_5	55.0 inches
L_6	28.0 inches
L_7	15.0 inches
Wing Carry-Through	
a	0
b	0
c	46.1 inches
Pylon	
a	31.2 inches
b	0
c	-19.0 inches

TABLE E-7
 IDENTIFICATION OF DEGREES OF FREEDOM FOR
 SYMMETRIC VIBRATION ANALYSIS

FUSELAGE

Beam #1

$q_1 - q_5$	Displs. } Slopes }	Vertical Bending
$q_6 - q_{10}$		
q_{11}	Axial Rigid Body Translation	

Beam #2

$q_{12} - q_{17}$	Displs. } Slopes }	Vertical Bending
$q_{18} - q_{23}$		
q_{24}	Axial Rigid Body Translation	

Beam #3

$q_{25} - q_{32}$	Displs. } Slopes }	Vertical Bending
$q_{33} - q_{40}$		
q_{41}	Axial Rigid Body Translation	

Wing Carry-Through Structure

$$q_{42} - q_{52}$$

WING

$q_{53} - q_{59}$	Displs. } Slopes }	Vertical Bending
$q_{60} - q_{66}$		
$q_{67} - q_{73}$	Displs. } Slopes }	Chordwise Bending
$q_{74} - q_{80}$		
$q_{81} - q_{87}$	Torsion	
q_{88}	Axial Rigid Body Translation	

TABLE E-7 (Concluded)

PYLON

Transmission/Engine Assembly

$q_{89} - q_{94}$ Rigid Body Translations & Rotations

Mast

$q_{95} - q_{106}$

PROPRTOR

$q_{107} - q_{112}$ Rigid Body Translations & Rotations

EMPENNAGE

Vertical Tail

$q_{113} - q_{117}$ Displs. }
 $q_{118} - q_{122}$ Slopes } Chordwise Bending

q_{123} Axial Rigid Body Translation

Horizontal Tail

$q_{124} - q_{127}$ Displs. }
 $q_{128} - q_{131}$ Slopes } Vertical Bending

$q_{132} - q_{135}$ Displs. }
 $q_{136} - q_{139}$ Slopes } Chordwise Bending

$q_{140} - q_{143}$ Torsion

q_{144} Axial Rigid Body Translation

TABLE E-8

CONSTRAINT EQUATIONS FOR SYMMETRIC VIBRATION ANALYSIS

$$a_{11} \cos \theta_1 - a_5 \sin \theta_1 - a_{24} = 0$$

$$a_{11} \sin \theta_1 + a_5 \cos \theta_1 - a_{12} = 0$$

$$-a_{10} + a_{18} = 0$$

$$a_{41} \cos \theta_2 - a_{25} \sin \theta_2 - a_{24} = 0$$

$$a_{41} \sin \theta_2 + a_{25} \cos \theta_2 - a_{17} = 0$$

$$-a_{33} + a_{23} = 0$$

$$a_{42} + L_1 a_{44} + a_{24} = 0$$

$$-L_1 a_{45} = 0$$

$$a_{43} - a_{17} = 0$$

$$-a_{45} = 0$$

$$a_{44} + a_{23} = 0$$

$$a_{46} = 0$$

$$a_{50} - a_{44} = 0$$

$$a_{47} = 0$$

$$a_{88} \cos \theta_3 - a_{67} \sin \theta_3 - a_{47} = 0$$

$$a_{88} \sin \theta_3 + a_{67} \cos \theta_3 - a_{48} = 0$$

$$a_{53} - a_{44} = 0$$

$$a_{81} \cos \theta_3 + a_{60} \sin \theta_3 - a_{50} = 0$$

$$a_{81} \sin \theta_3 - a_{60} \cos \theta_3 - a_{51} = 0$$

$$a_{74} - a_{52} = 0$$

TABLE E-8 (Continued)

$$\begin{aligned}
& a_{89} \cos \theta_3 + a_{90} \sin \theta_3 \cos \theta_4 - a_{91} \sin \theta_3 \sin \theta_4 \\
& \quad + a_{93} \sin \theta_4 [L_4 \sin \theta_3 + L_3 \cos \theta_3] \\
& \quad - a_{94} \cos \theta_4 [L_4 \sin \theta_3 + L_3 \cos \theta_3] - a_{88} = 0 \\
& -a_{89} \sin \theta_3 + a_{90} \cos \theta_3 \cos \theta_4 - a_{91} \cos \theta_3 \sin \theta_4 \\
& \quad + a_{93} \sin \theta_4 [L_4 \cos \theta_3 - L_3 \sin \theta_3] \\
& \quad - a_{94} \cos \theta_4 [L_4 \cos \theta_3 - L_3 \sin \theta_3] - a_{73} = 0 \\
& a_{92} \cos \theta_3 - a_{93} \sin \theta_3 \cos \theta_4 - a_{94} \sin \theta_3 \sin \theta_4 - a_{87} = 0 \\
& a_{90} \sin \theta_4 + a_{91} \cos \theta_4 + L_3 a_{92} - a_{93} L_4 \cos \theta_4 \\
& \quad - a_{94} L_4 \sin \theta_4 - a_{59} = 0 \\
& a_{92} \sin \theta_3 + a_{93} \cos \theta_3 \cos \theta_4 + a_{94} \cos \theta_3 \sin \theta_4 + a_{66} = 0 \\
& -a_{93} \sin \theta_4 + a_{94} \cos \theta_4 - a_{80} = 0 \\
& -a_{96} + L_5 a_{100} - a_{89} = 0 \\
& a_{95} - a_{90} = 0 \\
& a_{97} - L_5 a_{99} - a_{91} = 0 \\
& a_{99} - a_{92} = 0 \\
& -a_{98} + a_{93} = 0 \\
& a_{100} - a_{94} = 0 \\
& a_{101} - a_{95} = 0 \\
& a_{104} - a_{98} = 0 \\
& a_{107} - a_{101} = 0 \\
& a_{108} - a_{102} = 0 \\
& a_{109} - a_{103} = 0 \\
& -a_{110} + a_{104} = 0
\end{aligned}$$

TABLE E-8 (Concluded)

$$-a_{111} + a_{105} = 0$$

$$a_{112} - a_{106} = 0$$

$$a_{113} [-\cos \theta_2 \cos \theta_5 + \sin \theta_2 \sin \theta_5] + a_{123} [\cos \theta_2 \sin \theta_5 + \sin \theta_2 \cos \theta_5] + a_{118} L_7 \cos \theta_2 - a_{41} = 0$$

$$a_{113} [\sin \theta_2 \cos \theta_5 + \sin \theta_5 \cos \theta_2] + a_{123} [-\sin \theta_2 \sin \theta_5 + \cos \theta_2 \cos \theta_5] - a_{118} L_7 \sin \theta_2 - a_{32} = 0$$

$$-a_{118} + a_{40} = 0$$

$$a_{144} \cos \theta_6 + a_{132} \sin \theta_6 = 0$$

$$-a_{144} \cos \theta_5 \sin \theta_6 + a_{132} \cos \theta_5 \cos \theta_6 + a_{124} \sin \theta_5 - a_{115} = 0$$

$$a_{144} \sin \theta_5 \sin \theta_6 - a_{132} \sin \theta_5 \cos \theta_6 + a_{124} \cos \theta_5 - a_{123} = 0$$

$$a_{140} \cos \theta_6 - a_{128} \sin \theta_6 + a_{120} = 0$$

$$-a_{140} \cos \theta_5 \sin \theta_6 - a_{128} \cos \theta_5 \cos \theta_6 + a_{136} \sin \theta_5 = 0$$

$$a_{140} \sin \theta_5 \sin \theta_6 + a_{128} \sin \theta_5 \cos \theta_6 + a_{136} \cos \theta_5 = 0$$

TABLE E-9

IDENTIFICATION OF DEGREES OF FREEDOM FOR
ANTI-SYMMETRIC VIBRATION ANALYSIS

FUSELAGE

Beam #1

$q_1 - q_5$	Displs. } Slopes }	Side Bending
$q_6 - q_{10}$		
$q_{11} - q_{15}$	Torsion	

Beam #2

$q_{16} - q_{21}$	Displs. } Slopes }	Side Bending
$q_{22} - q_{27}$		
$q_{28} - q_{33}$	Torsion	

Beam #3

$q_{34} - q_{41}$	Displs. } Slopes }	Side Bending
$q_{42} - q_{49}$		
$q_{50} - q_{57}$	Torsion	

Wing Carry-Through Structure

 $q_{58} - q_{69}$ WING

$q_{70} - q_{76}$	Displs. } Slopes }	Vertical Bending
$q_{77} - q_{83}$		
$q_{84} - q_{90}$	Displs. } Slopes }	Chordwise Bending
$q_{91} - q_{97}$		
$q_{98} - q_{104}$	Torsion	
q_{105}	Axial Rigid Body Translation	

TABLE E-9 (Concluded)

PYLON

Transmission/Engine Assembly

 $q_{106} - q_{111}$

Rigid Body Translations & Rotations

Mast

 $q_{112} - q_{123}$ PROPROPOTOR $q_{124} - q_{129}$

Rigid Body Translations & Rotations

EMPENNAGE

Vertical Tail

 $q_{130} - q_{134}$

Displs. }

 $q_{135} - q_{139}$

Slopes }

Side Bending

 $q_{140} - q_{144}$

Torsion

Horizontal Tail

 $q_{145} - q_{148}$

Displs. }

 $q_{149} - q_{152}$

Slopes }

Vertical Bending

 $q_{153} - q_{156}$

Displs. }

 $q_{157} - q_{160}$

Slopes }

Chordwise Bending

 $q_{161} - q_{164}$

Torsion

 q_{165}

Axial Rigid Body Translation

TABLE E-10

CONSTRAINT EQUATIONS FOR ANTI-SYMMETRIC VIBRATION ANALYSIS

$$a_5 - a_{16} = 0$$

$$a_{15} \cos \theta_1 - a_{10} \sin \theta_1 - a_{28} = 0$$

$$a_{15} \sin \theta_1 + a_{10} \cos \theta_1 - a_{22} = 0$$

$$a_{34} - a_{21} = 0$$

$$a_{50} \cos \theta_2 - a_{42} \sin \theta_2 - a_{33} = 0$$

$$a_{50} \sin \theta_2 + a_{42} \cos \theta_2 - a_{27} = 0$$

$$a_{59} + L_1 a_{61} = 0$$

$$a_{58} - L_1 a_{62} - a_{21} = 0$$

$$a_{60} = 0$$

$$a_{62} + a_{33} = 0$$

$$a_{61} = 0$$

$$a_{63} - a_{27} = 0$$

$$a_{64} - a_{58} = 0$$

$$a_{105} \cos \theta_3 - a_{84} \sin \theta_3 - a_{64} = 0$$

$$a_{105} \sin \theta_3 + a_{84} \cos \theta_3 - a_{65} = 0$$

$$a_{70} - a_{66} = 0$$

$$a_{98} \cos \theta_3 + a_{77} \sin \theta_3 - a_{67} = 0$$

$$a_{98} \sin \theta_3 - a_{77} \cos \theta_3 - a_{68} = 0$$

$$a_{91} - a_{69} = 0$$

$$\begin{aligned} a_{106} \cos \theta_3 + a_{107} \sin \theta_3 \cos \theta_4 - a_{108} \sin \theta_3 \sin \theta_4 \\ + a_{110} \sin \theta_4 [L_4 \sin \theta_3 + L_3 \cos \theta_3] \\ - a_{111} \cos \theta_4 [L_4 \sin \theta_3 + L_3 \cos \theta_3] - a_{105} = 0 \end{aligned}$$

TABLE E-10 (Continued)

$$\begin{aligned}
& -a_{106} \sin \theta_3 + a_{107} \cos \theta_3 \cos \theta_4 - a_{108} \cos \theta_3 \sin \theta_4 \\
& \quad + a_{110} \sin \theta_4 [L_4 \cos \theta_3 - L_3 \sin \theta_3] \\
& \quad - a_{111} \cos \theta_4 [L_4 \cos \theta_3 - L_3 \sin \theta_3] - a_{90} = 0 \\
& a_{109} \cos \theta_3 - a_{110} \sin \theta_3 \cos \theta_4 - a_{111} \sin \theta_3 \sin \theta_4 - a_{104} = 0 \\
& a_{107} \sin \theta_4 + a_{108} \cos \theta_4 + L_3 a_{109} - a_{110} L_4 \cos \theta_4 \\
& \quad - a_{111} L_4 \sin \theta_4 - a_{76} = 0 \\
& -a_{109} \sin \theta_3 - a_{110} \cos \theta_3 \cos \theta_4 - a_{111} \cos \theta_3 \sin \theta_4 + a_{83} = 0 \\
& -a_{110} \sin \theta_4 + a_{111} \cos \theta_4 - a_{97} = 0 \\
& -a_{113} + L_5 a_{117} - a_{106} = 0 \\
& a_{112} - a_{107} = 0 \\
& a_{114} - L_5 a_{116} - a_{108} = 0 \\
& a_{116} - a_{109} = 0 \\
& -a_{115} + a_{110} = 0 \\
& a_{117} - a_{111} = 0 \\
& a_{118} - a_{112} = 0 \\
& a_{121} - a_{115} = 0 \\
& a_{124} - a_{118} = 0 \\
& a_{125} - a_{114} = 0 \\
& a_{126} - a_{120} = 0 \\
& -a_{127} + a_{121} = 0 \\
& -a_{128} + a_{122} = 0 \\
& a_{129} - a_{123} = 0 \\
& a_{130} - a_{135} L_7 \cos \theta_5 + a_{140} L_7 \sin \theta_5 - a_{41} = 0
\end{aligned}$$

TABLE E-10 (Concluded)

$$q_{135} [-\cos \theta_2 \cos \theta_5 + \sin \theta_2 \sin \theta_5] + q_{140} [\cos \theta_2 \sin \theta_5 + \sin \theta_2 \cos \theta_5] - q_{57} = 0$$

$$q_{135} [\sin \theta_2 \cos \theta_5 + \cos \theta_2 \sin \theta_5] + q_{140} [-\sin \theta_2 \sin \theta_5 + \cos \theta_2 \cos \theta_5] - q_{49} = 0$$

$$q_{165} \cos \theta_6 + q_{153} \sin \theta_6 - q_{132} = 0$$

$$-q_{165} \cos \theta_5 \sin \theta_6 + q_{153} \cos \theta_5 \cos \theta_6 + q_{145} \sin \theta_5 = 0$$

$$q_{165} \sin \theta_5 \sin \theta_6 - q_{153} \sin \theta_5 \cos \theta_6 + q_{145} \cos \theta_5 = 0$$

$$q_{161} \cos \theta_6 - q_{149} \sin \theta_6 = 0$$

$$-q_{161} \cos \theta_5 \sin \theta_6 - q_{149} \cos \theta_5 \cos \theta_6 + q_{157} \sin \theta_5$$

$$-q_{137} = 0$$

$$q_{161} \sin \theta_5 \sin \theta_6 + q_{149} \sin \theta_5 \cos \theta_6 + q_{157} \cos \theta_5 - q_{142} = 0$$

TABLE E-11
 FREE-FREE ELASTIC MODE FREQUENCIES OF MODEL 266 TILT-ROTOR (CPS)

Symmetric

θ_c Mode	0°	15°	30°	45°	60°	75°	90°
1	2.114	2.138	2.168	2.199	2.224	2.235	2.229
2	3.473	3.488	3.487	3.470	3.304	3.399	3.360
3	5.727	5.698	5.661	5.628	5.610	5.617	5.644
4	7.235	7.378	7.646	8.021	8.694	8.895	9.016
5	11.490	11.509	11.522	11.523	10.802	11.046	10.661

Anti-symmetric

θ_c Mode	0°	15°	30°	45°	60°	75°	90°
1	3.882	3.882	3.884	3.883	3.875	3.856	3.825
2	4.602	4.699	4.801	4.891	4.936	4.906	4.818
3	5.702	5.645	5.569	5.492	5.446	5.464	5.528
4	7.256	7.347	7.373	7.339	7.294	7.251	7.214
5	7.633	7.624	7.775	8.073	8.456	8.860	9.136

TABLE E-12

SYMMETRIC MODES OF MODEL 266 TILT-ROTOR ($\theta_c = 90^\circ$)

		First elastic mode	Second elastic mode	Third elastic mode	
Fuselage	Beam #1	Displs.	-1.5928679E-01	8.4360325E-02	8.1801437E-02
			-1.4951070E-01	5.6642165E-03	7.1173565E-02
			-1.4254418E-01	3.6955689E-03	6.3635950E-02
	Slopes	-1.3559451E-01	1.7167022E-03	5.8152093E-02	
		-1.2550424E-01	-1.0386461E-03	4.5792317E-02	
		2.7951211E-04	-7.9046777E-05	-3.0425986E-04	
	Axial RB	2.7852656E-04	-7.8976386E-05	-3.0236874E-04	
		2.7830655E-04	-7.8966551E-05	-3.0036132E-04	
		2.7756819E-04	-7.8834898E-05	-2.9805137E-04	
	Beam #2	Displs.	2.7582053E-04	-7.8724676E-05	-2.9249718E-04
			-1.4043819E-02	8.3722476E-02	8.7472417E-03
			-1.2645548E-01	1.2753016E-02	4.6680088E-02
	Slopes	-1.1550544E-01	9.6506954E-03	3.5013655E-02	
		-1.0601149E-01	6.9223407E-03	2.5163448E-02	
		-5.9319096E-02	4.9922614E-03	1.8350238E-02	
	Axial RB	-9.4037936E-02	3.4632477E-03	1.3070409E-02	
		-6.8836919E-02	1.9508381E-03	7.9751464E-03	
		2.7562053E-04	-7.8724676E-05	-2.9249718E-04	
Beam #3	Displs.	2.7294514E-04	-7.8264355E-05	-2.8538055E-04	
		2.6937382E-04	-7.7548967E-05	-2.7655576E-04	
		2.6580768E-04	-7.6813109E-05	-2.6866605E-04	
Slopes	2.6217676E-04	-7.6060747E-05	-2.5963402E-04		
	2.5778788E-04	-7.5152427E-05	-2.4960644E-04		
	6.9281822E-03	8.2745812E-02	1.0656589E-03		
Axial RB	-6.5689005E-02	-6.1331777E-03	7.8527009E-03		
	-8.0141184E-02	-8.8660579E-03	1.4967363E-03		
	-7.3065378E-02	-1.1167262E-02	-9.7245164E-03		
Wing carry-through	Displs.	-6.2531948E-02	-1.4801107E-02	-2.3166916E-02	
		-5.1292771E-02	-1.8525702E-02	-3.5064664E-02	
		-4.1816800E-02	-2.2676193E-02	-5.4073832E-02	
Slopes	-3.0098341E-02	-2.7785755E-02	-7.5255171E-02		
	-1.7107264E-02	-3.4217858E-02	-1.0225993E-01		
	2.5778788E-04	-7.5152427E-05	-2.4960644E-04		
Wing	Displs.	2.5360503E-04	-8.0535342E-05	-2.8246959E-04	
		2.5177358E-04	-8.4075577E-05	-3.0456161E-04	
		2.5015376E-04	-8.8692002E-05	-3.3391678E-04	
Fore and aft bending	Slopes	2.4950409E-04	-9.4545966E-05	-3.7073026E-04	
		2.4929164E-04	-1.0245818E-04	-4.1722547E-04	
		2.4943236E-04	-1.1456248E-04	-4.8005114E-04	
Torsion	Twists	2.5030770E-04	-1.3185848E-04	-5.5115406E-04	
		-1.7739865E-03	8.2541259E-02	1.8428040E-03	
		4.9558391E-03	-8.6210339E-02	-1.2576516E-02	
Vertical bending	Displs.	-8.8836919E-02	1.9508381E-03	7.9751464E-03	
		-2.5778788E-04	7.5152427E-05	2.4960644E-04	
		0.	0.	0.	
Wing	Displs.	1.2151127E-16	2.4222367E-15	8.3391115E-16	
		5.0368315E-03	-8.0765320E-02	-1.1240328E-02	
		-6.3375755E-02	1.8095548E-03	8.8212669E-03	
Fore and aft bending	Slopes	-2.5778788E-04	7.5152427E-05	2.4960644E-04	
		-2.5490658E-04	6.8051756E-05	-3.9561218E-05	
		3.4254823E-06	2.5665844E-04	6.2904912E-05	
Torsion	Twists	-8.3375755E-02	1.8095548E-03	8.8212669E-03	
		-7.2052205E-02	1.7195558E-03	1.0965762E-02	
		4.9351751E-02	1.4227768E-03	1.3880372E-02	
Fore and aft bending	Displs.	-7.6824638E-03	6.6454889E-04	1.7815040E-02	
		4.7876933E-02	-7.0676209E-04	2.2008150E-02	
		5.5056072E-02	-2.3571245E-03	2.5657318E-02	
Torsion	Twists	1.1917052E-01	-3.1202722E-03	2.7180723E-02	
		2.3389693E-04	-8.9177965E-07	5.5023205E-05	
		4.2758145E-04	-4.4550210E-06	6.6885349E-05	
Fore and aft bending	Slopes	6.6977867E-04	-1.0125667E-05	1.4502515E-05	
		5.8368683E-04	-2.0374753E-05	8.2277238E-05	
		1.3099311E-03	-3.7035759E-05	6.3132850E-05	
Torsion	Twists	1.5174160E-03	-5.4909295E-05	1.1149881E-04	
		1.5750089E-03	-6.2560268E-05	1.2374092E-04	
		5.0153231E-03	-8.0466519E-02	-1.1205678E-02	
Fore and aft bending	Displs.	5.1728598E-03	-6.8345751E-02	-8.2015934E-03	
		5.4640151E-03	-6.4882521E-02	-2.2315373E-03	
		5.9502158E-03	-3.1904117E-03	8.7748850E-03	
Torsion	Twists	6.5186936E-03	4.9846837E-02	2.3531209E-02	
		6.9757517E-03	9.6861543E-02	3.7430347E-02	
		7.1357928E-03	1.1502654E-01	4.3037242E-02	
Fore and aft bending	Slopes	3.4254823E-06	2.5665844E-04	6.2904912E-05	
		5.7604190E-06	4.5152867E-04	1.1309230E-04	
		8.3116032E-06	6.8586671E-04	1.7685136E-04	
Torsion	Twists	1.0903137E-05	9.6756039E-04	2.6059139E-04	
		1.2512905E-05	1.2248821E-03	3.5106870E-04	
		1.2703199E-05	1.3760031E-03	4.1936826E-04	
Fore and aft bending	Displs.	1.2513658E-05	1.4163055E-03	4.4312986E-04	
		-2.7699315E-04	7.5454999E-05	2.4573304E-04	
		-2.7070781E-04	1.1742777E-04	-1.0944181E-04	
Torsion	Twists	-2.6201822E-04	1.7722999E-04	-6.1541086E-04	
		-2.4879165E-04	2.6560671E-04	-1.3963080E-03	
		-2.3141536E-04	3.9660991E-04	-2.4166022E-03	
Fore and aft bending	Displs.	-2.1385121E-04	5.0862270E-04	-3.4073435E-03	
		-2.0627554E-04	5.9485769E-04	-3.7912780E-03	
		3.9471541E-04	-6.3323950E-03	-8.8190805E-04	

TABLE E-12 (CONCLUDED)

		First elastic mode	Second elastic mode	Third elastic mode	
Pylon	Transmission/engine	4.6047831E-05	8.7394562E-C3	3.2773473E-03	
		7.3614844E-03	1.3825277E-C1	5.0366586E-02	
		1.4753338E-01	-1.4241383E-C2	9.6422665E-02	
		-8.2065592E-05	5.4827869E-04	-3.7658821E-03	
		1.5863379E-03	-1.0590429E-04	4.2082041E-04	
		1.2513658E-05	1.4163095E-C3	4.4312986E-04	
		7.3614844E-03	1.3825277E-C1	5.0366586E-02	
		6.4220339E-04	6.9157565E-02	2.1094795E-C2	
		1.4301977E-01	1.5913945E-C2	-1.8892085E-01	
	Mast	1.5863379E-03	-1.0590429E-04	4.2082041E-04	
		-8.2065592E-05	5.4827869E-C4	-3.7698821E-03	
		1.2513658E-05	1.4163095E-C3	4.4312586E-04	
		7.3614844E-03	1.3825277E-C1	5.0366586E-C2	
		1.0003864E-03	1.1066805E-01	3.5625460E-02	
		1.4566661E-01	-2.5267681E-C5	1.0032911E-02	
		1.5863379E-03	-1.0590429E-C4	4.2082041E-04	
		-1.0155637E-04	5.9023436E-04	-4.7244149E-C3	
		1.3033502E-05	1.5550369E-C3	5.6625214E-04	
Rotor	7.3614844E-03	1.3825277E-C1	5.0366586E-02		
	1.0003864E-03	1.1066805E-C1	3.5625460E-02		
	1.4566661E-01	-2.5267681E-05	1.0032911E-02		
	1.5863379E-03	-1.0590429E-C4	4.2082041E-04		
	-1.0155637E-04	5.9023436E-C4	-4.7244149E-C3		
	1.3033502E-05	1.5550369E-03	5.6625214E-04		
	-3.7779922E-03	-9.0258036E-C2	-6.1130881E-C2		
	5.3449225E-03	-9.5217829E-C2	-8.1780206E-02		
	1.4161658E-02	-1.0026723E-01	-1.0276112E-01		
Vertical tail	Chordwise bending	2.3346279E-02	-1.0565410E-C1	-1.2532098E-01	
		3.2668229E-02	-1.1128767E-01	-1.4853214E-01	
		2.5030770E-04	-1.3185848E-C4	-5.5115406E-04	
		2.5069608E-04	-1.3987968E-04	-5.8100100E-04	
		2.5138789E-04	-1.4660358E-C4	-6.1055651E-04	
		2.5180924E-04	-1.5013029E-04	-6.2338419E-04	
	Axial RB	2.5201228E-04	-1.5170147E-04	-6.2930054E-04	
		-1.7214854E-02	1.3397245E-C2	-8.3589329E-02	
		-9.6176307E-03	-3.0225617E-02	-1.1918452E-01	
		-7.3684701E-03	-3.1952963E-02	-1.2946005E-01	
		-5.4768333E-03	-3.3935866E-C2	-1.4438611E-01	
		-3.2800790E-03	-3.6400908E-C2	-1.6351556E-01	
	Vertical bending	6.5064122E-05	-3.7943865E-C5	-1.5802401E-04	
		6.3634862E-05	-5.8062343E-05	-3.5949467E-04	
		6.2744410E-05	-7.0314937E-05	-5.4655575E-04	
		6.2744410E-05	-7.0314937E-05	-5.4655575E-04	
		1.9424593E-02	-9.3246476E-C2	-5.5840821E-C2	
		1.9435569E-02	-9.3410269E-C2	-5.6120310E-C2	
Horizontal tail	Chordwise bending	1.9470687E-02	-9.3750557E-02	-5.6701033E-02	
		1.9511804E-02	-9.4200293E-C2	-5.7468379E-02	
		0.	0.	0.	
		7.6217444E-07	-8.3356445E-C6	-1.4223562E-C5	
		1.1747801E-06	-1.2848482E-C5	-2.1924182E-05	
		1.1747801E-06	-1.2848482E-05	-2.1924182E-05	
	Torsion	Twists	-2.4282202E-04	1.4160816E-C4	5.8975220E-04
			-2.4291298E-04	1.4172878E-C4	5.5117443E-04
			-2.4302638E-04	1.4187916E-C4	5.5294759E-04
		Axial RB	-2.4302638E-04	1.4187916E-C4	5.5294759E-04
			-2.4302638E-04	1.4187916E-C4	5.5294759E-04
			-5.2048168E-03	2.4965379E-C2	1.4962539E-02

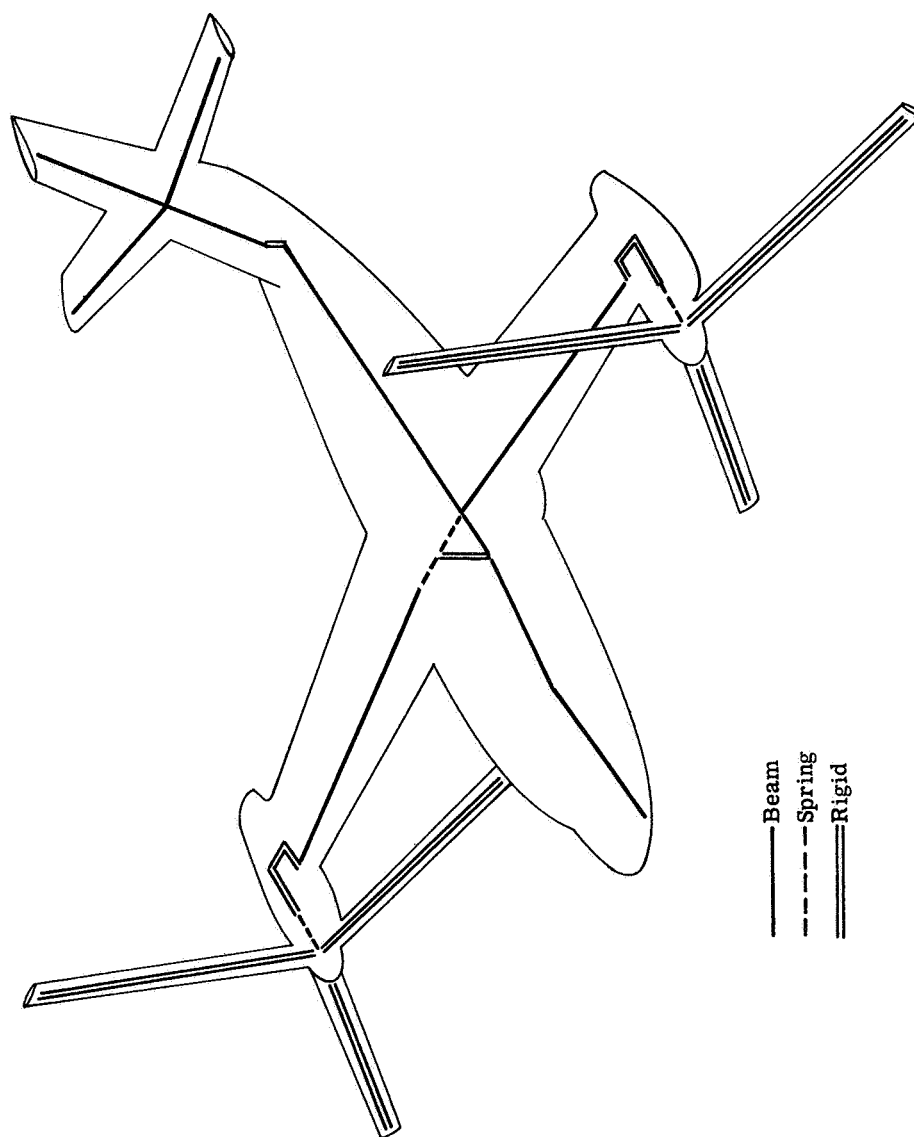


Figure E-1. "Stick" model of Bell Model 266 tilt-rotor aircraft.

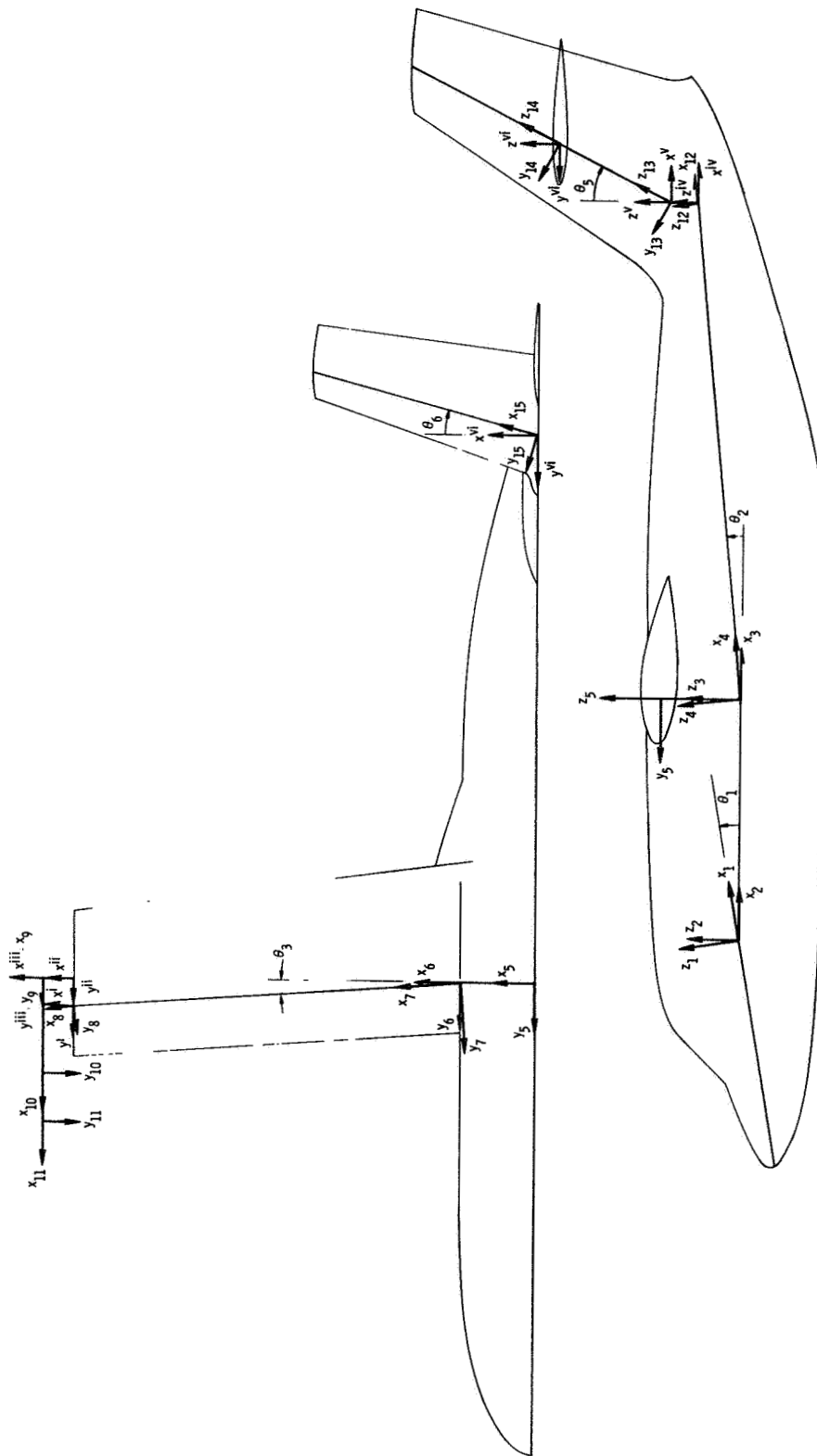


Figure E-2.- Coordinate systems employed in setting down the equations of deflection compatibility between adjacent substructures.

[K]_{CT} =

	q ₄₂	q ₄₃	q ₄₄	q ₄₅	q ₄₆	q ₄₇	q ₄₈	q ₄₉	q ₅₀	q ₅₁	q ₅₂
q ₄₂	$\frac{12EI_z}{L^3}$	0	0	0	$\frac{6EI_z}{L^2}$	0	$-\frac{12EI_z}{L^3}$	0	0	0	$\frac{6EI_z}{L^2}$
q ₄₃	$\frac{12EI_y}{L^3}$	$\frac{12EI_y}{L^3}$	0	$-\frac{6EI_y}{L^2}$	0	0	0	$-\frac{12EI_y}{L^3}$	0	$-\frac{6EI_y}{L^2}$	0
q ₄₄	0	$\frac{GI}{L}$	$\frac{GI}{L}$	0	0	0	0	0	$-\frac{GI}{L}$	0	0
q ₄₅	0	$-\frac{6EI_y}{L^2}$	$\frac{4EI_y}{L}$	0	0	0	0	$\frac{6EI_y}{L^2}$	0	$\frac{2EI_y}{L^2}$	0
q ₄₆	0	0	0	0	$\frac{4EI_z}{L}$	0	$-\frac{6EI_z}{L^2}$	0	0	0	$\frac{2EI_z}{L}$
q ₄₇	0	0	0	0	0	$\frac{AE}{L}$	0	0	0	0	0
q ₄₈	0	0	0	0	0	0	$\frac{12EI_z}{L^3}$	0	0	0	$-\frac{6EI_z}{L^2}$
q ₄₉	0	0	0	0	0	0	0	$\frac{12EI_y}{L^3}$	0	$\frac{6EI_y}{L^2}$	0
q ₅₀	0	0	0	0	0	0	0	$\frac{GI}{L}$	0	0	0
q ₅₁	0	0	0	0	0	0	0	0	$\frac{4EI_y}{L}$	0	0
q ₅₂	0	0	0	0	0	0	0	0	0	0	$\frac{4EI_z}{L}$

Symmetric

Figure E-3.- Stiffness matrix of wing carry-through beam-spring for symmetric vibration analysis.

$[K]_{\text{Mast}}$

q_{95}	q_{96}	q_{97}	q_{98}	q_{99}	q_{100}	q_{101}	q_{102}	q_{103}	q_{104}	q_{105}	q_{106}
$\frac{AE}{L}$	0	0	0	0	0	$-\frac{AE}{L}$	0	0	0	0	0
	$\frac{12EI_z}{L^3}$	0	0	0	$\frac{6EI_z}{L^2}$	0	$-\frac{12EI_z}{L^3}$	0	0	0	$\frac{6EI_z}{L^2}$
		$\frac{12EI_y}{L^3}$	0	$-\frac{6EI_y}{L^2}$	0	0	0	$-\frac{12EI_y}{L^3}$	0	$-\frac{6EI_y}{L^2}$	0
			$\frac{6J}{L}$	0	0	0	0	0	$-\frac{6J}{L}$	0	0
				$\frac{4EI_y}{L}$	0	0	0	$\frac{6EI_y}{L^2}$	0	$\frac{2EI_y}{L}$	0
					$\frac{4EI_z}{L}$	0	$-\frac{6EI_z}{L^2}$	0	0	0	$\frac{2EI_z}{L}$
						$\frac{AE}{L}$	0	0	0	0	0
							$\frac{12EI_z}{L^3}$	0	0	0	$-\frac{6EI_z}{L^2}$
								$\frac{12EI_y}{L^3}$	0	$\frac{6EI_y}{L^2}$	0
									$\frac{6J}{L}$	0	0
										$\frac{4EI_y}{L}$	0
											$\frac{4EI_z}{L}$

Symmetric

Figure E-4.- Stiffness matrix of pylon mast beam-spring for symmetric vibration analysis.

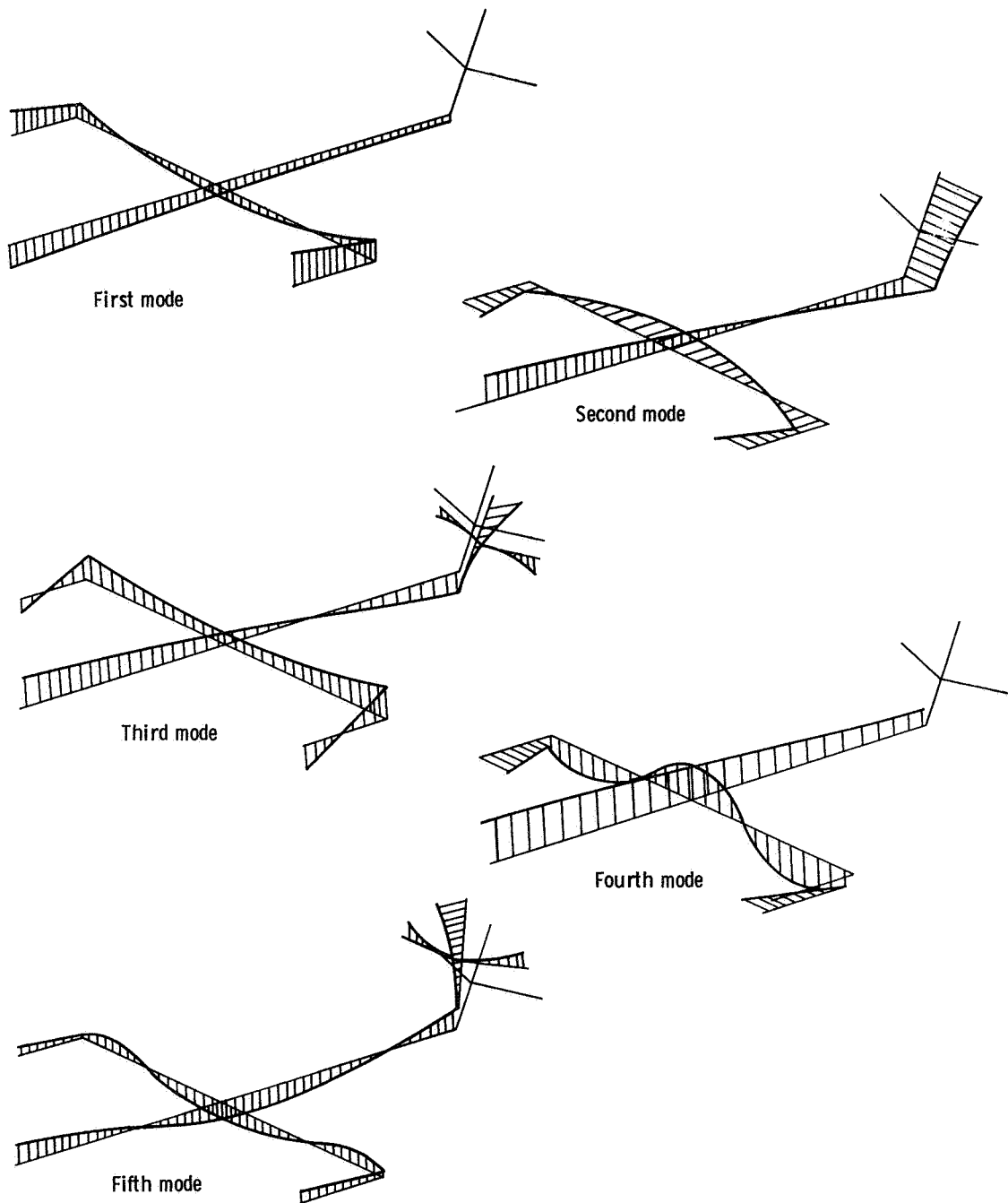


Figure E-5.- Symmetric elastic modes of Model 266 tilt-rotor.

APPENDIX F

SOME RESULTS BASED ON THE USE OF COMPONENT MODE SYNTHESIS

Presented herein are some comparative studies based on the application of the direct and component mode synthesis vibration analysis procedures developed in Chapter 6 to two simple structural systems. A comparison of the theoretical solutions with experimentally measured modes and frequencies of a model of one configuration is also presented. These studies are not intended to be an exhaustive or systematic comparative investigation for the purpose of delineating all the ramifications associated with the use of component mode synthesis. Rather, they are intended solely to provide an indication of the accuracy associated with partial modal coupling and to establish the validity of the theoretical analyses. Reference is also made to some analytical studies by others employing the component mode synthesis computer program developed in this dissertation.

Free-Free Beam

Consider a uniform beam of constant cross-section having the following properties*:

* These particular properties were employed in a different and unrelated study and simply adopted here for convenience.

L = total length = 54 inches

W = total weight = 29.25 lb

EI = sectional stiffness = 50,000 lb-in²

$\frac{I}{A}$ = $\frac{\text{section moment of inertia}}{\text{area of cross section}}$ = 29.16 in²

The distributed mass is taken to be lumped at ten equally spaced stations along the lengthwise axis of the beam in the manner shown in Fig. F-1a. Each station so established has two degrees of freedom: vertical translation and rotation. The direct solution is based on the 20 degree-of-freedom beam of Fig. F-1a. For the corresponding analysis by modal synthesis the complete beam was partitioned into the three unequal length beam segments shown in Fig. F-1b. In this partitioned form the unassembled beam segments have a total of 24 degrees of freedom. Table F-1 summarizes the physical properties of these lumped-mass systems.

Results showing a comparison of frequencies obtained by direct analysis of the complete beam with those obtained by both full modal synthesis and four combinations of partial modal synthesis employing only a few of the lower modes from each beam segment are given in Table F-2. A comparison of the displacements and slopes in the first four elastic modes, as obtained from a direct analysis, full modal coupling, and two combinations of partial modal coupling, is made in Table F-3. The results of the direct analysis constitute the basis from which to assess the accuracy of results obtained by partial modal coupling. The use of full modal

coupling is seen to yield results which are identical to those obtained by direct analysis. Good agreement is indicated in the modes shown for the case in which only half of the modes from each beam segment are employed. It is interesting to note that even when only one elastic mode from each beam segment is used the three predicted elastic frequencies still compare favorably with those given by the direct solution.

Airplane Beam Assembly

The availability of the lower modes and frequencies of a model consisting of an assembly of "beams" configured in the shape of an airplane provided the additional opportunity to compare the results of analysis with experimental measurements. This model is shown in Fig. F-2 as it appeared during the shake test.* Fig. F-3 summarizes the geometric properties of the model.

The partitioning scheme employed in the vibration analysis of this model is schematically depicted in Fig. F-4. Since only the symmetric modes of the model were available the analysis was restricted to the symmetric case. This permitted the analysis to be based on the explicit consideration of the fuselage and only one wing and tail. The fuselage, wing, and tail were treated as beams, the distributed mass of which was lumped at discrete points along the elastic axes of the respective members. Each

* Thanks are extended to Mr. Robert V. Doggett of the Aeroelasticity Branch of NASA-Langley for making the modal and geometric information pertaining to this model available to the author for the studies herein.

fuselage station had two degrees of freedom: vertical translation and rotation. In addition to these two degrees of freedom, each wing and tail station also had associated with it a torsional degree of freedom. Each member was also allocated a rigid body degree of freedom directed along its axis. The rotary inertia associated with each lumped mass was taken to be zero. The model properties, as discretized for the analysis, are given in Table F-4. 68 degrees of freedom are associated with the uncoupled system, 26 of which correspond to "massless" coordinates.

The results of some comparative studies pertaining to the model are summarized in Tables F-5 and F-6 and Fig. F-5. The results shown in the first two columns of Tables F-5 and F-6 indicate that the results of the direct analysis do not agree exactly with those obtained by modal synthesis using all of the calculated component modes. This discrepancy is a consequence of the fact that a modal expansion using all the calculated component modes is really incomplete since a set of modes equal in number to the number of massless degrees of freedom has been "lost" in solving for the subsystem modes and hence are "unavailable" for use in the synthesizing procedure. This incomplete expansion is equivalent to placing constraints on the beam segments, which will tend to give frequencies which are slightly higher than those obtained from a direct analysis. This is substantiated in Table F-5. A complete set of linearly independent shapes was established by calculating the component "modes" using an arbitrary value of 1.0 for all the rotary inertias.

Employing these shapes in a full modal synthesis then gave results which agreed exactly with those of the direct analysis.

Modal synthesis results employing only a few of the lowest modes from each subsystem are compared with solutions by the direct method and with experiment in Tables F-5 and F-6 and Fig. F-5. The results shown in Tables 5 and 6 for partial modal synthesis are for a single combination of the lowest component modes. In addition to the rigid body modes, these include: 6 fuselage bending modes, 5 wing modes (3 bending and 2 torsion), and 2 tail modes (1 bending and 1 torsion). The wing and tail modes corresponding to clamped-free*, pinned-free, and free-free beam end conditions, respectively, were used in conjunction with free-free fuselage modes to provide an indication of the type of component modes which lead to results most nearly in agreement with those obtained from a direct analysis. As might have been anticipated use of clamped-free modes for the wing and tail gave the best results. A comparison of the calculated mode shapes of the first four elastic modes is made in Table F-6.** Again, the direct solution results should be taken as a basis for the assessment of the accuracy of the results of partial modal synthesis. An assessment of the accuracy of the direct analysis procedure can be made by comparing the results obtained by

* A sample input for this case is included as part of the listing of the modal synthesis computer program in Appendix H.

** The zero rows correspond to the rigid body degree of freedom along the axis of each beam.

this method with those obtained experimentally. The frequency comparison, given in Table F-5, is considered to be quite good in view of the rather coarse spacing between stations, particularly on the fuselage and wing. The modes calculated by the direct method are compared with those obtained experimentally in Fig. F-5. Excellent agreement is shown through the highest mode for which data was available (the 7th elastic mode).

Additional Applications

The computer program for natural mode vibration analysis by component mode synthesis which has been developed in this dissertation has additionally been employed in two analytical studies by others.* The first study, directed at assessing the dependency of the rate of convergence on the type of component deflection shapes employed in the synthesizing procedure, concerned itself with comparing the free-free inplane frequencies and modes of a rectangular frame calculated on the basis of using selected free-free or clamped-free component modes by themselves and in conjunction with component static deflection shapes. The second application was to a dynamic model of an early space shuttle concept. This model consisted of a pair of tube-like beams arranged in a parallel "piggy-bank" fashion and joined together by two spring assemblies. The frequencies of the complete structure were calculated using 8 booster modes and 7 orbiter modes, each group

* Fralich, R. W., C. E. Green, and M. H. Rheinfurth: "Dynamic Analysis for Shuttle Design Verification", Paper no. 9, NASA Space Shuttle Technology Conference, April 12-14, 1972 (NASA TMX-2570, July 1972).

consisting of a mixture of free-free elastic modes, rigid-body modes, and static deflection shapes. The calculated frequencies are compared with those obtained experimentally in the reference cited in the footnote, to which the reader is referred for additional details.

TABLE F-1

DISCRETIZATION EMPLOYED FOR FREE-FREE UNIFORM BEAM

Direct Approach				
Station	Local Coordinate Position	Mass	RI	EI
	(inches)	lb-sec ² /in	lb-sec ² -in	(lb-in ²)
1	0.0	.004215	.136	50000.
2	6.0	.008430	.271	↓
3	12.0	↓	↓	↓
4	18.0	↓	↓	↓
5	24.0	↓	↓	↓
6	30.0	↓	↓	↓
7	36.0	↓	↓	↓
8	42.0	↓	↓	↓
9	48.0	.008430	.271	50000.
10	54.0	.004215	.136	-----
Modal Synthesis				
Beam #1				
1	0.0	.004215	.1360	50000.
2	6.0	.008430	.2710	50000.
3	12.0	.008430	.2710	50000.
4	18.0	.004215	.1355	-----
Beam #2				
1	0.0	.004215	.1355	50000.
2	6.0	.008430	.2710	50000.
3	12.0	.004215	.1355	-----
Beam #3				
1	0.0	.004215	.1355	50000.
2	6.0	.008430	.2710	50000.
3	12.0	.008430	.2710	50000.
4	18.0	.008430	.2710	50000.
5	24.0	.004215	.1360	-----

TABLE F-2
 COMPARISON OF CALCULATED FREQUENCIES FOR FREE-FREE UNIFORM BEAM (CPS)

Mode	Direct Solution	Modal Synthesis					
		Full	Partial	Partial	Partial	Partial	Partial
		(8,6,10)*	(6,5,7)	(4,4,4)	(4,3,5)	(3,3,3)	
1	0	0	0	0	0	0	0
2	0	0	0	0	0	0	0
3	5.7016	5.7016	5.7171	5.9313	5.8135	6.3517	6.3517
4	13.0848	13.0848	13.0890	13.3037	13.5910	14.0724	14.0724
5	21.7817	21.7817	21.8156	22.2553	22.2265	23.2227	23.2227
6	30.7180	30.7180	30.7484	31.4144	32.0870	-----	-----
7	39.0547	39.0547	39.0888	40.0870	41.4177	-----	-----
8	46.1034	46.1034	46.1238	49.5418	42.2940	-----	-----
9	51.4069	51.4069	51.4181	-----	-----	-----	-----
10	54.6867	54.6867	54.6937	-----	-----	-----	-----

*Numbers in parentheses indicate, respectively, the number of component modes selected from each of the three beam segments for use in the synthesizing procedure.

TABLE F-3

COMPARISON OF CALCULATED MODE SHAPES FOR FREE-FREE UNIFORM BEAM

FIRST ELASTIC MODE

	Direct Solution	Full Coupling (8, 6, 10)	Partial Coupling (6, 5, 7)	Partial Coupling (4, 3, 5)	
Beam Segment #1	Displs.	5.6940188E+00	5.6958846E+00	5.6952418E+00	
		2.6794610E+00	2.6774728E+00	2.6633156E+00	
	Slopes	-5.5572028E-02	-5.5572028E-02	-6.5671652E-02	-7.3671024E-02
		-2.1509378E+00	-2.1608378E+00	-2.1444832E+00	-2.1325959E+00
		-5.1147897E-01	-5.1147897E-01	-5.1129985E-01	-5.0060139E-01
		-4.8967741E-01	-4.8967741E-01	-4.8933868E-01	-5.0677401E-01
Beam Segment #2	Displs.	-4.1482535E-01	-4.1482535E-01	-4.0119731E-01	
		-2.7982716E-01	-2.7982716E-01	-2.8968755E-01	
	Slopes	-2.1608378E+00	-2.1608378E+00	-2.1444832E+00	-2.1325959E+00
		-3.3100605E+00	-3.3100605E+00	-3.3125993E+00	-3.3079176E+00
		-2.7982716E-01	-2.7982716E-01	-3.2947536E+00	-3.2578389E+00
		-9.8949691E-02	-9.8949691E-02	-2.8009756E-01	-2.8968755E-01
Beam Segment #3	Displs.	9.8949691E-02	9.8949691E-02	9.9060530E-02	
		-3.3100605E+00	-3.3100605E+00	1.0214705E-01	
	Slopes	-2.1608378E+00	-2.1608378E+00	-3.2947536E+00	-3.2578389E+00
		-5.5572028E-02	-5.5572028E-02	-2.1741467E+00	-2.1811187E+00
		2.6794610E+00	2.6794610E+00	-6.5085872E-02	-8.5820838E-02
		5.6940188E+00	5.6940188E+00	2.6802456E+00	2.6697264E+00
Slopes	9.8949691E-02	9.8949691E-02	5.7021592E+00	5.7166000E+00	
	2.7982716E-01	2.7982716E-01	9.9126083E-02	1.0214705E-01	
	4.1482535E-01	4.1482535E-01	2.8033523E-01	2.6405872E-01	
	4.8967741E-01	4.8967741E-01	4.1508683E-01	4.2999959E-01	
	5.1147897E-01	5.1147897E-01	4.9023537E-01	4.8184787E-01	
			5.1238555E-01	5.3009095E-01	

TABLE F-3 (Continued)

SECOND ELASTIC MODE

	Direct Solution	Full Coupling (8, 6, 10)	Partial Coupling (6, 5, 7)	Partial Coupling (4, 3, 5)
Beam Segment #1	Displs.	-4.0673964E+00	-4.0791726E+00	4.0425062E+00
		8.1516119E-02	8.1516119E-02	-1.2899686E-01
	Slopes	2.828564CE+00	2.828564CE+00	-2.7859925E+00
		3.2108920E+00	3.2108920E+00	-2.9007198E+00
Beam Segment #2	Displs.	7.4556765E-01	7.4755552E-01	-7.1891933E-01
		5.2249744E-01	6.2348352E-01	-6.5700230E-01
	Slopes	2.7983681E-01	2.7983681E-01	-2.1697653E-01
		-1.4640183E-01	-1.4584277E-01	1.6062843E-01
Beam Segment #3	Displs.	3.2108920E+00	3.2026757E+00	-2.9007198E+00
		1.3719184E+00	1.3694170E+00	-1.4618220E+00
	Slopes	-1.3719184E+00	-1.3816721E+00	1.0115774E+00
		-1.4640183E-01	-1.4584277E-01	1.6062843E-01
Beam Segment #3	Displs.	-4.3864237E-01	-4.3881534E-01	3.2602477E-01
		-4.3864237E-01	-4.3932858E-01	4.9142111E-01
	Slopes	-1.3719184E+00	-1.3816721E+00	1.0115774E+00
		-3.2108920E+00	-3.1993411E+00	3.1745654E+00
Beam Segment #3	Displs.	-2.828564CE+00	-2.8209529E+00	2.9858812E+00
		-8.1516119E-02	-8.4322303E-02	1.8339567E-01
	Slopes	4.0673964E+00	4.0571446E+00	-4.1982831E+00
		-4.3864237E-01	-4.3932858E-01	4.9142111E-01
Beam Segment #3	Displs.	-1.4640183E-01	-1.4717113E-01	2.0992139E-01
		2.7983681E-01	2.793977E-01	-2.7663558E-01
	Slopes	6.2249744E-01	6.2188428E-01	-6.4198220E-01
		7.4656765E-01	7.4565489E-01	-8.0277596E-01

TABLE F-3 (Continued)

THIRD ELASTIC MODE

	Direct Solution	Full Coupling (8, 6, 10)	Partial Coupling (6, 5, 7)	Partial Coupling (4, 3, 5)
Beam Segment #1	Displs.	2.6389073E+00	2.6211123E+00	-2.9018157E+00
		-1.6210115E+00	-1.6195568E+00	1.8070946E+00
		-2.6102932E+00	-2.6102932E+00	2.7750935E+00
		-3.4080647E-02	-3.4080647E-02	-1.9518656E-01
	Slopes	-9.6758759E-01	-8.658759E-01	9.6265155E-01
Beam Segment #2	Displs.	5.2738505E-01	-5.2738505E-01	5.7644265E-01
		1.9191076E-01	1.9473629E-01	-2.5600530E-01
		6.1165451E-01	6.1465465E-01	-7.0280977E-01
		-3.4080647E-02	-4.7012598E-02	-1.9518656E-01
	Slopes	2.9459317E+00	2.9144100E+00	-2.9709891E+00
Beam Segment #3	Displs.	2.9459317E+00	2.9140955E+00	-2.6091575E+00
		6.1165451E-01	6.1465465E-01	-7.0280977E-01
		3.2586496E-01	3.2434475E-01	-2.0116421E-01
		-3.2586496E-01	-3.3235156E-01	3.048135E-01
	Slopes	2.9459317E+00	2.9140955E+00	-2.6091575E+00
	-3.4080647E-02	-3.4280647E-02	-8.7152533E-02	
	-2.6102932E+00	-2.5930549E+00	2.3662273E+00	
	-1.6210115E+00	-1.6336420E+00	1.5524082E+00	
	2.6389073E+00	2.6326963E+00	-2.3748593E+00	
	-3.2586496E-01	-3.3235156E-01	3.048135E-01	
	-6.1165451E-01	-6.1836111E-01	5.3110866E-01	
	-1.9191076E-01	-1.9388272E-01	2.4436249E-01	
	5.2738505E-01	5.2972455E-01	-5.1956913E-01	
	8.6758759E-01	8.7114224E-01	-7.6537778E-01	

TABLE F-3 (Concluded)

FOURTH ELASTIC MODE

	Direct Solution			Full Coupling (8, 6, 10)	Partial Coupling (6, 5, 7)	Partial Coupling (4, 3, 5)
Beam Segment #1	Displs.	1.5407849E+00	1.5407849E+00	1.5277206E+00	1.0720708E+00	1.0720708E+00
		-2.1099470E+00	-2.1099470E+00	-2.1057819E+00	-1.6459134E+00	-1.6459134E+00
	Slopes	-8.6324372E-01	-8.6324372E-01	-7.9926286E-01	-4.8519823E-01	-4.8519823E-01
		2.4186786E+00	2.4186786E+00	2.3858377E+00	1.7102538E+00	1.7102538E+00
Beam Segment #2	Displs.	-9.1589550E-01	-9.1589550E-01	-9.1854928E-01	-7.9281501E-01	-7.9281501E-01
		-2.7198374E-01	-2.7198374E-01	-2.7269507E-01	-8.8633943E-02	-8.8633943E-02
	Slopes	6.3707187E-01	6.3707187E-01	6.4296516E-01	4.4316537E-01	4.4316537E-01
		3.7389223E-01	3.7389223E-01	3.8383215E-01	2.7372653E-01	2.7372653E-01
Beam Segment #3	Displs.	2.4186786E+00	2.4186786E+00	2.3858377E+00	1.8284178E+00	1.8284178E+00
		1.8153843E+00	1.8153843E+00	1.7831773E+00	1.7102538E+00	1.7102538E+00
	Slopes	-1.8153843E+00	-1.8153843E+00	-1.7570272E+00	-1.3720709E+00	-1.3720709E+00
		3.7389223E-01	3.7389223E-01	3.8383215E-01	2.7372653E-01	2.7372653E-01
Beam Segment #3	Displs.	-5.6685512E-01	-5.6685512E-01	-5.6202334E-01	-2.5686039E-01	-2.5686039E-01
		-5.6685512E-01	-5.6685512E-01	-5.6826866E-01	-7.8744731E-01	-7.8744731E-01
	Slopes	-1.8153843E+00	-1.8153843E+00	-1.7970272E+00	-1.3720709E+00	-1.3720709E+00
		-2.4186786E+00	-2.4186786E+00	-2.4279521E+00	-3.0063475E+00	-3.0063475E+00
Beam Segment #3	Displs.	8.6324372E-01	8.6324372E-01	8.5461047E-01	7.0630864E-01	7.0630864E-01
		2.1099470E+00	2.1099470E+00	2.1110319E+00	2.5721887E+00	2.5721887E+00
	Slopes	-1.5407849E+00	-1.5407849E+00	-1.5369871E+00	-1.6873487E+00	-1.6873487E+00
		-5.6685512E-01	-5.6685512E-01	-5.6826866E-01	-7.8744731E-01	-7.8744731E-01
Beam Segment #3	Displs.	3.7389223E-01	3.7389223E-01	3.7240325E-01	2.6499591E-01	2.6499591E-01
		6.3707187E-01	6.3707187E-01	6.3816020E-01	8.7039310E-01	8.7039310E-01
	Slopes	-2.7198374E-01	-2.7198374E-01	-2.7114062E-01	-3.2056058E-01	-3.2056058E-01
		-9.1589550E-01	-9.1589550E-01	-9.1620300E-01	-1.0648398E+00	-1.0648398E+00

TABLE F-4

DISCRETIZATION EMPLOYED FOR AIRPLANE BEAM ASSEMBLY

Station	Local Coordinate Position	Mass	Torsional Inertia	EI vertical	GJ
	(inches)	lb-sec ² /in	lb-sec ² -in	(lb-in ²)	(lb-in ²)
Fuselage					
1	0.0	.0002083	N/A	47790.	N/A
2	4.0	.0004166	↓	↓	↓
3	8.0	.0004166	↓	↓	↓
4	12.0	.0004166	↓	↓	↓
5	16.0	.0003750	↓	↓	↓
6*	19.2	.0030066	↓	↓	↓
7	24.0	.0004583	↓	↓	↓
8	28.0	.0004166	↓	↓	↓
9	32.0	.0004166	↓	↓	↓
10	36.0	.0004166	↓	↓	↓
11	40.0	.0003750	↓	↓	↓
12	43.2	.0004166	↓	47790.	↓
13	48.0	.0002500	↓	-----	↓
Wing					
1	0.0	.0003704	.0001235	9440.	15720.
2	4.0	.0007409	.0002470	↓	↓
3	8.0	↓	↓	↓	↓
4	12.0	↓	↓	↓	↓
5	16.0	↓	↓	↓	↓
6	20.0	.0007409	.0002470	9440.	15720.
7	24.0	.0003704	.0001235	-----	-----
Horizontal Tail					
1	0.0	.0001852	.00006177	9440.	15720.
2	2.0	.0003704	.00012354	↓	↓
3	4.0	↓	↓	↓	↓
4	6.0	↓	↓	↓	↓
5	8.0	.0003704	.00012354	9440.	15720.
6	10.0	.0001852	.00006177	-----	-----
*Mass of shaker stem and coil included					
Total Masses: Fuselage = .005, Wing = .00444, Tail = .00185					

TABLE F-5
 COMPARISON OF CALCULATED AND MEASURED SYMMETRIC MODE FREQUENCIES FOR AIRPLANE BEAM ASSEMBLY (CFS)

Mode	Direct Solution RI=0	Full Modal Synthesis*		Partial Modal Synthesis**		Measured
		free-free RI=0	free-free "Dummy" RI	clamped-free RI=0	pinned-free RI=0	
1	0	0	0	0	0	---
2	0	0	0	0	0	---
3	7.3769	8.0234	7.3769	7.4157	8.2024	8.3214
4	21.4885	21.5986	21.4885	21.5053	21.6805	21.7254
5	45.9255	50.8958	45.9255	46.2597	53.2747	54.2784
6	51.8871	54.9862	51.8871	52.3714	57.9148	59.7710
7	84.3666	86.8019	84.3666	85.0963	90.5896	94.9088
8	115.6038	127.8944	115.6038	116.4056	133.1559	134.2964
9	151.8068	154.3213	151.8068	153.3172	159.3065	160.3770
10	174.2613	175.4510	174.2613	177.1566	184.0957	184.1293

* Free-free modes employed for fuselage, wing, and tail

** Free-free modes employed for fuselage; clamped-free, pinned-free, and free-free modes, respectively, employed for wing and tail.

TABLE F-6

COMPARISON OF CALCULATED SYMMETRIC MODE SHAPES FOR AIRPLANE BEAM MODEL

First elastic mode

	Direct solution	Full modal synthesis					
		free-free			clamped-free	pinned-free	free-free
		RI = 0	RI = 0	"Dummy" RI	RI = 0	RI = 0	RI = 0
Fuselage	Displs.	8.1994467E+00	-8.6647252E+00	8.1994463E+00	-8.2301740E+00	-8.8329788E+00	8.9524582E+00
		7.2145750E+00	-7.9379599E+00	7.2145750E+00	-7.2221876E+00	-7.6117049E+00	7.6944781E+00
		6.2360589E+00	-6.3979699E+00	6.2360589E+00	-6.2453095E+00	-6.4287874E+00	6.4766499E+00
		5.2772632E+00	-5.2630893E+00	5.2772629E+00	-5.2846346E+00	-5.2672979E+00	5.2789637E+00
		4.3590319E+00	-4.1883757E+00	4.3590316E+00	-4.3350461E+00	-4.1223567E+00	4.1016349E+00
	Slopes	3.6716820E+00	-3.3947177E+00	3.6716817E+00	-3.6566888E+00	-3.3083695E+00	3.2644699E+00
		2.9991299E+00	-2.6317854E+00	2.9991296E+00	-2.9873633E+00	-2.5167216E+00	2.4919737E+00
		2.8597615E+00	-2.6648796E+00	2.8597614E+00	-2.8319021E+00	-2.3519436E+00	2.2943689E+00
		3.0203286E+00	-2.7475811E+00	3.0203282E+00	-3.0027202E+00	-2.5893778E+00	2.5318037E+00
		3.4068488E+00	-3.1871147E+00	3.4068483E+00	-3.4032480E+00	-3.1112302E+00	3.0726899E+00
		3.9490188E+00	-3.8249225E+00	3.9490183E+00	-3.9490183E+00	-3.6491957E+00	3.8002935E+00
		4.48501423E+00	-4.4441117E+00	4.4850141E+00	-4.4500965E+00	-4.4458936E+00	4.4647444E+00
		5.2306733E+00	-5.3976226E+00	5.2306732E+00	-5.2306227E+00	-5.4802697E+00	5.5241833E+00
		-2.4642260E-01	2.8964192E-01	-2.4642259E-01	2.5375983E-01	3.0747785E-01	-3.1671968E-01
		-2.4580837E-01	2.8872895E-01	-2.4580836E-01	2.4847017E-01	3.0098232E-01	-3.1004570E-01
-2.4288478E-01	2.8580921E-01	-2.4288477E-01	2.4100783E-01	2.9157278E-01	-3.0040376E-01		
-2.3953663E-01	2.8244766E-01	-2.3953663E-01	2.4066322E-01	2.9064741E-01	-2.9922508E-01		
-2.2233897E-01	2.6439205E-01	-2.2233897E-01	2.2903683E-01	2.7955097E-01	-2.8350722E-01		
-2.0639969E-01	2.2461870E-01	-2.0639969E-01	1.8864590E-01	2.2551788E-01	-2.3181352E-01		
-7.8713515E-02	9.2482200E-02	-7.8713524E-02	8.9465573E-02	9.8520702E-02	-1.0089500E-01		
5.8047472E-03	-1.2856129E-03	5.8047374E-03	-5.8047374E-03	-1.3287095E-02	1.4355918E-02		
7.1393950E-02	-6.9090166E-02	7.1393942E-02	-7.5967074E-02	-9.9864362E-02	1.0364396E-01		
1.1893386E-01	-1.4458335E-01	1.1893385E-01	-1.2126469E-01	-1.4679585E-01	1.6623091E-01		
1.4938862E-01	-1.8400648E-01	1.4938861E-01	-1.4939444E-01	-1.9174736E-01	1.9948587E-01		
1.6215916E-01	-1.9740674E-01	1.6215915E-01	-1.6234515E-01	-2.0783702E-01	2.1508225E-01		
1.5283636E-01	-1.0053135E-01	1.5283635E-01	-1.6908046E-01	-2.1618480E-01	2.2369772E-01		
0.	0.	0.	0.	0.	0.		
Wing	Displs.	3.6716320E+00	-3.3947177E+00	3.6716317E+00	-3.6566888E+00	-3.3083695E+00	3.2644698E+00
		2.3575210E+00	-2.3325949E+00	2.3575207E+00	-2.3574015E+00	-2.5161598E+00	2.4873823E+00
		-4.9587356E-01	1.3735622E-01	-4.9687391E-01	4.7562672E-01	-5.4563452E-02	1.1685655E-01
		-4.4838233E+00	4.1868338E+00	-4.4838237E+00	4.4634789E+00	4.0820565E+00	-4.0217537E+00
		-9.2030487E+00	9.0312162E+00	-9.2030489E+00	9.1928445E+00	9.0097425E+00	-8.9913169E+00
	Slopes	1.4303972E+01	1.4370035E+01	1.4303973E+01	1.4302634E+01	1.4342519E+01	1.4323634E+01
		-1.9536017E+01	1.4984223E+01	-1.9536018E+01	1.4556109E+01	1.9998137E+01	-2.0048062E+01
		-1.0320066E+01	1.1230957E+01	-1.0320066E+01	9.4325148E+00	1.1279080E+01	-1.1591701E+01
		-5.3773995E-01	4.1964447E-01	-5.3773995E-01	5.3369522E-01	3.6837212E-01	-3.5098165E-01
		-8.7225846E-01	6.6580105E-01	-8.7225845E-01	6.7225845E-01	8.5410696E-01	-8.4086635E-01
		-1.1042409E+00	1.1274136E+00	-1.1042409E+00	1.1042409E+00	1.1641278E+00	-1.1769050E+00
		-1.2464107E+00	1.2538554E+00	-1.2464107E+00	1.2439291E+00	1.2876112E+00	-1.2906439E+00
		-1.2992283E+00	1.3632291E+00	-1.2992283E+00	1.3029957E+00	1.3808134E+00	-1.3881798E+00
		-1.3124027E+00	1.3764509E+00	-1.3124026E+00	1.3159469E+00	1.4304311E+00	-1.4491953E+00
		1.7874725E-01	-1.7627939E-01	1.7874725E-01	-1.6793549E-01	1.9939300E-01	-2.0077358E-01
1.7888022E-01	-1.7649641E-01	1.7888023E-01	-1.6349371E-01	-1.9536240E-01	-5.0084271E-01		
1.7898904E-01	-1.7648367E-01	1.7898905E-01	-1.6359285E-01	-1.9952383E-01	-2.0100628E-01		
1.7907370E-01	-1.7646478E-01	1.7907370E-01	-1.6367973E-01	-1.9957843E-01	-2.0116887E-01		
1.7913418E-01	-1.7645076E-01	1.7913418E-01	-1.6373684E-01	-1.9976771E-01	-2.0126434E-01		
1.7917047E-01	-1.7643704E-01	1.7917047E-01	-1.6376747E-01	-1.9979146E-01	-2.0128968E-01		
1.7918256E-01	-1.7642895E-01	1.7918257E-01	-1.6377812E-01	-1.9979144E-01	-2.0128970E-01		
0.	0.	0.	0.	0.	0.		
Tail	Displs.	4.4501423E+00	-4.4401188E+00	4.4501418E+00	-4.4500965E+00	-4.4559363E+00	4.4447444E+00
		4.6315379E+00	-4.6449213E+00	4.6315369E+00	-4.6305470E+00	-4.6667085E+00	4.6818061E+00
		4.8417709E+00	-4.8847969E+00	4.8417695E+00	-4.8406811E+00	-4.8935800E+00	4.9099117E+00
		5.0586965E+00	-5.1461457E+00	5.0686961E+00	-5.0584193E+00	-5.1444270E+00	5.1575511E+00
		5.3035189E+00	-5.4111747E+00	5.3035184E+00	-5.3065860E+00	-5.4157354E+00	5.4263242E+00
	Slopes	5.5403055E+00	-5.4900490E+00	5.5408050E+00	-5.5481415E+00	-5.4560944E+00	5.7059413E+00
		3.1079754E-02	-5.8736666E-02	3.1079749E-02	-6.1127466E-02	-1.0391873E-01	1.0754435E-01
		9.9044487E-02	-1.1078366E-01	9.9044483E-02	-9.8379766E-02	-1.0831640E-01	1.1020378E-01
		1.1016441E-01	-1.2675866E-01	1.1016440E-01	-1.1028539E-01	-1.1922124E-01	1.1849144E-01
		1.1603662E-01	-1.3316411E-01	1.1603662E-01	-1.1728722E-01	-1.3114994E-01	1.2574793E-01
		1.1833193E-01	-1.3613437E-01	1.1833193E-01	-1.2032267E-01	-1.3884917E-01	1.3803560E-01
		1.1879899E-01	-1.3649944E-01	1.1879899E-01	-1.2100530E-01	-1.4114657E-01	1.4069502E-01
		-1.4043386E-01	1.7097618E-01	-1.4043385E-01	1.4059492E-01	1.7999911E-01	-1.8627175E-01
		-1.4045520E-01	1.7095952E-01	-1.4045519E-01	1.4061405E-01	1.7999953E-01	-1.8627976E-01
		-1.4047180E-01	1.7101382E-01	-1.4047180E-01	1.4053131E-01	1.8001921E-01	-1.8630072E-01
-1.4048366E-01	1.7103091E-01	-1.4048366E-01	1.4064501E-01	1.8004333E-01	-1.8632663E-01		
-1.4049078E-01	1.7104118E-01	-1.4049077E-01	1.4065380E-01	1.8006321E-01	-1.8634796E-01		
-1.4049319E-01	1.7104457E-01	-1.4049314E-01	1.4065483E-01	1.8007979E-01	-1.8635960E-01		
0.	0.	0.	0.	0.	0.		

TABLE F-6 (Continued)

COMPARISON OF CALCULATED SYMMETRIC MODE SHAPES FOR AIRPLANE BEAM MODEL

Second elastic mode

		Direct solution	Full modal synthesis		Partial modal synthesis			
		RI = 0	free-free RI = 0	free-free "Dummy" RI	clamped-free RI = 0	pinned-free RI = 0	free-free RI = 0	
Fuselage	Displs.	3.1432893E+01	3.1377025E+01	3.1432894E+01	-3.1449878E+01	3.1439939E+01	-3.1434168E+01	
		2.2880832E+01	2.2837459E+01	2.2880832E+01	-2.2889095E+01	2.2875090E+01	-2.2868236E+01	
		1.4527396E+01	1.4498197E+01	1.4527396E+01	-1.4529235E+01	1.4513085E+01	-1.4505568E+01	
		8.7500701E+00	8.7468044E+00	8.7500702E+00	-8.7499653E+00	8.7389037E+00	-8.729392E+00	
		7.8666463E-02	7.8609270E-02	7.8666524E-02	-7.8609142E-02	7.8491365E-02	-7.8421790E-02	
	Slopes	-4.0631702E+00	-4.07123153E+00	-4.0631701E+00	4.0662239E+00	-4.0159726E+00	4.0110031E+00	-4.0110031E+00
		-7.8515473E+00	-7.8437012E+00	-7.8515473E+00	7.8451431E+00	-7.7145749E+00	7.6916089E+00	-7.6916089E+00
		-6.8791451E+00	-6.87270378E+00	-6.8791451E+00	6.8649203E+00	-6.6575066E+00	6.6180421E+00	-6.6180421E+00
		-8.1576139E+00	-8.1597785E+00	-8.1576139E+00	8.1454662E+00	-7.8629343E+00	7.8072790E+00	-7.8072790E+00
		-5.9556871E+00	-5.9136486E+00	-5.9556871E+00	5.9226794E+00	-5.4722354E+00	5.5025900E+00	-5.5025900E+00
Wing	Displs.	-2.6213953E+00	-2.6334309E+00	-2.6213953E+00	2.5626310E+00	-2.1557355E+00	2.0747171E+00	
		5.8905333E-01	5.9472303E-01	5.8905332E-01	-5.2345628E-01	1.0671942E+00	-1.1552738E+00	
		5.7629438E+00	5.7148012E+00	5.7629437E+00	-5.7333370E+00	5.2738200E+00	-5.3202290E+00	
		-2.1446759E+00	-2.1418319E+00	-2.1446759E+00	2.1461146E+00	-2.1479597E+00	2.1481837E+00	
		-2.1246952E+00	-2.1214319E+00	-2.1246952E+00	2.1261084E+00	-2.1278765E+00	2.1288112E+00	
	Slopes	-2.0356669E+00	-2.0315642E+00	-2.0356669E+00	2.0369343E+00	-2.0372102E+00	2.0374413E+00	
		-1.8300338E+00	-1.8247424E+00	-1.8300338E+00	1.8301265E+00	-1.8267811E+00	1.8261046E+00	
		-1.4807450E+00	-1.4765066E+00	-1.4807450E+00	1.4799291E+00	-1.4778936E+00	1.4688304E+00	
		-1.0916450E+00	-1.0856375E+00	-1.0916450E+00	1.0967184E+00	-1.0877825E+00	1.0755677E+00	
		-4.9231796E-01	-4.9173782E-01	-4.9231796E-01	4.9183435E-01	-4.8947879E-01	4.8947879E-01	
Tail	Displs.	-2.8941470E-02	-2.8969747E-02	-2.8941472E-02	2.9267329E-02	-9.9489639E-03	5.811779E-03	
		3.783892E-01	3.7119420E-01	3.7838921E-01	-3.7996149E-01	3.9805904E-01	-4.0186437E-01	
		7.0799985E-01	7.0303111E-01	7.0799985E-01	-7.1610799E-01	7.3173109E-01	-7.3492733E-01	
		9.4196235E-01	9.4457425E-01	9.4196235E-01	-9.4627325E-01	9.4938078E-01	-9.4768175E-01	
		1.0528923E+00	1.0422831E+00	1.0528923E+00	-1.0627325E+00	1.0468917E+00	-1.0468773E+00	
	Slopes	1.0591134E+00	1.0570785E+00	1.0591133E+00	-1.0787073E+00	1.0880351E+00	-1.0886861E+00	
		-4.0631702E+00	-4.07123153E+00	-4.0631701E+00	4.0662239E+00	-4.0159726E+00	4.0110031E+00	
		5.7230907E+00	5.7230907E+00	5.7230907E+00	5.7174935E+00	-5.4841815E+00	5.4929711E+00	
		-5.8681369E+00	-5.8786669E+00	-5.8681369E+00	5.8824218E+00	-6.1893324E+00	6.2636163E+00	
		-4.1913669E+00	-4.1612011E+00	-4.1913669E+00	4.2180206E+00	-4.4165860E+00	4.4262317E+00	
Twist	Displs.	-8.5936277E-01	-8.5909395E-01	-8.5936281E-01	8.9880814E-01	-9.3943947E-01	9.3844564E-01	
		3.4582143E+00	3.4309642E+00	3.4582142E+00	-3.44751676E+00	3.6515167E+00	-3.6888548E+00	
		8.2418579E+00	8.2426148E+00	8.2418572E+00	-8.2544396E+00	8.769616E+00	-8.894510E+00	
		-5.4982364E-01	-5.424489E-01	-5.4982364E-01	5.4834037E-01	-6.137979E-01	5.3077466E-01	
		-2.4941994E-01	-2.4953392E-01	-2.4941994E-01	2.49428150E-01	-3.1840623E-01	3.186169E-01	
	Slopes	1.8977832E-01	1.7912748E-01	1.8977831E-01	-1.8321788E-01	1.8483019E-01	-1.7777152E-01	
		6.3909955E-01	6.0139007E-01	6.3909955E-01	-6.4095936E-01	6.7978228E-01	-6.5348515E-01	
		9.8340409E-01	9.7218145E-01	9.8340409E-01	-9.7066262E-01	1.0931064E+00	-1.0424779E+00	
		1.6446995E+00	1.2196126E+00	1.6446995E+00	-1.1643072E+00	1.7369932E+00	-1.2518833E+00	
		1.2116312E+00	1.265712E+00	1.2116311E+00	-1.2090959E+00	1.3079027E+00	-1.3262294E+00	
Twist	Displs.	9.4539160E-01	9.3571221E-01	9.4539161E-01	-9.4978134E-01	9.3768678E-01	-9.3492182E-01	
		9.5143913E-01	9.4578135E-01	9.5143914E-01	-9.5464539E-01	9.3999662E-01	-9.3715244E-01	
		9.5639659E-01	9.475757E-01	9.5639659E-01	-9.6083192E-01	9.4513399E-01	-9.4246779E-01	
		9.6025829E-01	9.544443E-01	9.6025830E-01	-9.6488717E-01	9.5040896E-01	-9.4766571E-01	
		9.6301982E-01	9.5741813E-01	9.6301982E-01	-9.6761938E-01	9.544370E-01	-9.5078256E-01	
	Slopes	9.6467800E-01	9.5908364E-01	9.6467800E-01	-9.6914623E-01	9.642387E-01	-9.5152979E-01	
		9.6523093E-01	9.5954390E-01	9.6523094E-01	-9.6962822E-01	9.624761E-01	-9.5113335E-01	
		5.8905333E-01	5.9472603E-01	5.8905332E-01	-5.2345628E-01	1.0671942E+00	-1.1552738E+00	
		1.8317064E+00	1.8428306E+00	1.8317063E+00	1.8447206E+00	-2.1376824E+00	-2.2178188E+00	
		3.3731439E+00	3.3731439E+00	3.3731438E+00	-3.3631710E+00	3.3378473E+00	-3.2644655E+00	
Twist	Displs.	5.1015979E+00	4.714052E+00	5.1015978E+00	-5.0737620E+00	6.7309186E+00	-6.8764894E+00	
		6.9247308E+00	6.5800764E+00	6.9247307E+00	-6.8847863E+00	8.2480133E+00	-8.1357853E+00	
		8.7796872E+00	8.273521E+00	8.7796870E+00	-8.7306435E+00	7.8235240E+00	-7.6852181E+00	
		5.2644729E+00	5.211111E+00	5.2644728E+00	-5.1813149E+00	5.2341159E+00	-5.2435476E+00	
		7.0589589E-01	6.158741E-01	7.0589589E-01	-6.9399725E-01	5.8909097E-01	-5.4502789E-01	
	Slopes	8.2610514E-01	7.537128E-01	8.2610513E-01	-8.1561166E-01	6.4693178E-01	-6.0932772E-01	
		9.4452019E-01	8.1515500E-01	9.4452019E-01	-8.0715825E-01	7.4321809E-01	-6.9666113E-01	
		9.2326622E-01	8.444646E-01	9.2326620E-01	-9.1817322E-01	8.7544489E-01	-7.6096096E-01	
		9.2954644E-01	8.4905362E-01	9.2954644E-01	-9.2515040E-01	8.239106E-01	-7.8156409E-01	
		-9.1183087E-01	-8.0264040E-01	-9.1183087E-01	8.9742753E-01	-8.0657290E-01	9.0827580E-01	
Twist	Displs.	-9.1300963E-01	-8.138153E-01	-9.1300962E-01	8.9945717E-01	-9.0683792E-01	9.0854242E-01	
		-9.1392640E-01	-8.41307E-01	-9.1392639E-01	8.9593802E-01	-9.075176E-01	9.092445E-01	
		-9.1458710E-01	-8.0535157E-01	-9.1458709E-01	9.0012131E-01	-9.0839939E-01	9.1010326E-01	
		-9.1497536E-01	-8.5757820E-01	-9.1497535E-01	9.0075943E-01	-9.0909323E-01	9.108129E-01	
		-9.1510646E-01	-8.0591639E-01	-9.1510645E-01	9.0075941E-01	-9.0934825E-01	9.1106791E-01	

TABLE F-6 (Continued)

COMPARISON OF CALCULATED SYMMETRIC MODE SHAPES FOR AIRPLANE BEAM MODEL

Third elastic mode

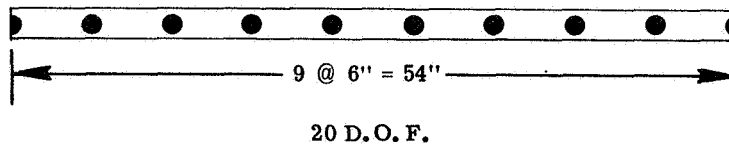
	Direct solution	Full modal synthesis			Partial modal synthesis		
	RI = 0	free-free RI = 0	free-free "Dummy" RI	clamped-free RI = 0	pinned-free RI = 0	free-free RI = 0	
Fuselage	Displs	-2.163285E+00	-4.7156173E-01	2.1632255E+00	2.417057E+00	-4.1272633E+00	5.9515454E+00
		-7.5934222E-01	1.1113112E-01	7.5934222E-01	9.6517439E-01	-1.9884308E+00	2.9702894E+00
		5.884744E-01	6.8152897E-01	-5.8847450E-01	-5.5459672E-01	2.0940100E-01	-1.3595892E-02
		1.8050778E+00	1.2377963E+00	1.8050778E+00	-1.8875300E+00	1.9826154E+00	-2.3722846E+00
		2.8417021E+00	1.8170478E+00	-2.8417021E+00	-2.8366791E+00	2.8976361E+00	2.9138035E+00
		3.5587440E+00	2.345292E+00	-3.5587440E+00	3.650715E+00	3.4298666E+00	-3.9396104E+00
		5.7466620E+00	5.0367644E+00	-5.7466620E+00	-5.8214370E+00	5.2322950E+00	5.1788832E+00
		8.1904292E+00	8.3839498E+00	-8.1904292E+00	-8.1530999E+00	7.5121605E+00	-6.8826861E+00
		9.9310250E+00	1.0584578E+01	-9.9310250E+00	-9.9119453E+00	9.3007321E+00	-8.1884037E+00
		1.0174970E+01	1.1584270E+01	-1.0174970E+01	-1.0088879E+01	9.3342221E+00	-7.9587818E+00
		8.3785382E+00	9.5253592E+00	-8.3785382E+00	-8.3410048E+00	7.1785368E+00	-5.6254451E+00
		6.0345970E+00	6.7857763E+00	-6.0345970E+00	-5.8537105E+00	4.2049385E+00	-3.0684280E+00
	1.5055797E+00	1.0753390E+00	-1.5055797E+00	-1.2078373E+00	-1.2528838E+00	1.8822721E+00	
	3.537966E-01	1.4593422E-01	-3.537966E-01	-3.5653299E-01	5.2674700E-01	-7.3882865E-01	
	3.467934E-01	1.4518971E-01	-3.467934E-01	-3.752523E-01	5.5063047E-01	-7.5828468E-01	
	3.235644E-01	1.3812309E-01	-3.235644E-01	-3.7090375E-01	5.2322950E-01	-7.0189140E-01	
	2.823308E-01	1.4725676E-01	-2.823308E-01	-2.8053383E-01	1.3473999E-01	-6.4107945E-01	
	2.3705086E-01	1.2448309E-01	-2.3705086E-01	-2.1810454E-01	1.5400783E-01	-1.5894333E-01	
	2.149536E-01	2.9589922E-01	-2.149536E-01	-3.2293817E-01	2.2549201E-01	-1.5061390E-01	
	6.0781166E-01	7.7597125E-01	-6.0781166E-01	-5.595792E-01	5.1691092E-01	-3.7482546E-01	
	5.6459529E-01	8.1022644E-01	-5.6459529E-01	-5.5885271E-01	5.6668128E-01	-4.2811948E-01	
	2.7207962E-01	4.4548398E-01	-2.7207962E-01	-2.7300789E-01	2.6737621E-01	-1.6983690E-01	
	-1.6450767E-01	-1.1691884E-01	1.6450767E-01	1.9933423E-01	-2.6361993E-01	3.0039530E-01	
	-6.2841384E-01	-7.7372173E-01	6.2841384E-01	6.4933866E-01	-7.8279297E-01	7.4047469E-01	
	-4.4797023E-01	-1.1197701E-00	4.4797023E-01	8.8532279E-01	-1.0483964E+00	6.5449255E-01	
	-4.4039930E-01	-1.2246273E+00	4.4039930E-01	1.0051740E+00	-1.1923713E+00	1.0679098E+00	
	0.	0.	0.	0.	0.	0.	
	3.5587440E+00	2.3632902E+00	-3.5587440E+00	-3.6066715E+00	3.4298666E+00	-3.9306164E+00	
	-4.3171297E-01	-1.2100630E+00	4.3171297E-01	3.3451359E-01	2.2944433E+00	-2.7045754E+00	
	-3.0603009E+00	-8.0527528E+00	3.0603009E+00	8.0158888E+00	-5.3809232E+00	5.0910498E+00	
	-1.2098924E+01	-1.1584977E+01	1.2098924E+01	1.2173616E+01	-1.3186449E+01	1.3550208E+01	
	-8.5848709E+00	-9.1516310E+00	8.5848709E+00	8.7146784E+00	-1.1036973E+01	1.1675827E+01	
	2.1141767E+00	1.2327317E+00	-2.1141767E+00	-2.0473514E+00	1.3866776E+00	-1.3245108E+00	
	1.6344163E+01	1.6277276E+01	-1.6344163E+01	-1.6557771E+01	1.7699148E+01	-1.8383939E+01	
	1.0747703E+01	1.4779692E+01	-1.0747703E+01	-1.6140543E+01	1.1279624E+01	-7.5307110E+00	
	-1.7744122E+00	-1.1420148E+00	1.7744122E+00	1.7936250E+00	-1.0770024E+00	1.0701420E+00	
	-1.7091119E+00	-1.6932724E+00	1.7091119E+00	1.7288883E+00	-2.3902288E+00	2.4935040E+00	
	-1.394832E-01	-6.6117566E-01	1.394832E-01	1.6814910E-01	-9.7290895E-01	1.1469331E+00	
	1.8813777E+00	1.6539174E+00	-1.8813777E+00	-1.8773910E+00	2.0117269E+00	-2.0721689E+00	
	3.2738630E+00	3.8791662E+00	-3.2738630E+00	-3.3244610E+00	3.8393962E+00	-4.0125714E+00	
	3.7011869E+00	3.8931150E+00	-3.7011869E+00	-3.7791018E+00	4.2903771E+00	-4.3618071E+00	
	-1.8615515E-01	-2.3198759E-01	1.8615515E-01	2.7967246E-01	-1.9536827E-01	1.3043537E-01	
	-1.9196771E-01	-2.587966E-01	1.9196771E-01	2.8814331E-01	-1.9837152E-01	1.252402E-01	
	-1.9665997E-01	-2.7406491E-01	1.9665997E-01	2.9516012E-01	-2.0948803E-01	1.3747359E-01	
	-2.0304559E-01	-2.8046780E-01	2.0304559E-01	3.0154457E-01	-2.126391E-01	1.4246438E-01	
	-2.0465349E-01	-2.8506810E-01	2.0465349E-01	3.0559103E-01	-2.1680594E-01	1.4534775E-01	
	-2.0519060E-01	-2.878418E-01	2.0519060E-01	3.0784186E-01	-2.1797472E-01	1.4616246E-01	
	0.	0.	0.	0.	0.	0.	
	4.2389695E+00	4.7357783E+00	-4.2389695E+00	-4.0780047E+00	4.2049385E+00	-3.0686280E+00	
	9.8657037E-01	1.6063077E+00	-9.8657037E-01	-8.7199094E-01	1.0690648E+00	-6.2241143E-01	
	-3.2983643E+00	-3.4429517E+00	3.2983643E+00	3.2887637E+00	-2.0177262E+00	1.5852906E+00	
	-8.1392754E+00	-9.3505261E+00	8.1392754E+00	7.8727777E+00	-6.9710849E+00	4.4891782E+00	
	-1.7398612E-01	-1.5466427E-01	1.7398612E-01	1.2653673E-01	-1.0586338E-01	7.8188222E-01	
	-1.2947773E+00	-1.5598422E-01	1.2947773E+00	4.4266234E-01	-5.2319932E-01	4.7924749E-01	
	1.9205249E+00	1.2418078E+00	-1.9205249E+00	-1.2888829E+00	-7.3238108E-01	5.7705913E-01	
	-2.3171639E+00	-2.2420858E+00	2.3171639E+00	1.8743895E+00	-1.2510869E+00	8.1185889E-01	
	-2.4968680E+00	-2.7711941E+00	2.4968680E+00	2.2187276E+00	-1.8184888E+00	1.2958629E+00	
	2.5427814E+00	2.0410184E+00	-2.5427814E+00	-2.369072E+00	-2.1851826E+00	1.6006469E+00	
	8.2049657E-01	9.1003914E+00	-8.2049657E-01	-2.9427814E+00	2.4017780E+00	-1.6984546E+00	
	8.2589693E-01	9.69748E+00	-8.2589693E-01	-2.056573E-01	-7.6671149E-01	8.3007866E-01	
	9.2967230E-01	9.7868994E-01	-9.2967230E-01	-2.2585943E-01	-7.702572E-01	8.3161823E-01	
	8.3239935E-01	9.8241708E-01	-8.3239935E-01	-2.2967230E-01	-7.745372E-01	8.3564807E-01	
	8.3403701E-01	9.8638709E-01	-8.3403701E-01	-2.3239935E-01	-7.7748270E-01	8.4063101E-01	
	8.3458314E-01	9.877107E-01	-8.3458314E-01	-2.3403701E-01	-7.7937381E-01	8.4466165E-01	
	0.	9.856696E-01	0.	-8.3458314E-01	-7.8002544E-01	8.4620122E-01	
	0.	0.	0.	0.	0.	0.	

TABLE F-6 (Concluded)

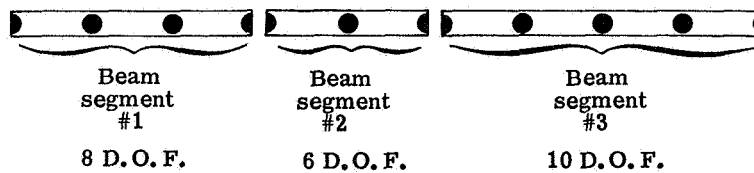
COMPARISON OF CALCULATED SYMMETRIC MODE SHAPES FOR AIRPLANE BEAM MODEL

Fourth elastic mode

	Direct solution						Full modal synthesis			Partial modal synthesis		
	RI = 0						free-free	free-free	clamped-free	pinned-free	free-free	
	RI = 0						RI = 0	"Dummy" RI	RI = 0	RI = 0	RI = 0	
Fuselage	Displ.	1.6521193E+01	1.7304901E+01	1.6521193E+01	1.6594463E+01	1.7608114E+01	1.7819170E+01	1.6521193E+01	1.6594463E+01	1.7608114E+01	1.7819170E+01	
		2.0329730E+00	1.4326893E+00	2.0329730E+00	1.9038620E+00	1.9038620E+00	1.9038620E+00	1.9038620E+00	1.9038620E+00	1.9038620E+00	1.9038620E+00	
		-3.3890805E+00	-4.0861526E+00	-3.3890805E+00	-3.5027696E+00	-4.4415989E+00	-4.4415989E+00	-4.4415989E+00	-3.5027696E+00	-4.4415989E+00	-4.4415989E+00	
		-5.1889494E+00	-6.7570397E+00	-5.1889494E+00	-6.1886494E+00	-6.2011387E+00	-6.2011387E+00	-6.2011387E+00	-6.1886494E+00	-6.2011387E+00	-6.2011387E+00	
		-5.9109087E+00	-6.1161571E+00	-5.9109087E+00	-5.9109087E+00	-5.8895563E+00	-5.8895563E+00	-5.8895563E+00	-5.9109087E+00	-5.8895563E+00	-5.8895563E+00	
		-1.3862320E+00	-1.0515346E+00	-1.3862320E+00	-1.4702655E+00	-1.6787879E+00	-1.6787879E+00	-1.6787879E+00	-1.4702655E+00	-1.6787879E+00	-1.6787879E+00	
	Slopes	7.6700795E+00	6.4619585E+00	7.6700795E+00	8.2944168E+00	1.2886464E+01	1.2886464E+01	1.2886464E+01	8.2944168E+00	1.2886464E+01	1.2886464E+01	
		1.0942433E+01	1.1088374E+01	1.0942433E+01	1.0942433E+01	1.1361834E+01	1.1361834E+01	1.1361834E+01	1.0942433E+01	1.1361834E+01	1.1361834E+01	
		1.1717232E+01	1.0912538E+01	1.1717232E+01	1.1717232E+01	1.1875342E+01	1.1875342E+01	1.1875342E+01	1.1717232E+01	1.1875342E+01	1.1875342E+01	
		1.0611212E+01	8.6551343E+00	1.0611212E+01	1.0505466E+01	1.0505466E+01	1.0505466E+01	1.0505466E+01	1.0611212E+01	1.0505466E+01	1.0505466E+01	
		7.3731216E+00	-4.0321336E+00	7.3731216E+00	7.3731216E+00	-1.8425407E+00	-1.8425407E+00	-1.8425407E+00	7.3731216E+00	-1.8425407E+00	-1.8425407E+00	
		-1.9037704E+00	-2.0675109E+00	-1.9037704E+00	-1.9037704E+00	-1.9041170E+00	-1.9041170E+00	-1.9041170E+00	-1.9037704E+00	-1.9041170E+00	-1.9041170E+00	
Wing	Displ.	1.8425407E+00	-1.6967112E+00	1.8425407E+00	-1.8425407E+00	-1.8425407E+00	-1.8425407E+00	-1.8425407E+00	-1.8425407E+00	-1.8425407E+00		
		-1.5922319E+00	-1.7024147E+00	-1.5922319E+00	-1.5922319E+00	-1.6207477E+00	-1.6207477E+00	-1.6207477E+00	-1.5922319E+00	-1.6207477E+00		
		-1.0711854E+00	-1.1064666E+00	-1.0711854E+00	-1.0711854E+00	-1.0647673E+00	-1.0647673E+00	-1.0647673E+00	-1.0711854E+00	-1.0647673E+00		
		-2.8936322E-01	-1.9402322E-01	-2.8936322E-01	-2.8936322E-01	-2.8936322E-01	-2.8936322E-01	-2.8936322E-01	-2.8936322E-01	-2.8936322E-01	-2.8936322E-01	
		4.7927251E-01	5.9545194E-01	4.7927251E-01	4.7927251E-01	4.5389674E-01	4.5389674E-01	4.5389674E-01	4.7927251E-01	4.5389674E-01	4.5389674E-01	
		1.1286242E+00	1.2570124E+00	1.1286242E+00	1.1286242E+00	1.1894047E+00	1.1894047E+00	1.1894047E+00	1.1286242E+00	1.1894047E+00	1.1894047E+00	
	Slopes	1.2623677E+00	1.2862844E+00	1.2623677E+00	1.3134399E+00	1.6173894E+00	1.6173894E+00	1.6173894E+00	1.2623677E+00	1.6173894E+00	1.6173894E+00	
		1.0320514E+00	9.4845450E-01	1.0320514E+00	1.0320514E+00	1.0099215E+00	1.0099215E+00	1.0099215E+00	1.0320514E+00	1.0099215E+00	1.0099215E+00	
		5.1796050E-01	3.2436225E-01	5.1796050E-01	5.1796050E-01	4.0710466E-01	4.0710466E-01	4.0710466E-01	5.1796050E-01	4.0710466E-01	4.0710466E-01	
		-1.4122561E-01	-4.4408212E-01	-1.4122561E-01	-1.4122561E-01	-1.9327917E-01	-1.9327917E-01	-1.9327917E-01	-1.4122561E-01	-1.9327917E-01	-1.9327917E-01	
		-6.6461082E-01	-6.7778124E-01	-6.6461082E-01	-6.6461082E-01	-5.6728038E-01	-5.6728038E-01	-5.6728038E-01	-6.6461082E-01	-5.6728038E-01	-5.6728038E-01	
		6.1738434E-01	-1.0037323E+00	6.1738434E-01	6.1738434E-01	8.3010708E-01	8.3010708E-01	8.3010708E-01	6.1738434E-01	8.3010708E-01	8.3010708E-01	
Displ.	5.9109087E+00	-6.1161571E+00	5.9109087E+00	-5.9109087E+00	-5.8895563E+00	-5.8895563E+00	-5.8895563E+00	-5.9109087E+00	-5.8895563E+00	-5.8895563E+00		
	-2.8247060E+00	3.8420514E+00	-2.8247060E+00	2.8247060E+00	2.8247060E+00	2.8247060E+00	2.8247060E+00	2.8247060E+00	2.8247060E+00	2.8247060E+00		
	2.3852849E+00	2.3852849E+00	2.3852849E+00	2.3852849E+00	2.3852849E+00	2.3852849E+00	2.3852849E+00	2.3852849E+00	2.3852849E+00	2.3852849E+00		
	5.8943198E+00	1.1401205E+00	5.8943198E+00	5.8943198E+00	5.8943198E+00	5.8943198E+00	5.8943198E+00	5.8943198E+00	5.8943198E+00	5.8943198E+00		
	4.8362074E+00	6.1930195E+00	4.8362074E+00	4.8362074E+00	4.8362074E+00	4.8362074E+00	4.8362074E+00	4.8362074E+00	4.8362074E+00	4.8362074E+00		
	-6.8898880E-01	-7.0890464E-01	-6.8898880E-01	-6.8898880E-01	-5.1401759E-01	-5.1401759E-01	-5.1401759E-01	-6.8898880E-01	-5.1401759E-01	-5.1401759E-01		
Slopes	-3.5402782E+00	-1.0570233E+01	-3.5402782E+00	-8.5602784E+00	-8.5602784E+00	-8.5602784E+00	-8.5602784E+00	-3.5402782E+00	-8.5602784E+00	-8.5602784E+00		
	2.3963676E-01	2.9772640E-01	2.3963676E-01	2.3963676E-01	2.2694885E-01	2.2694885E-01	2.2694885E-01	2.3963676E-01	2.2694885E-01	2.2694885E-01		
	1.1859534E+00	1.1111252E+00	1.1859534E+00	1.1859534E+00	1.1645964E+00	1.1645964E+00	1.1645964E+00	1.1859534E+00	1.1645964E+00	1.1645964E+00		
	1.2384949E+00	1.4374508E+00	1.2384949E+00	1.2384949E+00	1.1803297E+00	1.1803297E+00	1.1803297E+00	1.2384949E+00	1.1803297E+00	1.1803297E+00		
	3.6853644E-01	5.6325477E-01	3.6853644E-01	3.6853644E-01	3.9115005E-01	3.9115005E-01	3.9115005E-01	3.6853644E-01	3.9115005E-01	3.9115005E-01		
	-8.7464862E-01	-1.0197802E+00	-8.7464862E-01	-8.7464862E-01	-8.1131846E-01	-8.1131846E-01	-8.1131846E-01	-8.7464862E-01	-8.1131846E-01	-8.1131846E-01		
Twists	-1.7774235E+00	-2.2476897E+00	-1.7774235E+00	-1.7774235E+00	-1.7377283E+00	-1.7377283E+00	-1.7377283E+00	-1.7774235E+00	-1.7377283E+00	-1.7377283E+00		
	-2.0530218E+00	-2.4445144E+00	-2.0530218E+00	-2.0530218E+00	-2.0476219E+00	-2.0476219E+00	-2.0476219E+00	-2.0530218E+00	-2.0476219E+00	-2.0476219E+00		
	-4.1506188E-01	-1.1567514E-01	-4.1506188E-01	-4.1506188E-01	-3.9308585E-01	-3.9308585E-01	-3.9308585E-01	-4.1506188E-01	-3.9308585E-01	-3.9308585E-01		
	-4.317798E-01	-5.202184E-01	-4.317798E-01	-4.317798E-01	-4.086502E-01	-4.086502E-01	-4.086502E-01	-4.317798E-01	-4.086502E-01	-4.086502E-01		
	-4.4563976E-01	-6.7884190E-01	-4.4563976E-01	-4.4563976E-01	-4.2254942E-01	-4.2254942E-01	-4.2254942E-01	-4.4563976E-01	-4.2254942E-01	-4.2254942E-01		
	-6.9464882E-01	-8.7420957E-01	-6.9464882E-01	-6.9464882E-01	-6.3363765E-01	-6.3363765E-01	-6.3363765E-01	-6.9464882E-01	-6.3363765E-01	-6.3363765E-01		
Displ.	4.7054675E-01	5.9416754E-01	4.7054675E-01	4.7054675E-01	4.4950713E-01	4.4950713E-01	4.4950713E-01	4.7054675E-01	4.4950713E-01	4.4950713E-01		
	0.	0.	0.	0.	0.	0.	0.	0.	0.	0.		
	1.0412129E+01	8.6515348E+00	1.0412129E+01	8.0967546E+00	8.0967546E+00	8.0967546E+00	8.0967546E+00	1.0412129E+01	8.0967546E+00	8.0967546E+00		
	8.9945339E+00	7.1294458E+00	8.9945339E+00	8.9945339E+00	8.1211010E+00	8.1211010E+00	8.1211010E+00	8.9945339E+00	8.1211010E+00	8.1211010E+00		
	2.8958563E+00	2.7226446E+00	2.8958563E+00	2.8958563E+00	2.7227309E+00	2.7227309E+00	2.7227309E+00	2.8958563E+00	2.7227309E+00	2.7227309E+00		
	-4.3742001E+00	-3.7625238E+00	-4.3742001E+00	-4.3742001E+00	-4.5888874E+00	-4.5888874E+00	-4.5888874E+00	-4.3742001E+00	-4.5888874E+00	-4.5888874E+00		
Slopes	-1.2820274E+01	-1.1432720E+01	-1.2820274E+01	-1.2820274E+01	-1.2900508E+01	-1.2900508E+01	-1.2900508E+01	-1.2820274E+01	-1.2900508E+01	-1.2900508E+01		
	-2.1699619E+01	-1.0539728E+01	-2.1699619E+01	-2.1699619E+01	-2.1576928E+01	-2.1576928E+01	-2.1576928E+01	-2.1699619E+01	-2.1576928E+01	-2.1576928E+01		
	-3.3230612E-01	-4.7890705E-01	-3.3230612E-01	-3.3230612E-01	-3.3230612E-01	-3.3230612E-01	-3.3230612E-01	-3.3230612E-01	-3.3230612E-01	-3.3230612E-01		
	-1.9377348E+00	-1.40453439E+00	-1.9377348E+00	-1.9377348E+00	-1.9377348E+00	-1.9377348E+00	-1.9377348E+00	-1.9377348E+00	-1.9377348E+00	-1.9377348E+00		
	-3.1911635E+00	-2.8330356E+00	-3.1911635E+00	-3.1911635E+00	-3.2606742E+00	-3.2606742E+00	-3.2606742E+00	-3.1911635E+00	-3.2606742E+00	-3.2606742E+00		
	-4.0009223E+00	-3.0009223E+00	-4.0009223E+00	-4.0009223E+00	-3.9730493E+00	-3.9730493E+00	-3.9730493E+00	-4.0009223E+00	-3.9730493E+00	-3.9730493E+00		
Twist	-4.3793420E+00	-3.0052929E+00	-4.3793420E+00	-4.3793420E+00	-4.2819077E+00	-4.2819077E+00	-4.2819077E+00	-4.3793420E+00	-4.2819077E+00	-4.2819077E+00		
	4.4693031E+00	4.0052929E+00	4.4693031E+00	4.4693031E+00	4.313611E+00	4.313611E+00	4.313611E+00	4.4693031E+00	4.313611E+00	4.313611E+00		
	5.7955945E-01	7.0013454E-01	5.7955945E-01	5.7955945E-01	5.1725922E-01	5.1725922E-01	5.1725922E-01	5.7955945E-01	5.1725922E-01	5.1725922E-01		
	5.7996372E-01	6.6471491E-01	5.7996372E-01	5.7996372E-01	5.2083997E-01	5.2083997E-01	5.2083997E-01	5.7996372E-01	5.2083997E-01	5.2083997E-01		
	5.833912E-01	7.1866767E-01	5.833912E-01	5.833912E-01	5.2405274E-01	5.2405274E-01	5.2405274E-01	5.833912E-01	5.2405274E-01	5.2405274E-01		
	5.8583993E-01	7.7545633E-01	5.8583993E-01	5.8583993E-01	5.2667445E-01	5.2667445E-01	5.2667445E-01	5.8583993E-01	5.2667445E-01	5.2667445E-01		



(a) Complete beam



(b) Partitioned beam

Figure F-1.- Lumped mass representation for vibration analysis of uniform beam.

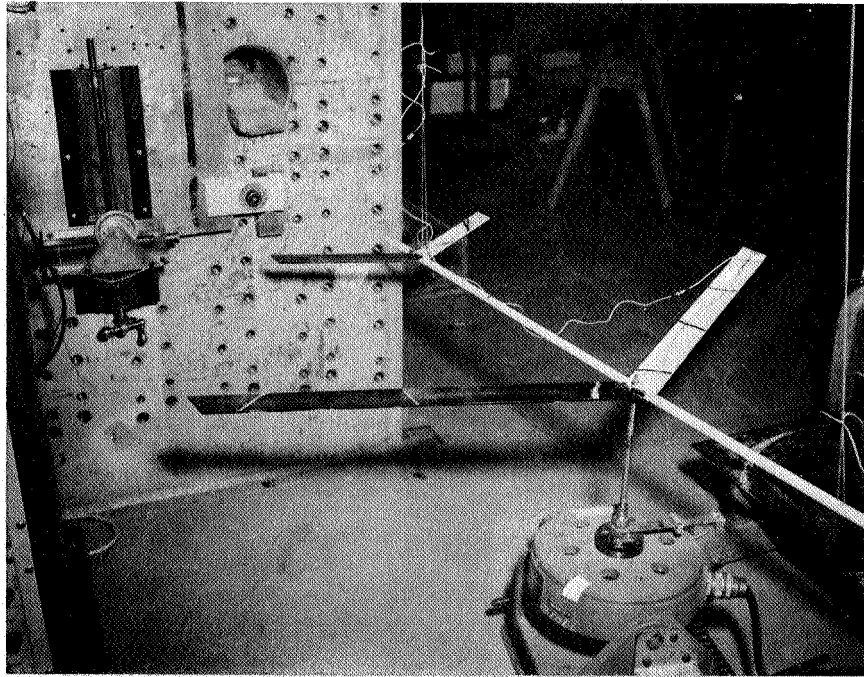


Figure F-2.- Airplane beam model during shake test.

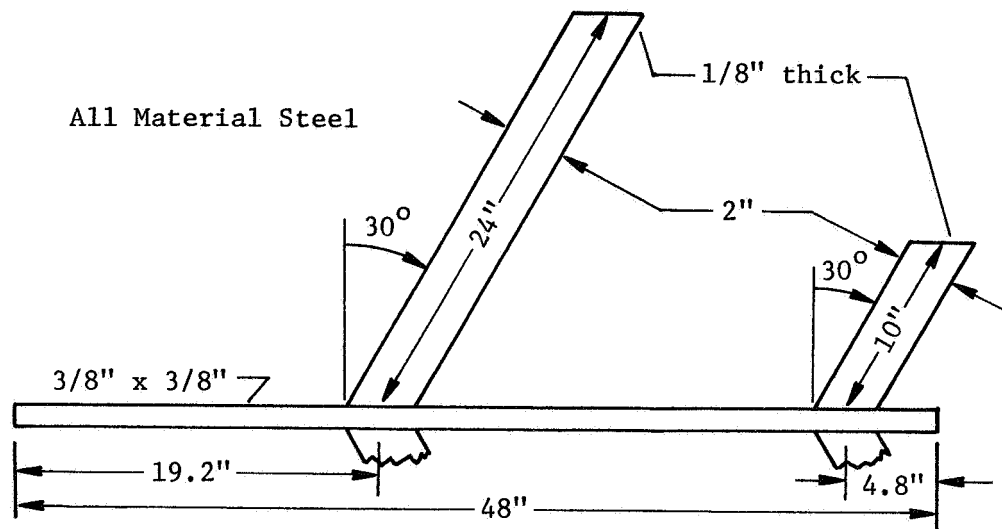


Figure F-3.- Geometric properties of model.

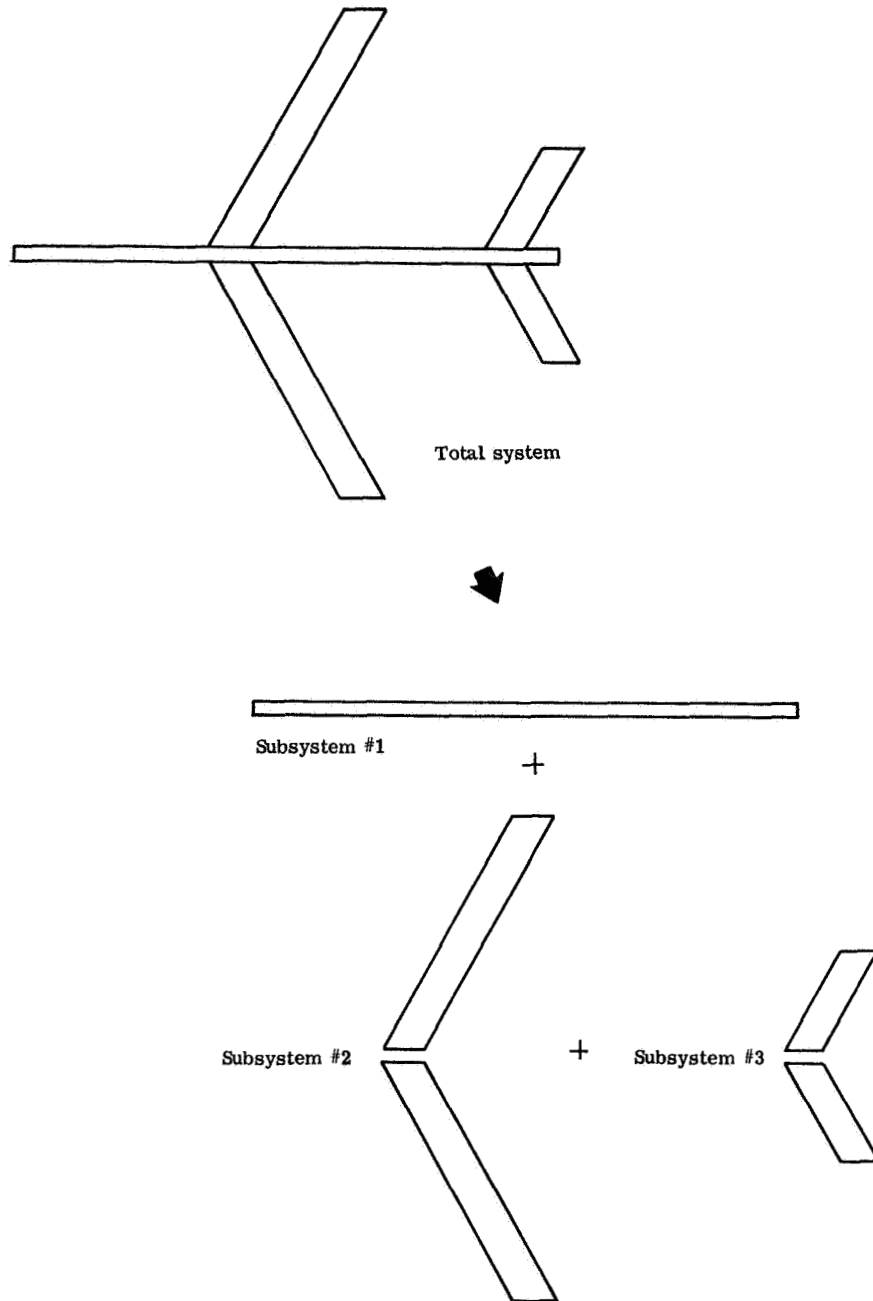


Figure F-4.- Partitioning scheme applied in vibration analysis of model.

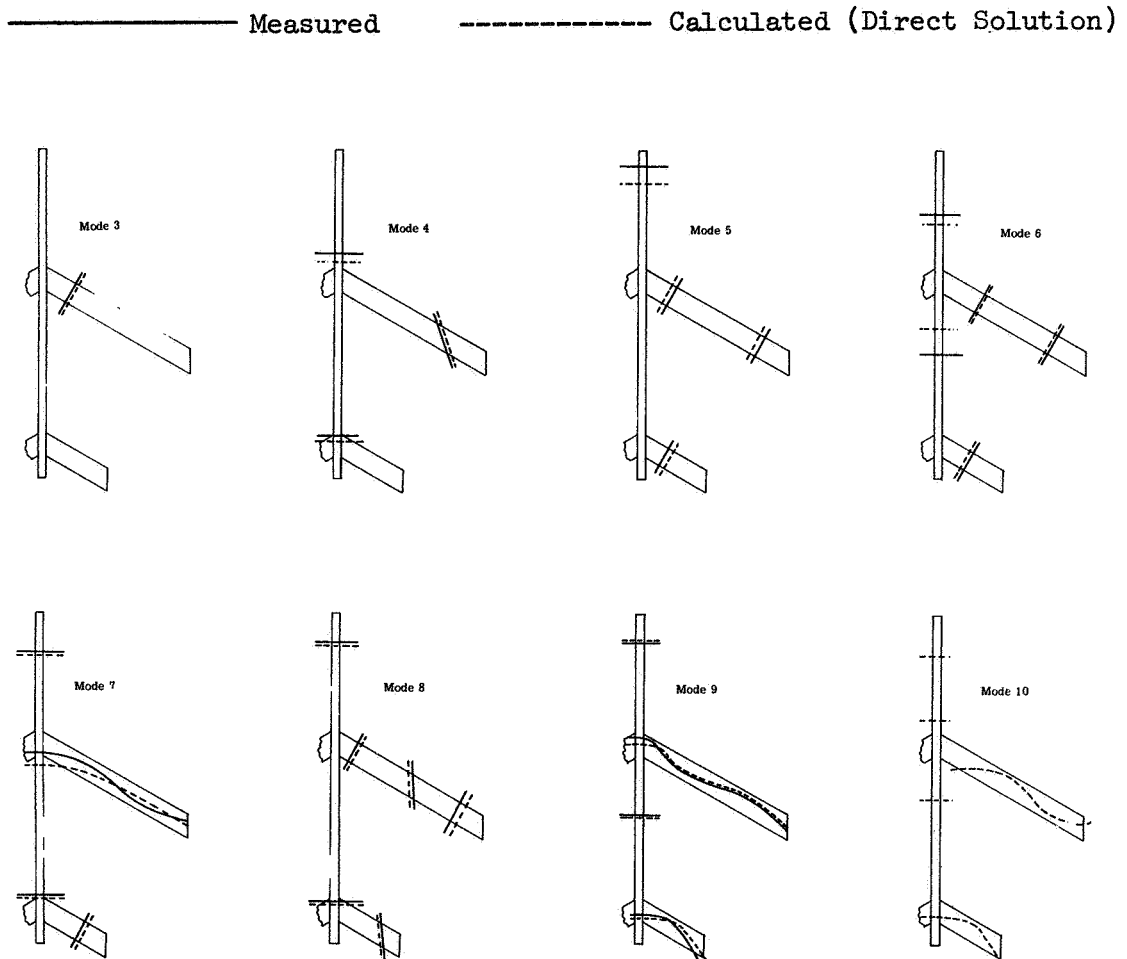


Figure F-5.- Comparison of measured and calculated nodal patterns for symmetric modes of model.

APPENDIX G

A GYROSCOPIC FINITE ELEMENT FOR USE IN DYNAMIC ANALYSES OF GYROSCOPICALLY COUPLED ELASTIC SYSTEMS

In dynamic analyses* of elastic systems having large rotating components, such as propellers or propellers on propeller- or propeller-driven aircraft or the fans of high bypass ratio ducted fanjet engines on turbo-fan jet powered aircraft, the gyroscopic effects arising from rotation may have a non-negligible influence on either the overall or local system dynamic characteristics. For dynamic analysis purposes the primary gyroscopic effects of such rotating components can be accounted for by idealizing each component as a rigid rotating disc. A finite element stiffness model based on this idealization which has the convenience of being readily incorporated into either a direct or modal formulation for dynamic analyses within the Lagrangian scheme for establishing equations of motion is derived below. The approach taken here is that of modifying the Lagrangian potential for the uncoupled system to account for the gyroscopic effects of any rotating components.

* Within the context of this discussion "dynamic analysis" includes both natural mode vibration analysis and structural response to time-dependent external excitation.

Within the finite element methodology the complete structure is partitioned into a number of simpler substructures. The spinning component is taken to be one such discrete substructure which is idealized as a rigid disc rotating with constant angular velocity Ω about its polar axis. The kinetic energy of a spinning disc performing translational and angular motions in space can be derived on the basis of the three sets of orthogonal axes shown in Fig. G-1. Coordinate axes $x_o y_o z_o$, the primary reference axes, are fixed in space. The axis systems $x_r y_r z_r$ and xyz are both moving coordinate systems located at the disc center of mass, denoted by O . The $x_r y_r z_r$ system moves only in translation, its coordinate axes remaining parallel to the corresponding axes of the space-fixed axes. To maintain the identity of the spin speed of the disc about the x axis as a distinct quantity the body axis triad xyz is fixed in the disc only to the extent that it participates in the variable (perturbation) angular motions of the disc in space. These axes are oriented such that the x axis remains normal to the plane of the disc; the plane formed by the yz axes lies in the plane of the disc. The disc spins about the x axis with angular velocity Ω with respect to the xyz system. Eulerian-type* angles θ , ψ , and ϕ are taken to define the

*Here the angles refer to rotations about mutually perpendicular axes in contrast to the unsymmetric definition of the Euler angles. A discussion of these alternative angles for describing the angular motion of a rigid body in space is given by L. A. Pars: A Treatise on Analytical Dynamics, John Wiley and Sons, Inc., New York, 1965, pp. 103-104.

orientation of the disc with respect to the translating axes $x_r y_r z_r$. The Cartesian coordinates of the center of mass in space-fixed axes together with the "Eulerian" angles completely describe the position of the disc in space and thus constitute a suitable set of generalized coordinates for the substructure.

The order of rotation in transforming from the translating axes $x_r y_r z_r$ to the body axes xyz is a positive pitch θ about the y_r axis, followed by a positive yaw ψ about the displaced z_r axis, followed by a positive rotation about the displaced x_r axis, as indicated in Fig. G-1. Since the axes moving with the disc are at the center of mass, the motion of the center of mass in the space-fixed system can be treated independently of the angular motion of the disc about its center of mass. The disc has velocity components $\dot{x}_O, \dot{y}_O, \dot{z}_O, \dot{\theta}, \dot{\psi}, \dot{\phi}$, and Ω . If ω_x, ω_y , and ω_z are the angular velocity components relative to the body axes xyz , the total kinetic energy of the disc can be written in vector notation as

$$T_G = \frac{1}{2} M \dot{\bar{r}} \cdot \dot{\bar{r}} + \frac{1}{2} \bar{\omega} \cdot \bar{H} \quad (G-1)$$

where

$$\dot{\bar{r}} = \dot{x}_O \bar{i}_O + \dot{y}_O \bar{j}_O + \dot{z}_O \bar{k}_O$$

$$\bar{\omega} = \omega_x \bar{i} + \omega_y \bar{j} + \omega_z \bar{k} \quad (G-2)$$

$$\bar{H} = I_x \omega_x \bar{i} + I_y \omega_y \bar{j} + I_z \omega_z \bar{k}$$

Because of polar symmetry the mass moments of inertia in the expression for \bar{H} are constant even though the body axes xyz are not fixed in the disc. From Fig. G-1 the angular velocity components relative to the xyz coordinate system can be written as

$$\begin{aligned}\omega_x &= \Omega + \dot{\theta} \sin \psi + \dot{\phi} \\ \omega_y &= \dot{\theta} \cos \psi \cos \phi + \dot{\psi} \sin \phi \\ \omega_z &= \dot{\psi} \cos \phi - \dot{\theta} \cos \psi \sin \phi\end{aligned}\tag{G-3}$$

For small angles, such as assumed in small vibration theory, Eqs. G-3 reduce to

$$\begin{aligned}\omega_x &\approx \Omega + \dot{\theta}\psi + \dot{\phi} \\ \omega_y &\approx \dot{\theta} + \dot{\psi}\phi \\ \omega_z &\approx \dot{\psi} - \dot{\theta}\phi\end{aligned}\tag{G-4}$$

We can also write

$$\begin{aligned}\dot{x}_O &\approx \dot{x} \\ \dot{y}_O &\approx \dot{y} \\ \dot{z}_O &\approx \dot{z}\end{aligned}\tag{G-5}$$

Substituting Eqs. G-2, G-4, and G-5 into Eq. G-1 and noting that $I_y = I_z$ from symmetry, the kinetic energy of the disc, to second order in the perturbation quantities, is given by

$$T_G = \frac{1}{2} M (\dot{x}^2 + \dot{y}^2 + \dot{z}^2) + \frac{1}{2} I_x (\Omega^2 + \underline{2\Omega\dot{\theta}\psi} + \dot{\phi}^2 + 2\Omega\dot{\phi}) + \frac{1}{2} I_y (\dot{\theta}^2 + \dot{\psi}^2) \quad (G-6)$$

The gyroscopic coupling term occurring as a consequence of spin is underlined. Eq. G-6 can be written in the matrix form

$$T_G = \frac{1}{2} \begin{Bmatrix} x \\ y \\ z \\ \theta \\ \psi \\ \phi \\ \psi \end{Bmatrix}^T \begin{bmatrix} M & 0 & 0 & 0 & 0 & 0 & 0 \\ 0 & M & 0 & 0 & 0 & 0 & 0 \\ 0 & 0 & M & 0 & 0 & 0 & 0 \\ 0 & 0 & 0 & I_y & 0 & 0 & \Omega I_x \\ 0 & 0 & 0 & 0 & I_y & 0 & 0 \\ 0 & 0 & 0 & 0 & 0 & I_x & 0 \\ 0 & 0 & 0 & \Omega I_x & 0 & 0 & 0 \end{bmatrix} \begin{Bmatrix} x \\ y \\ z \\ \theta \\ \psi \\ \phi \\ \psi \end{Bmatrix} \quad (G-7)^*$$

or, in abbreviated notation

$$T_G = \frac{1}{2} \begin{Bmatrix} \{\dot{\gamma}\} \\ \{\psi\} \end{Bmatrix}^T \begin{bmatrix} [\bar{M}]_G & [\bar{E}] \\ [\bar{E}]^T & [0] \end{bmatrix} \begin{Bmatrix} \{\dot{\gamma}\} \\ \{\psi\} \end{Bmatrix} \quad (G-8)$$

*The term $1/2 I_x(\Omega^2 + 2\Omega\dot{\phi})$ has been deleted because it will not contribute to the final equations of motion.

To accommodate a spin direction opposite to that shown in Fig. G-1 simply replace Ω in Eq. G-7 by $-\Omega$. Gravity has been removed from explicit consideration by assuming that all perturbations of the coupled system are to be measured from the static equilibrium position assumed by the structure with all the components spinning and gravity acting.

The corresponding potential energy expression is given by

$$V_G = \frac{1}{2} \{\gamma\}^T [\bar{K}]_G \{\gamma\} \quad (G-9)$$

where

$$[\bar{K}]_G = [\text{Null}] \quad (G-10)$$

since a rigid body has no strain energy associated with its displacement.

Eqs. G-8 and G-9 constitute the desired kinetic and potential energy expressions for a rigid rotating disc approximation to a spinning structural component such as a propeller, propotor, or fan. There is one such pair of expressions for each rotating component of a partitioned structure. These are simply grouped with the kinetic and potential energy expressions for the nonrotating substructures, a transformation to system generalized coordinates effected by enforcing inter-substructure displacement compatibility, and the resulting expressions substituted into Lagrange's equation to obtain the system equations of motion.

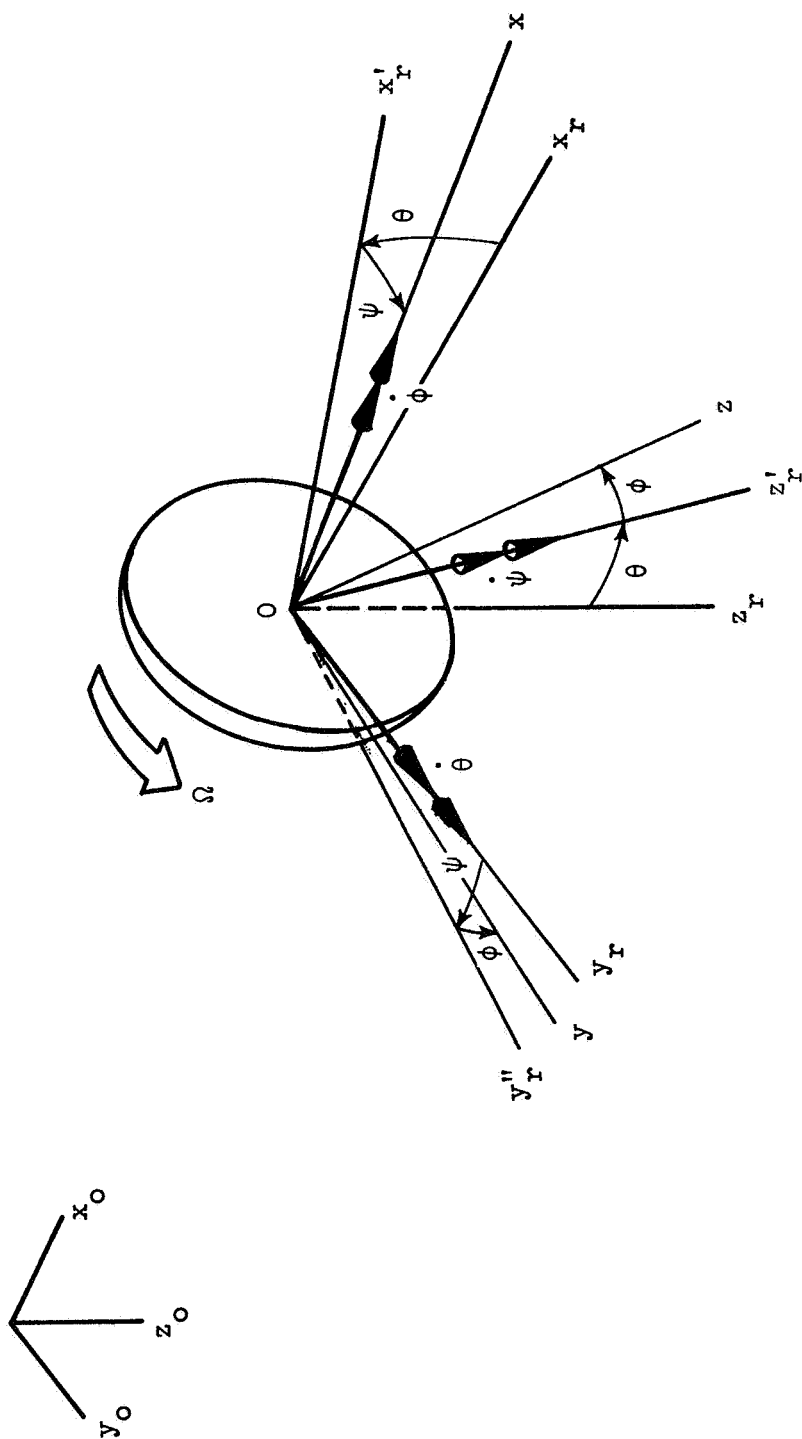


Figure G-1.- Coordinate systems employed for deriving the kinetic energy of a spinning disc which is performing translational and angular motions in space.

APPENDIX H

COMPUTER PROGRAMS

This appendix contains a listing of the computer programs employed in the numerical studies of this dissertation. These include three proprotor programs:

PRSTAB6 - Proprotor/Pylon Stability

HFORCE1 - Proprotor Force and Moment Derivatives

ROTDER4 - Proprotor Flapping Derivatives

and two computer "packages" for natural mode vibration analysis, each "package" consisting of an assembly of programs executed sequentially with disc communication between them:

DSTIFF/BJD5 - Vibration Analysis by a Direct Method

COSMOS/MODALC/BJD5M - Vibration Analysis by Component Mode Synthesis

A sample input is included with each of the programs.

The programs are written in FORTRAN IV for the CDC 6000 series computers with the Langley Research Center version of the SCOPE 3.0 operating system and the RUN compiler.

The author takes this opportunity to again acknowledge the programming assistance provided by Barbara J. Durling* and

* Structural Mechanics Branch, NASA-Langley

Robert N. Desmarais.* In addition to providing consultative services several subroutines from their personal computer program libraries were made available to the author for use herein. Specifically, computer program BJD5 and subroutines WMTXC, FREQ, and ZEROM used in the computer package for natural mode vibration analysis by the direct method were written by Barbara Durling. Program BJD5M and subroutine ALLEIG represent modifications of BJD5 by the author for use in the computer package for natural mode vibration analysis by component mode synthesis. The subroutines WMTXC, FREQ, and ZEROM were also employed in this latter assembly of programs. The function subprogram CIRC for evaluating Theodorsen's Circulation Function in program PRSTAB6 was written by Robert Desmarais.

* Aeroelasticity Branch, NASA-Langley

PROPROPOTOR/PYLON STABILITY

```
PROGRAM PRSTAB6(INPUT,OUTPUT,TAPE1,TAPE2,TAPE3,TAPE4,TAPE5=INPUT)
```

```
*****
*
*   THIS PROGRAM FORMULATES THE LINEAR EIGENVALUE PROBLEM
*   FOR THE DETERMINATION OF THE FLUTTER MODES AND
*   FREQUENCIES OF AN ISOLATED PROPROPOTOR/PYLON SYSTEM. THE
*   MATHEMATICAL MODEL ASSUMES A RIGID PYLON HAVING THREE
*   TRANSLATIONAL AND THREE ROTATIONAL DEGREES OF FREEDOM
*   AND A RIGID-BLADE GIMBALED ROTOR HAVING TIP-PATH-PLANE
*   FREEDOMS IN PITCH AND YAW. THE PROPROPOTOR IS TAKEN TO
*   BE FULLY CONVERTED FORWARD, REPRESENTING A HIGH-SPEED
*   AIRPLANE CRUISE MODE OF OPERATION. EITHER THEODORSEN
*   UNSTEADY AERODYNAMICS OR QUASI-STEADY AERODYNAMICS
*   MAY BE EMPLOYED FOR THE DISTRIBUTED BLADE LOADING.
*   BECAUSE THE RESULTING EQUATIONS CONTAIN NONPROPORTIONAL
*   DAMPING, THE N EQUATIONS OF SECOND ORDER ARE TRANSFORMED
*   TO AN EQUIVALENT SET OF 2N FIRST ORDER EQUATIONS IN
*   ORDER TO REDUCE THE MATRIX EQUATIONS TO STANDARD
*   EIGENVALUE FORM.
*
*****
```

```
C      KASE=1 -TPP PITCH AND YAW AND PYLON PITCH AND YAW
C      KASE=2 -PYLON PITCH AND YAW
C      KASE=3 -TPP PITCH AND YAW
C      KASE=4 -PYLON PITCH, YAW, AND VERTICAL TRANSLATION
C      KASE=5 -TPP PITCH AND YAW AND PYLON PITCH, YAW, AND
C              VERTICAL TRANSLATION
C      KASE=6 -TPP PITCH AND YAW AND PYLON PITCH
C      KASE=7 -TPP PITCH AND YAW AND PYLON PITCH, YAW,
C              AND AXIAL TRANSLATION
C      KASE=8 -TPP PITCH AND YAW AND PYLON PITCH, YAW,
C              VERTICAL TRANSLATION AND AXIAL TRANSLATION
C      KASE=9 -TPP PITCH AND YAW AND PYLON VERTICAL TRANSLATION

C      IAERO=1 -THEODORSEN UNSTEADY AERODYNAMICS
C      IAERO=2 -QUASI-STEADY AERODYNAMICS
C      IAERO=3 -NO AERODYNAMICS (SOLUTION GIVES NATURAL MODES)

C      IMACH=1 -PRANDTL-GLAUERT MACH NUMBER CORRECTION
C      IMACH=2 -MACH AND COMPRESSIBLE FLOW ASPECT RATIO CORRECTIONS
C      IMACH=3 -NO CORRECTIONS

C      IDAMP=1 -VISCIOUS STRUCTURAL DAMPING EMPLOYED FOR PYLON/WING
C      IDAMP=2 -COMPLEX STRUCTURAL DAMPING EMPLOYED FOR PYLON/WING
```

```
CCOMPLEX BM(8,8),BC(8,8),BK(8,8),H(16,16),W(16,16),LAMBDA(16),DET,
1      A(8,8),B(8,8),P(16),Q(16),AS(16,16),C,AT(16,16),
2      PQR(16),AST(16,17)
DIMENSION IPIVOT(8),INDEX(8,2),INTH(16,2),VKNOTS(60),FREQ(20),
1      T(16,3),U(8,8),TT(8,8),IR(8),RQ(8),FREQ1(20)
REAL MACH
```

```

COMMON HEAD1(12)
DIMENSION Z(16)
COMMON/UNSTDY/SUM(16),S,HSQ,MACH,R,BCH,VEL,FREQ1,II,IAERO,IMACH
COMPLEX A1,A2,A3,A4,A5,B1,B2,B3
EXTERNAL AERO
NAMELIST/ROTOR/NB,RI,RM,BU,PRECONE,H1,H2,R,BCH,DEN,DENSL,
1          AO,DELTA3,HSLONG,HSLAT,HDLONG,HDLAT,REF,SWPLONG,
2          SWPLAT,EPSILON,TD,VS
NAMELIST/PYLON/PM,PIROLL,PIPITCH,PIYAW,HB1,HB2,PSROLL,PSPITCH,
1          PSYAW,PSX,PSY,PSZ,PDX,PDY,PDZ,PDROLL,PDPITCH,
2          PDYAW,CB,WEMZ
1 READ 1000,(HEAD1(I),I=1,12)
IF(EOF,5)8998,8999
8997 FORMAT(1H1/* PROGRAM PRSTAB6 STOPPED ON (EOF,5)*)
8999 CCNTINUE
1000 FORMAT(8A10)
READ 1010,KASE,NFREQ,NVEL,IAERO,IMACH,LDAMP
1010 FORMAT(20I4)
READ 1020,(FREQ(I),I=1,NFREQ)
READ 1020,(VKNOTS(I),I=1,NVEL)
READ 1009,ETA1,ETA2,INC
IF(IAERO.EQ.1) READ 1020,(FREQ1(I),I=1,NFREQ)
1009 FORMAT(2E10.4,I10)
1020 FORMAT(8F10.4)
READ ROTOR
READ PYLON
RI=(NB*BI)/2
HDLONG=HDLONG*2*SQR(T(RI*HSLONG))
HDLAT=HDLAT*2*SQR(T(RI*HSLAT))
IF(LDAMP.EQ.1) GO TO 5
PGX=2*PDX $ PGY=2*PDY $ PGZ=2*PDZ
PGPITCH=2*PDPITCH $ PGYAW=2*PDYAW $ PGROLL=2*PDROLL
PCX=PDY=PDZ=PDPITCH=PDYAW=PDROLL=0.0
GO TO 6
5 PCX=PGY=PGZ=PGPITCH=PGYAW=PGROLL=0.0
PCX=PDX*2*SQR(T((PM+RM)*PSX))
PCY=PDY*2*SQR(T((PM+RM)*PSY))
PCZ=PDZ*2*SQR(T((PM+RM+WEMZ)*PSZ))
PDPITCH=PDPITCH*2*SQR(T((RM*(H1**2)+PIPITCH+PM*(HB1**2)
+PM*(CB**2))*PSPITCH))
1 PDYAW=PDYAW*2*SQR(T((RM*(H2**2)+PIYAW+PM*(HB2**2))*PSYAW))
PDROLL=PDROLL*2*SQR(T((NB*BI+PIROLL+PM*(CB**2))*PSROLL))
6 CONTINUE
RIJ=(NB*RI)/2
DELTA3=DELTA3/57.2957795130823
EPSILON=EPSILON/57.2957795130823
PRECONE=PRECONE/57.2957795130823
IF(IAERO.EQ.3) DEN=0.0
GAMMA=(DEN*AO*BCH*(P**4))/BI
RB=REF*R
DO 500 II=1,NFREQ
AF=FREQ(II)
FRFQ(II)=(6.28318531*FREQ(II))/60
IF(IAERO.EQ.1) FREQ1(II)=6.28318531*FREQ1(II)
DO 500 JJ=1,NVEL
DO 10 I=1,8
DO 10 J=1,8
BM(I,J)=0.0
BC(I,J)=0.0
10 BK(I,J)=0.0

```

```

BM(1,1)=BM(2,2)=BM(3,3)=RM+PM $ BM(4,4)=BM(5,5)=RI
BM(3,3)=BM(3,3)+WEMZ
BM(6,6)=NB*RI+PIROLL+PM*(CB**2)
BM(7,7)=RI+RM*(H1**2)+2.*RU*PRECCONE*H1+PIPITCH+PM*(HB1**2)
BM(7,7)=BM(7,7)+PM*(CB**2)
BM(8,8)=RI+RM*(H2**2)+2.*RU*PRECCONE*H2+PIYAW+PM*(HB2**2)
BM(2,5)=RU*PRECCONE $ BM(2,8)=RM*H2+RU*PRECCONE+PM*HB2
BM(3,4)=-RU*PRECCONE $ BM(3,7)=-RM*H1-RU*PRECCONE-PM*HB1
BM(4,7)=RI+RU*PRECCONE*H1 $ BM(5,8)=RI+RU*PRECCONE*H2
BM(5,2)=BM(2,5) $ BM(7,3)=BM(3,7) $ BM(7,4)=BM(4,7)
BM(8,2)=BM(2,8) $ BM(8,5)=BM(5,8)
BM(1,7)=BM(7,1)=-PM*CB
VEL=VKNOTS(JJ)/.592
MACH=VEL/VS
S=VEL/(FREQ(II)*R)
HSQ=S**2
PHI=ATAN(VEL/(FREQ(II)*RB))
IF(IAERO.EQ.3) GO TO 11
CALL MGAUSS(ETA1,ETA2,INC,SUM,AERO,Z,16)
A1=CMPLX(SUM(9),SUM(10)) $ A3=CMPLX(SUM(3),SUM(4))
A5=CMPLX(SUM(5),SUM(6)) $ B1=CMPLX(SUM(7),SUM(8))
B3=CMPLX(SUM(1),SUM(2)) $ B2=CMPLX(SUM(11),SUM(12))
A2=CMPLX(SUM(13),SUM(14)) $ A4=CMPLX(SUM(15),SUM(16))
11 CFM=.5*GAMMA*(FREQ(II)**2)*RI
CFH=CFM*S/R
CFMB=CFM*S*PRECCONE
IF(IAFRO.NE.3) GO TO 12
A1=A2=A3=A4=A5=B1=B2=B3=0.0
12 CCNTINUE
BC(1,1)=TD*((GAMMA*RI*FREQ(II)*A3)/(R**2))+PDX
BC(2,4)=BC(2,7)=CFH*A3/FREQ(II)
BC(2,2)=CFH*A1*S/(FREQ(II)*R)+PDY
BC(2,8)=CFH*A1*S*H2/(FREQ(II)*R)
BC(3,3)=CFH*A1*S/(FREQ(II)*R)+PDZ
BC(3,5)=BC(3,8)=CFH*A3/FREQ(II) $ BC(4,4)=CFM*A5/FREQ(II)+HDLONG
BC(3,7)=-CFH*A1*S*H1/(FREQ(II)*R)
BC(4,7)=CFM*A5/FREQ(II)+CFMB*A2*H1*S/(FREQ(II)*R)
BC(4,2)=CFM*A3*S/(FREQ(II)*R)
BC(4,8)=2.*RI*FREQ(II)+CFM*A3*S*H2/(FREQ(II)*R)-CFMB*A4/FREQ(II)
BC(4,5)=2.*RI*FREQ(II)-CFMB*A4/FREQ(II)
BC(4,3)=-CFMB*A2*S/(FREQ(II)*R) $ BC(5,5)=CFM*A5/FREQ(II)+HDLAT
BC(5,8)=CFM*A5/FREQ(II)+CFMB*A2*S*H2/(FREQ(II)*R)
BC(5,3)=CFM*A3*S/(FREQ(II)*R) $ BC(5,2)=CFMB*A2*S/(FREQ(II)*R)
BC(5,7)=-2.*RI*FREQ(II)-CFM*A3*H1*S/(FREQ(II)*R)+CFMB*A4/FREQ(II)
BC(5,4)=-2.*RI*FREQ(II)+CFMB*A4/FREQ(II) $ BC(7,4)=CFM*A5/FREQ(II)
BC(6,1)=-GAMMA*RI*FREQ(II)*S*A3/R $ BC(6,6)=PDROLL
BC(7,7)=CFM*A5/FREQ(II)+CFMB*A2*H1*S/(FREQ(II)*R)+CFH*A1*S*H1*H1/
1 (FREQ(II)*R)+PDPITCH $ BC(7,2)=CFM*A3*S/(FREQ(II)*R)
BC(7,8)=2.*RI*FREQ(II)+CFM*A3*S*H2/(FREQ(II)*R)-CFMB*A4/FREQ(II)-
1 CFH*A3*H1/FREQ(II)
BC(7,5)=2.*RI*FREQ(II)-CFMB*A4/FREQ(II)-CFH*A3*H1/FREQ(II)
BC(7,3)=-CFMB*A2*S/(FREQ(II)*R)-CFH*A1*S*H1/(FREQ(II)*R)
BC(8,5)=CFM*A5/FREQ(II) $ BC(8,3)=CFM*A3*S/(FREQ(II)*R)
BC(8,8)=CFM*A5/FREQ(II)+CFMB*A2*S*H2/(FREQ(II)*R)+CFH*A1*S*H2*H2/
1 (FREQ(II)*R)+PDYAW
BC(8,7)=-2.*RI*FREQ(II)-CFM*A3*H1*S/(FREQ(II)*R)+CFMB*A4/FREQ(II)
1 +CFH*A3*H2/FREQ(II)
BC(8,4)=-2.*RI*FREQ(II)+CFMB*A4/FREQ(II)+CFH*A3*H2/FREQ(II)
BC(8,2)=CFMB*A2*S/(FREQ(II)*R)+CFH*A1*S*H2/(FREQ(II)*R)
BK(1,1)=CMPLX(PXS,PSX*PGX) $ BK(2,2)=CMPLX(PSY,PSY*PGY)

```

```

RK(3,3)=CMPLX(PSZ,PSZ*PGZ) $ RK(6,6)=CMPLX(PSROLL,PSROLL*PGROLL)
RK(2,4)=CFH*F1*TAN(DELTA3) $ RK(2,5)=CFH*A3
RK(2,8)=-CFH*HSQ*A1+CFH*SWPLAT*B1*CCS(EPSILON)
RK(3,5)=CFH*B1*TAN(DELTA3) $ RK(2,7)=CFH*SWPLONG*SIN(EPSILON)*B1
RK(3,7)=CFH*A1*HSQ-CFH*B1*SWPLONG*CCS(EPSILON) $ BK(3,4)=-CFH*A3
RK(3,8)=CFH*B1*SWPLAT*SIN(EPSILON)
BK(4,4)=HSLONG+CFM*B3*TAN(DELTA3)+CFM*A4 $ BK(4,8)=-CFM*A3*HSQ+
1 CFM*B3*SWPLAT*CCS(EPSILON)-CFM*B2*SWPLAT*SIN(EPSILON)
RK(4,5)=CFM*A5-CFM*B2*TAN(DELTA3)
BK(4,7)=CFM*B3*SWPLONG*SIN(EPSILON)-CFM*A2*HSQ+CFM*SWPLONG*B2*
1 CCS(EPSILON)
RK(5,5)=HSLAT+CFM*B3*TAN(DELTA3)+CFM*A4
FK(5,4)=-CFM*A5+CFM*B2*TAN(DELTA3)
BK(5,7)=CFM*A3*HSQ-CFM*B3*SWPLONG*CCS(EPSILON)+CFM*B2*SWPLONG*
1 SIN(EPSILON) $ BK(5,8)=CFM*B3*SWPLAT*SIN(EPSILON)-CFM*B
2 A2*HSQ+CFM*B2*SWPLAT*CCS(EPSILON)
BK(7,4)=CFM*B3*TAN(DELTA3)+CFM*A4+CFH*A3*H1
BK(7,5)=CFM*A5-CFM*B2*TAN(DELTA3)-CFH*B1*H1*TAN(DELTA3)
BK(7,7)=CMPLX(PSPITCH,PSPITCH*PGPITCH)+CFM*B3*SWPLONG*SIN(EPSILON)
1 -CFM*A2*HSQ+CFM*SWPLONG*B2*CCS(EPSILON)-CFH*A1*HSQ*H1+
2 CFH*B1*SWPLONG*H1*CCS(EPSILON)
BK(7,8)=CFM*B3*SWPLAT*CCS(EPSILON)-CFM*B2*SWPLAT*SIN(EPSILON)-CFH
1 *B1*SWPLAT*H1*SIN(EPSILON)-CFM*A3*HSQ
BK(8,5)=CFM*B3*TAN(DELTA3)+CFM*A4+CFH*A3*H2
BK(8,4)=-CFM*A5+CFM*B2*TAN(DELTA3)+CFH*B1*H2*TAN(DELTA3)
BK(8,7)=CFM*A3*HSQ+CFH*B1*SWPLONG*H2*SIN(EPSILON)-CFM*B3*
1 SWPLONG*CCS(EPSILON)+CFM*B2*SWPLONG*SIN(EPSILON)
RK(8,8)=CMPLX(PSYAW,PSYAW*PGYAW)+CFM*B3*SWPLAT*SIN(EPSILON)-CFM*B
1 A2*HSQ+CFM*B2*SWPLAT*CCS(EPSILON)-CFH*A1*HSQ*H2
2 +CFH*B1*SWPLAT*H2*CCS(EPSILON)
FEWIND 1
FEWIND 3
WRITE(1)((RM(I,J),J=1,8),I=1,8)
WRITE(1)((RC(I,J),J=1,8),I=1,8)
WRITE(1)((BK(I,J),J=1,8),I=1,8)
DO 8 I=1,8
DO 8 J=1,8
8 U(I,J)=0.0
DO 9 I=1,8
9 L(I,I)=1.0
GO TO(21,22,23,24,25,26,27,28,29)KASE
21 NDF=4
IR(1)=4 $ IR(2)=5 $ IR(3)=7 $ IR(4)=8
GO TO 30
22 NDF=2
IR(1)=7 $ IR(2)=8
GO TO 30
23 NDF=2
IR(1)=4 $ IR(2)=5
GO TO 30
24 NDF=3
IR(1)=3 $ IR(2)=7 $ IR(3)=8
GO TO 30
25 NDF=5
IR(1)=3 $ IR(2)=4 $ IR(3)=5 $ IR(4)=7 $ IR(5)=8
GO TO 30
26 NDF=3
IR(1)=4 $ IR(2)=5 $ IR(3)=7
GO TO 30

```



```

27 NDF=5
   IR(1)=1 $ IR(2)=4 $ IR(3)=5 $ IR(4)=7 $ IR(5)=8
   GO TO 30
28 NDF=6
   IR(1)=1 $ IR(2)=3 $ IR(3)=4 $ IR(4)=5 $ IR(5)=7 $ IR(6)=8
   GO TO 30
29 NDF=3
   IR(1)=3 $ IR(2)=4 $ IR(3)=5
   GO TO 30
30 CCNTINUE
   DO 50 KK=1,NDF
   I=IR(KK)
   DO 50 J=1,8
50 TT(KK,J)=U(I,J)
   REWIND 2
   DO 330 I=1,NDF
330 WRITE(2)(TT(I,J),J=1,8)
   REWIND 1
   DO 333 KL=1,3
   READ(1)((BM(I,J),J=1,8),I=1,8)
   RFWIND 2
   DO 331 J=1,NDF
   READ(2)(RQ(I),I=1,8)
   DO 331 I=1,8
   BC(I,J)=0.0
   DO 331 IJ=1,8
331 BC(I,J)=BC(I,J)+BM(I,IJ)*RQ(IJ)
   REWIND 2
   DO 332 I=1,NDF
   READ(2)(RQ(J),J=1,8)
   DO 332 J=1,NDF
   BM(I,J)=0.0
   DO 332 IJ=1,8
332 BM(I,J)=BM(I,J)+RQ(IJ)*BC(IJ,J)
   WRITE(3)((BM(I,J),J=1,NDF),I=1,NDF)
333 CCNTINUE
   REWIND 3
   READ(3)((BM(I,J),J=1,NDF),I=1,NDF)
   READ(3)((BC(I,J),J=1,NDF),I=1,NDF)
   READ(3)((BK(I,J),J=1,NDF),I=1,NDF)
   NDFT2=2*NDF
   CALL EIG2N(BM,BC,BK,NDF,NDFT2,W,LAMBDA)
   DO 13 I=1,NDFT2
   T(I,1)=AIMAG(LAMBDA(I))/6.28318530717959
   T(I,2)=(T(I,1)*60.)/AF
   IF(AIMAG(LAMBDA(I)).EQ.0.0) GO TO 13
   T(I,3)=(REAL(LAMBDA(I))/ABS(AIMAG(LAMBDA(I))))*100.
13 CCNTINUE
   PRINT 1014,HEAD1
1014 FORMAT(1H1//12A10////)
   VKEAS=VKNOTS(JJ)*SQRT(DEN/DENSL)
   AR=3.14159265358979*VEL/(FREQ(II)*R)
   PHI=PHI*57.2957795130823
   IF(DEN.NE.0.0) GO TO 1015
   VEL=VKNOTS(JJ)=AR=PHI=0.0
1015 PRINT 1013
1013 FCRMAT(1H0,3X,*ROTOR RPM*,28X,*VELOCITY*,27X,*ADVANCE RATIO*,
18X,*LOCK NUMBER*.9X,*INFLOW ANGLE**//26X,*FT/SEC*.11X,*KNOTS*,
213X,*KEAS*.17X,*J*.39X,*PHI**//)
   PRINT 1012,AF,VEL,VKNOTS(JJ),VKEAS,AR,GAMMA,PHI

```

```

1012 FORMAT(1X,F15.9,6X,F15.8,2X,F15.8,2X,E15.8,5X,F15.8,5X,F15.8,
15X,F15.8////)
      IF(KASE.FQ.2) GO TO 123
      IF(HSLONG.NE.HSLA*) GO TO 123
      SAVE1=1.0+HSLONG/(R1*FREQ(I1)**2)+.50*GAMMA*B3*TAN(DELTA3)
      IF(SAVE1.LT.0.0) GO TO 123
      BFF=SQRT(SAVE1)
      BDR=25*GAMMA*A5/BFF
      PRINT 1016,BFF,BDR
1016 FORMAT(1X,43H**** BLADE FLAPPING FREQUENCY(CYCLES/REV) =,F10.3,
1      20X,38H**** BLADE DAMPING(PERCENT CRITICAL) =,F10.3////)
123 CONTINUE
      PRINT 1011
1011 FORMAT(11X,*SYSTEM EIGENVALUES*,28X,*FREQUENCY*,24X,*DAMPING*///
1      8X,*REAL*,12X,*IMAGINARY*,17X,*CPS*,13X,*CYCLES/REV*,
2      10X,*PERCENT CRITICAL*)
      PRINT 1040,(LAMBDA(I),(T(I,J),J=1,3),I=1,NDFT2)
1040 FORMAT(// (2X,E15.8,4X,E15.8,8X,E15.8,4X,E15.8,8X,E15.8) )
      CALL WCM(W,NDFT2,NDFT2)
500 CONTINUE
      GO TO 1
8998 PRINT 8997
      END

```

```

SUBROUTINE EIG2N(BM,BC,BK,N,NT2,W,LAMBDA)
  COMPLEX BM(8,8),BC(8,8),BK(8,8),H(16,16),W(16,16),LAMBDA(16),DET,
1      A(8,8),B(8,8),P(16),Q(16),AS(16,16),C,AT(16,16),
2      PQR(16),AST(16,17)
  DIMENSION IPIVOT(8),INDEX(8,2),INTH(16,2),VKNOTS(20),FREQ(20),
1      T(16,3),U(8,8),TT(8,8),IR(8),PQ(8)
  INTH(1,1)=NT2 $ INTH(2,1)=NT2
  CALL CXINV(BM,N,C,O,DET,IPIVOT,INDEX,8,ISCALE)
  CALL CMULT(BM,BC,A,N)
  CALL CMULT(BM,BK,B,N)
  DO 20 I=1,N
  DO 20 J=1,N
  A(I,J)=-A(I,J)
20 B(I,J)=-B(I,J)
  DO 50 I=1,N
  DO 50 J=1,NT2
  F(I,J)=0.0
  DO 55 I=1,N
  J=N+I
55 F(I,J)=1.0
  MN = N+1
  DO 60 I=MN,NT2
  K=I-N
  DO 60 J=1,N
60 F(I,J)=B(K,J)
  DO 65 I = MN,NT2
  K=I-N
  DO 65 J = MN,NT2
  L=J-N
65 H(I,J)=A(K,L)
  CALL CFIG(H,LAMBDA,NT2,16,P,Q,PQR,AST,W,NT2)
  RETURN $ END

```

```

SUBROUTINE CMULT(A,B,C,N)
  COMPLEX A(8,8),B(8,8),C(8,8)
  DO 10 I=1,N
  DO 10 J=1,N
  C(I,J)=0.0
  DO 10 K=1,N
10 C(I,J)=C(I,J)+A(I,K)*B(K,J)
  RETURN $ END

SUBROUTINE WCM(A,NR,NC)
  COMPLEX A(16,16)
  COMMON HEAD1(12)
  KE=0
  KSFT=NC/4
  KLEFT=MOD(NC,4)
  IF(KLEFT.NE.0) KSET=KSET+1
  DO 10 KT=1,KSFT
  KB=KE+1
  KE=KE+4
  IF(KT.EQ.KSET) KE=NC
  PRINT 5001,HEAD1,(J,J=KB,KE)
5001 FCRMAT(1H1//12A10//1X,* SYSTEM EIGENVECTORS *///10H ROW COL,8X,
1I4.3(26X14)//10X,*REAL*,9X,*IMAGINARY*,3(8X,*REAL*,9X,*IMAGINARY*)
2//)
  DO 10 I=1,NR
  10 PRINT 5002,I,(A(I,J),J=KB,KE)
5002 FCRMAT(14.8E15.7)
  RETURN
  END

SUBROUTINE AERO(X,Z)
  DIMENSION Z(16),FREQ1(20)
  COMMON/UNSTDY/SUM(16),S,HSQ,MACH,R,BCH,VEL,FREQ1,II,[AERO,IMACH]
  COMPLEX CIRC,C,CCNST
  REAL MACH
  IF(IAERO.EQ.2) GO TO 91
  RFREQ=FREQ1(II)*BCH*S/(2*VEL*SQRT(-HSQ+X**2))
  C=CIRC(RFREQ,F,G)
  GO TO 92
91 C=(1.0,0.0)
92 IF(IMACH.EQ.1) CCMCOR=1.0/SQRT(1.0-((MACH**2/HSQ)*(HSQ+X**2)))
  IF(IMACH.EQ.2) CCMCOR=R/(2.*BCH+R*SQRT(1.-(MACH**2/HSQ)*
1 (HSQ+X**2)))
  IF(IMACH.EQ.3) CCMCOR=1.0
  CCNST=C*CCMCOR
  PQ=SQRT(HSQ+X**2)
  Z(1)=REAL(CONST*(X**2)*PQ) $ Z(2)=AIMAG(CONST*(X**2)*PQ)
  Z(3)=REAL(CONST*(X**2)/PQ) $ Z(4)=AIMAG(CONST*(X**2)/PQ)
  Z(5)=REAL(CONST*(X**4)/PQ) $ Z(6)=AIMAG(CONST*(X**4)/PQ)
  Z(7)=REAL(CONST*PQ) $ Z(8)=AIMAG(CONST*PQ)
  Z(9)=REAL(CONST/PQ) $ Z(10)=AIMAG(CONST/PQ)
  Z(11)=REAL(CONST*X*PQ) $ Z(12)=AIMAG(CONST*X*PQ)
  Z(13)=REAL(CONST*X/PQ) $ Z(14)=AIMAG(CONST*X/PQ)
  Z(15)=REAL(CONST*(X**3)/PQ) $ Z(16)=AIMAG(CONST*(X**3)/PQ)
  RETURN $ END

```

```

COMPLEX FUNCTION CIRC(X,F,G) $ REAL JO,J1 $ COMPLEX D,P,W,CSQRT
COMPILATION FIELD LENGTH IS 36300. SUBPROGRAM LENGTH IS 504.
DATA PI,GAMMA/3.14159265358979,.577215664901533/
IF(X.LT.1.E-4) GO TO 2 $ IF(X.GT.20) GO TO 4 $ Z=2/X
A=GAMMA-ALOG(Z) $ N=1.3+.75*SQRT(X*(X+28)) $ K=N+1 $ S=-(-1)**N
J1=Y1=0 $ JO=1.E-100 $ YO=-S*JO/K $ DO 1 I=1,N $ K=K-1
J1=(2*K+2)*Z*JO-J1 $ Y1=Y1+S*(2*K+1)*J1/(K*(K+1.))
JO=(2*K+1)*Z*J1-JO $ YO=YO+S*JO/K
1 S=-S $ J1=2*Z*JO-J1 $ JO=Z*J1-JO $ YO=A*JO+2*YO
Y1=-JO/X+(A-1)*J1+Y1 $ J1=.5*PI*J1 $ JO=.5*PI*JO
D=CMPLX(YO,JO)/CMPLX(Y1,J1) $ CIRC=1/(1+(D.,1.)*D) $ F=REAL(CIRC)
G=AIMAG(CIRC) $ RETURN
2 IF(X.LE.0) GO TO 3 $ D=GAMMA+ALOG(.5*X)+(0.,.5)*PI
D=-X*D/(1-(D-1)*.5*X*X) $ CIRC=1/(1+(D.,1.)*D) $ F=REAL(CIRC)
G=AIMAG(CIRC) $ RETURN
3 F=1 $ G=0 $ CIRC=CMPLX(F,G) $ RETURN
4 W=(0.,4.)*X $ N=120/SQRT(X) $ P=.5*(-1+CSQRT(1+4*N/W)) $ N=2*N+1
5 N=N-2 $ P=N/(W+N/(1+P)) $ IF(N.GT.1) GO TO 5 $ CIRC=1-.5/(1+P)
F=REAL(CIRC) $ G=AIMAG(CIRC) $ RETURN
END          COMPLEX FUNCTION CIRC

```

PROPRTOR STABILITY KORRELATION - LANGLEY TDT TEST 139 - RUN NO.3
PYLON YAW UNLOCKED (298 RPM)

	8	1	21	2	3	2	
298.							
100.		120.		140.		160.	180.
260.		280.		300.		320.	340.
420.		440.		460.		480.	500.
.12		1.0				10	

\$ROTOR NB=3, BI=900., RM=45., BU=138., PRECONE=3., H1=6.92, H2=6.92, R=19.25,
BCH=1.92, DEN=.00222, DENSL=.00222, AO=5.85, DELTA3=-22.5, HSLONG=0.0,
HSLAT=0.0, HDLUNG=0.0, HDLAT=0.0, REF=.75, SWPLUNG=0.0, S#PLAT=0.0,
EPSILON=0.0, TD=1.0, VS=1116.0\$
\$PYLON PM=84.2, PIRDLL= 0.0 , PIPITCH=845., PIYAW=845., HB1=2.39, HB2=2.39,
PSKOLL=0.0, PSPITCH=230000., PSYAW= 500000., PSX=42300., PSY=0.0,
PSZ=25200., PDY=0.0, PDZ=.013, PDROLL=0.0, PDPTCH=.013,
PDYAW=.013, CB=1.10, WEMZ=5.37\$

PROPROTOR FORCE AND MOMENT DERIVATIVES

PROGRAM HFORCE1(INPUT,OUTPUT,TAPE5=INPUT)

```

*****
*
*       THIS PROGRAM CALCULATES THE DYNAMIC PROPROTOR FORCE
*       AND MOMENT DERIVATIVES ARISING FROM SINUSOIDAL
*       PITCHING OSCILLATIONS OF THE PYLON. THE RIGID-BLADE
*       MATHEMATICAL MODEL EMPLOYED HAS TIP-PATH-PLANE PITCH
*       AND YAW AND PYLON PITCH DEGREES OF FREEDOM. A QUASI-STEADY
*       AERODYNAMIC THEORY IS EMPLOYED FOR THE DISTRIBUTED
*       BLADE LOADING.
*
*****

```

```

      COMPLEX A(2,2),B(2),DET,HZ(80),HY(80),MY(80),MZ(80)
      DIMENSION HEAD1(12),RPM(20),VKNCTS(20),FREQ(80),IPIVOT(2),T(80,3),
1      INDEX(2,2),TT(80,4),TU(80,4)
      NAMELIST/ROTOR/NB,BI,BU,PRECONE,H1,R,BCH,DEN,AO,DELTA3,HSLONG,
1      HSLAT,SWPLONG,EPSILON
      NAMELIST/PYLON/PHIYO
1      READ 1000,(HEAD1(I),I=1,12)
      IF(EOF,5)8998,8999
8997  FORMAT(1H1/** PROGRAM HFORCE1 STOPPED ON (EOF,5)*)
8999  CONTINUE
1000  FORMAT(8A10)
      READ 1010,NRPM,NVEL,NFREQ
1010  FORMAT(20I4)
      READ 1020,(RPM(I),I=1,NRPM)
      READ 1020,(VKNCTS(I),I=1,NVEL)
      READ 1020,(FREQ(I),I=1,NFREQ)
1020  FORMAT(RE10.4)
      READ 1020,ETA1,ETA2
      READ ROTOR
      READ PYLON
      RI=(NB*BI)/2
      RU=(NR*BU)/2
      DELTA3=DELTA3/57.2957795130823
      EPSILON=EPSILON/57.2957795130823
      PRECONE=PRECONE/57.2957795130823
      GAMMA=(DEN*AO*BCH*(R**4))/BI
      PA=PHIYO
      PHIYO=PHIYO/57.2957795130823
      DO 500 II=1,NRPM
      AF=RPM(II)
      RPM(II)=(A.28318531*RPM(II))/60
      DO 500 JJ=1,NVEL
      DO 490 KK=1,NFREQ
      BF=FREQ(KK)
      FREQ(KK)=FREQ(KK)*RPM(II)
      T(KK,1)=BF
      T(KK,2)=FREQ(KK)/6.28318530717959
      T(KK,3)=FREQ(KK)
      VFL=VKNCTS(JJ)/.592
      S=VFL/(RPM(II)*R)

```

```

HSQ=S**2
WW1=SQRT(HSQ+ETA1**2)
WW2=SQRT(HSQ+ETA2**2)
FQ=ETA2*WW2-ETA1*WW1
A1=ALOG((ETA2+WW2)/(ETA1+WW1))
A2=WW2-WW1
A3=.5*(PQ-HSQ*A1)
A4=(1./3.)*(WW2**3-WW1**3)-HSQ*(WW2-WW1)
A5=.25*((ETA2**3)*WW2-(ETA1**3)*WW1)-(3./8.)*HSQ*(PQ-HSQ*A1)
R1=.5*(PQ+HSQ*A1)
R2=(1./3.)*(WW2**3-WW1**3)
R3=.25*(ETA2*WW2**3-ETA1*WW1**3)-(1./8.)*HSQ*(PQ+HSQ*A1)
CFM=.5*GAMMA*(RPM(II)**2)*R1
CFH=CFM*S/R
CFMB=CFM*S*PRECONE
FS=FREQ(KK)**2
A(1,1)=CMPLX(-PI*FS+HSLONG+CFM*B3*TAN(DELTA3)+CFMB*A4,
1      FREQ(KK)*CFM*A5/RPM(II))
A(1,2)=CMPLX(CFM*A5-CFMB*B2*TAN(DELTA3),FREQ(KK)*(2*I*FPM(II)
1      -CFMB*A4/RPM(II)))
A(2,1)=CMPLX(-CFM*A5+CFMB*B2*TAN(DELTA3),FREQ(KK)*(-2*R1*RPM(II)
1      +CFMB*A4/RPM(II)))
A(2,2)=CMPLX(-PI*FS+HSLAT+CFM*B3*TAN(DELTA3)+CFMB*A4,
1      FREQ(KK)*CFM*A5/RPM(II))
P(1)=CMPLX((FS*(R1+R2*PRECONE*H1)-CFM*B3*SWPLONG*SIN(EPSILON)
1      +CFMB*HSQ*A2-CFMB*B2*SWPLONG*CCS(EPSILON))*PHIYO,
2      -FREQ(KK)*PHIYO*(CFM*A5/RPM(II)+CFMB*S*A2*H1/
3      (RPM(II)*R)))
P(2)=CMPLX((-CFM*HSQ*A3+CFM*SWPLONG*B3*CCS(EPSILON)-CFMB*B2*
1      SWPLONG*SIN(EPSILON))*PHIYO,FREQ(KK)*PHIYO*
2      (2*I*RPM(II)+CFM*S*A3*H1/(RPM(II)*R)-CFM*B4/RPM(II)))
CALL CXTRV(A,2,R,1,DET,IPIVOT,INDEX,2,ISCALE)
DET=(0.0,1.0)
HY(KK)=CFH*(-R1*B(1)*TAN(DELTA3)-A3*B(2)-SWPLONG*R1*SIN(EPSILON)*
1      PHIYO)-CFH*DET*BF*A3*(B(1)+PHIYO)
HZ(KK)=-CFH*(R1*B(2)*TAN(DELTA3)+HSQ*A1*PHIYO-A3*B(1)-SWPLONG*
1      R1*CCS(EPSILON)*PHIYO)-CFH*DET*(BF*B(2)*A3-BF*S*A1*
2      H1*PHIYO/R)
MY(KK)=-CFM*(R3*B(1)*TAN(DELTA3)+A5*B(2)+SWPLONG*B3*SIN(EPSILON)*
1      PHIYO)-CFM*DET*(BF*B(1)+BF*PHIYO)*A5+CFMB*(B2*B(2)
2      *TAN(DELTA3)+HSQ*A2*PHIYO-A4*B(1)-B2*SWPLONG*CCS(EPSILON)
3      *PHIYO)+CFMB*DET*(BF*B(2)*A4-BF*S*A2*H1*PHIYO/R)
490 MZ(KK)=-CFM*(R3*B(2)*TAN(DELTA3)+HSQ*A3*PHIYO-A5*B(1)-B3*SWPLONG
1      *CCS(EPSILON)*PHIYO)-CFM*DET*(BF*B(2)*A5-BF*S*A3*H1*PHIYO
2      /R)+CFMB*(-B2*B(1)*TAN(DELTA3)-A4*B(2)-B2*SWPLONG*
3      SIN(EPSILON)*PHIYO)-CFM*DET*(BF*B(1)+BF*PHIYO)
DO 33 IJ=1,NFREQ
TT(IJ,1)=FEAL(HZ(IJ))/PHIYO
TT(IJ,2)=AIMAG(HZ(IJ))/(FREQ(IJ)*PHIYO)
TT(IJ,3)=FEAL(MY(IJ))/PHIYO
TT(IJ,4)=AIMAG(MY(IJ))/(FREQ(IJ)*PHIYO)
TU(IJ,1)=FEAL(HY(IJ))/PHIYO
TU(IJ,2)=AIMAG(HY(IJ))/(FREQ(IJ)*PHIYO)
TU(IJ,3)=FEAL(MZ(IJ))/PHIYO
32 TU(IJ,4)=AIMAG(MZ(IJ))/(FREQ(IJ)*PHIYO)
VKFAS=VKFNCTS(JJ)*SQRT(DEN/.00238)
AP=3.14159265358979*VEL/(RPM(II)*R)
PRINT 1030,HEAD1
1030 FORMAT(1H1//12A10////)
PRINT 103

```

```

1031 FORMAT(1H0,3X,*ROTOR RPM*,28X,*VELOCITY*,27X,*ADVANCE RATIO*,10X,
1      *PYLON PITCH AMPLITUDE*///26X,*FT/SEC*,11X,*KNOTS*,13X,
2      *KEAS*,17X,*J*,15X,*DEGREE S*,10X,*RADIANS*//)
      PRINT 1032,AF,VEL,VKNOTS(JJ),VKEAS,AR,PA,PHIYO
1032 FORMAT(1X,E15.8,5X,E15.8,2X,E15.8,2X,E15.8,4X,E15.8,3X,E15.8,2X,
1      E15.8////)
      PRINT 1033
1033 FORMAT(16X,*PYLON PITCH FREQUENCY*,28X,*ROTOR INPLANE H-FORCE*,
1      14X,*H-FORCE DERIVATIVES*///5X,*CYCLES/REV*,11X,*CPS*,
2      12X,*RAD/SEC*,16X,*REAL*,11X,*IMAGINARY*,1CX,*H-ALPHA*,
3      7X,*H-ALPHA DOT*)
      PRINT 1034,(((T(I,J),J=1,3),HZ(I),(TT(I,K),K=1,2)),I=1,NFREQ)
1034 FORMAT(//(2X,E15.8,2X,E15.8,2X,E15.8,8X,E15.8,2X,E15.8,2X,E15.8,
1      2X,E15.8))
      PRINT 1035
1035 FORMAT(1H1/16X,*PYLON PITCH FREQUENCY*,28X,*ROTOR INPLANE Y-FORCE*
1      ,14X,*Y-FORCE DERIVATIVES*///5X,*CYCLES/REV*,11X,*CPS*,
2      12X,*RAD/SEC*,16X,*REAL*,11X,*IMAGINARY*,1CX,*Y-ALPHA*,
3      7X,*Y-ALPHA DOT*)
      PRINT 1036,(((T(I,J),J=1,3),HY(I),(TU(I,K),K=1,2)),I=1,NFREQ)
1036 FORMAT(//(2X,E15.8,2X,E15.8,2X,E15.8,8X,E15.8,2X,E15.8,2X,E15.8,
1      2X,E15.8))
      PRINT 1037
1037 FORMAT(1H1/16X,*PYLON PITCH FREQUENCY*,28X,*ROTOR PITCHING MOMENT*
1      ,10X,*PITCHING MOMENT DERIVATIVES*///5X,*CYCLES/REV*,11X,
2      *CPS*,12X,*RAD/SEC*,16X,*REAL*,11X,*IMAGINARY*,10X,
3      *M-ALPHA*,7X,*M-ALPHA DOT*)
      PRINT 1034,(((T(I,J),J=1,3),MY(I),(TT(I,K),K=3,4)),I=1,NFREQ)
      PRINT 1038
1038 FORMAT(1H1/16X,*PYLON PITCH FREQUENCY*,29X,*ROTOR YAWING MOMENT*,
1      12X,*YAWING MOMENT DERIVATIVES*///5X,*CYCLES/REV*,11X,
2      *CPS*,12X,*RAD/SEC*,17X,*REAL*,11X,*IMAGINARY*,9X,
3      *N-ALPHA*,7X,*N-ALPHA DOT*)
      PRINT 1034,(((T(I,J),J=1,3),MZ(I),(TU(I,K),K=3,4)),I=1,NFREQ)
      DO 22 I=1,NFREQ
      22 FREQ(I)=T(I,1)
      500 CONTINUE
      GO TO 1
8998 PRINT 8<97
      END

```

PROPRTOR OSCILLATORY FORCE AND MOMENT DERIVATIVES - SAMPLE INPUT LISTING

```

      2      1      32
238.      298.
350.
0.0      .02      .04      .06      .08      .1      .12      .14
.16      .18      .2      .24      .28      .3      .4      .6
.8      1.0      1.2      1.4      1.5      1.6      1.64      1.7
1.74      1.8      1.84      1.9      2.0      2.4      3.0      10.0
0.0      1.0
$ROTOR NB=3,RI=791.0,BU=138.,PRECONE=0.0,H1=6.92,R=19.25,BCH=1.92,
DEN=.00238,AO=5.73,DELTA3=-22.5,HSLONG=20000.0,HSLAT=20000.0,
SWPLONG=0.0,EPSILON=0.0$
$PYLON PHIYO=6.0$

```

PROPROPOTOR FLAPPING DERIVATIVES

PROGRAM ROTDER4(INPUT,OUTPUT,TAPES=INPUT)

```

*****
*
*       THIS PROGRAM CALCULATES THE DYNAMIC PROPROPOTOR FLAPPING
*       DERIVATIVES ARISING FROM SINUSOIDAL PITCHING OR YAWING
*       OSCILLATIONS OF THE PYLON. THE RIGID-BLADE MATHEMATICAL
*       MODEL EMPLOYED HAS TIP-PATH-PLANE PITCH AND YAW AND
*       PYLON PITCH AND YAW DEGREES OF FREEDOM. A QUASI-STEADY
*       AERODYNAMIC THEORY IS EMPLOYED FOR THE DISTRIBUTED
*       BLADE LOADING.
*
*****

      COMPLEX A11,A12,A21,A22,B11,B21,B12,B22,DEL,DA1Y(80),DB1Y(80),
1      DA1Z(80),DB1Z(80),DBETAY(80),DBETAZ(80)
      DIMENSION HEAD1(12),KPM(20),VKNCTS(20),FREQ(80),T(80,3),TT(80,6),
1      TU(80,6)
      NAMELIST/ROTOR/NB,BI,BU,PRECONF,H1,H2,R,BCH,DEA,AC,DELTA3,HSLONG,
1      HSLAT,SWPLNG,SWPLAT,EPSILON,REF
1 READ 1000,(HEAD1(I),I=1,12)
      IF(EOF,5)8998,8999
8997 FORMAT(1H1/** PROGRAM ROTDER4 STOPPED ON (EOF,5)*)
8999 CONTINUE
1000 FORMAT(8A10)
      READ 1010,NRPM,NVEL,NFREQ
1010 FORMAT(20I4)
      READ 1020,(RPM(I),I=1,NRPM)
      READ 1020,(VKNCTS(I),I=1,NVEL)
      READ 1020,(FREQ(I),I=1,NFREQ)
      READ 1020,ETA1,ETA2
1020 FORMAT(8F10.4)
      READ ROTOR
      RI=(NB*BI)/2
      RU=(NB*BU)/2
      DELTA3=DELTA3/57.2957795130823
      PRECONF=PRECONF/57.2957795130823
      EPSILON=EPSILON/57.2957795130823
      GAMMA=(DEA*AO*BCH*(R**4))/BI
      RB=REF*R
      DO 500 II=1,NRPM
      AF=RPM(II)
      RPM(II)=(6.28318531*RPM(II))/60
      DO 500 JJ=1,NVEL
      DO 490 KK=1,NFREQ
      BF=FREQ(KK)
      FREQ(KK)=FREQ(KK)*RPM(II)
      T(KK,1)=BF
      T(KK,2)=FREQ(KK)/6.28318530717959
      T(KK,3)=FREQ(KK)
      VEL=VKNCTS(JJ)/.592
      PHI=ATAN(VEL/(RPM(II)*RB))
      S=VEL/(RPM(II)*R)
      HSQ=S**2
      WW1=SQRT(HSQ+ETA1**2)
      WW2=SQRT(HSQ+ETA2**2)

```



```

PW=ETAZ*WZ-ETA1*W1
A1=ALOG((ETAZ+WZ)/(ETA1+W1))
AZ=WZ-W1
A3=.5*(PW-HSQ*A1)
A4=(1./3.)*(WZ**3-W1**3)-HSQ*(WZ-W1)
A5=.25*((ETAZ**3)*WZ-(ETA1**3)*W1)-(3./8.)*HSQ*(PW-HSQ*A1)
B1=.5*(PW+HSQ*A1)
B2=(1./3.)*(WZ**3+W1**3)
B3=.25*(ETAZ*WZ**3-ETA1*W1**3)-(1./8.)*HSQ*(PW+HSQ*A1)
CFM=.5*GAMMA*(RPM(11)**2)*K1
CFMB=CFM*S*PRECONE
FS=FREQ(KK)**2
A11=CMPLX(-FS*RI+HSLUNG+CFM*B3*TAN(DELTA3)+CFMB*A4,BF*CFM*A5)
A12=CMPLX(CFM*A5-CFMB*B2*TAN(DELTA3),FREQ(KK)*(2.*RPM(11)*RI-
1 CFMB*A4/RPM(11)))
A21=CMPLX(-CFM*A5+CFMB*B2*TAN(DELTA3),FREQ(KK)*(CFMB*A4/RPM(11)-
1 2.*RPM(11)*RI))
A22=CMPLX(-FS*RI+HSLAT+CFM*B3*TAN(DELTA3)+CFMB*A4,BF*CFM*A5)
B11=CMPLX(FS*(K1+K0*PRECONE*F1)-CFM*B3*SWPLUNG* SIN(EPSILUN)+
1 CFMB*(HSQ*A2-B2*SWPLUNG*COS(EPSILUN)), -BF*(A5*CFM+
2 CFMB*S*A2*H1/R))
B12=CMPLX(CFM*(HSQ*A3-B3*SWPLAT*COS(EPSILUN))+CFMB*B2*SWPLAT*
1 SIN(EPSILUN), BF*(CFM*A4-2.*RI*RPM(11)**2-CFM*S*A3*H2/R))
B21=CMPLX(CFM*(B3*SWPLUNG*COS(EPSILUN)-HSQ*A3)-CFMB*B2*SWPLUNG*
1 SIN(EPSILUN), BF*(2.*RI*RPM(11)**2+CFM*S*A3*H1/R-
2 CFMB*A4))
B22=CMPLX(FS*(K1+K0*PRECONE*F2)-CFM*B3*SWPLAT*SIN(EPSILUN)+
1 CFMB*(HSQ*A2-SWPLAT*B2*COS(EPSILUN)),
2 -BF*(CFM*A5+CFMB*S*A2*H2/R))
DEL=A11*A22-A12*A21
DA1Y(KK)=(B11*A22-A12*B21)/DEL
DB1Y(KK)=(A11*B21-B11*A21)/DEL
DA1Z(KK)=(B12*A22-A12*B22)/DEL
DB1Z(KK)=(A11*B22-B12*A21)/DEL
490 CONTINUE
DO 33 IJ=1,NFREQ
TT(IJ,1)=REAL(DA1Y(IJ))
TT(IJ,2)=AIMAG(DA1Y(IJ))/FREQ(IJ)
TT(IJ,3)=REAL(DB1Y(IJ))
TT(IJ,4)=AIMAG(DB1Y(IJ))/FREQ(IJ)
TT(IJ,5)=SQRT(TT(IJ,1)**2+TT(IJ,3)**2)
TT(IJ,6)=SQRT(TT(IJ,2)**2+TT(IJ,4)**2)
TU(IJ,1)=REAL(DA1Z(IJ))
TU(IJ,2)=AIMAG(DA1Z(IJ))/FREQ(IJ)
TU(IJ,3)=REAL(DB1Z(IJ))
TU(IJ,4)=AIMAG(DB1Z(IJ))/FREQ(IJ)
TU(IJ,5)=SQRT(TU(IJ,1)**2+TU(IJ,3)**2)
TU(IJ,6)=SQRT(TU(IJ,2)**2+TU(IJ,4)**2)
33 CONTINUE
VKEAS=VKNUIS(JJ)*SQRT(DEN/.00230)
AR=.14159265358979*VEL/(RPM(11)*K)
PHI=PHI*.7.2957795130625
PRINT 1030,HEAD1
1030 FORMAT(1H1//12A10//)
PKINI 1029
1029 FORMAT(1HU,3X,*RPM*,20X,*VELOCITY*,27X,*ADVANCE RATIO*,
18X,*LOCK NUMBER*,9X,*INFLUW ANGLE**//20X,*FT/SEC*,11X,*KNUIS*,
21X,*KEAS*,17X,*J*,39X,*PHI**//)
PRINT 1020,AF,VEL,VKNUIS(JJ),VKEAS,AR,GAMMA,PHI

```

```

1028 FORMAT(1X,F15.8,6X,E15.8,2X,E15.8,2X,E15.8,5X,E15.8,5X,E15.8,
15X,E15.8////)
      IF(HSLONG.NE.HSLAT) GO TO 123
      BFF=SQRT(1.+HSLONG/(RI*RPM(II)**2)+.50*GAMMA*B3*TAN(DELTA3))
      BCR=25*GAMMA*A5/BFF
      PRINT 1015,BFF,BCR
1016 FORMAT(1X,43H**** BLADE FLAPPING FREQUENCY(CYCLES/REV) =,F10.3,
1      20X,38H**** BLADE DAMPING(PERCENT CRITICAL) =,F10.3////)
1023 CCNTINUE
      PRINT 1031
1031 FORMAT(31X,73H***** PROPRTOR DYNAMIC FLAPPING CERIVATIVES DUE T
10 PYLON PITCH *****//)
      PRINT 1032
1032 FORMAT(9X,*PYLON PITCH FREQUENCY*,24X,*COMPONENT FLAPPING DERIVATI
IVES*,16X,*TOTAL FLAPPING DERIVATIVE*//2X,*CYCLES/REV*,7X,*CPS*,
2      8X,*RAD/SEC*,8X,*A1/PHIY*,4X,*A1/PHIY DOT*,4X,*B1/PHIY*,
3      4X,*B1/PHIY DOT*, 8X,*BETA/PHIY*,3X,*BETA/PHIY DOT*)
      PRINT 1033,(((T(I,J),J=1,3),(TT(I,K),K=1,6)),I=1,NFREQ)
1033 FORMAT(//(1X,F11.4,2X,E11.4,2X,E11.4,5X,E11.4,2X,E11.4,2X,E11.4,
1      2X,E11.4,7X,E11.4,2X,E11.4))
      PRINT 1034
1034 FORMAT(///32X,71H***** PROPRTOR DYNAMIC FLAPPING DERIVATIVES D
UE TO PYLON YAW *****//)
      PRINT 1035
1035 FORMAT(10X,*PYLON YAW FREQUENCY*,25X,*COMPONENT FLAPPING DERIVATIV
IFS*,16X,*TOTAL FLAPPING DERIVATIVE* //2X,*CYCLES/REV*,7X,*CPS*,
2      8X,*RAD/SEC*,8X,*A1/PHIZ*,4X,*A1/PHIZ DOT*,4X,*B1/PHIZ*,
3      4X,*B1/PHIZ DOT*, 8X,*BETA/PHIZ*,3X,*BETA/PHIZ DOT*)
      PRINT 1036,(((T(I,J),J=1,3),(TU(I,K),K=1,6)),I=1,NFREQ)
1036 FORMAT(//(1X,F11.4,2X,E11.4,2X,E11.4,5X,E11.4,2X,E11.4,2X,E11.4,
1      2X,E11.4,7X,E11.4,2X,E11.4))
      DO 22 I=1,NFREQ
22 FREQ(I)=T(I,1)
500 CCNTINUE
      GO TO 1
8998 PRINT 8997
      FND

```

PROPRTOR OSCILLATORY FLAPPING DERIVATIVES - SAMPLE INPUT LISTING

2	1	20					
238.		298.					
350.							
.0001	.05	.10	.2	.4	.6	.8	1.0
1.2	1.4	1.6	1.8	2.0	2.2	2.4	2.6
2.8	3.0	5.0	10.0				
0.0	1.0						

\$RDTOR NB=3,RI=791.0,BU=138.,PRECONE=0.0,H1=6.92,H2=6.92,R=19.25,
PC4=1.92,DEN=.00238,A0=5.73,DELTA3=-22.5,HSLONG=20000.0,HSLAT=20000.0,
SWPLNG=0.0,SWPLAT=0.0,EPSILON=0.0,REF=.75\$

VIBRATION ANALYSIS BY A DIRECT STIFFNESS METHOD

```

PROGRAM DSTIFF(INPUT,OUTPUT,TAPE5=INPUT,TAPE6,TAPE8,
1           TAPE3,TAPE4,TAPE30,TAPE31)

```

```

*****
*
*   PROGRAMS DSTIFF AND BJD5 COMPRISE A COMPUTER PACKAGE
*   FOR THE VIBRATION ANALYSIS OF COMPLEX STRUCTURAL
*   SYSTEMS BY A DIRECT STIFFNESS TECHNIQUE.
*
*   THE STRUCTURE IS IDEALIZED AS AN ASSEMBLY OF BEAM,
*   SPRING, AND RIGID MASS SUBSYSTEMS. A FINITE-ELEMENT
*   APPROACH IS EMPLOYED TO GENERATE THE MASS AND STIFFNESS
*   MATRICES FOR THE UNCOUPLED SUBSYSTEMS. USER WRITTEN
*   CONSTRAINT EQUATIONS ENFORCING INTER-SUBSYSTEM DISPLACEMENT
*   COMPATIBILITY ARE APPLIED ACCORDING TO THE METHOD OF
*   NASA TR R-326. A CONDENSATION OF THE SYSTEM GENERALIZED
*   STIFFNESS MATRIX IS PERFORMED, IF NECESSARY, AND THE
*   RESULTANT EQUATIONS CAST INTO A FORM TO WHICH THE
*   THRESHOLD VARIATION OF THE JACOBI ALGORITHM FOR FINDING
*   EIGENVALUES AND EIGENVECTORS IS APPLIED.
*
*****

```

```

C   KASE=1, DIAGONAL MASS ONLY (NO NULL VALUES)
C   KASE=2, DIAGONAL MASS AND ROTARY INERTIA (NO NULL VALUES)
C   KASE=3, NON-DIAGONAL MASS AND ROTARY INERTIA (NULL VALUES
C           CAN BE ON DIAGONAL)
C   KASE=4, DIAGONAL TORSIONAL INERTIA OR AXIAL MASS (NO NULL
C           VALUES ON DIAGONAL)
C   KASE=5, DIAGONAL TORSIONAL INERTIA OR AXIAL MASS (NULL
C           VALUES CAN BE ON DIAGONAL)

C   KK=ORDER OF BLOCK

C   LOC=1, BEAM BENDING
C   LOC=2, BEAM TORSION
C   LOC=3, BEAM AXIAL
C   LOC=4, SPRING OR RIGID BODY ELEMENT

C   FOR SPRING OR RIGID BODY ELEMENTS ---
C   MK=1, READ STIFFNESS MATRIX FROM CARDS
C   MK=0, NO READ

C   MM=1, READ MASS MATRIX FROM CARDS
C   MM=0, NO READ

```

```

C      FOR A SYMMETRIC OR ANTI-SYMMETRIC FORMULATION OF THE
C      PROBLEM, THE MASS AND STIFFNESS MATRICES CORRESPONDING
C      TO STRUCTURAL BLOCKS OUT OF THE VERTICAL PLANE OF SYMMETRY
C      MUST BE MULTIPLIED BY 2.0
C      ISYM=1, MULTIPLY BLOCK MASS AND STIFFNESS MATRIX BY 2.0
C      ISYM=0, NO MULTIPLICATION

C      MASS AND/OR STIFFNESS TERMS ARISING FROM WING AND TAIL STATIC
C      UNBALANCE AND FROM ASSIMILATING THE MASS MATRIX OF A RIGID
C      BODY OR THE STIFFNESS MATRIX OF A MASSLESS SPRING ELEMENT
C      INTO THE CORRESPONDING MATRICES OF THE MEMBER(S) TO WHICH
C      THEY ARE CONNECTED WILL COUPLE BLOCKS IN THE UNCOUPLED
C      SYSTEM MASS AND STIFFNESS MATRICES. THESE TERMS ARE
C      INTRODUCED SEPARATELY.
C      MASADD = NUMBER OF MASS TERMS TO BE ADDED ON AND ABOVE
C      DIAGONAL OF THE UNCOUPLED SYSTEM MASS MATRIX.
C      PROGRAM WILL PROVIDE SYMMETRY AS REQUIRED.
C      NSPADD = NUMBER OF SPRING TERMS TO BE ADDED ON AND ABOVE
C      DIAGONAL OF THE UNCOUPLED SYSTEM STIFFNESS
C      MATRIX. PROGRAM WILL PROVIDE SYMMETRY.

      DIMENSION A(12,12),B(12,12),C(12,12),DM(12),RI(12),X(8),S(8),
1         E(16),ES(8),EC(8),IR(16,2),AA(16,16),BB(16,16),
2         BK(144,144),BM(144,144),D(49,144),DTD(144,144),
3         EIGV(144),BC(144,144),BETA(144,144),R(144)
      COMMON HMTX(12)
      EQUIVALENCE (BM(1,1),DTD(1,1),BETA(1,1)),(BK(1,1),BC(1,1)),
1         (D(1,1),EIGV(1))
      MAX=12
      MAXT2=16
      MAX2=2
      FCUN=1.0
      1 READ 1010,(HMTX(J),J=5,12)
1010  FORMAT(8A10)
      IF(EOF,5) 8998,8999
8998  WRITE(6,8997)
      PRINT 8997
      GO TO 2300
8997  FORMAT(1H1/** PROGRAM BBSTIFF STOPPED ON (EOF,5)*)
8999  CONTINUE
C      READ NUMBER OF BLOCKS IN UNCOUPLED SYSTEM MASS AND STIFFNESS
C      MATRICES, ORDER OF SYSTEM, AND NUMBER OF CONSTRAINT EQUATIONS
      READ 1020,NBLKS,NORDER,NCEQS
      WRITE(6,1011) NBLKS,NORDER,NCEQS
      PRINT 1011,NBLKS,NORDER,NCEQS
1011  FORMAT(1H1/** NUMBER BLOCKS IN UNCOUPLED SYSTEM MASS AND STIFFNESS
1         MATRICES = *,I3/** ORDER OF SYSTEM = *,I3/** NUMBER OF CONSTRAINT
2         EQUATIONS = *,I3)
C      READ NUMBER OF MASSES TO BE ADDED ON OR ABOVE DIAGONAL OF
C      MASS MATRIX AND/OR NUMBER OF SPRING CONSTANTS TO BE ADDED ON
C      OR ABOVE DIAGONAL OF STIFFNESS MATRIX
      READ 1020,MASADD,NSPADD
      WRITE(6,1012) MASADD,NSPADD
      PRINT 1012,MASADD,NSPADD
1012  FORMAT(1H /** NUMBER OF MASSES TO BE ADDED = *,I3/** NUMBER OF SP
RING CONSTANTS TO BE ADDED = *,I3)

```

```

CALL ZFROM(BK,NCPDER,NORDEF,NORDER,NORDER)
CALL ZFROM(BM,NORDEF,NORCFR,NORDER,NORDER)
NCB=1 $ NRB=1
NCF=0 $ NRF=0
ID=0 $ MI=0 $ KI=0
DO 200 NRLOCK=1,NBLKS
WRITE(6,1019) NRLOCK
PRINT 1019,NRLOCK
1019 FORMAT(1H //1X,19H*****//1X,19H*          */
1      1X,14H* BLOCK NUMBER ,I3,2H */1X,19H*          */
2      1X,19H*****//1X,19H*          */
      READ 1020, KK, LOC, MK, MM, ISYM
1020 FORMAT(20I4)
      ID=ID+1
      IF(ID.EQ.1) GO TO 1021
      MI=KI
1021 CONTINUE
      NRF=NRF+KK
      NCF=NCF+KK
      GO TO (110,120,120,130), LOC

*****
* BEAM BENDING *
*****

C      FOR BEAM BENDING, FREE-FREE STIFFNESS MATRIX IS
C      GENERATED IN THE PARTITIONED FORM (A B)
C      (BT C)
C      WHERE A=(K*K), R=(K*N), BT=(N*K), C=(N*N)
C      FOR THE FREE-FREE CASE, K=N

110 READ 1020,K,N,KASE
WRITE(6,1030) K,N,KASE
PRINT 1030,K,N,KASE
1030 FORMAT(//9X,*K*,9X,*N*,8X,*KASE*//3I10)
1040 FOPMAT(5E14.8)
      KM1=K-1
      CALL ZEROM(A,K,K,MAX,MAX)
      CALL ZEROM(B,K,N,MAX,MAX)
      CALL ZEROM(C,N,N,MAX,MAX)
      CALL ZEROM(DM,K,1,MAX,1)
      CALL ZEROM(RI,N,1,MAX,1)
      READ 1040,(X(I),I=1,K)
      READ 1040,(S(I),I=1,KM1)
      READ 1040,(DM(I),I=1,K)
      IF(KASE.NE.1) READ 1040,(RI(I),I=1,N)
      PRINT 1050,(J,X(J),S(J),DM(J),RI(J),J=1,KM1)
      WRITE(6,1050)(J,X(J),S(J),DM(J),RI(J),J=1,KM1)
      PRINT 1051,K,X(K),DM(K),RI(K)
      WRITE(6,1051)K,X(K),DM(K),RI(K)
1050 FORMAT(//3X,*J*,7X,*X(J)*,11X,*EI(J)*,10X,*MASS(J)*,10X,*RI(J)*,
1      //(I4,4E16.8))
1051 FORMAT(I4,E16.8,16X,2E16.8)
      DO 40 L=1,KM1
      40 E(L)=1.0/(X(L+1)-X(L))

```

```

      DO 41 I=1,KM1
41  FS(L)=F(L)*F(L)
      DO 42 I=1,KM1
42  EC(L)=F(L)*ES(L)
C   FORM MATRIX A
      A(1,1)=12.0*S(1)*EC(1)
      A(1,2)=-A(1,1)
      A(K,KM1)=-12.0*S(KM1)*EC(KM1)
      A(K,K)=-A(K,KM1)
      M=0
      DO 50 L=2,KM1
      M=M+1
      A(L,M)=-12.0*S(M)*EC(M)
      A(L,M+2)=-12.0*S(M+1)*EC(M+1)
50  A(L,M+1)=-(A(L,M)+A(L,M+2))
C   FORM MATRIX B
      B(1,1)=6.0*S(1)*ES(1)
      B(1,2)=B(1,1)
      B(K,KM1)=-6.0*S(KM1)*FS(KM1)
      B(K,K)=B(K,KM1)
      M=0
      DO 61 L=2,KM1
      M=M+1
      B(L,M)=-6.0*S(M)*ES(M)
      B(L,M+2)=6.0*S(M+1)*FS(M+1)
61  B(L,M+1)=B(L,M)+B(L,M+2)
C   FORM MATRIX C
      C(1,1)=4.0*S(1)*F(1)
      C(1,2)=2.0*S(1)*E(1)
      C(K,KM1)=2.0*S(KM1)*E(KM1)
      C(K,K)=4.0*S(KM1)*E(KM1)
      M=0
      DO 71 L=2,KM1
      M=M+1
      C(L,M)=2.0*S(M)*E(M)
      C(L,M+2)=2.0*S(M+1)*E(M+1)
71  C(L,M+1)=4.0*(S(M+1)*E(M+1)+S(M)*E(M))
C   FORM FREE-FREE BENDING STIFFNESS AND MASS MATRICES
      KPN=K+N
      KP1=K+1
      CALL ZEROM(AA,KPN,KPN,MAXT2,MAXT2)
      CALL ZEROM(BB,KPN,KPN,MAXT2,MAXT2)
      REWIND 3
      WRITE(3)((A(I,J),J=1,K),I=1,K),((B(I,J),J=1,N),I=1,K),((B(I,J),
1      I=1,K),J=1,N),((C(I,J),J=1,N),I=1,N),((DM(J),J=1,K),
2      (RI(J),J=1,N)
      PEWIND 3
      READ(3)((AA(I,J),J=1,K),I=1,K),((AA(I,J),J=KP1,KPN),I=1,K),
1      ((AA(I,J),J=1,K),I=KP1,KPN),((AA(I,J),J=KP1,KPN),I=KP1,KPN),
2      (BR(J,J),J=1,KPN)
C   MULTIPLY FREE-FREE STIFFNESS MATRIX BY 2.0 IF ISYM = 1
      IF(ISYM.EQ.0) GO TO 1068
      DO 1065 I=1,KPN
      DO 1065 J=1,KPN
1065 AA(I,J)=2.0*AA(I,J)
1068 CONTINUE

```

```

C   MULTIPLY FREE-FREE MASS MATRIX BY 2.0 IF ISYM = 1
      IF (ISYM.EQ.0) GO TO 95
      DO 96 I=1,KPN
      DO 96 J=1,KPN
96   BB(I,J)=2.0*BB(I,J)
95   CONTINUE
      DO 11 I=NRB,NRF
      DO 11 J=NCB,NCF
      BK(I,J)=AA(I-MI,J-MI)
11   BM(I,J)=BB(I-MI,J-MI)
      KI=KI+KK
      NRB=NRB+KK
      NCB=NCB+KK
      GO TO 200
*****
* BEAM TORSION OR AXIAL *
*****

C           FREE-FREE STIFFNESS MATRIX IS OF ORDER K

120  READ 1020,K,KASE
      WRITE(6,1090)K,KASE
      PRINT 1090,K,KASE
1090  FORMAT(//9X,*K*,8X,*KASE*//2I10)
      KM1=K-1
      CALL ZERCM(A,K,K,MAX,MAX)
      CALL ZEROM(B,K,K,MAX,MAX)
      READ 1040,(X(I),I=1,K)
      READ 1040,(S(I),I=1,KM1)
      READ 1040,(RI(I),I=1,K)
      IF(LOC.EQ.2) GO TO 1098
      WRITE(6,1102)(J,X(J),S(J),RI(J),J=1,KM1)
      WRITE(6,1101) K,X(K),PI(K)
      PRINT 1102,(J,X(J),S(J),RI(J),J=1,KM1)
      PRINT 1101,K,X(K),RI(K)
      GO TO 1099
1098  WRITE(6,1100)(J,X(J),S(J),RI(J),J=1,KM1)
      WRITE(6,1101) K,X(K),PI(K)
      PRINT 1100,(J,X(J),S(J),PI(J),J=1,KM1)
      PRINT 1101,K,X(K),RI(K)
1100  FORMAT(//3X,*J*,7X,*X(J)*,11X,*GJ(J)*,10X,*RI(J)*,/(14,3E16.8))
1101  FORMAT(14,E16.8,16X,E16.8)
1102  FORMAT(//3X,*J*,7X,*X(J)*,11X,*AE(J)*,10X,*DM(J)*,/(14,3E16.8))
C   FORM FREE-FREE STIFFNESS MATRIX
1099  DO 121 L=1,KM1
121  E(L)=1.0/(X(L+1)-X(L))
      DO 122 J=1,KM1
122  S(J)=S(J)*E(J)
      A(1,1)=S(1)
      A(1,2)=-S(1)
      A(K,K-1)=-S(KM1)
      A(K,K)=S(KM1)
      KTB=0
      DO 123 J=2,KM1
      KD=KTB+J
      A(KD,KD-1)=-S(J-1)
      A(KD,KD)=S(J-1)+S(J)
123  A(KD,KD+1)=-S(J)

```

```

C MULTIPLY FREE-FREE STIFFNESS MATRIX BY 2.0 IF ISYM = 1
  IF(ISYM.EQ.0) GO TO 129
  DO 129 I=1,K
  DO 129 J=1,K
129 A(I,J)=2.0*A(I,J)
128 CONTINUE
  DO 13 J=1,K
  13 B(J,J)=R(I,J)
C MULTIPLY FREE-FREE MASS MATRIX BY 2.0 IF ISYM = 1
  IF(ISYM.EQ.0) GO TO 1261
  DO 1262 I=1,K
  DO 1262 J=1,K
1262 B(I,J)=2.0*B(I,J)
1261 CONTINUE
  DO 1263 I=NRB,NRF
  DO 1263 J=NCB,NCF
  BK(I,J)=A(I-MI,J-MI)
1263 BM(I,J)=B(I-MI,J-MI)
  KI=KI+KK
  NRB=NRB+KK
  NCB=NCB+KK
  GO TO 200
*****
* SPRING OR RIGID BODY ELEMENT *
*****

  130 CALL ZEROM(A, KK, KK, MAX, MAX)
  CALL ZEROM(B, KK, KK, MAX, MAX)
  IF(MK.EQ.0) GO TO 131
  PRINT 1301
  WRITE(6,1301)
1301 FORMAT(1H //1X,* SPRING ELEMENT - STIFFNESS MATRIX WILL BE READ
1FROM CARDS. MASS MATRIX IS NULL.*)
  READ 1040, ((A(I,J), J=1, KK), I=1, KK)
  131 IF(MM.EQ.0) GO TO 132
  PRINT 1302
  WRITE(6,1302)
1302 FORMAT(1H //1X,* RIGID BODY ELEMENT - MASS MATRIX WILL BE READ F
1FROM CARDS. STIFFNESS MATRIX IS NULL.*)
  READ 1040, ((B(I,J), J=1, KK), I=1, KK)
  132 CONTINUE
C MULTIPLY FREE-FREE MASS AND STIFFNESS MATRICES BY 2.0 IF ISYM = 1
  IF(ISYM.EQ.0) GO TO 135
  DO 134 I=1, KK
  DO 134 J=1, KK
  A(I,J)=2.0*A(I,J)
134 B(I,J)=2.0*B(I,J)
135 CONTINUE
  DO 138 I=NRB,NRF
  DO 138 J=NCB,NCF
  BK(I,J)=A(I-MI, J-MI)
138 BM(I,J)=B(I-MI, J-MI)
  IF(MK.NE.0.OR.MM.NE.0) GO TO 133
  PRINT 1303
  WRITE(6,1303)
1303 FORMAT(1H //1X,* MASS AND STIFFNESS MATRICES ARE BOTH NULL *)
  133 CONTINUE

```



```

KI=KI+KK
NPB=NRB+KK
NCB=NCR+KK
200 CONTINUE
C NOTE -- FOR SYMMETRIC OR ANTI-SYMMETRIC FORMULATION THE MASSES
C AND/OR SPRINGS TO BE ADDED MUST BE MULTIPLIED BY 2.0
IF(MASADD.EQ.0) GO TO 20
READ 1060, (IR(J,1),IR(J,2),E(J),J=1,MASADD)
1060 FORMAT(4(I3,E14.8))
WRITE(6,1061)(J,IR(J,1),IR(J,2),E(J),J=1,MASADD)
PRINT 1061, (J,IR(J,1),IR(J,2),E(J),J=1,MASADD)
1061 FORMAT(/4X,*J*,2X,*ROW*,2X,*COL*,8X,*MASS(J)*//(3I5,E22.14))
DO 20 J=1,MASADD
NROW=IR(J,1)
NCOL=IR(J,2)
BM(NROW,NCOL)=BM(NROW,NCOL)+E(J)
IF(NROW.NE.NCOL) BM(NCOL,NROW)=BM(NROW,NCOL)
20 CONTINUE
IF(NSPADD.EQ.0) GO TO 90
READ 1060, (IR(J,1),IR(J,2),E(J),J=1,NSPADD)
WRITE(6,1062)(J,IR(J,1),IR(J,2),E(J),J=1,NSPADD)
PRINT 1062, (J,IR(J,1),IR(J,2),E(J),J=1,NSPADD)
1062 FORMAT(/4X,*J*,2X,*ROW*,2X,*COL*,7X,*SPRING(J)*//(3I5,E22.14))
DO 90 J=1,NSPADD
NROW=IR(J,1)
NCOL=IR(J,2)
BK(NROW,NCOL)=BK(NROW,NCOL)+E(J)
IF(NROW.NE.NCOL) BK(NCOL,NROW)=BK(NROW,NCOL)
90 CONTINUE
C WRITE SYSTEM FREE-FREE STIFFNESS AND MASS MATRICES ON TAPE 6
HMTX(1)=10H FREE-FREE $ HMTX(2)=10H SYSTEM ST
HMTX(3)=10H STIFFNESS MA $ HMTX(4)=10H TRIX
CALL WMTXC(BK,NORDER,NORDER,NORDER,NORDER)
HMTX(1)=10H FREE-FREE $ HMTX(2)=10H SYSTEM MA
HMTX(3)=10H SS MATRIX $ HMTX(4)=10H
CALL WMTXC(BM,NORDER,NORDER,NORDER,NORDER)
C WRITE MASS MATRIX ON TAPE 30 BY ROWS, ONE RECORD
REWIND 30
WRITE(30)((BM(I,J),J=1,NORDER),I=1,NORDER)
C WRITE STIFFNESS MATRIX ON TAPE 31 BY ROWS, ONE RECORD
REWIND 31
WRITE(31)((BK(I,J),J=1,NORDER),I=1,NORDER)
CALL CONEQS(D,NCEQS,NORDER)
C EVALUATE D TRANSPOSE * D BY CALLING ROWS OF D AS COLUMNS OF DT
DO 300 J=1,NORDER
DO 300 I=1,NORDER
DTD(I,J)=0.0
DO 300 IJ=1,NCEQS
300 DTD(I,J)=DTD(I,J)+D(IJ,I)*D(IJ,J)
C SOLVE FOR EIGENVALUES AND EIGENVECTORS OF DTD
CALL JACTV(NORDER,NORDER,1,DTD,EIGV,RC,DUM1,DUM2,DUM3,DUM4,NERR)
IF(NERR.EQ.1) GO TO 2200

C TEST FOR NUMBER OF FINITE(POSITIVE) EIGENVALUES OF DTD. MODAL
C COLUMNS OF DTD CORRESPONDING TO THE ZERO EIGENVALUES ARE THEN TAKEN
C TO BE THE COLUMNS OF THE BETA MATRIX

```

```

NFEV=NORDER
DO 75 J=2,NORDER
  IJ=J-1
  IF(EIGV(J).LE.0.0) GO TO 76
  IF((EIGV(IJ)/EIGV(J)).GE.1000000.0) GO TO 76
75 CONTINUE
76 IF(NFEV.NE.IJ) NFEV=IJ
  PRINT 14,NFEV
  14 FORMAT(//* NUMBR OF FINITE EIGENVALUES OF DTD = *,I3//)
C WRITE EIGENVALUES OF D TRANSPOSE * D ON TAPE 6
  WRITE(6,1111)(EIGV(I),I=1,NORDER)
1111 FORMAT(//* EIGENVALUES OF DTD *//(2X,E15.8))
  WRITE(6,14) NFEV
  NCBETA=NORDER-NFEV
  DO 80 I=1,NORDER
    DO 80 J=1,NCBETA
      80 BETA(I,J)=BC(I,NFEV+J)
  NRBETA=NORDER
C BETA WRITTEN ON TAPE 3 FOR USE IN BJD5
C WRITE ORDER BETA ON TAPE 3, ONE RECORD
C WRITE BETA ON TAPE 3 BY POWS, NRBETA RECORDS
  REWIND 3
  WRITE(3)NRBETA,NCBETA
  DO 66 I=1,NRBETA
    66 WRITE(3) (BETA(I,J),J=1,NCBETA)
C WRITE BETA ON TAPE 9 BY COLUMNS, NCBETA RECORDS
  REWIND 9
  DO 351 J=1,NCBETA
    351 WRITE(9)(BETA(I,J),I=1,NRBETA)

C FORM COUPLED MASS MATRIX BY THE MATRIX PRODUCT
C BETA TRANSPOSE * BM * BETA

C READ MASS MATRIX FROM TAPE 30
  REWIND 30
  READ(30)((BM(I,J),J=1,NORDER),I=1,NORDER)
  REWIND 8
C POST-MULTIPLY MASS MATRIX BY BETA
  DO 114 J=1,NCBETA
C READ COLUMN OF BETA
  READ(8)(R(I),I=1,NRBETA)
  DO 114 I=1,NRBETA
    BC(I,J)=0.0
  DO 114 IJ=1,NRBETA
    114 BC(I,J)=BC(I,J)+BM(I,IJ)*R(IJ)
  REWIND 8
C PRE-MULTIPLY MATRIX JUST COMPUTED BY BETA TRANSPOSE
  DO 115 I=1,NCBETA
C READ COLUMN OF BETA AS ROW OF TRANSPOSE
  READ(8)(R(J),J=1,NRBETA)
  DO 115 J=1,NCBETA
    BM(I,J)=0.0
  DO 115 IJ=1,NRBETA
    115 BM(I,J)=BM(I,J)+R(IJ)*BC(IJ,J)
C WRITE COUPLED MASS MATRIX ON TAPE 4 BY COLUMNS, ONE RECORD
  REWIND 4
  WRITE(4) ((BM(I,J),I=1,NCBETA),J=1,NCBETA)

```

```

C FORM COUPLED STIFFNESS MATRIX BY THE MATRIX PRODUCT
C BETA TRANSPOSE * BK * BETA

C READ STIFFNESS MATRIX FROM TAPE 31
  REWIND 31
  READ(31)((BK(I,J),J=1,NORDEP),I=1,NORDER)
  REWIND 8
C POST-MULTIPLY STIFFNESS MATRIX BY BETA
  DO 352 J=1,NCBETA
C READ COLUMN OF BETA
  READ(8)(R(I),I=1,NRBETA)
  DO 352 I=1,NRBETA
  BETA(I,J)=0.0
  DO 352 IJ=1,NRBETA
352 BETA(I,J)=BETA(I,J)+BK(I,IJ)*R(IJ)
  REWIND 8
C PRE-MULTIPLY MATRIX JUST COMPUTED BY BETA TRANSPOSE
  DO 113 I=1,NCBETA
C READ COLUMN OF BETA AS ROW OF TRANSPOSE
  READ(8)(R(J),J=1,NRBETA)
  DO 113 J=1,NCBETA
  BK(I,J)=0.0
  DO 113 IJ=1,NRBETA
113 BK(I,J)=BK(I,J)+R(IJ)*BETA(IJ,J)
C WRITE COUPLED STIFFNESS MATRIX ON TAPE 4 BY COLUMNS, ONE RECORD
  WRITE(4)((BK(I,J),I=1,NCBETA),J=1,NCBETA)
  REWIND 3
  REWIND 4
  IF(NERR.EQ.0) GO TO 2300
2200 WRITE(6,2210)
  PRINT 2210
2210 FORMAT(/** ERROR RETURN FROM JACTV - DTD CALL *)
2300 CONTINUE
  END

  SUBROUTINE CONEQS(D,NCEQS,NORDER)
C MATRIX OF CONSTRAINT EQUATIONS IN PHYSICAL COORDINATES
  DIMENSION D(NCEQS,NORDER)
  CALL ZEROM(D,NCEQS,NORDER,NCEQS,NORDER)
  D(1,24)=-1.0 $ D(1,11)=COS(.1658) $ D(1,5)=-SIN(.1658)
  D(2,12)=-1.0 $ D(2,11)=SIN(.1658) $ D(2,5)=COS(.1658)
  D(3,18)=1.0 $ D(3,10)=-1.0 $ D(4,24)=-1.0 $ D(4,41)=COS(.09774)
  D(4,25)=-SIN(.09774) $ D(5,17)=-1.0 $ D(5,41)=SIN(.09774)
  D(5,25)=COS(.09774) $ D(6,23)=1.0 $ D(6,33)=-1.0
  D(7,24)=1.0 $ D(7,42)=1.0 $ D(7,44)=46.1 $ D(8,45)=-46.1
  D(9,17)=1.0 $ D(9,43)=-1.0 $ D(10,45)=-1.0 $ D(11,23)=1.0
  D(11,44)=1.0 $ D(12,46)=1.0 $ D(13,50)=1.0 $ D(13,44)=-1.0
  D(14,47)=1.0 $ D(15,47)=-1.0 $ D(15,88)=COS(.07854)
  D(15,67)=-SIN(.07854) $ D(16,48)=-1.0 $ D(16,88)=SIN(.07854)
  D(16,67)=COS(.07854) $ D(17,49)=-1.0 $ D(17,53)=1.0
  D(18,50)=-1.0 $ D(18,81)=COS(.07854) $ D(18,60)=SIN(.07854)
  D(19,51)=-1.0 $ D(19,81)=SIN(.07854) $ D(19,60)=-COS(.07854)
  D(20,52)=-1.0 $ D(20,74)=1.0
  D(21,88)=-1.0

```

```

D(21,89)=COS(.07854) $ D(21,90)=SIN(.07854)
D(21,94)=-(.17.0*SIN(.07854) +.17.0*COS(.07854))
D(22,73)=-1.0 $ D(22,90)=COS(.07854)
D(22,94)=-(.17.0*COS(.07854)-.17.0*SIN(.07854))
D(22,89)=-SIN(.07854) $ D(23,87)=-1.0 $ D(23,92)=COS(.07854)
D(23,93)=-SIN(.07854) $ D(24,59)=-1.0 $ D(24,91)=1.0
D(24,92)=17.0 $ D(24,93)=-17.0 $ D(25,66)=1.0
D(25,92)=-SIN(.07854) $ D(25,93)=-COS(.07854) $ D(26,80)=-1.0
D(26,94)=1.0
D(27,89)=-1.0 $ D(27,96)=-1.0 $ D(27,100)=55.0
D(28,90)=-1.0 $ D(28,95)=1.0 $ D(29,91)=-1.0 $ D(29,97)=1.0
D(29,99)=-55.0 $ D(30,92)=-1.0 $ D(30,99)=1.0
D(31,93)=1.0 $ D(31,98)=-1.0 $ D(32,94)=-1.0 $ D(32,100)=1.0
D(33,101)=1.0 $ D(33,95)=-1.0 $ D(34,104)=1.0
D(34,98)=-1.0 $ D(35,101)=-1.0 $ D(35,107)=1.0 $ D(36,102)=-1.0
D(36,108)=1.0 $ D(37,103)=-1.0 $ D(37,109)=1.0 $ D(38,104)=-1.0
D(38,110)=1.0 $ D(39,105)=-1.0 $ D(39,111)=1.0
D(40,106)=-1.0 $ D(40,112)=1.0 $ D(41,41)=-1.0
D(41,113)=-COS(.09774)*COS(.4363)+SIN(.09774)*SIN(.4363)
D(41,123)=COS(.09774)*SIN(.4363) + SIN(.09774)*COS(.4363)
D(41,118)=15.0*COS(.09774) $ D(42,32)=-1.0
D(42,113)=SIN(.09774)*COS(.4363) + SIN(.4363)*COS(.09774)
D(42,123)=-SIN(.09774)*SIN(.4363) + COS(.09774)*COS(.4363)
D(42,118)=-15.0*SIN(.09774) $ D(43,40)=1.0 $ D(43,118)=-1.0
D(44,144)=COS(.2618) $ D(44,132)=SIN(.2618) $ D(45,115)=-1.0
D(45,124)=SIN(.4363) $ D(45,144)=-COS(.4363)*SIN(.2618)
D(45,132)=COS(.4363)*COS(.2618) $ D(46,123)=-1.0
D(46,124)=COS(.4363) $ D(46,144)=SIN(.4363)*SIN(.2618)
D(46,132)=-SIN(.4363)*COS(.2618) $ D(47,120)=1.0
D(47,140)=COS(.2618) $ D(47,128)=-SIN(.2618)
D(48,140)=-COS(.4363)*SIN(.2618)
D(48,129)=-COS(.4363)*COS(.2618) $ D(48,136)=SIN(.4363)
D(49,140)=SIN(.4363)*SIN(.2618)
D(49,128)=SIN(.4363)*COS(.2618) $ D(49,136)=COS(.4363)
RETURN
END

```

```

SUBROUTINE WMTXC(A,NP,NC,MAXR,MAXC)
C NR=ROWS OF A, NC=COLS OF A, MAXR=MAX ROWS OF A, MAXC=MAX COLS OF A
DIMENSION A(MAXR,MAXC)
COMMON HMTX(12)
KE=0
KSET=NC/8
KLEFT=MOD(NC,8)
IF(KLEFT.NE.0) KSFT=KSET+1
DO 10 KT=1,KSET
KB=KE+1
KE=KE+9
IF(KT.EQ.KSET) KE=NC
WRITE(6,5001) HMTX,{J,J=KB,KE}
DO 10 I=1,NR
10 WRITE(6,5002) I,(A(I,J),J=KB,KE)
5001 FORMAT(1H1//12A10///10H ROW COL,I4,7(11X14))
5002 FORMAT(14,8E15.7)
RETURN
END

```

```

SUBROUTINE ZEROM(A,M,L,MMAX,LMAX)
DIMENSION A(MMAX,LMAX)
DO 10 I=1,M
DO 10 J=1,L
10 A(I,J)=0.0
RETURN
END

```

FULL-SCALE TILT ROTOR SYMMETRIC FREE-FLIGHT MODES--90 DEG CONVERSION ANGLE

```

20 144 49
10 0
10 1 0 0 0
5 5 1
0.0 35.0 60.0 95.0 120.0
3400000000.0 8000000000.0 16000000000.0 32000000000.0
.1040 .1200 .3000 1.4400 2.1600
1 4 0 1 0
4.124
12 1 0 0 0 0
6 6 1
0.0 40.0 75.0 100.0 120.0
140.0
80000000000.0 136000000000.0 160000000000.0 166000000000.0 168000000000.0
2.160 5.280 2.040 .240 .960
.840
1 4 0 1 0
11.520
16 1 0 0 0
8 8 1
0.0 35.0 63.0 105.0 150.0
188.0 235.0 287.0
168000000000.0 166000000000.0 146000000000.0 90000000000.0 45000000000.0
30000000000.0 18000000000.0
.840 1.878 2.900 10.560 2.556
.720 .350 .600
1 4 0 1 0
20.404
11 4 1 0 1
5980000.0 0.0 0.0 0.0 125400000.0
0.0 -5980000.0 0.0 0.0 0.0
125400000.0 0.0 2550000.0 0.0 -53400000.0
0.0 0.0 0.0 -2550000.0 0.0
-53400000.0 0.0 0.0 0.0 0.0
0.0 0.0 0.0 0.0 0.0
0.0 0.0 0.0 0.0 -53400000.0
0.0 150000000.0 0.0 0.0 0.0
53400000.0 0.0 75000000.0 0.0 125400000.0
0.0 0.0 0.0 352000000.0 0.0
-125400000.0 0.0 0.0 0.0 1760000000.0
0.0 0.0 0.0 0.0 0.0
0.0 0.0 0.0 0.0 0.0
0.0 -5980000.0 0.0 0.0 0.0
-125400000.0 0.0 5980000.0 0.0 0.0
0.0 -125400000.0 0.0 -2550000.0 0.0

```

53400000.0	0.0	0.0	0.0	2550000.0
0.0	53400000.0	0.0	0.0	0.0
0.0	0.0	0.0	0.0	0.0
0.0	0.0	0.0	0.0	0.0
-53400000.0	0.0	750000000.0	0.0	0.0
0.0	53400000.0	0.0	1500000000.0	0.0
125400000.0	0.0	0.0	0.0	1760000000.0
0.0	-125400000.0	0.0	0.0	0.0
3520000000.0				
14 1 0	0 1			
7 7 1				
0.0	34.0	75.0	125.0	173.0
209.0	222.0			
15000000000.0	12400000000.0	9200000000.0	6000000000.0	4600000000.0
4150000000.0				
.381	.705	.518	.648	.357
1.48	0.0			
14 1 0	0 1			
7 7 1				
0.0	34.0	75.0	125.0	173.0
209.0	222.0			
35000000000.0	30000000000.0	24000000000.0	18000000000.0	15000000000.0
14200000000.0				
.381	.705	.518	.648	.357
1.48	0.0			
7 2 0	0 1			
7 4				
0.0	34.0	75.0	125.0	173.0
209.0	222.0			
12300000000.0	10400000000.0	8200000000.0	6000000000.0	4600000000.0
42000000000.0				
389.0	414.0	246.0	231.0	251.0
526.0	0.0			
1 4 0	1 1			
4.59				
6 4 0	1 1			
7.25	0.0	0.0	0.0	137.8
-226.0	0.0	7.25	0.0	137.8
0.0	0.0	0.0	0.0	7.25
226.0	0.0	0.0	0.0	137.8
226.0	16627.0	0.0	0.0	137.8
0.0	0.0	0.0	6417.0	-4297.8
-226.0	0.0	0.0	0.0	-4297.8
13180.0				
12 4 1	0 1			
0.0	0.0	0.0	0.0	0.0
0.0	0.0	0.0	0.0	0.0
0.0	0.0	0.0	1366618.076	0.0
0.0	0.0	19132653.06	0.0	-1366618.076
0.0	0.0	0.0	19132653.06	0.0
0.0	1366618.076	0.0	-19132653.06	0.0
0.0	0.0	-1366618.076	0.0	-19132653.06
0.0	0.0	0.0	0.0	0.0
0.0	0.0	0.0	0.0	0.0
0.0	0.0	0.0	0.0	0.0
0.0	0.0	0.0	0.0	0.0
-19132653.06	0.0	357142857.1	0.0	0.0
0.0	19132653.06	0.0	178571428.55	0.0
0.0	19132653.06	0.0	0.0	0.0
357142857.1	0.0	-19132653.06	0.0	0.0
0.0	178571428.55	0.0	0.0	0.0

0.0	0.0	0.0	0.0	0.0
C.0	0.0	0.0	0.0	0.0
-1366618.076	0.0	0.0	0.0	-19132653.06
0.0	1366618.076	0.0	0.0	0.0
-19132653.06	0.0	0.0	-1366618.076	0.0
19132653.06	0.0	0.0	0.0	1366618.076
C.0	19132653.06	0.0	0.0	0.0
C.0	0.0	0.0	0.0	0.0
C.0	0.0	0.0	0.0	0.0
C.0	0.0	-19132653.06	0.0	178571428.55
C.0	0.0	0.0	19132653.06	0.0
357142857.1	0.0	0.0	19132653.06	0.0
C.0	0.0	178571428.55	0.0	-19132653.06
C.0	0.0	0.0	357142857.1	0.0
6 4 0	1 1			
3.64	0.0	0.0	0.0	0.0
C.0	0.0	3.64	0.0	0.0
0.0	0.0	0.0	0.0	3.64
C.0	0.0	0.0	0.0	0.0
C.0	28476.0	0.0	0.0	0.0
C.0	0.0	0.0	14238.0	0.0
C.0	0.0	0.0	0.0	0.0
14238.0				
10 1 0	0 0			
5 5 1				
C.0	36.4	71.5	108.0	145.0
1520000000.0	800000000.0	340000000.0	180000000.0	0.0
.0863	.1306	.1244	.1166	.0833
1 4 0	1 0			
.542				
8 1 0	0 1			
4 4 1				
C.0	35.0	65.0	100.0	
45000000.0	20000000.0	12000000.0	0.0	
C.0	0.0	.36	0.0	
8 1 0	0 1			
4 4 1				
C.0	35.0	65.0	100.0	
300000000.0	150000000.0	75000000.0	0.0	
C.0	0.0	.36	0.0	
4 2 0	0 1			
4 4				
C.0	35.0	65.0	100.0	
40000000.0	27500000.0	10000000.0	0.0	
0.0	0.0	21.8	0.0	
1 4 0	1 1			
.36				
17 17 .88	23 23 2595.0	23 24 -40.6	24 24 .88	
53 81 -10.36	54 82 -12.96	55 83 -9.84	56 84 -11.14	
57 85 -12.96	58 86 -18.64			

```

PROGRAM BJD5(INPUT,OUTPUT,TAPE3,TAPE4,TAPE6,TAPE8,TAPE9,
1          TAPE50,TAPE5=INPUT)
DIMENSION CM(99,99),V(99,99),EM(99),CS(99,99),E(99),BETA(144,99),
1          R(99),P(99),C(99,99),CINVT(99,99),BCBT(99,99),
2          IPIVOT(99),INDEX(99,2)
COMMON HMTX(12),FCOM
EQUIVALENCE(BETA(1,1),CM(1,1),CS(1,1),CINVT(1,1),INDEX(1,1)),
1          (V(1,1),C(1,1),BCBT(1,1))

```

```

      MAX=99
      MBETA=144
C      ON ENTRY TO THIS PROGRAM - - - -
C      TAPE3 HAS ORDER AND BETA MATRIX
C      TAPE4 HAS COUPLED MASS AND STIFFNESS MATRICES
      1 READ(5,5001) (HMTX(J),J=5,12)
5001 FORMAT(8A10)
      IF(EOF,5) 8998,8999
8998 WRITE(6,8997)
      PRINT 8997
      STOP 500
8997 FORMAT(/** PROGRAM BJD5 STOPPED ON (EOF,5)*)
8999 CONTINUE
      READ(5,5001) (HMTX(I),I=1,4)
      NERR=0
      FCON=1.0
      REWIND 3
C READ ORDER OF BETA FROM TAPE 3
      READ(3) NRB,NCB
      REWIND 4
C READ COUPLED MASS MATRIX FROM TAPE4
      READ(4)((CM(I,J),I=1,NCB),J=1,NCB)
C SOLVE FOR EIGENVALUES AND EIGENVECTORS OF COUPLED MASS MATRIX
      CALL JACTV(NCB,MAX,1,CM,EM,V,DUM1,DUM2,DUM3,DUM4,IERR)
      IF(IERR.EQ.1) GO TO 1500
C TEST FOR NUMBER OF FINITE EIGENVALUES OF COUPLED MASS MATRIX
      DO 10 J=2,NCB
        IJ=J-1
        IF(EM(J).LE.0.0) GO TO 11
        IF((EM(IJ)/EM(J)).GE.1.000000.0) GO TO 11
        IF (J.EQ.NCB) IJ=NCB
      10 CONTINUE
      11 NFMEV=IJ
C WRITE EIGENVALUES OF COUPLED MASS MATRIX ON TAPE 6
      WRITE(6,12)(EM(I),I=1,NCB)
      12 FORMAT(/** EIGENVALUES OF COUPLED MASS MATRIX **/(2X,E15.8))
      WRITE(6,13) NFMEV
      13 FORMAT(/** NUMBER OF FINITE MASS EIGENVALUES = *,I3/**)
C READ COUPLED STIFFNESS MATRIX FROM TAPE4
      READ(4)((CS(I,J),I=1,NCB),J=1,NCB)
C REWIND TAPE4 AND WRITE COLUMNS OF VECTOR MATRIX ON TAPE4
C REWIND TAPE9 AND WRITE ROWS OF VECTOR MATRIX ON TAPE9
      REWIND 4
      REWIND 9
      DO 20 J=1,NCB
        WRITE(9)(V(J,I),I=1,NCB)
      20 WRITE(4)(V(I,J),I=1,NCB)
C MULTIPLY STIFFNESS BY VECTOR AND STORE IN V
      REWIND 4
      DO 30 J=1,NCB
C      READ COLUMN OF VECTOR MATRIX
        READ(4)(R(I),I=1,NCB)
        DO 30 I=1,NCB
          V(I,J)=0.0
          DO 30 IJ=1,NCB
            30 V(I,J)=V(I,J)+CS(I,IJ)*R(IJ)
C COMPUTE VT*(CS*V)
      REWIND 4
      DO 40 I=1,NCB
C      READ COLUMN OF VECTOR MATRIX AS ROW OF VECTOR TRANSPOSE

```



```

      RFAD(4)(R(J),J=1,NCB)
      DO 40 J=1,NCB
      CS(I,J)=0.0
      DO 40 IJ=1,NCB
40 CS(I,J)=CS(I,J)+R(IJ)*V(IJ,J)
      K=NFMEV
      N=NCB-NFMEV
C IF THE NUMBER OF FINITE MASS EIGENVALUES (NFMEV) IS EQUAL TO THE
C ORDER OF THE COUPLED MASS MATRIX CM, BYPASS PARTITIONING OF THE
C COUPLED STIFFNESS MATRIX CS.
      IF(N.EQ.0) GO TO 79
      KP1=K+1
C CS WILL BE PARTITIONED AS FOLLOWS----- (A B)
C (BT C)
C WHERE A=(K*K), B=(K*N), BT=(N*K), C=(N*N)
      REWIND 4
C STORE MATRIX A ON TAPE4 BY COLUMNS, 1 RECORD
      WRITE(4)((CS(I,J),I=1,K),J=1,K)
      REWIND 8
C STORE MATRIX C ON TAPE 8 BY COLUMNS, 1 RECORD
      WRITE(8)((CS(I,J),I=KP1,NCB),J=KP1,NCB)
C STORE MATRIX B ON TAPE8 BY ROWS, K RECORDS
      DO 50 I=1,K
50 WRITE(8) (CS(I,J),J=KP1,NCB)
C READ MATRIX C FROM TAPE8 AND COMPUTE THE INVERSE OF C
      REWIND 8
      READ(8)((C(I,J),I=1,N),J=1,N)
      CALL MATINV(C,N,BI,0,DET,PIVOT,INDEX,MAX,ISCALE)
C COMPUTE C INVERSE TIMES B TRANSPOSE
      DO 60 J=1,K
C READ ROW OF B AS COLUMN OF B TRANSPOSE
      READ(8)(P(I),I=1,N)
      DO 60 I=1,N
      CINVBT(I,J)=0.0
      DO 60 IJ=1,N
60 CINVBT(I,J)=CINVBT(I,J)+C(I,IJ)*P(IJ)
      REWIND 8
C THE NEXT READ STATEMENT IS A DUMMY READ TO POSITION TAPE8
      READ(8) SKIPREC
C COMPUTE P * (C INVERSE * B TRANSPOSE)
      DO 70 I=1,K
C READ ROW OF B
      READ(8)(P(J),J=1,N)
      DO 70 J=1,K
      BCBT(I,J)=0.0
      DO 70 IJ=1,N
70 BCBT(I,J)=BCBT(I,J)+P(IJ)*CINVBT(IJ,J)
      REWIND 8
C STORE C INVERSE TIMES B TRANSPOSE ON TAPE8 BY COLUMNS, 1 RECORD
      WRITE(8)((CINVBT(I,J),I=1,N),J=1,K)
      REWIND 4
C READ MATRIX A FROM 4
      READ(4)((CS(I,J),I=1,K),J=1,K)
C COMPUTE A - (B*CINV*BT)
C REPLACE THE FIRST K (FINITE) EIGENVALUES OF THE MASS MATRIX BY
C 1.0/(SQUARE ROOT OF EIGENVALUE)
79 DO 81 I=1,K
      EM(I)=1.0/SQRT(EM(I))
      IF(N.EQ.0) GO TO 81
      DO 80 J=1,K

```

```

80 CS(I,J)=CS(I,J)-BCBT(I,J)
81 CONTINUE
C PRE- AND POST-MULTIPLY THE CS MATRIX BY 1./SQRT(MASS EIGENVALUES)
  DO 90 I=1,K
  DO 90 J=1,K
90 CS(I,J)=EM(I)*CS(I,J)
  DO 100 J=1,K
  DO 100 I=1,K
100 CS(I,J)=CS(I,J)*EM(J)
  CALL JACTV(K,MAX,K,CS,E,V,DUM1,DUM2,DUM3,DUM4,NERR)
  IF(NERR.NE.0) GO TO 1500
  CALL FREQ(E,CS,K,MAX)
C PRE-MULTIPLY VECTOR MATRIX BY 1./SQRT(MASS EIGENVALUES)
  DO 110 I=1,K
  DO 110 J=1,K
110 V(I,J)=EM(I)*V(I,J)
  REWIND 4
C STORE X SUB 1 VECTORS ON TAPE4, BY COLUMNS, K RECORDS
  DO 115 J=1,K
115 WRITE(4)(V(I,J),I=1,K)
  IF(N.EQ.0) GO TO 144
  REWIND 8
C READ C INVERSE * B TRANSPOSE MATRIX FROM TAPE8
  READ(8)((CS(I,J),I=1,N),J=1,K)
  REWIND 4
C MULTIPLY (C INVERSE * B TRANSPOSE) BY X SUB 1 VECTOR MATRIX
  DO 120 J=1,K
C READ COLUMN OF X SUB 1 MATRIX FROM TAPE4
  READ(4)(P(I),I=1,K)
  DO 120 I=1,N
  V(I,J)=0.0
  DO 120 IJ=1,K
120 V(I,J)=V(I,J)+CS(I,IJ)*P(IJ)
C X SUB 2 VECTOR MATRIX = - VECTOR MATRIX JUST COMPUTED
  DO 125 I=1,N
  DO 125 J=1,K
125 V(I,J)=-V(I,J)
C STORE X SUB 2 VECTOR MATRIX ON TAPE4 BY ROWS, 1 RECORD
  WRITE(4)((V(I,J),J=1,K),I=1,N)
C REWIND 4, THEN READ X SUB 1 VECTORS INTO FIRST K ROWS OF CS AND
C READ X SUB 2 VECTORS INTO (K+1) TO NCB ROWS OF CS
C THE CS MATRIX IS NOW (NCB * K)
144 REWIND 4
  DO 145 J=1,K
145 READ(4)(CS(I,J),I=1,K)
  IF(N.NE.0) READ(4)((CS(I,J),J=1,K),I=K+1,NCB)
C MULTIPLY MASS VECTOR MATRIX BY CS MATRIX
  PEWIND 9
  DO 146 I=1,NCB
C READ ROW OF MASS VECTOR MATRIX
  READ(9)(R(J),J=1,NCB)
  DO 146 J=1,K
  V(I,J)=0.0
  DO 146 IJ=1,NCB
146 V(I,J)=V(I,J)+R(IJ)*CS(IJ,J)
C COMPUTE BETA * THE FINAL VECTOR MATRIX
  REWIND 8
  DO 151 I=1,NRB
C READ ROW OF BETA MATRIX
  READ(3)(R(J),J=1,NCB)

```

```

      DO 150 J=1,K
      P(J)=0.0
      DO 150 IJ=1,NCR
150  P(J)=P(J)+P(IJ)* V(IJ,J)
151  WRITE(8)(P(J),J=1,K)
      REWIND 8
      DO 160 I=1,NRR
160  READ(8)(BETA(I,J),J=1,K)
      CALL WMTXC(BETA,NRR,K,MBETA,MAX)
      REWIND 8
      WRITE(50)((BETA(I,J),I=1,NCR),J=1,K)
      GO TO 1
1500 IF(IERR.EQ.1) WRITE(6,1501)
      IF(NERR.NE.0) WRITE(6,1502)
1501 FORMAT(/** ERROR RETURN FROM JACTV - FIRST CALL - COUPLED MASS*)
1502 FORMAT(/** ERROR RETURN FROM JACTV - SECOND CALL - STIFFNESS*)
      GO TO 1
      END

```

```

      SUBROUTINE WMTXC(A,NP,NC,MAXR,MAXC)
C   NR=ROWS OF A, NC=COLS OF A, MAXR=MAX ROWS OF A, MAXC=MAX COLS OF A
      DIMENSION A(MAXR,MAXC)
      COMMON HMTX(12)
      KE=0
      KSET=NC/8
      KLEFT=MOD(NC,8)
      IF(KLEFT.NE.0) KSET=KSET+1
      DO 10 KT=1,KSET
      KB=KE+1
      KE=KE+8
      IF(KT.EQ.KSET) KE=NC
      WRITE(6,5001) HMTX,(J,J=KB,KE)
      DO 10 I=1,NP
10  WRITE(6,5002) I,(A(I,J),J=KB,KE)
5001 FORMAT(1H1//12A10///10H ROW COL,I4,7(11X14))
5002 FORMAT(14,9E15.7)
      RETURN
      END

```

```

      SUBROUTINE FREQ(E,A,K,MAX)
      DIMENSION F(MAX),A(MAX,MAX)
      COMMON HMTX(12),FCON
      DO 10 I=1,K
      A(I,1)=E(I)
      A(I,2)=FCON*E(I)
      A(I,3)=SQRT(ABS(A(I,2)))
10  A(I,4)=A(I,3)/6.28318530717959
      PRINT 5014,(HMTX(J),J=5,12),FCON,(I,(A(I,J),J=1,4),I=1,K)
      WRITE(6,5014)(HMTX(J),J=5,12),FCON,(I,(A(I,J),J=1,4),I=1,K)
5014 FORMAT(1H1//1X8A10//7H FCON =,E22.14//4X1HJ9X9HLAMBDA(J)14X12HOMEG
1A SQ (J)14X8HCMEGA(J)14X13HFREQ.(J), CPS/34X13H(FCON * LAMBDA(J))1
22X6H(REAL)///(15,4E24.14))
      RETURN
      END

```

FULL-SCALE TILT ROTOR SYMMETRIC FREE-FLIGHT MODES--90 DEG CONVERSION ANGLE
FINAL MODAL MATRIX

VIBRATION ANALYSIS BY COMPONENT MODE SYNTHESIS

```
PROGRAM COSMOS(INPUT,OUTPUT,TAPE5=INPUT,TAPE3,TAPE4,TAPE6,TAPE8,
1 TAPE9,TAPE10,TAPE11,TAPE12,TAPE20)
```

```
*****
*
* PROGRAMS COSMOS,MODALC,AND BJD5M COMPRISE A COMPUTER
* PACKAGE FOR THE NATURAL MODE VIBRATION ANALYSIS OF
* COMPLEX STRUCTURAL SYSTEMS BY THE METHOD OF COMPONENT
* MODE SYNTHESIS.
*
* THE STRUCTURE IS IDEALIZED AS AN ASSEMBLY OF BEAM,SPRING,
* AND RIGID MASS SUBSYSTEMS. A FINITE-ELEMENT APPROACH
* IS EMPLOYED TO GENERATE THE MASS AND STIFFNESS MATRICES
* FOR THE UNCOUPLED SYSTEM AND THOSE REQUIRED FOR
* SUBSYSTEM MODAL ANALYSES. SUBSYSTEM BEAM BOUND CONDITIONS
* CAN BE FREE-FREE, PINNED-FREE, OR CLAMPED-FREE. PROGRAM
* PERMITS OPTION OF EXPRESSING MODAL EXPANSION MATRIX
* AS A COMBINATION OF CALCULATED SUBSYSTEM NATURAL MODES
* AND ADDITIONAL USER-INPUT DEFLECTION SHAPES (SUCH AS
* MEASURED MODE SHAPES,STATIC DEFLECTION SHAPES,OR
* ASSUMED DEFLECTION SHAPES). USER-WRITTEN CONSTRAINT
* EQUATIONS ENFORCING INTER-SUBSYSTEM DISPLACEMENT
* COMPATIBILITY ARE APPLIED ACCORDING TO THE METHOD OF
* NASA TR R-326. A CONDENSATION OF THE SYSTEM GENERALIZED
* STIFFNESS MATRIX IS PERFORMED,IF NECESSARY,AND THE
* RESULTANT EQUATIONS CAST INTO A FORM TO WHICH THE
* THRESHOLD VARIATION OF THE JACOBI ALGORITHM FOR FINDING
* EIGENVALUES AND EIGENVECTORS IS APPLIED.
*
*****
```

```

DIMENSION A(13,13),B(13,13),C(13,13),DM(13),PI(13),X(13),S(13),
1 E(26),FS(13),EC(13),IP(26,2),AA(26,26),BB(26,26),
2 EIGV(26),V(26,26),EM(26),R(26),IPIVOT(13),INDEX(13,2),
3 CINVT(13,13),P(13),BCINVT(13,13),EV(26)
COMMON/SAME/HMTX(12),FCON,KASE,IFFPC,IRITALL
MAX=13 $ MAX2=26 $ MAX3=39
MAX2=2
FCON=1.0
FEWIND 11
FEWIND 12
FEWIND 20
1 READ 1-17,(HMTX(J),J=5,12)
1010 FGMAT(8A10)
IF(EOF,5) 8998,8999
8997 FORMAT(1H1/** PROGRAM COSMOS STOPPED ON EOF,5 *)
8999 CONTINUE
```

```

C KASE=1, DIAGONAL MASS ONLY (NO NULL VALUES)
C KASE=2, DIAGONAL MASS AND ROTARY INERTIA (NO NULL VALUES)
C KASE=3, NON-DIAGONAL MASS AND ROTARY INERTIA (NULL VALUES
C CAN BE ON DIAGONAL)
C KASE=4, DIAGONAL TORSIONAL INERTIA OR AXIAL MASS (NO NULL
C VALUES ON DIAGONAL)
C KASE=5, DIAGONAL TORSIONAL INERTIA OR AXIAL MASS (NULL
C VALUES CAN BE ON DIAGONAL)
```

```

C      ---BEAM END CONDITIONS---
C      IFFPC=1, FREE-FREE
C      IFFPC=2, PINNED-FREE
C      IFFPC=3, CLAMPED-FREE

C      STATIC UNBALANCE TERMS ARISING FROM MASSES OFF THE
C      ELASTIC AXIS COUPLE BENDING AND TORSION
C      ICBT=1, COUPLED BENDING-TORSION
C      ICBT=0, BENDING AND TORSION UNCOUPLED (OR NOT APPLICABLE)

C      FOR SPRING OR RIGID BODY SUBSYSTEMS NO MODAL EXPANSIONS
C      WILL BE PERFORMED. USER HAS OPTION TO BYPASS MODAL
C      EXPANSIONS FOR ANY BEAM SUBSYSTEM.
C      IEXPAND=1, MODAL EXPANSION WILL BE PERFORMED
C      IEXPAND=0, NO MODAL EXPANSION (OR NOT APPLICABLE)

C      NSPADD = NUMBER OF SPRING CONSTANTS TO BE ADDED ON AND ABOVE
C      DIAGONAL OF FREE-FREE STIFFNESS MATRIX IN A GIVEN
C      BLOCK. PROGRAM WILL PROVIDE SYMMETRY AS REQUIRED.
C      --NOTE--THESE SPRINGS TIE BEAM OR RIGID BODY
C      ELEMENTS TO GROUND ONLY AND NOT TO OTHER ELEMENTS.

C      MASADD = NUMBER OF MASSES TO BE ADDED ON AND ABOVE
C      DIAGONAL OF THE FREE-FREE MASS-ROTARY INERTIA
C      MATRIX IN A GIVEN BLOCK. THE PROGRAM WILL
C      PROVIDE SYMMETRY AS REQUIRED.

C      MASCBT = NUMBER OF STATIC UNBALANCE TERMS ABOVE DIAGONAL
C      OF COUPLED BENDING-TORSION MASS MATRIX. THE
C      PROGRAM WILL PROVIDE SYMMETRY AS REQUIRED.

C      IRITALL CONTROLS INTERMEDIATE OUTPUT TO TAPE 6 WHICH
C      MAY BE ROUTED.
C      IRITALL=1, SUBSYSTEM MASS AND STIFFNESS MATRICES
C      FOR FREE-FREE AND RESTRAINED CONDITIONS
C      WILL BE OUTPUT
C      IRITALL=0, ABOVE NOT OUTPUT

C      NBLKS = NUMBER OF BLOCKS IN UNCOUPLED, FREE-FREE SYSTEM
C      MASS AND STIFFNESS MATRICES

C      NORDER = ORDER OF UNCOUPLED, FREE-FREE SYSTEM

C  READ NUMBER OF BLOCKS IN UNCOUPLED SYSTEM MASS AND STIFFNESS
C  MATRICES AND ORDER OF SYSTEM
      READ 1020,NBLKS,NORDER
      WRITE(6,1011) NBLKS,NORDER
      PRINT 1011,NBLKS,NORDER
1011 FORMAT(1H1/* NUMBER BLOCKS IN UNCOUPLED SYSTEM MASS AND STIFFNESS
1  MATRICES = *,I3/* ORDER OF SYSTEM = *,I3)
      DO 200 NBLOCK=1,NBLKS
      WRITE(6,1019) NBLOCK
      PRINT 1019,NBLOCK
1019 FORMAT(1H //1X,19H*****//1X,19H*           */
1      1X,14H* BLOCK NUMBER ,I3,2H */1X,19H*           */
2      1X,19H*****))

```

```

C      KK=ORDER OF BLOCK

C      LOC=1, BEAM BENDING
C      LOC=2, BEAM TORSION
C      LOC=3, BEAM AXIAL
C      LOC=4, SPRING OR RIGID BODY ELEMENT

C      FOR SPRING OR RIGID BODY ELEMENTS ----
C      MK=1, READ STIFFNESS FROM CARDS
C      MK=0, NO READ

C      MM=1, READ MASS FROM CARDS
C      MM=0, NO READ

C      FOR A SYMMETRIC OR ANTI-SYMMETRIC FORMULATION OF THE
C      PROBLEM, THE MASS AND STIFFNESS MATRICES FOR BLOCKS
C      CORRESPONDING TO SUBSYSTEMS OUT OF THE VERTICAL PLANE
C      OF SYMMETRY MUST BE MULTIPLIED BY 2.0
C      ISYM=1, MULTIPLY BLOCK MASS AND STIFFNESS MATRIX BY 2.0
C      ISYM=0, NO MULTIPLICATION

      READ 1020, KK, LOC, MK, MM, IEXPAND, ISYM
1020 FORMAT(20I4)
      GO TO (110, 120, 120, 130), LOC

*****
* BEAM BENDING *
*****

C      FOR BEAM BENDING, FREE-FREE STIFFNESS MATRIX IS
C      GENERATED IN THE PARTITIONED FORM (A B)
C      (BT C)
C      WHERE A=(K*K), B=(K*N), BT=(N*K), C=(N*N)
C      FOR THE FREE-FREE CASE, K=N

110 READ 1020, K, N, KASE, ICBT, IFFPC, NSPADD, MASADD, IRITALL
   WRITE(6, 1030) K, N, KASE, ICBT, IFFPC, NSPADD, MASADD, IRITALL
   PRINT 1030, K, N, KASE, ICBT, IFFPC, NSPADD, MASADD, IRITALL
1030 FORMAT(/, 9X, *K*, 9X, *N*, 8X, *KASE*, 6X, *ICBT*, 7X, *IFFPC*, 7X, *NSPADD*,
1      6X, *MASADD*, 5X, *IRITALL*/, 4I10, 4I12)
1040 FORMAT(5E14.8)
   IF (ICBT.EQ.1) KASESAV=KASE
   KM1=K-1
   CALL ZEROM(A, K, K, MAX, MAX)
   CALL ZEROM(B, K, N, MAX, MAX)
   CALL ZEROM(C, N, N, MAX, MAX)
   CALL ZEROM(DM, K, 1, MAX, 1)
   CALL ZEROM(RI, N, 1, MAX, 1)
   READ 1040, (X(I), I=1, K)
   READ 1040, (S(I), I=1, KM1)
   READ 1040, (DM(I), I=1, K)
   IF (KASE.NE.1) READ 1040, (RI(I), I=1, N)
   PRINT 1050, (J, X(J), S(J), DM(J), RI(J), J=1, KM1)
   WRITE(6, 1050) (J, X(J), S(J), DM(J), RI(J), J=1, KM1)
   PRINT 1051, K, X(K), DM(K), RI(K)
   WRITE(6, 1051) K, X(K), DM(K), RI(K)

```

```

1050 FORMAT(///3X,*J*,7X,*X(J)*,11X,*E[(J)*,10X,*MASS(J)*,10X,*R[(J)*,
1      //(14,4E16.8))
1051 FORMAT(14,E16.8,16X,2E16.8)
      DC 40 L=1,KM1
      40 E(L)=1.0/(X(L+1)-X(L))
      DC 41 L=1,KM1
      41 ES(L)=E(L)*E(L)
      DC 42 L=1,KM1
      42 EC(L)=E(L)*ES(L)
C   FORM MATRIX A
      A(1,2)=-A(1,1)
      A(K,KM1)=-12.0*S(KM1)*EC(KM1)
      A(K,K)=-A(K,KM1)
      M=0
      DO 50 L=2,KM1
      M=M+1
      A(L,M)=-12.0*S(M)*EC(M)
      A(L,M+2)=-12.0*S(M+1)*EC(M+1)
50   A(L,M+1)=-A(L,M)+A(L,M+2)
C   FORM MATRIX B
      B(1,1)=6.0*S(1)*ES(1)
      B(1,2)=B(1,1)
      B(K,KM1)=-6.0*S(KM1)*ES(KM1)
      B(K,K)=B(K,KM1)
      M=0
      DO 61 L=2,KM1
      M=M+1
      B(L,M)=-6.0*S(M)*ES(M)
      B(L,M+2)=6.0*S(M+1)*ES(M+1)
61   B(L,M+1)=B(L,M)+B(L,M+2)
C   FORM MATRIX C
      C(1,1)=4.0*S(1)*E(1)
      C(1,2)=2.0*S(1)*E(1)
      C(K,KM1)=2.0*S(KM1)*E(KM1)
      C(K,K)=4.0*S(KM1)*E(KM1)
      M=0
      DO 71 L=2,KM1
      M=M+1
      C(L,M)=2.0*S(M)*E(M)
      C(L,M+2)=2.0*S(M+1)*E(M+1)
71   C(L,M+1)=4.0*(S(M+1)*E(M+1)+S(M)*E(M))
      IF(NSPADD.EQ.0) GO TO 90
      READ 1060,(IR(J,1),IR(J,2),E(J),J=1,NSPADD)
1060  FORMAT(4(2I3,E14.8))
      WRITE(6,1061)(J,IR(J,1),IR(J,2),E(J),J=1,NSPADD)
1061  FORMAT(//4X,*J*,2X,*R[J]*,2X,*COL*,7X,*SPRING(J)*// (3I5,E22.14))
      DO 90 JJ=1,NSPADD
      NROW=IR(JJ,1)
      NCOL=IR(JJ,2)
      IF(NROW.GT.K) GO TO 89
      IF(NCOL.GT.K) GO TO 88
      A(NROW,NCOL)=A(NROW,NCOL)+E(JJ)
      IF(NROW.NE.NCOL) A(NCOL,NROW)=A(NCOL,NROW)+E(JJ)
      GO TO 90
88   NCOL=NCOL-K
      B(NROW,NCOL)=B(NROW,NCOL)+E(JJ)
      GO TO 90

```

```

89 NROW=NR0W-K
   NCOL=NCOL-K
   C(NROW,NCOL)=C(NROW,NCOL)+E(JJ)
   IF(NROW.NF.NCOL) C(NCOL,NROW)=C(NCOL,NROW)+E(JJ)
90 CONTINUE
C FORM FREE-FREE BENDING STIFFNESS AND MASS MATRICES
  KPN=K+N
  KP1=K+1
  IF(ICBT.EQ.1) KK=KK+KK/2
  IF(ICBT.EQ.1) KKSAY=KK
  IF(ICBT.EQ.1) MAXT2=MAXT3
  CALL ZEROM(AA,KK,KK,MAXT2,MAXT2)
  CALL ZEROM(BB,KK,KK,MAXT2,MAXT2)
  REWIND 3
  WRITE(3)((A(I,J),J=1,K),I=1,K),((B(I,J),J=1,N),I=1,K),((B(I,J),
1      I=1,K),J=1,N),((C(I,J),J=1,N),I=1,N),((D(I,J),J=1,K),
2      (PI(J),J=1,N)
  REWIND 3
  READ(3)((AA(I,J),J=1,K),I=1,K),((AA(I,J),J=KP1,KPN),I=1,K),
1      ((AA(I,J),J=1,K),I=KP1,KPN),((AA(I,J),J=KP1,KPN),I=KP1,KPN),
2      (BB(J,J),J=1,KPN)
  IF(ICBT.NE.1) GO TO 1064
  REWIND 9
  WRITE(9)((AA(I,J),J=1,KPN),I=1,KPN)
C MULTIPLY FREE-FREE STIFFNESS MATRIX BY 2.0 IF ISYM = 1
1064 IF(ISYM.EQ.0) GO TO 1066
   DO 1065 I=1,KPN
   DO 1065 J=1,KPN
1065 AA(I,J)=2.0*AA(I,J)
1066 IF(ICBT.NE.1) GO TO 1068
   KP=K $ NP=N
   GO TO 1069
C WRITE ORDER AND FREE-FREE STIFFNESS MATRIX ON TAPE 11, 1 RECORD
1068 WRITE(11)KPN,((AA(I,J),J=1,KPN),I=1,KPN)
   IF(IRITALL.EQ.0) GO TO 1069
   HMTX(1)=10H FREE-FRE $ HMTX(2)=10HE BENDING
   HMTX(3)=10HSTIFFNESS $ HMTX(4)=10HMATRIX
   CALL WMTXC(AA,KPN,KPN,MAXT2,MAXT2)
1069 CONTINUE
   IF(MASADD.EQ.0) GO TO 93
   READ 1060,((IR(J,1),IR(J,2)),E(J),J=1,MASADD)
   DO 93 J=1,MASADD
   NRCW=IR(J,1)
   NCOL=IR(J,2)
   BB(NROW,NCOL)=BB(NROW,NCOL)+E(J)
   IF(NROW.NE.NCOL) BB(NCOL,NROW)=BB(NROW,NCOL)
93 CONTINUE
   IF(ICBT.NE.1) GO TO 99
   REWIND 10
   WRITE(10)((BB(I,J),J=1,KPN),I=1,KPN)
C MULTIPLY FREE-FREE MASS MATRIX BY 2.0 IF ISYM = 1
99 IF(ISYM.EQ.0) GO TO 98
   REWIND 8
   WRITE(8)((BB(I,J),J=1,KPN),I=1,KPN)
   DO 96 I=1,KPN
   DO 96 J=1,KPN
96 BB(I,J)=2.0*BB(I,J)
98 IF(ICBT.NE.1) GO TO 95
   GO TO 97

```



```

C WRITE ORDER AND FREE-FREE MASS MATRIX ON TAPE 12, 1 RECORD
95 WRITE(12)KPN,((BB(I,J),J=1,KPN),I=1,KPN)
   IF(IRITALL.EQ.0) GO TO 94
   HMTX(1)=1CH FREE-FRE $ HMTX(2)=1OHE BENDING
   HMTX(3)=1OHMASS MATRI $ HMTX(4)=1OHX
   CALL WMTXC(BB,KPN,KPN,MAXT2,MAXT2)
94 CONTINUE
   IF(ISYM.EQ.0) GO TO 97
   REWIND 8
   READ(8)((BB(I,J),J=1,KPN),I=1,KPN)
97 IF(ICBT.EQ.1) GO TO 200
   IF(IEXPAND.EQ.1) GO TO 1070
   CALL ZEROM(V,KK,KK,MAXT2,MAXT2)
   DO 1071 I=1,KK
     J=KK+1-I
1071 V(I,J)=1.0
     KPN=KK $ K=KK
     GO TO 7000
C APPLY BOUNDARY CONDITIONS TO FREE-FREE STIFFNESS AND MASS MATRICES
107C IBA=1
   IBC=1
   IF(IFFPC.GE.2) IBA=2
   IF(IFFPC.EQ.3) IBC=2
   KA=K+IBC
   REWIND 3
1   ((C(I,J),J=IBC,N),I=IBC,N),((BB(I,J),J=IBA,K),I=IBA,K),
2   ((BB(I,J),J=KA,KPN),I=IBA,K),((BB(I,J),J=IBA,K),
3   I=KA,KPN),((BB(I,J),J=KA,KPN),I=KA,KPN)
   IF(IBA.EQ.2) K=K-1
   IF(IBC.EQ.2) N=N-1
   HMTX(1)=1OH K,N AFTE $ HMTX(2)=1OHR APPLICAT
   HMTX(3)=1CHION OF BDR $ HMTX(4)=1OHY. COND.
   WRITE(6,1080)HMTX,K,N
   PRINT 1080,HMTX,K,N
1080 FORMAT(///12A10//5X,*K = *,I3,10X,*N = *,I3)
   REWIND 3
   KPN=K+N
   KP1=K+1
   READ(3)((AA(I,J),J=1,K),I=1,K),((AA(I,J),J=KP1,KPN),I=1,K),
1   ((AA(I,J),J=KP1,KPN),I=KP1,KPN),((BB(I,J),J=1,K),I=1,K),
2   ((BB(I,J),J=KP1,KPN),I=1,K),((BB(I,J),J=1,K),I=KP1,KPN),
3   ((BB(I,J),J=KP1,KPN),I=KP1,KPN)
   DO 11 I=KP1,KPN
     DO 11 J=1,K
11 AA(I,J)=AA(J,I)
   IF(IRITALL.EQ.0) GO TO 12
   HMTX(1)=1OH FINAL ST $ HMTX(2)=1OHIFNESS MA
   HMTX(3)=1OHTRIX $ HMTX(4)=1OH
   CALL WMTXC(AA,KPN,KPN,MAXT2,MAXT2)
   HMTX(1)=1OH FINAL MA $ HMTX(2)=1OHSS MATRIX
   HMTX(3)=1CH $ HMTX(4)=1OH
   CALL WMTXC(BB,KPN,KPN,MAXT2,MAXT2)
12 FEWIND 4
C WRITE ORDER, MASS MATRIX, AND STIFFNESS MATRIX ON TAPE 4, 1 RECORD
   WRITE(4)KPN,((BB(I,J),J=1,KPN),I=1,KPN),((AA(I,J),J=1,KPN),
1   I=1,KPN)
C CALL EIGENVALUE SUBROUTINE
   CALL ALLEIG(AA,BB,KPN,MAXT2,MAX,MAX2,K,N,C,IPIVOT,INDEX,P,
1   C INVBT,BC INVBT,EM,EIGV,V,EV,R,KPR,ICBT)

```

```

      GC TO(105,102,102)IFFPC
C   ADD RIGID BODY TRANSLATION MODE TO MODAL MATRIX
102 N=KPN/2
      K=K+1 $ J=N
      DO 103 I=1,N
      J=J+1
      V(I,K)=1.0
103 V(J,K)=0.0
      IF(IFFPC.EQ.2) GO TO 105
C   ADD RIGID BODY ROTATION MODE TO MODAL MATRIX
      K=K+1 $ J=N
      DO 104 I=1,N
      J=J+1
      V(I,K)=X(I)
104 V(J,K)=1.0
105 CONTINUE
C   WRITE ORDER AND MODES (BY COLUMNS) ON TAPE 20, 2 RECCROS
7000 WRITE(20) KPN,K
      WRITE(20)((V(I,J),I=1,KPN),J=1,K)
      IF(NBLJCK.EQ.NBLKS.AND.NBLKS.EQ.1) GO TO 1
      GO TO 200

*****
* BEAM TORSION OR AXIAL *
*****

C       FREE-FREE STIFFNESS MATRIX IS OF ORDER K

120 READ 1020,K,KASE,IFFPC,NSPADD,MASADD,IRITALL
      WRITE(6,1090)K,KASE,IFFPC,NSPADD,MASADD,IRITALL
      PRINT 1090,K,KASE,IFFPC,NSPADD,MASADD,IRITALL
1090 FORMAT(//3X,*K*,8X,*KASE*,5X,*IFFPC*,5X,*NSPADD*,4X,*MASADD*,
1       3X,*IRITALL*//6I10)
      KM1=K-1
      IF(ICBT.EQ.1) KASE=KASESAV
      CALL ZEROM(A,K,K,MAX,MAX)
      CALL ZEROM(B,K,K,MAX,MAX)
      READ 1040,(X(I),I=1,K)
      READ 1040,(S(I),I=1,KM1)
      READ 1040,(RI(I),I=1,K)
      IF(LOC.EQ.2) GO TO 1098
      WRITE(6,1102)(J,X(J),S(J),RI(J),J=1,KM1)
      WRITE(6,1101) K,X(K),RI(K)
      PRINT 1102,(J,X(J),S(J),RI(J),J=1,KM1)
      PRINT 1101,K,X(K),RI(K)
      GO TO 1099
1098 WRITE(6,1100)(J,X(J),S(J),RI(J),J=1,KM1)
      WRITE(6,1101) K,X(K),RI(K)
      PRINT 1100,(J,X(J),S(J),RI(J),J=1,KM1)
      PRINT 1101,K,X(K),RI(K)
1100 FORMAT(//3X,*J*,7X,*X(J)*,11X,*GJ(J)*,10X,*RI(J)*,/(I4,3E16.8))
1101 FORMAT(I4,E16.8,16X,E16.8)
1102 FOPMAT(//3X,*J*,7X,*X(J)*,11X,*AE(J)*,10X,*DM(J)*,/(I4,3E16.8))
C   FORM FREE-FREE STIFFNESS MATRIX
1099 DO 121 L=1,KM1
      121 E(L)=1.0/(X(L+1)-X(L))
      DO 122 J=1,KM1
      122 S(J)=S(J)*E(J)
      A(1,1)=S(1)
      A(1,2)=-S(1)
      A(K,K-1)=-S(KM1)
      A(K,K)=S(KM1)

```

```

KTB=0
DO 123 J=2,KM1
KC=KTB+J
A(KD,KD-1)=-S(J-1)
A(KD,KD)=S(J-1)+S(J)
123 A(KD,KD+1)=-S(J)
IF(NSPADD.EQ.0) GO TO 124
READ 1060,(IR(J,1),IR(J,2),E(J),J=1,NSPADD)
WRITE(6,1C61)(J,IR(J,1),IR(J,2),E(J),J=1,NSPADD)
DO 124 JJ=1,NSPADD
NROW=IR(JJ,1)
NCOL=IR(JJ,2)
A(NROW,NCOL)=A(NROW,NCOL)+E(JJ)
IF(NROW.NE.NCOL) A(NCOL,NROW)=A(NROW,NCOL)
124 CONTINUE
IF(ICBT.EQ.1) GO TO 125
IF(IRITALL.EQ.0) GO TO 125
HMTX(1)=10H FREE-FRE $ HMTX(2)=10HE TORSION
HMTX(3)=10HSTIFFNESS $ HMTX(4)=10HMATRIX
CALL WMTXC(A,K,K,MAX,MAX)
125 CONTINUE
IF(ICBT.NE.1) GO TO 119
WRITE(9)((A(I,J),J=1,K),I=1,K)
C MULTIPLY FREE-FREE STIFFNESS MATRIX BY 2.0 IF ISYM = 1
119 IF(ISYM.EQ.0) GO TO 128
REWIND 8
WRITE(8)((A(I,J),J=1,K),I=1,K)
DO 129 I=1,K
DO 129 J=1,K
129 A(I,J)=2.0*A(I,J)
128 CONTINUE
IF(ICBT.NE.1) GO TO 1292
C FORM FREE-FREE COUPLED BENDING-TORSION STIFFNESS MATRIX
KPNPK=KPN+K $ KPNP1=KPN+1
DO 1293 I=KPNP1,KPNPK
II=I-KPN
DO 1293 J=KPNP1,KPNPK
JJ=J-KPN
1293 AA(I,J)=A(II,JJ)
C WRITE ORDER AND FREE-FREE COUPLED BENDING-TORSION STIFFNESS MATRIX
C (BY ROWS) ONTO TAPE11, 1 RECCRD
WRITE(11)KPNPK,((AA(I,J),J=1,KPNPK),I=1,KPNPK)
GO TO 1294
C WRITE ORDER AND FREE-FREE STIFFNESS MATRIX (BY ROWS) ON
C TAPE 11, 1 RECORD
1292 WRITE(11)K,((A(I,J),J=1,K),I=1,K)
1294 IF(ISYM.EQ.0) GO TO 1291
REWIND 8
READ(8)((A(I,J),J=1,K),I=1,K)
1291 CCNTINUE
DO 13 J=1,K
13 B(J,J)=PI(J)
IF(MASADD.EQ.0) GO TO 126
READ 1060,(IR(J,1),IR(J,2),E(J),J=1,MASADD)
DO 126 J=1,MASADD
NROW=IR(J,1)
NCCL=IR(J,2)
B(NROW,NCOL)=B(NROW,NCOL)+E(J)
IF(NROW.NE.NCOL) B(NCOL,NROW)=B(NROW,NCOL)
126 CONTINUE

```

```

      IF(ICBT.NE.1) GO TO 1259
      WRITE(10)((B(I,J),J=1,K),I=1,K)
C   MULTIPLY FREE-FREE MASS MATRIX BY 2.0 IF ISYM = 1
1259 IF(ISYM.EQ.0) GO TO 1260
      REWIND 8
      WRITE(8)((B(I,J),J=1,K),I=1,K)
      DO 1262 I=1,K
      DO 1262 J=1,K
1262 B(I,J)=2.0*B(I,J)
126C IF(ICBT.NE.1) GO TO 1261
C   FORM FREE-FREE COUPLED BENDING-TORSION MASS MATRIX
      DO 1264 I=KPNP1,KPNPK
      II=I-KPN
      DO 1264 J=KPNP1,KPNPK
      JJ=J-KPN
1264 BB(I,J)=B(II,JJ)
      READ 1020,MASCBT
      READ 1060,(IR(J,1),IR(J,2),E(J),J=1,MASCBT)
      IF(ISYM.EQ.0) GO TO 1265
      DO 1266 J=1,MASCBT
1266 E(J)=2*E(J)
1265 DO 127 J=1,MASCBT
      NROW=IR(J,1)
      NCOL=IR(J,2)
      BB(NROW,NCOL)=BB(NROW,NCOL)+E(J)
127 BB(NCOL,NROW)=BB(NROW,NCOL)
C   WRITE ORDER AND FREE-FREE COUPLED BENDING-TORSION MASS MATRIX
C   (BY ROWS) ONTO TAPE 12, 1 RECORD
      WRITE(12) KPNPK,((BB(I,J),J=1,KPNPK),I=1,KPNPK)
      REWIND 10
      CALL ZEROM(BB,KPNPK,KPNPK,MAXT2,MAXT2)
      READ(10)((BB(I,J),J=1,KPN),I=1,KPN)
      READ(10)((BB(I,J),J=KPNP1,KPNPK),I=KPNP1,KPNPK)
      DO 1267 J=1,MASCBT
      IF(ISYM.EQ.1) E(J)=.5*E(J)
      NROW=IR(J,1)
      NCOL=IR(J,2)
      BB(NROW,NCOL)=BB(NROW,NCOL)+E(J)
1267 BB(NCOL,NROW)=BB(NROW,NCOL)
      GO TO 1268
C   WRITE ORDER AND FREE-FREE MASS MATRIX (BY ROWS) ON TAPE 12, 1 RECORD
1261 WRITE(12)K,((B(I,J),J=1,K),I=1,K)
1268 IF(ISYM.EQ.0) GO TO 1263
      REWIND 8
      READ(8)((B(I,J),J=1,K),I=1,K)
1263 REWIND 3
      IF(IEXPAND.EQ.1.AND.ICBT.NE.1) GO TO 1270
      IF(IEXPAND.EQ.0.AND.ICBT.NE.1) 1275,1276
1275 CALL ZEROM(V,KK,KK,MAXT2,MAXT2)
      DO 1075 I=1,KK
      J=KK+1-I
1075 V(I,J)=1.0
      KPN=KK $ K=KK
      GO TO 2051
C   APPLY BOUNDARY CONDITIONS TO FREE-FREE MASS AND STIFFNESS MATRICES
1276 REWIND 9
      READ(9)((AA(I,J),J=1,KPN),I=1,KPN)
      READ(9)((AA(I,J),J=KPNP1,KPNPK),I=KPNP1,KPNPK)

```

```

IF(IEXPAND.EQ.1) GO TO 1277
CALL ZEROM(V,KKSAV,KKSAV,MAXT2,MAXT2)
DC 1278 I=1,KKSAV
J=KKSAV+1-I
1278 V(I,J)=1.0
KPN=KKSAV $ K=KKSAV
GC TO 2051
1277 IF(IFFPC.EQ.1) GO TO 1269
IBA=1 $ IBC=1
IF(IFFPC.GE.2) IBA=2
IF(IFFPC.EQ.3) IBC=2
REWIND 3
J1=KPN+IBC $ J2=KPN+IBC
WRITE(3) ((AA(I,J),J=IBA,KP),I=IBA,KP),((AA(I,J),J=J1,KPN),
1 I=IBA,KP),((AA(I,J),J=J2,KPNPK),I=IBA,KP),((AA(I,J),
2 J=IBA,KP),I=J1,KPN),((AA(I,J),J=J1,KPN),I=J1,KPN),
3 ((AA(I,J),J=J2,KPNPK),I=J1,KPN),((AA(I,J),J=IBA,KP),
4 I=J2,KPNPK),((AA(I,J),J=J1,KPN),I=J2,KPNPK),
5 ((AA(I,J),J=J2,KPNPK),I=J2,KPNPK)
REWIND 10
WRITE(10)((BB(I,J),J=IBA,KP),I=IBA,KP),((BB(I,J),J=J1,KPN),
1 I=IBA,KP),((BB(I,J),J=J2,KPNPK),I=IBA,KP),((BB(I,J),
2 J=IBA,KP),I=J1,KPN),((BB(I,J),J=J1,KPN),I=J1,KPN),
3 ((BB(I,J),J=J2,KPNPK),I=J1,KPN),((BB(I,J),J=IBA,KP),
4 I=J2,KPNPK),((BB(I,J),J=J1,KPN),I=J2,KPNPK),
5 ((BB(I,J),J=J2,KPNPK),I=J2,KPNPK)
IF(IBA.EQ.2) KP=KP-1
IF(IBC.EQ.2) NP=NP-1
KPN=KP+NP $ KPP1=KP+1
KPNP1=KPN+1 $ KPNPK=KPN+NP
REWIND 3
READ(3)((AA(I,J),J=1,KP),I=1,KP),((AA(I,J),J=KPP1,KPN),I=1,KP),
1 ((AA(I,J),J=KPNP1,KPNPK),I=1,KP),((AA(I,J),J=1,KP),
2 I=KPP1,KPN),((AA(I,J),J=KPP1,KPN),I=KPP1,KPN),
3 ((AA(I,J),J=KPNP1,KPNPK),I=KPP1,KPN),((AA(I,J),J=1,KP),
4 I=KPNP1,KPNPK),((AA(I,J),J=KPP1,KPN),I=KPNP1,KPNPK),
5 ((AA(I,J),J=KPNP1,KPNPK),I=KPNP1,KPNPK)
REWIND 10
READ(10)((BB(I,J),J=1,KP),I=1,KP),((BB(I,J),J=KPP1,KPN),I=1,KP),
1 ((BB(I,J),J=KPNP1,KPNPK),I=1,KP),((BB(I,J),J=1,KP),
2 I=KPP1,KPN),((BB(I,J),J=KPP1,KPN),I=KPP1,KPN),
3 ((BB(I,J),J=KPNP1,KPNPK),I=KPP1,KPN),((BB(I,J),J=1,KP),
4 I=KPNP1,KPNPK),((BB(I,J),J=KPP1,KPN),I=KPNP1,KPNPK),
5 ((BB(I,J),J=KPNP1,KPNPK),I=KPNP1,KPNPK)
C WRITE ORDER AND FINAL MASS AND STIFFNESS MATRICES ONTO TAPE 4
1269 REWIND 4
WRITE(4)KPNPK,((BB(I,J),J=1,KPNPK),I=1,KPNPK),((AA(I,J),
1 J=1,KPNPK),I=1,KPNPK)
CALL ALLEIG(AA,BB,KPN,MAXT2,MAX,MAX2,K,N,C,PIVOT,INDEX,P,
1 CINVBT,BCINVBT,EM,EIGV,V,EV,R,KPR,ICBT)
GC TC(205,206,206) IFFPC
C ADD RIGID BODY TRANSLATION MODE TO MODAL MATRIX
206 N=KPN/3
K=K+1
DO 207 I=1,N
207 V(I,K)=1.0
NT2=2*N $ J=N
CC 208 I=1,NT2
J=J+1
208 V(J,K)=0.0

```

```

      IF(IFFPC.EQ.2) GO TO 205
C   ADD RIGID BODY ROTATIONAL MODE TO MODAL MATRIX
      K=K+1 $ J=N $ JJ=NT2
      DO 209 I=1,N
        J=J+1 $ JJ=JJ+1
        V(I,K)=X(I)
        V(J,K)=1.0
209  V(JJ,K)=0.0
C   ADD RIGID BODY TORSION MODE TO MODAL MATRIX
      K=K+1
      DO 210 I=1,NT2
210  V(I,K)=0.0
        J=NT2
        DO 211 I=1,N
          J=J+1
211  V(J,K)=1.0
205  CONTINUE
      GO TO 2051
CUTOUT      1184
127C IBA=1
      IF(IFFPC.EQ.3) IBA=2
      WRITE(3)((A(I,J),J=IBA,K),I=IBA,K),((B(I,J),J=IBA,K),I=IBA,K)
      IF(IFFPC.EQ.3) K=K-1
      HMTX(1)=10H K AFTER $ HMTX(2)=10HAPPLICATIO
      HMTX(3)=10HN OF BDRY. $ HMTX(4)=10HCOND.
      WRITE(6,1200)HMTX,K
1200  FORMAT(////12A10//5X,*K = *,I3)
      REWIND 3
      KPN=K
      READ(3)((A(I,J),J=1,K),I=1,K),((B(I,J),J=1,K),I=1,K)
      HMTX(1)=10H FINAL ST $ HMTX(2)=10HIFNESS MA
      HMTX(3)=10HTP IX $ HMTX(4)=10H
      CALL WMTXC(A,K,K,MAX,MAX)
      HMTX(1)=10H FINAL MA $ HMTX(2)=10HSS MATRIX
      HMTX(3)=10H $ HMTX(4)=10H
      CALL WMTXC(B,K,K,MAX,MAX)
      REWIND 4
C   WRITE ORDER AND FINAL MASS AND STIFFNESS MATRICES ON TAPE 4, 1 RECORD
      WRITE(4)KPN,((B(I,J),J=1,KPN),I=1,KPN),((A(I,J),J=1,KPN),I=1,KPN)
C   CALL EIGENVALUE SUBROUTINE
      CALL ALLEIG(AA,BB,KPN,MAXT2,MAX,MAX2,K,N,C,IPIVOT,INDEX,P,
1      C INVB,BCINVB,EM,EIGV,V,EV,R,KPR,ICBT)
      GO TO(204,204,202)IFFPC
C   ACC RIGID BODY TORSION OR AXIAL MODE TO MODAL MATRIX
202  K=K+1
      DO 203 I=1,K
203  V(I,K)=1.0
204  CCNTINUE
C   WRITE ORDER AND MODES (BY COLUMNS) ON TAPE 20, 2 REGRDS
2051  WRITE(20) KPN,K
      WRITE(20)((V(I,J),I=1,KPN),J=1,K)
      IF(NBLJCK.EQ.NBLKS.AND.NBLKS.EQ.1) GO TO 1
      GO TO 200

```

```

*****
* SPRING OR RIGID BODY ELEMENT *
*****

130 CALL ZEROM(A, KK, KK, MAX, MAX)
CALL ZEROM(B, KK, KK, MAX, MAX)
IF(MK.EQ.0) GO TO 131
PRINT 1301
WRITE(6,1301)
1301 FORMAT(1H //1X,* SPRING ELEMENT - STIFFNESS MATRIX WILL BE READ
FROM CARDS. MASS MATRIX IS NULL.*)
READ 1040,((A(I,J),J=1, KK),I=1, KK)
C MULTIPLY FREE-FREE STIFFNESS MATRIX BY 2.0 IF ISYM = 1
IF(ISYM.EQ.0) GO TO 131
REWIND 8
WRITE(8)((A(I,J),J=1, KK),I=1, KK)
DO 135 I=1, KK
DO 135 J=1, KK
135 A(I,J)=2.0*A(I,J)
131 WRITE(11)KK,((A(I,J),J=1, KK),I=1, KK)
IF(MM.EQ.^) GO TO 132
PRINT 1302
WRITE(6,1302)
1302 FORMAT(1H //1X,* RIGID BODY ELEMENT - MASS MATRIX WILL BE READ F
FROM CARDS. STIFFNESS MATRIX IS NULL.*)
READ 1040,((B(I,J),J=1, KK),I=1, KK)
C MULTIPLY FREE-FREE MASS MATRIX BY 2.0 IF ISYM = 1
IF(ISYM.EQ.0) GO TO 132
REWIND 9
WRITE(9)((B(I,J),J=1, KK),I=1, KK)
DO 136 I=1, KK
DO 136 J=1, KK
136 B(I,J)=2.0*B(I,J)
132 WRITE(12)KK,((B(I,J),J=1, KK),I=1, KK)
IF(MK.NE.0.OR.MM.NE.0) GO TO 133
PRINT 1303
WRITE(6,1303)
1303 FORMAT(1H //1X,* MASS AND STIFFNESS MATRICES ARE BOTH NULL *)
133 CONTINUE
HMTX(1)=10H FINAL ST $ HMTX(2)=10HSTIFFNESS MA
HMTX(3)=10HTPIX $ HMTX(4)=10H
CALL WMTXC(A, KK, KK, MAX, MAX)
HMTX(1)=10H FINAL MA $ HMTX(2)=10HSS MATRIX
HMTX(3)=10H $ HMTX(4)=10H
CALL WMTXC(B, KK, KK, MAX, MAX)
CALL ZEROM(V, KK, KK, MAX2, MAX2)
DO 134 I=1, KK
J=KK+1-I
134 V(I,J)=1.0
HMTX(1)=10H FINAL MO $ HMTX(2)=10HVAL MATRIX
HMTX(3)=10H $ HMTX(4)=10H
CALL WMTXC(V, KK, KK, MAX2, MAX2)
WRITE(20) KK, KK
WRITE(20)((V(I,J),I=1, KK),J=1, KK)
IF(NBLOCK.EQ.NBLKS.AND.NBLKS.EQ.1) GO TO 1
200 CONTINUE
8998 WRITE(6,8997)
PRINT 8997
END

```

```

SUBROUTINE ALLEIG(AA,BB,KPN,MAX2,MAX,MAX2,K,N,C,IPIVOT,INDEX,P,
1          CINVBT,BCINVBT,EM,EIGV,V,EV,R,KPR,ICBT)
DIMENSION AA(MAX2,MAX2),BB(MAX2,MAX2),C(MAX,MAX),IPIVOT(MAX),
1          INDEX(MAX,MAX2),P(MAX),CINVBT(MAX,MAX),BCINVBT(MAX,MAX),
2          EM(MAX2),EIGV(MAX2),V(MAX2,MAX2),EV(MAX2),R(MAX2)
COMMON/SAFE/HMTX(12),FCOIN,KASE,IFFPC,IRITALL
REWIND 4
C READ ORDER AND MASS AND STIFFNESS MATRICES FROM TAPE 4 BY ROWS
READ(4) KPN,((BB(I,J),J=1,KPN),I=1,KPN),((AA(I,J),J=1,KPN),
1          I=1,KPN)
GO TO (210,220,230,220,230),KASE
C SOLVE FOR EIGENVALUES AND EIGENVECTORS OF MASS MATRIX
230 CALL JACTV(KPN,MAX2,1,BB,EM,V,DUM1,DUM2,DUM3,DUM4,IERR)
IF(IERR.EQ.1) GO TO 1500
C TEST FOR NUMBER OF FINITE EIGENVALUES
DO 10 J=2,KPN
IJ=J-1
IF(EM(J).LE.0.0) GO TO 11
IF(EM(IJ)/EM(J).GE.1000000.0) GO TO 11
IF(J.EQ.KPN) IJ=KPN
10 CONTINUE
11 NFMEV=IJ
C REWIND TAPE 4 AND WRITE COLUMNS OF MASS VECTOR MATRIX ON TAPE 4
C REWIND TAPE 9 AND WRITE ROWS OF MASS VECTOR MATRIX ON TAPE 9
231 REWIND 4
REWIND 9
DO 20 J=1,KPN
WRITE(9)(V(J,I),I=1,KPN)
20 WRITE(4)(V(I,J),I=1,KPN)
C POST-MULTIPLY STIFFNESS MATRIX BY MASS VECTOR MATRIX AND STORE IN V
REWIND 4
DO 30 J=1,KPN
C READ COLUMN OF MASS VECTOR MATRIX
READ(4)(R(I),I=1,KPN)
DO 30 I=1,KPN
V(I,J)=0.0
DO 30 IJ=1,KPN
30 V(I,J)=V(I,J)+AA(I,IJ)*R(IJ)
C COMPUTE V TRANSPOSE * (AA * V)
REWIND 4
DO 40 I=1,KPN
C READ COLUMNS OF MASS VECTOR MATRIX AS ROWS OF VECTOR TRANSPOSE
READ(4)(R(J),J=1,KPN)
DO 40 J=1,KPN
AA(I,J)=0.0
DO 40 IJ=1,KPN
40 AA(I,J)=AA(I,J)+R(IJ)*V(IJ,J)
K=NFMEV
N=KPN-NFMEV
C IF THE NUMBER OF FINITE MASS EIGENVALUES (NFMEV) IS EQUAL TO THE
C ORDER OF THE MASS MATRIX BB, BYPASS PARTITIONING OF THE STIFFNESS
C MATRIX AA
IF(N.EQ.0) GO TO 220
210 KPI=K+1
C          STIFFNESS MATRIX AA WILL BE PARTITIONED AS FOLLOWS ----(A  B)
C                                     (BT C)
C          WHERE A=(K*K), B=(K*N), BT(N*K), C(N*N)
REWIND 4

```



```

C STORE MATRIX A ON TAPE 4 BY COLUMNS, 1 RECORD
  WRITE(4)((AA(I,J),I=1,K),J=1,K)
  REWIND 8
C STORE MATRIX C ON TAPE 8 BY COLUMNS, 1 RECORD
  WRITE(8)((AA(I,J),I=KPI,KPN),J=KPI,KPN)
C STORE MATRIX B ON TAPE 8 BY ROWS, K RECORDS
  DO 50 I=1,K
  50 WRITE(8){AA(I,J),J=KPI,KPN)
C READ MATRIX C FROM TAPE 8 AND COMPUTE INVERSE OF C
  REWIND 8
  READ(8)((C(I,J),I=1,N),J=1,N)
  CALL MATINV(C,N,BI,0,DET,IPIVOT,INDEX,MAX,ISCALE)
C COMPUTE C INVERSE * B TRANSPOSE
  DO 60 J=1,K
C READ ROW OF B AS COLUMN OF B TRANSPOSE
  READ(8){P(I),I=1,N)
  DO 60 I=1,N
  CINVBT(I,J)=0.0
  DO 60 IJ=1,N
  60 CINVBT(I,J)=CINVBT(I,J)+C(I,IJ)*P(IJ)
  REWIND 8
C THE NEXT STATEMENT IS A DUMMY READ TO POSITION TAPE 8
  READ(8)
C COMPUTE B * (C INVERSE * B TRANSPOSE)
  DO 70 I=1,K
C READ ROW OF B
  READ(8){P(J),J=1,N)
  DO 70 J=1,K
  BCINVBT(I,J)=0.0
  DO 70 IJ=1,N
  70 BCINVBT(I,J)=BCINVBT(I,J)+P(IJ)*CINVBT(IJ,J)
  REWIND 8
C STORE C INVERSE * B TRANSPOSE ON TAPE 8 BY COLUMNS, 1 RECORD
  WRITE(8)((CINVBT(I,J),I=1,N),J=1,K)
  REWIND 4
C READ MATRIX A FROM TAPE 4
  READ(4)((AA(I,J),I=1,K),J=1,K)
C COMPUTE A - (B * CINV * BT)
  IF(KASE.NE.1) GO TO 220
  DO 212 I=1,K
  212 EM(I)=BB(I,I)
  220 IK=K
  IF(KASE.EQ.2.OR.KASE.EQ.4) K=KPN
  IF(KASE.EQ.2.OR.KASE.EQ.4) N=0
  IF(KASE.EQ.2.OR.KASE.EQ.4) 222,225
  222 DO 223 I=1,K
  223 EM(I)=BB(I,I)
  225 DO 81 I=1,K
  EM(I)=1.0/SQRT(EM(I))
  IF(N.EQ.0) GO TO 81
  DO 80 J=1,K
  80 AA(I,J)=AA(I,J)-BCINVBT(I,J)
  81 CONTINUE
C PRE- AND POST-MULTIPLY STIFFNESS MATRIX BY 1.0/SQRT(MASS)
  DO 90 I=1,K
  DO 90 J=1,K
  90 AA(I,J)=EM(I)*AA(I,J)
  DO 100 J=1,K
  DO 100 I=1,K
  100 AA(I,J)=AA(I,J)*EM(J)

```

```

      CALL JACTV(K,MAXT2,1,AA,EIGV,V,DUM1,DUM2,DUM3,DUM4,NERR)
      IF(NERR.NE.0) GO TO 1500
      CALL FREQ(EIGV,AA,K,MAXT2)
C   PRE-MULTIPLY VECTOR MATRIX BY 1.0/SQRT(MASS)
      DO 110 I=1,K
      CC 110 J=1,K
      110 V(I,J)=EM(I)*V(I,J)
      REWIND 4
C   STORE X SUB 1 VECTORS ON TAPE 4 BY COLUMNS, K RECORDS
      DO 115 J=1,K
      115 WRITE(4)(V(I,J),I=1,K)
      IF(N.EQ.0) GO TO 144
      REWIND 8
C   READ C INVERSE * B TRANSPOSE FROM TAPE 8
      READ(8)((AA(I,J),I=1,N),J=1,K)
      REWIND 4
C   MULTIPLY (C INVERSE * B TRANSPOSE) BY X SUB 1 VECTOR MATRIX
      DO 120 J=1,K
C   READ COLUMN OF X SUB 1 MATRIX FROM TAPE 4
      READ(4)(P(I),I=1,K)
      DO 120 I=1,N
      V(I,J)=0.0
      DO 120 IJ=1,K
      120 V(I,J)=V(I,J)+AA(I,IJ)*P(IJ)
C   X SUB 2 VECTOR MATRIX = - VECTOR MATRIX JUST COMPUTED
      DO 125 I=1,N
      DO 125 J=1,K
      125 V(I,J)=-V(I,J)
C   STORE X SUB 2 VECTOR MATRIX ON TAPE 4 BY ROWS, 1 RECCRD
      WRITE(4)((V(I,J),J=1,K),I=1,N)
C   REWIND TAPE 4, THEN READ X SUB 1 VECTORS INTO FIRST K ROWS OF AA AND
C   READ X SUB 2 VECTORS INTO (K+1) TO KPN ROWS OF AA
C   THE AA MATRIX IS NOW (KPN * K)
      144 REWIND 4
      DO 145 J=1,K
      145 READ(4)(AA(I,J),I=1,K)
      IF(N.NE.0) READ(4)((AA(I,J),J=1,K),I=K+1,KPN)
      IF(KASE.LE.2.OR.KASE.EQ.4) GO TO 150
C   PCST-MULTIPLY MASS VECTOR MATRIX BY AA MATRIX
      REWIND 9
      CC 146 I=1,KPN
C   READ ROW OF MASS VECTOR MATRIX
      READ(9)(R(J),J=1,KPN)
      DO 146 J=1,K
      V(I,J)=0.0
      DO 146 IJ=1,KPN
      146 V(I,J)=V(I,J)+R(IJ)*AA(IJ,J)
      150 CCNTINUE
      IF(KASE.LE.2.OR.KASE.EQ.4) 151,160
      151 DO 155 I=1,KPN
      DO 155 J=1,K
      155 V(I,J)=AA(I,J)
      160 CCNTINUE
      IF(N.EQ.0.AND.KASE.EQ.3) KASE=2
      IF(IFFPC.EQ.1) GO TO 170
      GO TO (161,162,161,163,163),KASE
      161 KPR=KPN
      KPN=K
      GO TO 169

```

```

162 K=IK
    KPR=KPN
    GO TO 169
163 IF(IFFPC.EQ.2) GO TO 170
    IFFPC=2
    KPR=KPN
169 CALL ADDBACK(V,E,IGV,K,KPN,KPR,MAXT2,ICBT)
    IF(KASE.EQ.4.OR.KASE.EQ.5) IFFPC=3
    K=KPN
    KPN=KPR
170 HMTX(1)=IOH FINAL MO $ HMTX(2)=IOHDAL MATRIX
    HMTX(3)=IOH $ HMTX(4)=IOH
    CALL WMTXC(V,KPN,K,MAXT2,MAXT2)
150C IF(IERR.EQ.1) WRITE(6,1501)
    IF(NERR.NE.0) WRITE(6,1502)
1501 FORMAT(/** ERROR RETURN FROM JACTV - FIRST CALL - MASS *)
1502 FORMAT(/** ERROR RETURN FROM JACTV - SECOND CALL - STIFFNESS *)
    RETURN
    END

SUBROUTINE ADCBACK(V,E,K,KPN,KPR,MAXT2,ICBT)
DIMENSION V(MAXT2,MAXT2),E(MAXT2)
COMMON/SAME/HMTX(12),FCGN,KASE,IFFPC,IRITALL
CALL ZEROM(E,KPN,1,MAXT2,1)
REWIND 4
IF(IFFPC.EQ.3) GO TO 9
WRITE(4)(E(J),J=1,KPN),((V(I,J),J=1,KPN),I=1,KPR)
KPR=KPR+1
GO TO 20
9 IF(ICBT.NE.1) GO TO 10
KLM=KPN/3 $ KLMP1=KLM+1
KLMT2=2*KLM $ KLMT2P1=KLMT2+1
WRITE(4)(E(J),J=1,KPN),((V(I,J),J=1,KPN),I=1,KLM),(E(J),J=1,KPN),
1 ((V(I,J),J=1,KPN),I=KLMP1,KLMT2),(E(J),J=1,KPN),
2 ((V(I,J),J=1,KPN),I=KLMT2P1,KPN)
KPR=KPR+3
GO TO 20
10 KP1=K+1
WRITE(4)(E(J),J=1,KPN),((V(I,J),J=1,KPN),I=1,K),
1 (E(J),J=1,KPN),((V(I,J),J=1,KPN),I=KP1,KPR)
KPR=KPR+2
20 REWIND 4
READ(4)((V(I,J),J=1,KPN),I=1,KPR)
RETURN
END

SUBROUTINE ZEROM(A,M,L,MMAX,LMAX)
DIMENSION A(MMAX,LMAX)
DO 10 I=1,M
DO 10 J=1,L
10 A(I,J)=0.0
RETURN
END

```

```

SUBROUTINE WMTXC(A,NR,NC,MAXR,MAXC)
C NR=ROWS OF A, NC=COLS OF A, MAXR=MAX ROWS OF A, MAXC=MAX COLS OF A
  DIMENSION A(MAXR,MAXC)
  COMMON/SAME/HMTX(12),FCON,KASE,IFFPC,IRITALL
  KE=0
  KSET=NC/8
  KLEFT=MOD(NC,8)
  IF(KLEFT.NE.0) KSET=KSET+1
  DO 10 KT=1,KSET
  KB=KE+1
  KE=KE+8
  IF(KT.EQ.KSET) KE=NC
  WRITE(6,5001) HMTX,(J,J=KB,KE)
  DO 10 I=1,NR
10 WRITE(6,5002) I,(A(I,J),J=KB,KE)
5001 FORMAT(1H1//12A10///10H ROW COL,I4,7(11X14))
5002 FORMAT(14,8E15.7)
  RETURN
  END

SUBROUTINE FREQ(E,A,K,MAX)
DIMENSION E(MAX),A(MAX,MAX)
COMMON/SAME/HMTX(12),FCON,KASE,IFFPC,IRITALL
DO 10 I=1,K
  A(I,1)=E(I)
  A(I,2)=FCON*E(I)
  A(I,3)=SQRT(ABS(A(I,2)))
10 A(I,4)=A(I,3)/6.28318530717959
  PRINT 5014,(HMTX(J),J=5,12),FCON,(I,(A(I,J),J=1,4),I=1,K)
  WRITE(6,5014)(HMTX(J),J=5,12),FCON,(I,(A(I,J),J=1,4),I=1,K)
5014 FORMAT(1H1//1X8A10//7H FCON =,E22.14//4X1HJ9X9HLAMBDA(J)14X12HOMEG
1A SQ (J)14X8HOMEGA(J)14X13HFREQ.(J), CPS/34X18H(FCCN * LAMBDA(J))1
22X6H(REAL)//(15,4E24.14))
  RETURN
  END

```



```

PROGRAM MODALC(INPUT,OUTPUT,TAPE20,TAPE2,TAPE3,TAPE4,TAPE6,
1 TAPE11,TAPE12,TAPE8,TAPE9)

```

```

*****
*
* PROGRAM MODALC FORMULATES THE EIGENVALUE PROBLEM FOR
* THE DETERMINATION OF THE COUPLED MODES AND FREQUENCIES
* OF THE COMPLETE (ASSEMBLED) STRUCTURE.
*
*****

```

```

DIMENSION A(26,26),U(68,68),C(10,68),D(10,68),DTD(68,68),
1 EIGV(68),BB(68,68),BETA(68,68),BK(68,68),BM(68,68),
2 R(68)
EQUIVALENCE (BK(1,1),BM(1,1),U(1,1),C(1,1),DTD(1,1),BETA(1,1)),
1 (D(1,1),BB(1,1),A(1,1)),(EIGV(1),R(1))
INTEGER BMS(10),DOF(10),SM(40),ISTATIC(4)
COMMON HMTX(12)

```

```

C LD SPECIFIES THE SOURCE OF THE MODAL DATA FOR THE SUBSYSTEMS
C LD=1 - MODAL DATA ON MAGNETIC TAPE AND COPIED ONTC TAPE20
C VIA CONTROL CARDS
C LD=2 - MODAL DATA READ FROM CARDS
C LD=3 - MODAL DATA GENERATED IN PROGRAM BRANCHB

C NB - NUMBER OF SUBSYSTEMS INTO WHICH STRUCTURE IS PARTITIONED

C NMS - TCTAL NUMBER OF SUBSYSTEM MODE SETS

C NCEQS - NUMBER OF CONSTRAINT EQUATIONS

C BMS(I) - NUMBER OF MASS STATIONS ON EACH BEAM SUBSYSTEM

C DOF(I) - DEGREEES OF FREEDOM IN EACH MODE SET

C SM(I) - NUMBER OF CALCULATED MODES SELECTED FROM EACH MODE SET

C ISTATIC(I) - NUMBER OF ADDITIONAL DEFLECTION SHAPES (SUCH AS
C MEASURED MODES, STATIC DEFLECTION SHAPES, OR ASSUMED
C DEFLECTION SHAPES) TO BE ADDED TO THE CALCULATED
C MODES SELECTED FROM EACH SUBSYSTEM MODE SET

C NMC - TCTAL NUMBER OF DEGREES OF FREEDOM FOR UNCOUPLED SYSTEM

C NMT - TCTAL NUMBER OF MODES SELECTED FOR SYNTHESIS

C CN ENTRY TO THIS PROGRAM ---
C TAPE 11 HAS ORDER AND FREE-FREE STIFFNESS MATRIX FOR
C EACH SUBSYSTEM
C TAPE 12 HAS ORDER AND FREE-FREE MASS MATRIX FOR EACH SUBSYSTEM
C TAPE 20 HAS OPDER AND MODES FOR EACH SUBSYSTEM

```

```

      READ 141, (HMTX(I), I=5, 12)
141  FCRMAT(8A10)
      READ 1C, LD, NB, NMS, NCEQS
10  FCRMAT(20I4)
      READ 10, (BMS(I), I=1, NB)
      READ 10, (DOF(I), I=1, NMS)
      READ 10, (SM(I), I=1, NMS)
      READ 10, (ISTATIC(I), I=1, NMS)
      PRINT 11, LD, NB, NMS, NCEQS
      WRITE(6, 11) LD, NB, NMS, NCEQS
11  FORMAT(1H1/* LD=*, I3, 10X, *NB=*, I3, 10X, *NMS=*, I3, 10X, *NCEQS=*, I3)
      PRINT 12, (I, BMS(I), DOF(I), SM(I), ISTATIC(I), I=1, NB)
      WRITE(6, 12) (I, BMS(I), DOF(I), SM(I), ISTATIC(I), I=1, NB)
12  FORMAT(1H0//4X, 1HJ, 9X, 6HBMS(J), 9X, 6HDOF(J), 9X, 5HSM(J), 9X,
1    10HISTATIC(J)//(I5, 9X, I3, 12X, I3, 12X, I3, 13X, I3))
      IF (NB.EQ.NMS) GO TO 9
      IM=NB+1
      PRINT 13, (I, DOF(I), SM(I), ISTATIC(I), I=IM, NMS)
      WRITE(6, 13) (I, DOF(I), SM(I), ISTATIC(I), I=IM, NMS)
13  FORMAT((I5, 24X, I3, 12X, I3, 13X, I3))
9   CONTINUE
      IF (LD.EQ.1.OR.LD.EQ.3) GO TO 5000
      REWIND 20

C   FOR EACH SUBSYSTEM MODAL SET ---
C   READ ORDER OF MODAL MATRIX
C   READ MODES (BY COLUMNS) FROM HIGHEST TO LOWEST
C   WRITE ON TAPE 20

      DO 5050 IK=1, NMS
      READ 15, K, N
15  FCRMAT(2I4)
      READ 16, ((A(I, J), I=1, K), J=1, N)
16  FCRMAT(4E16.8)
      WRITE(20) K, N
5050 WRITE(20) ((A(I, J), I=1, K), J=1, N)
5000 CCNTINUE
      REWIND 20
      NMC=0
      DO 30 I=1, NMS
30  NMC=NMC+DOF(I)
      PRINT 31, NMC
      WRITE(6, 31) NMC
31  FORMAT(// * TOTAL NUMBER OF DEGREES OF FREEDOM = *, I3)
      NMT=0
      DO 40 I=1, NMS
40  NMT=NMT+SM(I)+ISTATIC(I)
      PRINT 41, NMT
      WRITE(6, 41) NMT
41  FORMAT(// * TOTAL NUMBER OF MODES EMPLOYED = *, I3)

C   FORM THE MODAL EXPANSION MATRIX FROM THE SELECTED MODES

      NPF=0 $ NCF=0 $ KK=0 $ ID=0
      NCB=1 $ NRB=1
      DO 100 IJ=1, NMS
      READ(20) K, N
      READ(20) ((A(I, J), I=1, K), J=1, N)
      IF (ISTATIC(IJ).EQ.0) GO TO 42

```

```

      IST=ISTATIC(IJ)
      DO 43 J=1,IST
43  REAU 17,(A(I,J+N),I=1,K)
      17 FUKMAT(5E14.8)
      N=N+ISTATIC(IJ)
42  NRF=NRF+K
      ID=ID+1
      NCF=NCF+SM(IJ)+ISTATIC(IJ)
      M=0
      IF(IC.EQ.1) GO TO 11)
      M=KK
110  JJ=N+NCB
      DO 120 I=NRB,NRF
      DO 120 J=1,NMT
120  U(I,J)=0.0
      DO 130 I=NRB,NRF
      DO 130 J=NCB,NCF
130  U(I,J)=A(I-M,JJ-J)
      NCB=NCB+SM(IJ)+ISTATIC(IJ)
      NRB=NRB+K
      KK=KK+K
100  CCNTINUE
      HMTX(1)=10H MODAL EX $ HMTX(2)=10HPANSION MA
      HMTX(3)=10HTFIX U $ HMTX(4)=10H
      CALL WMTXC(U,NMC,NMT,NMC,NMC)
C   WRITE ORDER U ON TAPE 2, ONE RECORD
C   WRITE U MATRIX ON TAPE 2 BY ROWS, NMC RECORDS
      REWIND 2
      WRITE(2)NMC,NMT
      DO 150 I=1,NMC
150  WRITE(2)(U(I,J),J=1,NMT)
      REWIND 2
C   WRITE U MATRIX ON TAPE 8 BY COLUMNS, NMT RECORDS
      REWIND 8
      DO 151 J=1,NMT
151  WRITE(8) (U(I,J),I=1,NMC)
      CALL CONEQS(C,NCEQS,NMC)
C   MATRIX OF CONSTRAINT EQUATIONS IN PHYSICAL COORDINATES IS
C   TRANSFORMED TO ONE IN MODAL COORDINATES VIA THE MATRIX
C   OPERATION C * U = D.
      REWIND 8
      DO 152 J=1,NMT
      READ(8) (R(I),I=1,NMC)
      DO 152 I=1,NCEQS
      D(I,J)=0.0
      DO 152 IJ=1,NMC
152  D(I,J)=D(I,J)+C(I,IJ)*R(IJ)
C   WRITE D MATRIX ON TAPE 9 BY COLUMNS, NMT RECORDS
      REWIND 9
      DO 153 J=1,NMT
153  WRITE(9) (D(I,J),I=1,NCEQS)
      REWIND 9
C   READ COLUMNS OF D AS ROWS OF D TRANSPOSE
      DO 154 I=1,NMT
154  READ(9) (BB(I,J),J=1,NCEQS)
C   EVALUATE MATRIX PRODUCT D TRANSPOSE * D
      REWIND 9
      DO 155 J=1,NMT

```



```

      READ(9) (R(I),I=1,NCEQS)
      DO 155 I=1,NMT
        DTD(I,J)=0.0
        DO 155 IJ=1,NCEQS
          155 DTD(I,J)=DTD(I,J)+BB(I,IJ)*R(IJ)
C SOLVE FOR EIGENVALUES AND EIGENVECTORS OF DTD
      CALL JACTV(NMT,NMC,1,DTD,EIGV,BB,DUM1,DUM2,DUM3,DUM4,NERR)
      IF(NERR.EQ.1) GO TO 2200

C TEST FOR NUMBER OF FINITE(POSITIVE) EIGENVALUES OF DTD. MODAL
C COLUMNS OF DTD CORRESPONDING TO THE ZERO EIGENVALUES ARE THEN TAKEN
C TO BE THE COLUMNS OF THE BETA MATRIX

      MFEV=NMT
      DO 75 J=2,NMT
        IJ=J-1
        IF(EIGV(J).LE.0.0) GO TO 76
        IF((EIGV(IJ)/EIGV(J)).GE.1000000.0) GO TO 76
      75 CONTINUE
      76 IF(NFEV.NE.IJ) NFEV=IJ
        PRINT 14,NFEV
      14 FORMAT(/ * NUMBER OF FINITE EIGENVALUES OF DTD = *,I3//)
C WRITE EIGENVALUES OF D TRANSPOSE * D ON TAPE 6
      WRITE(6,1111)(EIGV(I),I=1,NMT)
      1111 FORMAT(/ * EIGENVALUES OF DTD * // (2X,E15.8) )
      WRITE(6,14) NFEV
      NCBETA=NMT-NFEV
      DO 80 I=1,NMT
        DO 80 J=1,NCBETA
          80 BETA(I,J)=BB(I,NFEV+J)
C WRITE BETA MATRIX ON TAPE 9 BY COLUMNS, NCBETA RECORDS
      REWIND 9
      DO 81 J=1,NCBETA
        81 WRITE(9) (BETA(I,J),I=1,NMT)
      NRBETA=NMT
C WRITE ORDER BETA ON TAPE 3, ONE RECORD
C WRITE BETA ON TAPE 3 BY ROWS, NRBETA RECORDS
      REWIND 3
      WRITE(3)NRBETA,NCBETA
      DO 66 I=1,NRBETA
        66 WRITE(3) (BETA(I,J),J=1,NCBETA)
C READ MATRIX U FROM TAPE 8
      REWIND 8
      DO 82 J=1,NMT
        82 READ(8) (U(I,J),I=1,NMC)
      REWIND 9
      DO 83 J=1,NCBETA
        READ(9) (R(I),I=1,NMT)
        DO 83 I=1,NMC
          BB(I,J)=0.0
          DO 83 IJ=1,NRBETA
            83 BB(I,J)=BB(I,J)+U(I,IJ)*R(IJ)
C WRITE U*BETA ON TAPE 8 BY COLUMNS
      REWIND 8
      DO 84 J=1,NCBETA
        84 WRITE(8) (BB(I,J),I=1,NMC)
C FORM MASS MATRIX OF UNCOUPLED SYSTEM
      REWIND 12
      NRB=1 $ NRF=0 $ KK=0 $ ID=0
      NCB1=1 $ NCF1=0

```

```

DC 200 IJ=1,NMS
READ(12) KPN, ((A(I,J), J=1,KPN), I=1,KPN)
NRF=NRF+KPN
ID=ID+1
NCF1=NCF1+DOF(IJ)
M=0
IF(IC.NE.1) M=KK
DO 220 I=NRB,NRF
DO 220 J=1,NMC
220 BM(I,J)=0.0
DO 231 I=NRB,NFF
DO 231 J=NCB1,NCF1
231 BM(I,J)=A(I-M,J-M)
NCB1=NCB1+DOF(IJ)
NRF=NRB+KPN
KK=KK+KPN
2CC CONTINUE
HMTX(1)=10H UNCOUPLE $ HMTX(2)=10HD SYSTEM M
HMTX(3)=10HASS MATRIX $ HMTX(4)=10H
CALL WMTXC(BM,NMC,NMC,NMC,NMC)
C GENERATE MASS MATRIX FOR COUPLED SYSTEM
C FORM MATRIX PRODUCT M*(U*BETA)
REWIND 8
DO 85 J=1,NCBETA
READ(8) (R(I),I=1,NMC)
DO 85 I=1,NMC
BB(I,J)=0.0
DO 85 IJ=1,NMC
85 BB(I,J)=BB(I,J)+BM(I,IJ)*R(IJ)
C WRITE PRODUCT ON TAPE 9 BY COLUMNS
REWIND 9
DO 86 J=1,NCBETA
86 WRITE(9) (BB(I,J),I=1,NMC)
C READ COLUMNS OF U*BETA AS ROWS OF TRANSPOSE
REWIND 8
DO 87 I=1,NCBETA
87 READ(8) (BB(I,J),J=1,NMC)
C FORM MATRIX PRODUCT BETA TRANSPOSE * U TRANSPOSE * (M * U * BETA)
REWIND 9
DO 88 J=1,NCBETA
READ(9) (R(I),I=1,NMC)
DO 88 I=1,NCBETA
BM(I,J)=0.0
DO 88 IJ=1,NMC
88 BM(I,J)=BM(I,J)+BB(I,IJ)*R(IJ)
C WRITE COUPLED MASS MATRIX ON TAPE 4 BY COLUMNS, ONE RECORD
REWIND 4
WRITE(4) ((BM(I,J),I=1,NCBETA),J=1,NCBETA)
C FORM STIFFNESS MATRIX OF UNCOUPLED SYSTEM
REWIND 11
NRF=1 $ NRF=0 $ KK=0 $ ID=0
NCB1=1 $ NCF1=0
DO 300 IJ=1,NMS
READ(11) KPN, ((A(I,J), J=1,KPN), I=1,KPN)
NRF=NRF+KPN
ID=ID+1
NCF1=NCF1+DOF(IJ)
M=0
IF(ID.NE.1) M=KK

```

```

DO 320 I=NRB,NRF
DO 320 J=1,NMC
320 BK(I,J)=0.0
DO 331 I=NRB,NRF
DO 331 J=NCB1,NCF1
331 BK(I,J)=A(I-M,J-M)
NCB=NCB+SM(IJ)
NCB1=NCB1+DOF(IJ)
NRB=NRB+KPN
KK=KK+KPN
300 CONTINUE
HMTX(1)=10H UNCOUPLE $ HMTX(2)=10HD SYSTEM S
HMTX(3)=10HTIFFNESS M $ HMTX(4)=10HATRIX
CALL WMTXC(BK,NMC,NMC,NMC,NMC)
C GENERATE STIFFNESS MATRIX FOR COUPLED SYSTEM
C FORM MATRIX PRODUCT K*(U*BETA)
REWIND 8
DO 95 J=1,NCBETA
FEAD(8) (P(I),I=1,NMC)
DO 95 I=1,NMC
BB(I,J)=0.0
DO 95 IJ=1,NMC
95 BB(I,J)=BB(I,J)+BK(I,IJ)*R(IJ)
C WRITE PRODUCT ON TAPE 9 BY COLUMNS
REWIND 9
DO 96 J=1,NCBETA
96 WRITE(9) (BB(I,J),I=1,NMC)
C READ COLUMNS OF U*BETA AS ROWS OF TRANSPOSE
REWIND 8
DO 97 I=1,NCBETA
97 READ(8) (BB(I,J),J=1,NMC)
C FORM MATRIX PRODUCT BETA TRANSPOSE * U TRANSPOSE * (K * U * BETA)
REWIND 9
DO 98 J=1,NCBETA
READ(9) (R(I),I=1,NMC)
DO 98 I=1,NCBETA
BK(I,J)=0.0
DO 98 IJ=1,NMC
98 BK(I,J)=BK(I,J)+BB(I,IJ)*R(IJ)
C WRITE COUPLED STIFFNESS MATRIX ON TAPE 4 BY COLUMNS, ONE RECORD
WRITE(4) ((BK(I,J),I=1,NCBETA),J=1,NCBETA)
REWIND 3
REWIND 4
IF(NERR.EQ.0) GO TO 2300
2200 WRITE(6,2210)
PRINT 2210
2210 FORMAT(//* ERROR RETURN FROM JACTV - DTD CALL *)
2300 CONTINUE
END

```



```

PROGRAM BJD5M(INPUT,OUTPUT,TAPE2,TAPE3,TAPE4,TAPE6,TAPE8,TAPE9,
1 TAPE5=INPUT)
DIMENSION CM(68,68),V(68,68),EM(68),CS(68,68),E(68),BETA(68,68),
1 R(68),P(68),C(68,68),CINVT(68,68),BCBT(68,68),
2 IPIVOT(68),INDEX(68,2),RU(68),PU(68),XVEC(68,68)
COMMON HMTX(12),FCON
EQUIVALENCE (XVEC(1,1),BETA(1,1),CM(1,1),CS(1,1),CINVT(1,1),
1 INDEX(1,1)),(V(1,1),C(1,1),BCBT(1,1)),(R(1),RU(1)),
2 (P(1),PU(1))
MAX=68 $ MBETA=68
C ON ENTRY TO THIS PROGRAM - - -
C TAPE2 HAS ORDER AND U MATRIX
C TAPE3 HAS ORDER AND BETA MATRIX
C TAPE4 HAS COUPLED MASS AND STIFFNESS MATRICES
1 READ(5,5001) (HMTX(J),J=5,12)
5001 FCRMAT(8A10)
IF(ECF,5) 8998,8999
8957 FORMAT(/** PROGRAM BJD5M STOPPED ON (EOF,5)*)
8999 CONTINUE
HMTX(1)=10H FINAL MO $ HMTX(2)=10HDAL MATRIX
HMTX(3)=10H $ HMTX(4)=10H
FCON=1.0
REWIND 3
C READ ORDER OF BETA FROM TAPE 3
READ(3) NFB,NCB
REWIND 4
C READ COUPLED MASS MATRIX FROM TAPE 4
READ(4)((CM(I,J),I=1,NCB),J=1,NCB)
C SOLVE FOR EIGENVALUES AND EIGENVECTORS OF COUPLED MASS MATRIX
CALL JACTV(NCB,MAX,NCB,CM,EM,V,DUM1,DUM2,DUM3,DUM4,IERR)
IF(IERR.EQ.1) GO TO 1500
C TEST FOR NUMBER OF FINITE EIGENVALUES
DO 10 J=2,NCB
IJ=J-1
IF(EM(J).LE.0.0) GO TO 11
IF((EM(IJ)/EM(J)).GE.1000000.0) GO TO 11
IF (J.EQ.NCB) IJ=NCB
10 CONTINUE
11 NFMEV=IJ
WRITE(6,1111)(EM(I),I=1,NCB)
1111 FORMAT(/** EIGENVALUES OF COUPLED MASS MATRIX *// (2X,E15.8))
PRINT 14,NFMEV
WRITE(6,14) NFMEV
14 FORMAT(/** NUMBER OF FINITE EIGENVALUES OF COUPLED MASS MATRIX = *
1,I3//)
C READ COUPLED STIFFNESS MATRIX FROM TAPE 4
READ(4)((CS(I,J),I=1,NCB),J=1,NCB)
C REWIND TAPE 4 AND WRITE COLUMNS OF VECTOR MATRIX ON TAPE 4
C REWIND TAPE 9 AND WRITE ROWS OF VECTOR MATRIX ON TAPE 9
REWIND 4
REWIND 9
DO 20 J=1,NCB
WRITE(9)(V(J,I),I=1,NCB)
20 WRITE(4)(V(I,J),I=1,NCB)
C MULTIPLY STIFFNESS BY VECTOR AND STORE IN V
REWIND 4
DO 30 J=1,NCB
C READ COLUMN OF VECTOR MATRIX
READ(4)(R(I),I=1,NCB)

```

```

      DO 30 I=1,NCB
      V(I,J)=0.0
      DO 30 IJ=1,NCB
30 V(I,J)=V(I,J)+CS(I,IJ)*R(IJ)
C   CCMPUTE VT*(CS*V)
      REWIND 4
      DO 40 I=1,NCB
C     READ COLUMN OF VECTOR MATRIX AS ROW OF VECTOR TRANSPSE
      READ(4)(R(J),J=1,NCB)
      DO 40 J=1,NCB
      CS(I,J)=0.0
      DO 40 IJ=1,NCB
40 CS(I,J)=CS(I,J)+R(IJ)*V(IJ,J)
      K=NFMEV
      N=NCB-NFMEV
C   IF THE NUMBER OF FINITE MASS EIGENVALUES (NFMEV) IS EQUAL TO THE
C   CRDER OF THE COUPLED MASS MATRIX CM, BYPASS PARTITIONING OF THE
C   CCUPLED STIFFNESS MATRIX CS.
      IF(N.EQ.0) GO TO 79
      KP1=K+1
      REWIND 4
C     CS WILL BE PARTITIONED AS FOLLOWS----- (A  B)
C                                           (BT C)
C     WHERE  A=(K*K),  B=(K*N),  BT=(N*K),  C=(N*N)
      REWIND 4
C     STORE MATRIX A ON TAPE4 BY COLUMNS,  1 RECORD
      WRITE(4)((CS(I,J),I=1,K),J=1,K)
      REWIND 8
C     STORE MATRIX C ON TAPE 8 BY COLUMNS,  1 RECORD
      WRITE(8)((CS(I,J),I=KP1,NCB),J=KP1,NCB)
C     STORE MATRIX B ON TAPE8 BY ROWS,  K RECORDS
      DO 50 I=1,K
50 WRITE(8) (CS(I,J),J=KP1,NCB)
C   READ MATRIX C FROM TAPE8 AND COMPUTE THE INVERSE OF C
      REWIND 8
      READ(8)((C(I,J),I=1,N),J=1,N)
      CALL MATINV(C,N,BI,0,DET,IPIVOT,INDEX,MAX,ISCALE)
C     COMPUTE C INVERSE TIMES B TRANSPSE
      DO 60 J=1,K
C     READ ROW OF B AS COLUMN OF B TRANSPSE
      READ(8)(P(I),I=1,N)
      DO 60 I=1,N
      CINVBT(I,J)=0.0
      DO 60 IJ=1,N
60 CINVBT(I,J)=CINVBT(I,J)+C(I,IJ)*P(IJ)
      REWIND 8
C   THE NEXT READ STATEMENT IS A DUMMY READ TO POSITION TAPE8
      READ(8) SKIPREC
C     COMPUTE B * (C INVERSE * B TRANSPSE)
      DO 70 I=1,K
C     READ ROW OF B
      READ(8)(P(J),J=1,N)
      DO 70 J=1,K
      ECBT(I,J)=0.0
      DO 70 IJ=1,N
70 ECBT(I,J)=ECBT(I,J)+P(IJ)*CINVBT(IJ,J)
C   REWIND TAPE8
      REWIND 8

```

```

C      STORE C INVERSE TIMES B TRANSPOSE ON TAPE8 BY COLUMNS, 1 RECORD
WRITE(8)((CINVT(I,J),I=1,N),J=1,K)
REWIND 4
C      READ MATRIX A FROM 4
READ(4)((CS(I,J),I=1,K),J=1,K)
C      COMPUTE A - (B*CINV*BT)
C      REPLACE THE FIRST K (FINITE) EIGENVALUES OF THE MASS MATRIX BY
C      1.0/(SQUARE ROOT OF EIGENVALUE)
79 DO 81 I=1,K
EM(I)=1.0/SQRT(EM(I))
IF(N.EQ.0) GO TO 81
CO 80 J=1,K
80 CS(I,J)=CS(I,J)-BCBT(I,J)
81 CONTINUE
C PRE- AND POST-MULTIPLY THE CS MATRIX BY 1./SQRT(MASS EIGENVALUES)
DO 90 I=1,K
DO 90 J=1,K
90 CS(I,J)=EM(I)*CS(I,J)
DO 100 J=1,K
DO 100 I=1,K
100 CS(I,J)=CS(I,J)*EM(J)
CALL JACTV(K,MAX,K,CS,E,V,DUM1,DUM2,DUM3,DUM4,NERR)
IF(NERR.NE.0) GO TO 1500
CALL FREQ(E,CS,K,MAX)
C PRE-MULTIPLY VECTOR MATRIX BY 1./SQRT(MASS EIGENVALUES)
DO 110 I=1,K
DO 110 J=1,K
110 V(I,J)=EM(I)*V(I,J)
REWIND 4
C      STORE X SUB 1 VECTORS ON TAPE4, BY COLUMNS, K RECORDS
DO 115 J=1,K
115 WRITE(4)(V(I,J),I=1,K)
IF(N.EQ.0) GO TO 144
REWIND 8
C      READ C INVERSE * B TRANSPOSE MATRIX FROM TAPE8
READ(8)((CS(I,J),I=1,N),J=1,K)
REWIND 4
C      MULTIPLY (C INVERSE * B TRANSPOSE) BY X SUB 1 VECTOR MATRIX
DO 120 J=1,K
C      READ COLUMN OF X SUB 1 MATRIX FROM TAPE4
READ(4)(P(I),I=1,K)
DO 120 I=1,N
V(I,J)=0.
DO 120 IJ=1,K
120 V(I,J)=V(I,J)+CS(I,IJ)*P(IJ)
C      X SUB 2 VECTOR MATRIX = - VECTOR MATRIX JUST COMPUTED
DO 125 I=1,N
DO 125 J=1,K
125 V(I,J)=-V(I,J)
C      STORE X SUB 2 VECTOR MATRIX ON TAPE4 BY ROWS, 1 RECORD
WRITE(4)((V(I,J),J=1,K),I=1,N)
C      REWIND 4, THEN READ X SUB 1 VECTORS INTO FIRST K ROWS OF CS AND
C      READ X SUB 2 VECTORS INTO (K+1) TO NCB ROWS OF CS
C      THE CS MATRIX IS NOW (NCB * K)
144 REWIND 4
DO 145 J=1,K
145 READ(4)(CS(I,J),I=1,K)
IF(N.NE.0) READ(4)((CS(I,J),J=1,K),I=K+1,NCB)
C      MULTIPLY MASS VECTOR MATRIX BY CS MATRIX
REWIND 9

```

```

      CO 146 I=1,NCB
C     READ ROW OF MASS VECTOR MATRIX
      READ(9)(R(J),J=1,NCB)
      CO 146 J=1,K
      V(I,J)=0.0
      DC 146 IJ=1,NCB
146 V(I,J)=V(I,J)+R(IJ)*CS(IJ,J)
C     COMPUTE BETA * THE FINAL VECTOR MATRIX
      REWIND 8
      CO 151 I=1,NRB
C     READ ROW OF BETA MATRIX
      READ(3)(R(J),J=1,NCB)
      DC 150 J=1,K
      P(J)=0.0
      CO 150 IJ=1,NCB
150 P(J)=P(J)+R(IJ)* V(IJ,J)
151 WRITE(8)(P(J),J=1,K)
      REWIND 8
      DC 160 I=1,NRB
160 READ(8)(BETA(I,J),J=1,K)
C     COMPUTE U * BETA MATRIX
      REWIND 2
      READ(2) NRU,NCU
      REWIND 8
      DC 166 I=1,NRU
C     READ ROW OF U MATRIX
      READ(2)(RU(J),J=1,NCU)
      DC 165 J=1,K
      PU(J)=0.0
      DC 165 IJ=1,NCU
165 PU(J)=PU(J)+RU(IJ)*BETA(IJ,J)
166 WRITE(8)(PU(J),J=1,K)
      REWIND 8
      CO 169 I=1,NRU
169 READ(8)(XVEC(I,J),J=1,K)
      CALL WMTXC(XVEC,NRU,K,MBETA,MAX)
      REWIND 9
      WRITE(9) NRU,K
      WRITE(9)(E(J),J=1,K)
      DC 170 J=1,K
170 WRITE(9)(XVEC(I,J),I=1,NRU)
      GO TO 1
1500 IF(IERR.EQ.1) WRITE(6,1501)
      IF(NERR.NE.0) WRITE(6,1502)
1501 FORMAT(/** ERROR RETURN FROM JACTV - FIRST CALL - COUPLED MASS*)
1502 FORMAT(/** EPROR RETURN FROM JACTV - SECOND CALL - STIFFNESS*)
      GO TO 1
8998 WRITE(6,8997)
      PRINT 8997
      END

```



```

      SUBROUTINE WMTXC(A,NR,NC,MAXR,MAXC)
C   NR=ROWS OF A, NC=COLS OF A, MAXR=MAX ROWS OF A, MAXC=MAX COLS OF A
      DIMENSION A(MAXR,MAXC)
      COMMON HMTX(12)
      KE=0
      KSET=NC/8
      KLEFT=MOD(NC,8)
      IF(KLEFT.NE.0) KSET=KSET+1
      DO 10 KT=1,KSET
      KB=KE+1
      KE=KE+8
      IF(KT.EQ.KSET) KE=NC
      WRITE(6,5001) HMTX,(J,J=KB,KE)
      GO 10 I=1,NR
10  WRITE(6,5002) I,(A(I,J),J=KB,KE)
5001 FORMAT(1H1//12A10///10H ROW   COL,14,7(11X14))
5002 FORMAT(14,8E15.7)
      RETURN
      END

      SUBROUTINE FREQ(E,A,K,MAX)
      DIMENSION E(MAX),A(MAX,MAX)
      COMMON HMTX(12),FCON
      DO 10 I=1,K
      A(I,1)=E(I)
      A(I,2)=FCON*A(I,1)
      A(I,3)=SQRT(ABS(A(I,2)))
10  A(I,4)=A(I,3)/6.28318530717959
      PRINT 5014,(HMTX(J),J=5,12),FCON,(I,(A(I,J),J=1,4),I=1,K)
      WRITE(6,5014)(HMTX(J),J=5,12),FCON,(I,(A(I,J),J=1,4),I=1,K)
5014 FORMAT(1H1//1X8A10//7H FCON =,E22.14//4X1HJ9X9HLAMBDA(J)14X12HOMEG
1A SQ (J)14X8HOMEGA(J)14X13HFREQ.(J), CPS/34X18H(FCON * LAMBDA(J))1
22X6H(REAL) //(15,4E24.14))
      RETURN
      END

```

AIRPLANE BEAM ASSEMBLY - SYMMETRIC MODES - CLAMPED-FREE MODES FOR WING AND TAIL